Errata

Page No.,	Line No.	Instead of	Read
p.16,	Title of Fig.1.6	Coordinates of Plates...	Coordinate axes of plates ...
p.23,	line 27	The collapse of practical steel structures is subjected...	The collapse of practical structures subjected ...
p.33, 1	line 17	... and pick up ...	... and can pick up ...
p.48,	line 2	$\frac{1}{2I} A_{ijk} v_j v_k$ ...	$\frac{1}{2I} (A_{ijk} + e A_{ijk\ell}) v_j v_k$
	line 15	"	"
p.57,	line 2	A comparison example of..	A companion example of ...
p.81,	line 13	... in Fig. 3.1 ...	... in Fig. 3.2 ...
p.82,	line 8	The basic reatures of the ...	The basic features ...
p.104,	line 5	... $\frac{1}{2I} A_{ijk} v_j v_k$	$\frac{1}{2I} (A_{ijk} + e A_{ijk\ell}) v_j v_k$
	line 15	.. $A_{ijk} v_{j_1} v_{k_1}$	$(A_{ijk} + e A_{ijk\ell} q_{\ell_1}) v_{j_1} v_{k_1}$
	line 16	.. $3A_{ijk} v_{j_1} v_{k_2}$	... $3(A_{ijk} + e A_{ijk\ell} q_{\ell_1}) v_{j_1} v_{k_2}$ + $3e_1 A_{ijk\ell} q_{\ell_1} q_{j_1} q_{k_1}$
p.162,	line 15	The critical load expressed in terms of K where ...	The critical load is expressed in terms of K where ...
p.173,	Fig.4.18(a)	$\varepsilon_{cr_o} = \sigma_{cr_o} = \frac{\pi^2}{12(1-\nu^2)} \left(\frac{h}{2L}\right)^2$	$\varepsilon_{cr_o} = \frac{\sigma}{E} cr_o = \frac{\pi^2}{3(1-\nu^2)} \left(\frac{h}{2L}\right)^2$
p.251,	line 24	The scope for extensions of the present work are discussed ...	The scope for extensions of the present work is discussed ...
p.286,	line 2	Contents: In this Appendix is described..	Contents: In this Appendix are described ..
p.87,	line 3	... $f_{1,6n} \cos 6n\pi\xi$	.... $f_{2,6n} \cos 6n\pi\xi$

ELASTIC POSTBUCKLING BEHAVIOUR AND CRINKLY COLLAPSE OF PLATE STRUCTURES

by

S. SRIDHARAN

A Thesis submitted for the degree of

Doctor of Philosophy

of the University of Southampton

November 1977

ACKNOWLEDGEMENTS

The author wishes to express his gratitude to Dr. T.R. Graves-Smith whose inspiring guidance, thoughtful criticism and valuable suggestions have made this thesis possible.

The author is grateful to the Association of the Commonwealth Universities, U.K. for granting him a Commonwealth Scholarship which enabled him to undertake and complete the studies reported herein.

The author is thankful to the University of Southampton Computing Services for their efficient service. Special thanks are also due to Messrs. D. Orchard and A.T. Rogerson for their kind technical assistance in the experimental work, Mr. J. A. Oldham for his kind help in the preparation of tracings of drawings and Mrs. A. Lampard for typing this thesis neatly.

Finally I must acknowledge the stabilising influence of my family throughout the period of research and in particular my wife Chandra who "strengthened failing courage and instilled faith in hours of despair".

UNIVERSITY OF SOUTHAMPTON

ABSTRACT

FACULTY OF ENGINEERING AND APPLIED SCIENCE

DEPARTMENT OF CIVIL ENGINEERING

Doctor of Philosophy

ELASTIC POSTBUCKLING BEHAVIOUR AND
CRINKLY COLLAPSE OF PLATE STRUCTURES

by S. Sridharan

The widespread use of structures built up of thin plate elements in engineering construction has made a study of their buckling, post-buckling and collapse behaviour very important.

In the present study methods of buckling and post-local-buckling analysis of prismatic plate structures have been developed using the finite strip approach. The buckling analysis presented takes into account the prebuckling stress distribution and can model localised buckling modes by a superposition of a chosen number of harmonics. The post-local-buckling analysis has been developed in two versions:

The first, a simpler version which neglects the coupling of inplane and out of plane displacements (and forces) of plates meeting along a common edge,

the second, the more general version which makes no such assumption. Brief parametric studies on the post-local-buckling behaviour of a few typical plate assemblies have been reported.

The plate structures are known to fail most frequently by a 'crinkly' buckling of one or more of their junctions; and this type of failure can occur entirely elastically. With the object of gaining an insight into this phenomenon, an analytical and experimental investigation on square box columns was undertaken as part of the present studies. The experimental study established that the elastic collapse loads of the box columns is very reproducible and the phenomenon of crinkly collapse under controlled compression, is the result of snap-buckling of the structure after reaching a limit point, to a remote state of equilibrium. Good agreement was found to exist between the theoretically predicted and experimental values of collapse loads. A theoretical mechanical model of a column resting on a nonlinear elastic foundation has been proposed, to explain the post-collapse "crinkly" displacement profile.

TABLE OF CONTENTS

Notation

$A_i, A_{ij}, A_{ijk}, A_{ijk\ell}$	Coefficients of the terms of energy expression
B	Width of plate
B_{ij}	Coefficients of terms of energy expression
C	Width of patch loading on a plate
C_{ij}	Coefficients of terms of energy expression
D	Flexural rigidity of plate per unit width
E	Young's Modulus of the material of the plate
N	Total number of degrees of freedom of plate strip
P	Applied patch load on plate
P_{cr}	Critical value of P
Q_i	A global degree of freedom
U	Total internal strain energy
V	Potential Energy of applied load
W	Total potential energy of a plate strip
X,Y,Z	Global axes of coordinates
a	Length of plate
b	Width of plate strip
e	Average strain of the plate structure
h	Thickness of plate
i,j,k,ℓ,m,n,p.q	integers
q_i	A local degree of freedom
u,v,w	Displacements in the longitudinal, transverse (inplane) and normal (out of plane) directions
x,y,z	Coordinates of a point in the longitudinal, transverse (inplane) and normal directions of a plate strip
Δ	End compression of a plate
α	= a/h

β	= b/h
γ	= a/B
δ	End compression of a plate
ε	Perturbation parameter in chapters 2 and 3; average strain of the plate elsewhere
$\varepsilon_x, \varepsilon_y, \gamma_{xy}$	Strain components at a point
η	Nondimensional 'y' coordinate of a point in plate strip (y/b)
λ	Halfwave length of buckling
ν	Poisson's ratio of the material of the plate
ξ	Nondimensional 'x' coordinate of a point in plate strip (x/a)
$\sigma_x, \sigma_y, \tau_{xy}$	Normal and shear stress components
σ_{cr}	Buckling stress
σ, σ_{av}	Average longitudinal stress
σ_{max}	Maximum membrane stress
	Airy's stress function
ϕ'	$\frac{\partial \phi}{\partial y}$
ϕ''	$\frac{\partial^2 \phi}{\partial y^2}$
ϕ^{iv}	$\frac{\partial^4 \phi}{\partial y^4}$
ω	A synonym for 'w' in Chapter 1.

All the other symbols have been defined when they are first introduced.

CHAPTER 1

REVIEW OF THE LITERATURE AND SCOPE OF THE PRESENT INVESTIGATION

1.1 Introduction

One of the major developments in modern civil, aeronautical and naval construction is the widespread use of structures composed of thin plate elements. The characteristic feature of thin-walled structures is that they are susceptible to local buckling when carrying longitudinal compression, i.e. the individual plates developing out of plane deformation while the junctions remain essentially straight. This results in the structure losing some of its stiffness after a certain critical load, but it can often have a great deal of reserve strength before it collapses.

The determination of the critical load is of importance as buckling is accompanied by a loss in stiffness and growth of out of plane deflections. This is especially true of supersonic aircraft construction where the prime necessity is the maintenance of the aerodynamic shape of the vehicle. A postbuckling analysis, which takes into account the geometric and material nonlinearities can provide information regarding the stiffness characteristics of the structure under loads in excess of the critical load and help to assess the collapse load; and this has become vitally important in the current design practice inspired as it is by the limit state design philosophy.

It is not surprising therefore, that the attention of several investigators has remained focussed on the subject of buckling, post-buckling behaviour and ultimate strength of plate structures in the past

five decades. Most of the investigators have tended to concentrate their studies on single plates rather than plate assemblies in spite of the widespread use of the latter in practice. This is especially true of postbuckling and ultimate strength analysis due, understandably, to the necessity of exploring fully the behaviour of the basic component of plate structures and the complexity of analysis of combinations of plates. In the present investigation, greater emphasis is laid on the analysis of plate assemblies, but attention is restricted to elastic behaviour. A characteristic feature of the plate assemblies is their mode of failure by a "crinkly" collapse of junctions, and interestingly this type of failure can occur entirely elastically. In the present investigation an attempt is made to understand and explain this mode of collapse of plate structures. Thus the present investigation is concerned mainly with the elastic postbuckling behaviour and crinkly collapse of plate assemblies. As a prelude to this study, an investigation into buckling of plate structures has been undertaken. In the review of literature that follows, an attempt has been made to place the present work in the context of earlier studies.

1.2 Review of literature

In this section, a brief review of the literature on flat plate structures is presented. Emphasis will be on structures carrying axial compression, these being the most relevant to the present thesis.

1.2.1 Initial buckling of plate structures

The literature on initial buckling of plates with various boundary conditions is very extensive as seen from references 1-4. The problem of initial buckling of plate assemblies has been studied extensively by

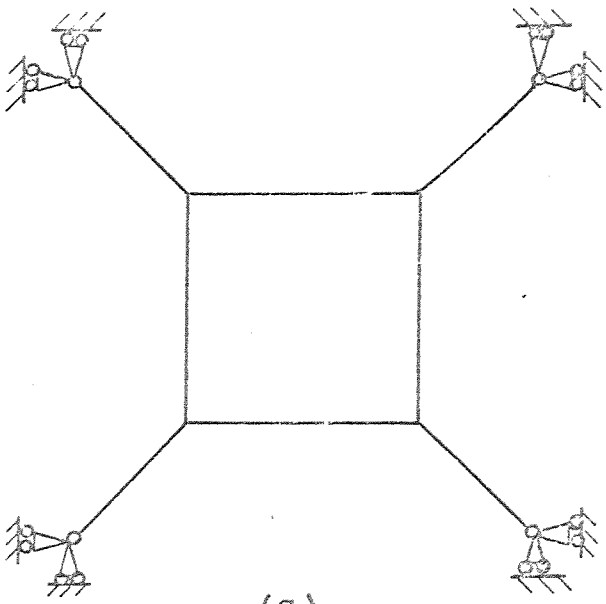

(a)

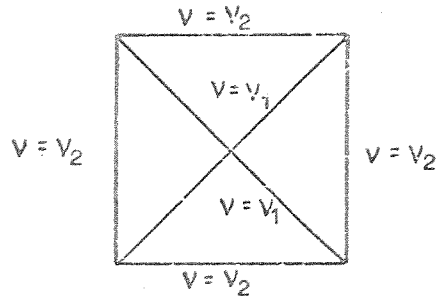

(b)

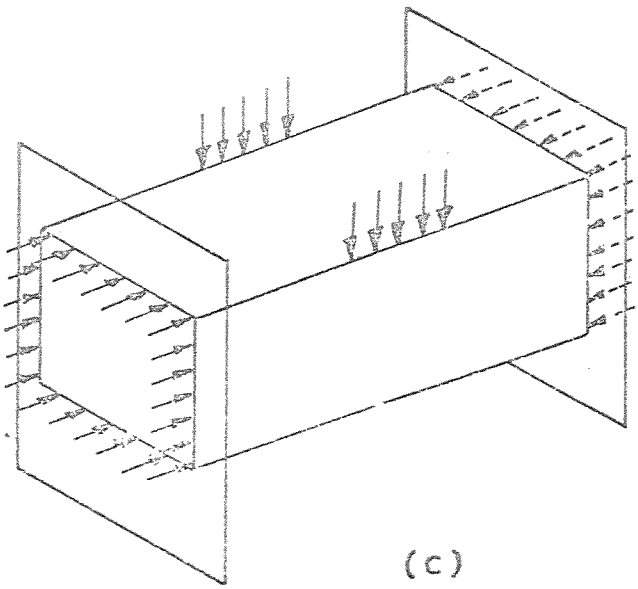

(c)

Fig. 1.1 Examples of Plate Assemblies with nontrivial Prebuckling Stress distribution.

Wittrick[5-9], who in a series of papers developed a generalised matrix approach for the problem. His approach was based on a solution of the governing differential equations as given by Novozhilov[10] in terms of displacements. In contrast to the previous analyses, it was possible in this approach to obtain the 'local','overall' or 'coupled' buckling modes and loads as eigenvectors and values of a single stiffness matrix.

Parallel to the development of the 'exact' method by Wittrick, a simpler finite strip method of buckling analysis has been developed by Turvey[11] and Cheung[12] independently. In this method, approximate polynomial functions were used to characterise the variation of the displacements in the transverse direction and a variational principle was invoked to generate the equilibrium equations. The main advantage of this approach over one based on solution of differential equations, is that it leads to a linear eigenvalue problem, which is capable of a direct solution for all the eigenvalues and vectors.

In all the above methods, the constituent plates are subjected to stresses (uniform or varying) whose values are known at the outset. In many situations in practice, the stress distribution can not be known a priori and can not be described adequately by simple expressions. Two examples will be cited to illustrate this point. In Fig. 1(a-b) are shown the configurations of plate assemblies which carry uniform longitudinal stresses applied at the ends of the structure. Due to the 'indeterminacy' of these structures, each of the constituent plates will carry varying magnitudes of stresses in the transverse direction due to Poisson's effect, the magnitudes of which are not known before hand. Fig. 1(c) shows a plate structure carrying a combination of axial and lateral patch loading. In this case the prebuckling stress distribution is too complex to be described in terms of sample expressions. In the foregoing problems, it is necessary first to obtain the prebuckling

stresses and feed their effect into the buckling analysis. In other words buckling must be treated as bifurcation from a "nontrivial"[13] equilibrium path. Such an investigation for plates carrying inplane patch loads has been made by Rockey and Bagchi[14] using a finite element approach. In chapter 2 of this thesis a finite strip approach has been developed to deal with similar problems.

1.2.2 Initial postbuckling analysis: General

The problem of postbuckling analysis of plate structures, is in general a difficult one, riddled as it is by the presence of finite deflections and progressive plastic yielding of regions of the plate. In this section, attention will be confined to postbuckling behaviour of plates and plate assemblies at loads which are not far in excess of the critical load, while the material is assumed to remain elastic.

The differential equations governing the problem of "large" deflections of plates were first established by von Karman[15] in 1910, and these are of fundamental importance in the study of nonlinear behaviour of plates. It must be noted that a few important assumptions[16,17] had been made in deriving these equations. These are briefly

$$\omega \gg u,v$$

$$\left(\frac{\partial \omega}{\partial x}\right) , \left(\frac{\partial \omega}{\partial y}\right) \ll 1 \qquad \ldots 1(a\text{-}b)$$

These assumptions are indeed valid for the postbuckling analysis of plates in the vast majority of practical situations, as has been demonstrated by analytical and experimental studies in the past five decades.

In the context of postbuckling behaviour of plate assemblies it is important to note that von Karman equations are not adequate for a study of post-overall-buckling problems, but only for post-local-buckling

studies. This can be clarified by reference to Fig. 1.2. In the local buckling problems, each plate undergoes normal displacements while the junctions undergo little or no displacements. (Fig. 1.2(a)). An overall buckling mode, on the other hand, is one in which the junctions undergo significant translations. In this case, some of the constituent plates will undergo inplane displacements in the transverse direction which may not be small in comparison with normal displacements, as for example the stiffeners in the stiffened plate shown in Fig. 1.2(b). This means that the assumption 1(a) of the von Karman theory is invalidated. In order to model the post-overall-buckling behaviour it is necessary to include the nonlinear terms in 'v' as well as in 'ω' in the strain displacement relations. Owing apparently to its complexity, it seems such an analysis has not been dealt with in literature so far. This is also true of the present studies which deal only with the post-local-buckling phenomena.

1.2.2.1 Initial postbuckling analysis of single plates.

With the exception of a small number of papers, most published work on the subject of postbuckling analysis of plate structures deal with single plates rather than of plate assemblies; and on this however a wealth of literature exists. The analytical procedures employed for the study of the problem fall under the following categories:

1. Solution of von Karman differential equations.

2. Solution of the von Karman compatibility equation together with the use of a variational method.

3. Variational procedures.

These will be considered briefly one by one in the following.

1.2.2.1.(a) Solutions based on differential equations

An "exact" solution of the von Karman equations for the case of a

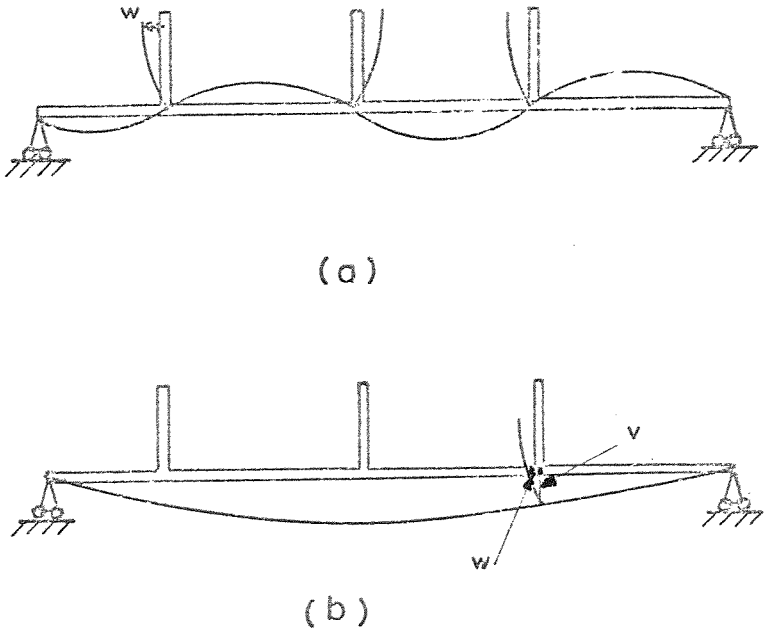

Fig. 1.2 Local and Overall Buckling Modes of a Stiffened Plate.

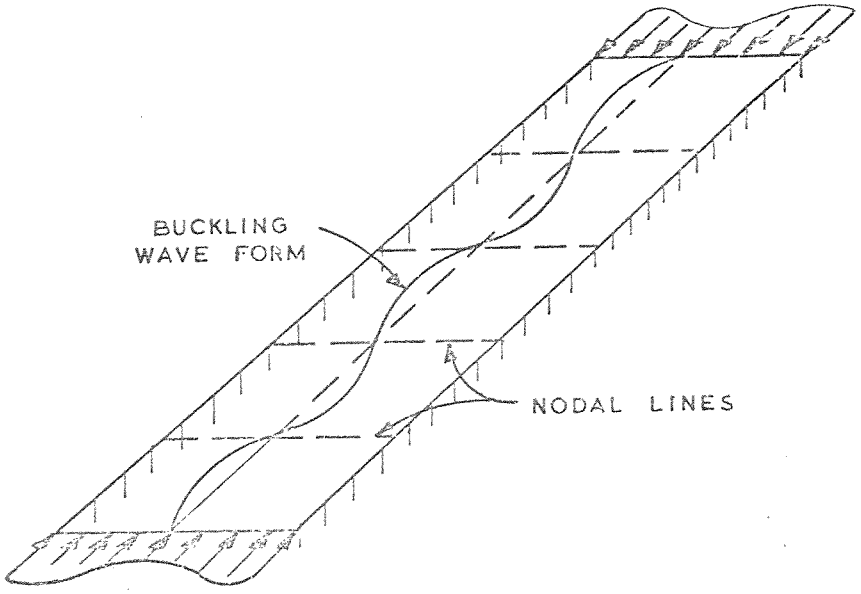

Fig. 1.3 Buckling Wave-form of a Long Plate under End Compression.

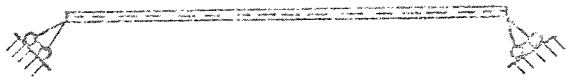

Fig. 1.4 Plate with Skew Boundary Conditions.

simply supported plate under uniform edge compression was obtained by Levy[18]. The method was based on the assumption of 'w' in the form of a double Fourier series. An extension of this method was due to Coan[19] who studied the behaviour of plates with initial imperfections with stress-free unloaded edges. Hemp[20] proposed an iterative solution of von Karman equations for the initial postbuckling analysis of rectangular plates with one pair of edges simply supported. Manuel Stein [21,22] employed a perturbation technique to solve the differential equations in order to study the problem of a simply supported rectangular plate.

Except for the simplest case of a plate simply supported on all its four edges, the solution of the von Karman equations is no easy task. For plates with various boundary conditions, a semivariational approach appears to be more fruitful and this will be discussed next.

1.2.2.1.(b) Semi-variational approach

This approach is based on the fact that it is fairly easy to characterise the normal deflection 'ω' by a relatively small number of terms (say one or two) but not the stress function. Once the function for 'ω' is assumed, it is often possible to solve the compatibility equation to obtain ϕ, in terms of the coefficients describing 'ω'; the arbitrary constants in the solution for 'ϕ' can be obtained from the inplane boundary conditions. Instead of attempting to satisfy the equilibrium equation with these expressions for 'ω' and 'ϕ', it is often simpler to invoke a variational principle to generate the required nonlinear algebraic equations in terms of the unknown coefficients in the function describing 'ω'.

The earliest application of this technique was by Marguerre[23] who solved the problem of a simply supported plate using upto three terms in the description of 'ω' and Ritz procedure to generate algebraic

equations governing the problem.

Yarmaki undertook a comprehensive investigation of the postbuckling behaviour of rectangular plates using the semivariational method[24]. Several combinations of inplane and out of plane boundary conditions were considered by him, such as simply supported and clamped edges for a pair of opposite edges as well as two sets of inplane boundary conditions along the unloaded edges - one in which the edges were allowed to freely wave and the other in which they were allowed to move but held straight. Galerkin's variational technique was used to generate the algebraic equations in terms of the unknown coefficients in the description of 'ω'. Numerical solutions were obtained for square plates with or without initial imperfections.

Similar method was used by Walker[25] in his investigation of simply supported square plates who used a perturbation technique to obtain the postbuckling characteristics. This obviated the necessity of solving nonlinear equations and an explicit solution for the deflection coefficients was found to be possible. In using a perturbation method, it is important to remember that the accuracy of the final solution depends on the perturbation parameter chosen and in general remains unknown (unless by comparison with an already available solution) on points not in the immediate vicinity of the critical load. But the path parameter chosen by Walker $\sqrt{(\sigma-\sigma_{cr})/\sigma_{cr}}$ - the same as the one used by Stein, was found to give very satisfactory results for the postbuckling problem.

A long rectangular plate, with all its edges supported in some manner, buckles under longitudinal compression with a deflection mode which can be satisfactorily represented by a sine wave at the initial stages of postbuckling behaviour. In such a case, the plate is subdivided into a sequence of independent buckles, with the nodal lines remaining

straight and carrying no shear stresses. Thus it is necessary and sufficient to consider the action of just one buckle between two successive nodal lines to obtain the initial postbuckling behaviour of the entire plate. Such an approach was taken by Rhodes and Harvey[26-28] all of whose solutions are based on the assumption of 'ω' in the form

$$\omega = \omega(y) \sin \frac{\pi x}{\lambda}$$

where 'λ' is the half wave length of buckling, (Fig. 1.3) and $\omega(y)$ is a function of y, which could be so chosen as to satisfy the out of plane boundary conditions. In one of their earlier papers[25], they studied the behaviour of plates elastically restrained along its longitudinal edges but resting on rigid supports. A two term trigonometric function was employed to describe the normal displacement in the transverse direction. The solution was found to be quite accurate upto twice the critical load. In a subsequent paper[27] a four term polynomial was used to describe the buckling mode and the postbuckling analysis was carried out making the assumption that the postbuckled deflected form is the same as the buckling mode. An analysis based on such an assumption can not depict the drop in postbuckling stiffness with increase in load as was found by Graves-Smith[59] in an earlier investigation, on rectangular columns. The same assumptions were made by Rhodes and Harvey, in their analysis of eccentrically compressed rectangular plates[28]. A summary of their findings may be found in a recent paper[29]. The chief contribution of these papers lies in producing a large body of useful results for the initial postbuckling stiffnesses for plates with various degrees of rotational restraints along the unloaded edges and subjected to linearly varying applied end compression.

The semivariational approach has proved to be quite a useful tech-

nique for the initial postbuckling analysis of rectangular plates. However the algebraic work involved becomes much too tedious if several harmonics have to be taken into account in the longitudinal direction as may be required for loads higher than twice the critical load. The secret of their success lies in the fact that the boundary conditions in 'ω' and 'ϕ' are not coupled in the problems considered (so that 'ω' can be described without reference to 'ϕ'). Such a coupling can occur when the plate is subjected to skewed boundary conditions as shown in Fig. 1.4.

1.2.2.1.(c) Variational methods

The solution of von Karman compatibility equation is often a very difficult task and may not be readily achieved for any set of boundary conditions, even for rectangular plates. In such situations it can often prove simpler to make use of a variational principle and convert the problem into one of a solution of algebraic equations in terms of unknowns describing the displacements. In this section, these methods will be briefly discussed in the context of postbuckling analysis of plates.

The following formulations of the variational method have been used in the past for a variety of structural problems:-

(i) The classical variational methods, such as Rayleigh-Ritz, Galerkin and Kantorovich methods.[30]

(ii) The finite element method.

(iii) The energy formulation of the finite difference method.

(i) Classical variational methods

The application of Rayleigh-Ritz method has been restricted to the simplest case of a simply supported rectangular plate .[31-32] The main difficulty lies in the description of inplane displacement across the plate in terms of a manageable number of unknowns. Inadequate description

of inplane displacements will lead to inaccuracies in the resulting postbuckling characteristics, as for example in Timoshenko's analysis[32] where the displacements were each described by one term.

Walker[33] applied Galerkin's method for the problem of rectangular plate carrying a nonuniform loading. In the analysis, both 'ω' and 'ϕ' were described by polynomials whose coefficients were so adjusted as to satisfy the boundary conditions. The solution procedure, though of interest from the point of view of the analytical technique used, was found to involve generally more arithmetical work than the semienergy method for obtaining an accurate result.

The main disadvantage associated with the classical methods is their lack of generality, in that it is very difficult to take into account the arbitrary geometry and boundary conditions of the plate.

(ii) Finite element method

This is a generalised version of the Ritz method. The method is based on the description of displacements in sub-domains (elements) instead of over the entire domain. Each element is connected to adjacent elements at joints, called nodal points, through which continuity of certain displacement parameters (called nodal degrees of freedom) is maintained. A stiffness relationship between the nodal forces and displacements can be established using the virtual work principle for each element.

The method has proved to be very powerful and is capable of dealing with complicated shapes and boundary conditions of plates[34-36]. The first attempt at including the geometric effects in the method for the purpose of studying the buckling problem was made by Turner[36] et al. in 1960. Later a long series of publications[37-46] has extended the method

to be applicable to various types of instability and large deflection problems. The finite element implementation may be based either on a total Lagrangian description of the displacements referred to a fixed coordinate system or on a formulation where the "local" coordinate frames are updated in a stepwise fashion. The total Lagrangian description has the merit of simplicity and computational ease and has been used extensively[38,43,46]. The formulation based on a movable 'local' coordinate systems used by Murray and Wilson removes the restriction on the displacement gradients $\frac{\partial \omega}{\partial x}$, $\frac{\partial \omega}{\partial y}$ that they be small.

While it is true that the finite element method is the most versatile and powerful for dealing with structural problems, it can often prove expensive in computation and can be recommended only when cheaper and more efficient methods can not be found for the problem. If the ends of the plate are simply supported, a finite strip approach would often prove more efficient. This has already been forcefully demonstrated by Cheung for the buckling problem. However the applications of this technique for nonlinear problems have been very few. Of these, Ref. 48-51 deal with the problem of rotational shells using ring elements. The major difficulty encountered herein, arises due to the coupling of several harmonics in the solution, leading to a large number of coefficients of nonlinear terms to be calculated. In order to simplify the analysis certain approximations have been made e.g. coupling of certain harmonics being neglected altogether or the quartic terms in the potential energy expression. The validity of these assumptions for the postbuckling analysis of plates is questionable. The ref. 47 deals with the nonlinear analysis of plates, with displacement functions which model satisfactorily neither the case of uniform end compression nor of uniform applied stress. In chapter 3,

of the thesis, this method is developed to deal with post-local-buckling problem of plate assemblies, where it is shown how the foregoing difficulties can be overcome.

(iii) Variational formulation of the finite difference method

Usually the finite difference method is used to satisfy at discrete points, the differential equations governing the problem. In this form, it has been used for large deflection problems by Wang[52] and more recently by Chapman[53-54]. However investigations in which the difference technique has been applied directly to the functionals associated with the differential equations, have been reported by Greenspan[55-56]. This approach has been utilised for structural problems by Almroth, Bushnell[57] and others. It is believed that the finite difference method in this form, could be successfully applied to the postbuckling problems of plates. Nevertheless, the method is less versatile than the finite element method being more difficult to apply in nonrectangular domains and in the presence of discontinuities.

1.2.2.2 Initial postbuckling analysis of plate assemblies

In contrast with single plates, the literature available on initial postbuckling analysis of combinations of plates is rather scanty. The most of the available solutions of the postbuckling problems of plates are based on solutions of differential equations and semi-variational approaches. These methods tend to make the analysis of arbitrarily given configuration very complicated, as they involve satisfaction of difficult equilibrium and compatibility conditions along the junctions of the plates. The finite element approach provides a general framework for dealing with this problem, but would prove very expensive for computation.

The first notable work on the subject is by Benthem[58] who used the semi-energy method for obtaining the reduction in stiffness of the plate assembly immediately after local buckling. From the point of view of postulating the boundary conditions, the junctions were classified by him into three specific types:

1) A "corner", i.e. a sharp bend between adjacent plates (Fig. 1.5(a))
2) A "transition" connecting two adjacent plates of unequal thickness. (Fig. 1.5(b))
3) A "branch point" where one plate branches off from a junction of two other plates in a line. (Fig. 1.5(c))

It can be readily seen that for a "transition" the boundary conditions in 'ω' and 'ϕ' are not coupled, but for a 'corner', they are coupled in a strict theoretical sense. But using a fairly lengthy mathematical argument, Benthem came to the conclusion that the following boundary conditions may be applied for each of the plates meeting at a 'corner':-

$$\frac{\partial^2\phi}{\partial x^2} \quad , \quad \text{the normal stress in the transverse direction} = 0$$

$$w \quad , \quad \text{the normal displacement} = 0$$

This set of conditions applied for each of the plates results in the violation of compatibility and equilibrium conditions along the junction, but can be justified on the following grounds: (i) The extensional rigidities of the plates are so great in comparison to flexural rigidities, that little resistance is encountered as each of the plates wave in their own plane and (ii) the inplane displacements for each of the plates along the common edge are small by an order of magnitude in comparison to the normal displacements, the bending energy involved in accommodating these displacements is negligibly small. (Fig. 1.6 and 1.7)

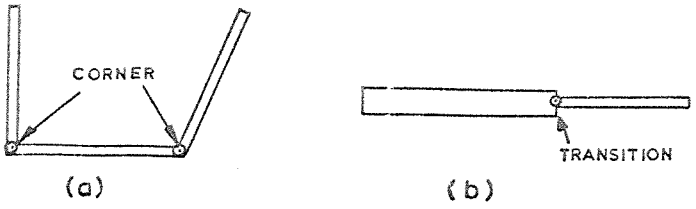

Fig. 1.5 Three types of Junctions in Benthem's Analysis.

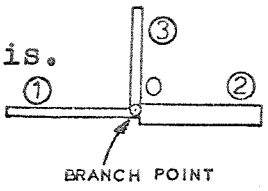

(c)

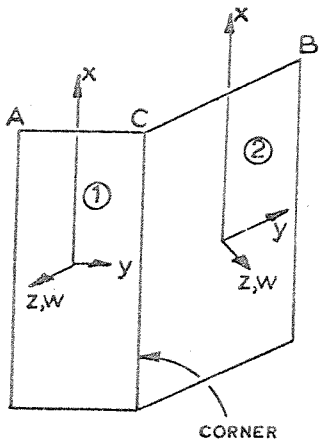

Fig. 1.6 Coordinates of Plates Meeting at a 'Corner'.

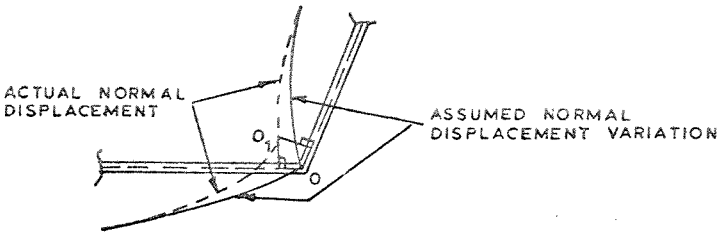

Fig. 1.7 Normal Displacements near a Junction.

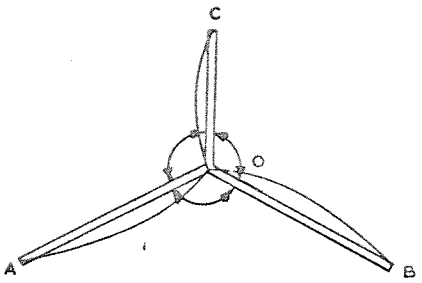

Fig. 1.8 A Junction with three plates meeting at equal angles.

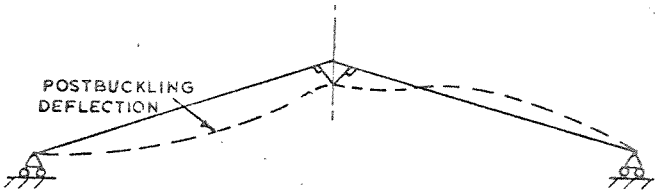

Fig. 1.9 Plates meeting at an Oblique Angle.

It will be of interest to consider the case of a junction where three plates meet at nearly equal angles (Fig. 1.8) and examine whether the above assumptions can be made. In this case, the inplane movements of each plate are resisted by those in the other two and thus each plate would carry a normal stress in the transverse direction at the common edge O. However two equilibrium equations can be written relating these forces while the normal displacements at O, for each of the plates can be assumed to vanish.

Another situation where Benthem's approximations become questionable is when two plates (such as AO and BO in Fig. 1.9) meet at a very oblique angle. Here even very small inplane displacements in the plates AO and BO would result in a comparatively large normal displacement at the common edge and this in turn can have a significant effect on the postbuckling characteristics of the plate structure. Such a problem is discussed in chapter 4.

However, it is apparent that Benthem's approximations are valid for the initial post-local-buckling analysis for a wide spectrum of cases of practical interest. But the major disadvantage of Benthem's approach is that it is not suitable for automated conputation, a consideration which becomes important when dealing with plate assemblies consisting of several plates.

An elastic post-local-buckling analysis of rectangular columns was presented by Graves-Smith[59] as part of his studies on the ultimate strength of columns. Semi-energy method was used and the boundary conditions along the junction were approximated in the same manner as in Benthem's analysis. Initial postbuckling stiffnesses were obtained for rectangular columns of various ratios of length to width of the cross-section. Since the deflection mode was not allowed any freedom to

change in the postbuckling range, it was not possible to obtain the reduction in postbuckling stiffness which occurs as the applied loads increase well beyond the critical. In a subsequent paper[60] Graves-Smith considered the post-local-buckling behaviour of a box beam subjected to end moments using a similar approach.

Another significant contribution on the subject of post local buckling behaviour of combinations of plates came from Rhodes and Harvey who studied the problem of plain and lipped channels[61-62] subjected to compression and bending using the semi-energy method. Their theoretical results showed good agreement with the experimental results published earlier by Winter.

Before concluding this subsection, it may not be inappropriate to refer to the earlier studies of the author on the problem of elastic postbuckling behaviour of plate assemblies, briefly summarised in Appendix I of the thesis. The solution is based on an assumption of 'ω' and 'ϕ' in the form of a trigonometric series, each term of which is associated with a finite difference grid in the transverse direction. By expanding certain terms in Fourier series again and using the perturbation technique, it was possible to reduce von Karman equations to sets of sequentially linear algebraic equations. The main advantage of this solution is that it uncouples the equations corresponding to each trigonometric term, which may be solved separately, thus resulting in saving of computing effort. However, this approach did not prove efficient for tracing the postbuckling equilibrium path in its highly nonlinear ranges, as is shown in Appendix I.

1.2.3 Advanced postbuckling analysis of plates and plate assemblies

As the applied load increases well beyond the critical, the struct-

ural response of the plate undergoes changes which can not be predicted by the relatively simple postbuckling analysis considered so far. The analysis must be capable of depicting

1. The possible changes in longitudinal wave form which can usually be accompanied by abrupt loss of stiffness of the buckled structure.

2. The interaction of local and overall buckling modes, which would occur if the plate structure is sufficiently long.

3. The phenomenon of progressive plastic yielding of the material leading to the collapse of the structure.

4. Collapse of the structure which is accompanied by 'crinkly buckling' of plate junctions, which is the sudden appearance of an extremely localised mechanism type of deformation or kink along the junction.

The study of these phenomena has proved, in general, very difficult and therefore it is not surprising that the literature available on these is rather limited.

1.2.3.1 Changes in wave form

The phenomenon of change of longitudinal wave from was first studied by Stein[22,63]. The possibility of change of wave form from one consisting of 'm' half waves, on a certain point on the primary postbuckling equilibrium path, to one consisting of 'n' half waves (secondary buckling path) depends upon the second variation of the potential energy of the structure with respect to the degrees of freedom corresponding to the two buckling modes. If it is positive definite, the primary buckling is stable; and if it ceases to be positive definite at some point, then a change of wave form is imminent.

Stein investigated the simpler problem of a mechanical model[17] resting on nonlinear elastic springs. With this it was possible to obtain the different possible paths of loading and unloading that could be followed. Some led to conditions of gradual transition from one mode to another and others to snapping or 'explosive' changes. In practice this change might be delayed or advanced by the presence of initial imperfections. However, Stein did not apply this rigorous procedure for the plate problem but based his results on a study of an infinitely long plate which was supposed to exhibit continuous change of wave form. The results of an experimental investigation on a plate resting on a number of intermediate supports subject to longitudinal compression were also reported. These results will be commented upon towards the end of this section.

The problem of changes in wave form of plates was studied by Supple[64] in a rigorous manner. His approach was based on a detailed study in general terms of the possible forms of coupled buckling modes for structural systems with two degrees of freedom which have symmetric uncoupled modes[65-66]. The plate was considered to have two degrees of freedom corresponding to any two given wave forms. Solutions were obtained for uncoupled and coupled buckling modes taking into consideration the initial imperfections of the plate. With these solutions, it is possible to predict whether any change of form will occur at all and if so to obtain the precise path of transition from one mode to another, in any given case.

It will be a matter of interest to examine Stein's experimental results in the light of Supple's theoretical conclusions. For an initially perfect simply supported, uniformly compressed plate with the unloaded edges free to move but held straight, Supple[66] has proved

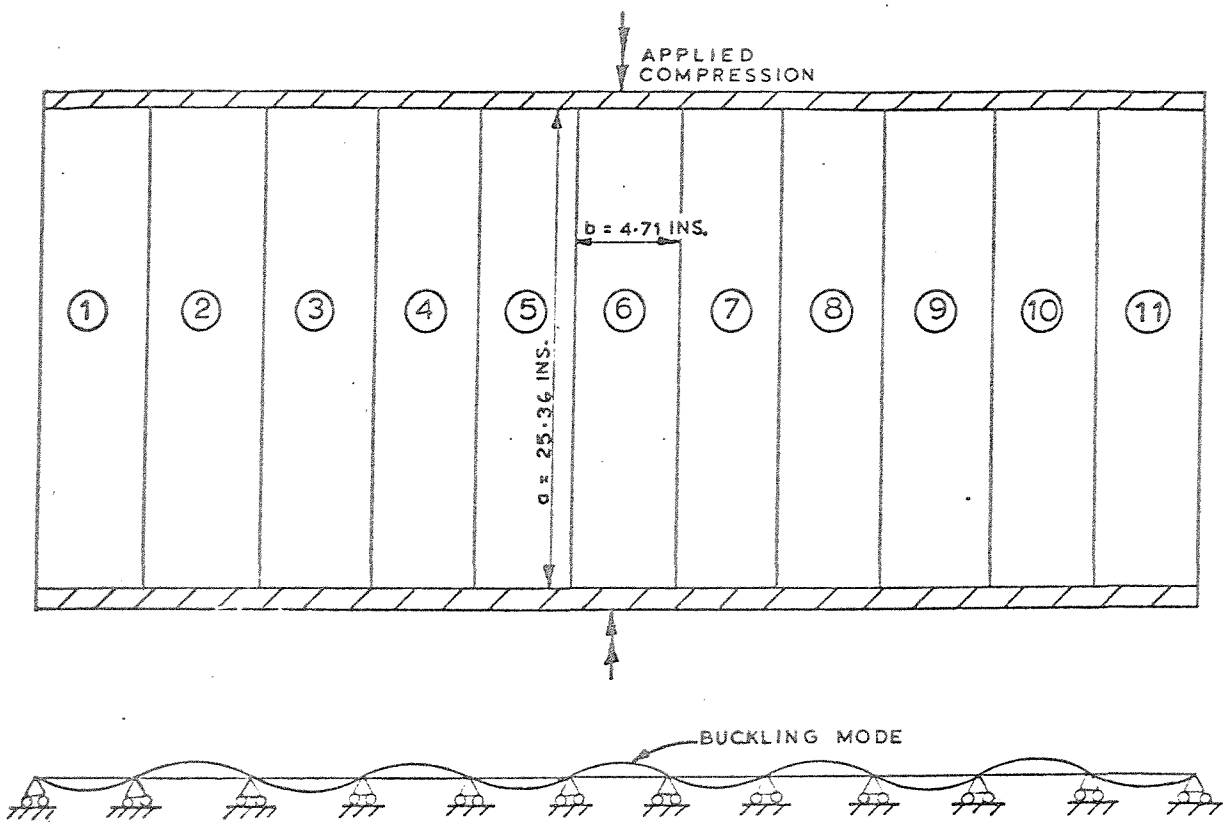

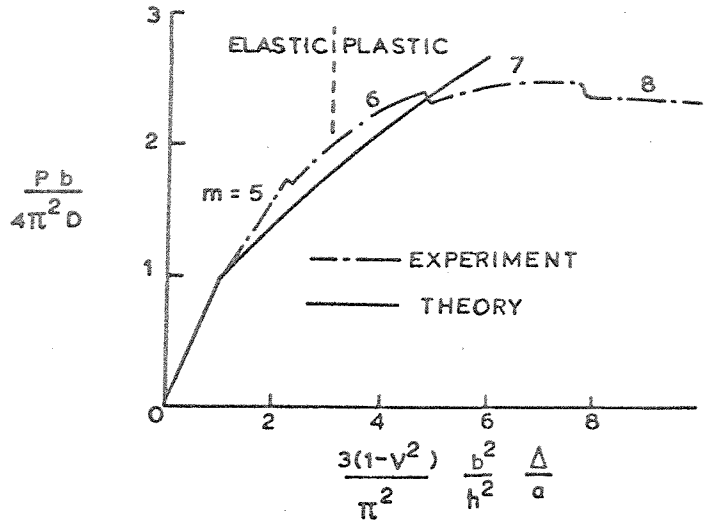

Fig.1.10 Stein's Test Set up and results.

that no change of wave form from the primary buckling mode will occur; on the other hand Stein's experimental study[21] on a plate which can be treated as having the above boundary conditions does show a change of wave form, the plate snapping from a mode with five half waves to another with six half waves, while it remains still elastic. (Ref. Fig. 1.10) Thus it would appear that Stein's experimental results can be explained only by the presence of initial imperfections (in the form of a sine wave with a half wave length equal to one sixth of the length of the plate). It may be noted that Stein's theoretical results, based on a hypothetical continuous change of wave form are a way off his experimental results.

In conclusion it may be stated that the results obtained by Supple are indeed of considerable interest, but his analysis is restricted to the case of simply supported plates on all the edges. In chapter 3 of this thesis, a method using finite strip technique for the problem is discussed.

1.2.3.2 Interaction of local and overall buckling

The local buckling of a plate assembly such as thin-walled columns results in a loss of stiffness of the structure, thus reducing the resistance of the structure to overall buckling; a coupled mode of buckling would set in if the length of the structure exceeds a certain critical value. The interaction of overall buckling, results in a further loss of stiffness often leading to a plastic failure of the material. The interaction of overall buckling and the consequent failure of the column can be hastened by the presence of 'overall' imperfections.

One of the early studies on the interactive buckling problem was by Graves-Smith[67]. He determined the resistance to overall buckling by

calculating the moment developed by the section by the application of a small bending strain to the column; from this it was possible to predict the load at which the overall buckling of the column would occur in the post-local-buckling equilibrium path of the structure. Thus in effect, the interaction problem is treated as a bifurcation problem. For a simple but representative model, van der Neut[68] takes the analysis a step further and determines in addition to the bifurcation load, the asymptotic postcritical behaviour of the column in the neighbourhood of the point of bifurcation. His results showed that for columns so proportioned that the local buckling stress is in the proximity of overall buckling stress, the bifurcation stress is substantially reduced in the presence of 'local imperfections' - a conclusion confirmed by Koiter[69]; and the equilibrium state at the bifurcation is unstable, indicating the sensitivity of the structure to overall imperfections. In a subsequent publication[70] van der Neut extended his analysis to take into account both the 'local' and 'overall' imperfections. Svensson and Croll[71] presented a more accurate solution of the van der Neut problem by treating the problem as one of large deflections; and they took into account plastic yielding of the material also for their prediction of ultimate load.

The interactive buckling problem for a stiffened panel was studied by Walker and his associates[72-74]. A simple mathematical model was proposed which though involving a number of assumptions did manifest the essential features of the problem. The experimental results showed good agreement with the theoretical predictions.

1.2.3.3 Effects of plastic yielding

The collapse of practical steel structures is subjected to axial compression, is almost always preceded by plastic yielding of the material.

Marguerre, Yamaki and Walker have taken the load at which the first yield occurs, as the ultimate load. But this is not an accurate definition of the ultimate load, for the structure can withstand higher loads by a redistribution of stresses. An elastoplastic analysis taking into account the geometric nonlinearities appears to be necessary in order to find the load at which the structure loses all its stiffness and starts shedding load. While the principles on which such an analysis may be based have been established for some time, it is still proving too expensive to obtain a complete solution to any but very simple cases.

Most of the work[78-82] on this problem is based on the von Mises yield criterion (or a modified version of the same) together with the use of Prandtl-Reuss equations which relate the increment of plastic strains to the corresponding deviatoric stress components. A variational approach is made use of to establish the equilibirum equations in an incremental form. Graves-Smith studied the problem of a thin-walled rectangular column[78] and corroborated his theoretical results by an extensive experimental investigation. Crisfield[79] used a finite element approach to study the problem of a rectangular plate and applied his results to predict the behaviour of a wide eccentrically stiffened plate subject to axial compression. This approach is being used currently to solve a variety of related problems[46,80-82] by, for instance Dowling and Bergan, to mention only two of the several investigators in the field.

The effort and expense involved in an elastoplastic large deflection analysis of plates and plate assemblies have given an impetus to a search for simpler ultimate load analysis of these structures using a rigid plastic mechanism approach[83-86], which has been very successful in the yield line analysis of reinforced concrete slabs. It is important to remember, however, that there is a basic difference in the analysis of

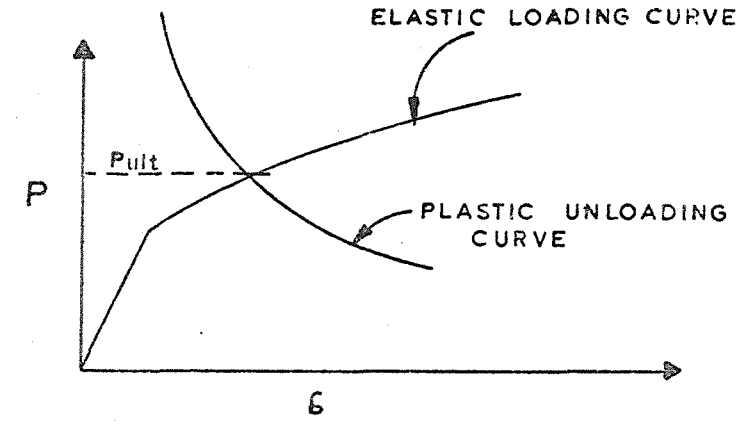

(a)

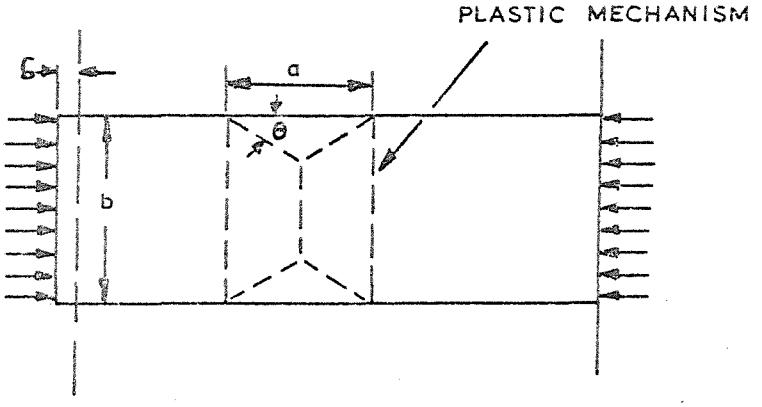

(b)

Fig.1.11 Ultimate Load Analysis of Plates by the Plastic Mechanism Approach.

plates under edge compression on the one hand and laterally loaded plates on the other. For a given shape and dimensions of a failure mechanism, the latter problem yields a certain ultimate load independent of the actual displacements the mechanism undergoes; whereas for a plate carrying edge compression, the applied load comes out as a function of the displacements the mechanism undergoes. Thus the analysis can yield only an "unloading curve" which relates the compressive load to the displacements of the structure; and there is a family of unloading curves depending upon the dimensions of the mechanism. According to the reasoning advanced in the previous studies on the strength of elements[87-88], the intersection of a plastic unloading curve with the elastic loading curve gives an estimate of the ultimate load. (Fig. 1.11) This procedure, though seemingly simple, is fraught with serious difficulties, some of which will now be discussed:

1. There seem to be no rational criteria for a proper choice of the shape and geometric parameters of the mechanism except perhaps experimental observation. Such an approach, though of interest for a specific problem, does not provide a general framework for the solution of a similar class of problems. On the other hand, one can generate a family of unloading curves varying the geometric parameters of the mechanism with the help of a computer, and the choice which gives the least load may be taken as the solution sought after - an assumption which need not have a basis on reality.

2. For the sake of simplicity, the mechanism is assumed to be made up of straight lines - an assumption which can not be justified by a proper elasto-plastic analysis.

3. Another unresolved question is regarding the parameter against which the load should be plotted in both the elastic loading and plastic unloading curves. Is it the end shortening, central deflection or any

other suitable parameter? The point of intersection of the curves and therefore the predicted collapse load depends upon the choice of the parameter.

Thus it would appear that the plastic mechanism approach, requires further development on a more rational basis before it can be applied extensively for the ultimate load analysis of plate structures.

1.2.3.4 'Crinkly buckling' of plate junctions

A striking feature of the behaviour of thin-walled structures is their mode of failure which is most frequently accompanied by the formation of kinks along one or more junctions of the plates. As soon as the structure loses its stiffness against axial compression, one or more of the junctions caves in; there occurs a dramatic change in the buckling mode, with a highly localised buckling mode making its appearance. Graves-Smith noted this type of failure[60,67,89] in his investigations of thin-walled columns and beams and called it the "crinkly buckling". (This nomenclature has been retained in the present thesis). It has also been mentioned by other investigators, notably Jombock and Clark[90] and Rawlings and Shapland[91]. It is important to note that the crinkly collapse of plate junctions can occur entirely elastically[92] as indicated by the preliminary experimental studies of the author. In the present investigation an attempt has been made to understand and explain the nature of this type of failure so frequently noticed in connection with plate structures.

The problems mentioned in the foregoing are some of the benchmarks in the frontiers of nonlinear behaviour of axially loaded plates and plate assemblies. These problems are difficult in the sense, a great deal of effort is required in the analysis, computation and experimentation in order to generate useful new information; and it is not surprising,

therefore, the progress in these directions has been rather slow.

1.2.4 Concluding remarks on the review of literature

The review presented herein, is indeed very brief considering the vast number of publications not cited in it, but it is believed that most, if not all, of the typical contributions have been touched upon. Attention, however, has been confined mainly to axially loaded plate structures as being the most relevant for the purposes of the present thesis.

1.3 Scope and Objectives of the present investigation

The foregoing review shows that while there is a wealth of literature available on the subject of postbuckling behaviour of single plates, not much has been published on the problem of plate assemblies; the possible computational advantage offered by the application of the finite strip method, so highly successful for initial buckling problems, has not been explored in the postbuckling analysis; and finally no attention has been given to the most frequent type of failure - the crinkly buckling of plate junctions - a phenomenon which can occur entirely elastically.

In the present work, therefore, analytical techniques based on the finite strip approach have been developed for the study of elastic post-local-buckling behaviour of plate assemblies upto a point when the crinkly collapse becomes imminent. In order to study the phenomenon of crinkly buckling, an experimental investigation on square box columns made up of Silocone rubber has been undertaken. Theoretical predictions of collapse loads are compared with experimental results. In order to gain an insight into the mechanics of snap through to the crinkly mode of deflection, a mechanical model of a column resting on discrete

nonlinear elastic supports has been investigated.

This chapter is concluded with an outline of the contents of the various chapters in the thesis. Chapter 2 is devoted to a discussion of the buckling problem. The novel feature of the analysis presented therein, is that the prebuckling stress distribution is generated as an integral part of the analysis and its effects fed into the buckling analysis. Such an approach provides a general scheme for the analysis of plate assemblies in which the axial loading causes transverse stresses in the constituent plates and those subjected to a combination of axial and lateral loading.

The finite strip method is further developed to deal with post-local-buckling problems of plate assemblies in chapter 3. Two versions of this method are described; one of them makes use of simpified boundary conditions as presented by Benthem, Graves-Smith and others and results in a particularly simple formulation, with the corresponding finite strip having only 10 degrees of freedom. As has already been pointed out, such an approach may not be sufficiently accurate, where the 'coupling' of inplane and out of plane quantities of constituent plates meeting along a common edge becomes significant. Such a coupling would become important in structures where the constituent plates meet at obtuse angles and in any case in advanced postbuckling behaviour when the displacement along the junction can no longer be neglected. In order to deal with these situations, a more general version of the finite strip method is developed and discussed in the same chapter. Examples presented deal with the convergence of solutions, effects of 'extra-buckling' harmonics in the solution, possible changes of wave form and problems involving coupled boundary conditions.

In chapter 4, the results of a study on the post-local-buckling

behaviour of channel section struts, plates with v-corrugation and stiffened panels are presented.

Chapter 5 deals with the problem of determination of elastic collapse loads for plate structures. It includes a parametric study on square box columns.

In part I of chapter 6, the details of the experimental investigation are presented. Part II is devoted to a discussion of the results and includes the description of a mechanical model to explain the phenomenon of crinkly collapse.

The thesis is concluded with a summary of findings and a discussion of scope for extension of the work begun in the present investigation.

CHAPTER 2

INITIAL BUCKLING ANALYSIS

2.1 Introduction

The determination of buckling stresses and modes of plate structures is an essential preliminary for a study of their postbuckling behaviour and forms, therefore, the subject matter of this chapter. The plate structures considered in the present investigation are assumed to consist of a set of thin rectangular plates, each of which is connected one or more of the others along one or both of its longitudinal edges. The most powerful technique for the initial buckling analysis of such structures is the finite strip method which retains most of the versatility of the finite element approach and in comparison, is extremely efficient in computation. In this chapter, the method is developed further to deal with the initial buckling problems in which the prebuckling stress distribution must be taken into account and buckling phenomenon treated as bifurcation from a "nontrivial" equilibrium path. Such a problem can arise even in the context of a plate assembly acted upon by only axial compressive forces at its ends, as will be shown later in the chapter.

2.1.1 Finite strip technique: Earlier studies

In buckling and postbuckling problems of plates and plate assemblies, the deflection mode can often be characterised by one or at worst, a small number of harmonics; and the facility with which the buckling mode can be described is fully exploited by the finite strip method. This is achieved by a modification of the finite element procedure by

(i) the use of rectangular strip elements spanning from end to end, and

(ii) the choice of the displacement functions which take the form of a continuously differentiable smooth series in the longitudinal direction satisfying the boundary conditions and polynomial functions in the transverse direction. Several applications of the method for a variety of structural problems have been discussed by Cheung[12]. The method was applied to initial buckling analysis of plate assemblies by Turvey[11].

A comparison of the computing effort involved in the finite element method using triangular elements and the finite strip method has been made by Yoshida[93], who found that the latter took only about 1 to 1.5% of the computing time required by the former for obtaining the buckling stress of a stiffened panel.

In the foregoing studies, the prebuckling stress distribution was assumed to be uniform in the longitudinal direction, and either uniform or uniformly varying in the transverse direction, so that it could always be described by simple expressions. In many practical situations, however, prebuckling stress distribution can not be known a priori or described simply e.g. a plate carrying inplane patch loading. This problem has been tackled among others by Khan[95] and Walker[94] using an energy method for relatively simple boundary conditions and also by Rockey and Bagchi[14] by the finite element method. A procedure to take into account the prebuckling stress distribution in the finite strip approach has been outlined by Benson and Hinton[96]. This has a few serious limitations, the most important of which are mentioned in the following:

(i) It was proposed that shear stresses may be neglected in the description of prebuckling stresses, presumably in the hope

of uncoupling the harmonics in the buckling analysis.

and (ii) The buckling mode was assumed to be made up of a single harmonic. In many problems where the influence of prebuckling stresses is significant, as for instance in the patch loaded plates, the buckling mode is a localised one and the description of the buckling mode by a single harmonic can often be very inadequate.

2.1.2 The present approach

The analysis outlined in this chapter may be considered as an advance in the finite strip approach to the buckling analysis of plate assemblies in that the prebuckling stresses are taken into account fully as an integral part of the procedure and the buckling mode is represented by a superposition of a number of harmonics, which can be chosen judiciously for the problem in hand. In these respects, the present analysis will be found to have much in common with the stability analysis of cylindrical shells under lateral pressures by Prabhu et al[109]. The formulation of the problem is quite comprehensive in that it takes into account combination of axial and lateral forces acting on the structure and pick up buckling modes which may be 'local', 'overall' or 'coupled'.

As stated earlier there are cases of plate assemblies subjected only to axial compression which would develop prebuckling stresses in the transverse direction of such magnitudes as to reduce significantly the buckling stress of the structure. This can be the result of

(i) some of the constituent plates carrying inplane constraints

and (ii) the 'indeterminacy' of the configuration.

These will be discussed further in the next paragraph.

The assumption of uniaxial compression, often the basis of buckling analyses of plate assemblies implies that the plates are free to expand in the transverse direction with a strain of $\nu\sigma/E$, where 'σ' is applied axial stress. This is generally valid owing to the small bending rigid-

ities of the constituent plates. The presence of inplane lateral constraints in one or more of the plates, (Fig. 1.1(a)) however, would prevent partly or fully the lateral expansion of plates and as a consequence there would develop transverse compressive stresses which are not negligible. The lateral expansion of the constituent plates can also be inhibited by the very nature of the configuration of the plates in the structure. (Fig.1.1(b))This can, however, happen only when the plates are subjected to a nonuniform applied stress distribution at the ends or when they are composed of materials with differing values of Poisson's ratio. This aspect will be discussed later in the chapter.

From the foregoing discussion, it is clear that an analysis of prebuckling stress distribution is important not only for structures carrying lateral loads but also for axially loaded plate structures in certain special cases. In the next section, the analytical technique employed is discussed at some length. Most of the ideas presented therein will be useful when the approach is extended for the postbuckling analysis in the next chapter. The chapter is concluded with a discussion on the results of a small number of worked examples.

2.2 Theory

We now outline the various steps involved in the analysis.

The first step is to choose a set of functions for the displacements u, v and w at the middle surface of the strip satisfying the boundary conditions at the ends of the strip. A Lagrangian description[16] which refers the displacements to a fixed coordinate system, is used in the analysis. The next step, is to express the potential energy of the

system in terms of displacements, with the aid of strain displacement relations. The principle of stationary potential energy is then invoked to generate the algebraic equations of equilibrium for the problem. The perturbation technique[13,97,98] is then employed to obtain the pre-buckling equilibrium path and "the sliding incremental displacement" technique is used to detect the bifurcation thereof. Each of these aspects will be discussed in some detail in the following paragraphs.

2.2.1 Displacement functions

A typical strip with dimensions (a,b,h) is shown in Fig. 2.1 with the positive directions of the middle surface displacements u, v and w.

As stated the displacement functions chosen must satisfy the boundary conditions at the ends of the plate which may be stated in the form

$$w = 0$$

$$\frac{\partial^2 w}{\partial x^2} = 0$$

$$v = 0$$

$$\frac{\partial u}{\partial x} = f(y) \qquad \ldots \text{ 2.1(a-d)}$$

conditions 2.1(a) and (b) mean that the plates are simply supported at their ends; 2.1(a) and (c) together represent a situation where the end cross-sections of the plate assembly remain undistorted. The last condition 2.1(d) implies that the plate assembly carries a longitudinal stress proportional to f(y) across the plate (provided the displacements remain small). Since most of the discussion in the present work will refer to plate assemblies carrying uniform stress, f(y) must be chosen as a constant. It must also be noted that the condition of uniform stress for columns is a very close approximation, in the prebuckling

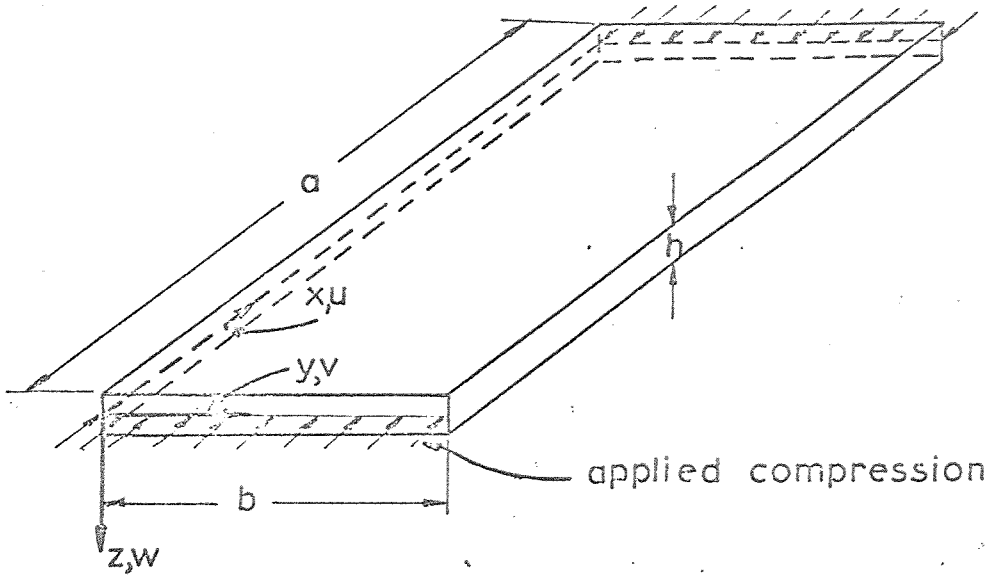

Fig. 2.1 Coordinate axes and Dimensions of a Strip.

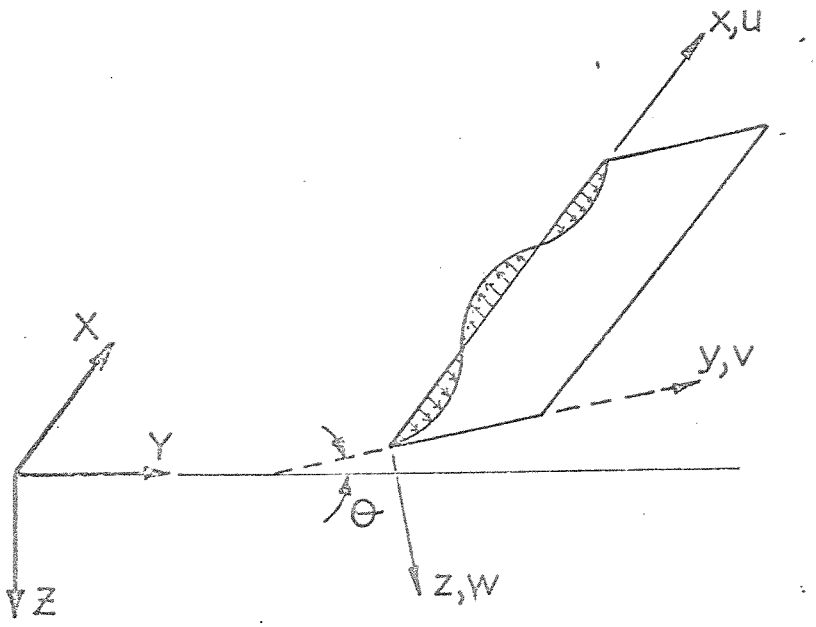

Fig. 2.2 Local and Global Coordinate Systems.

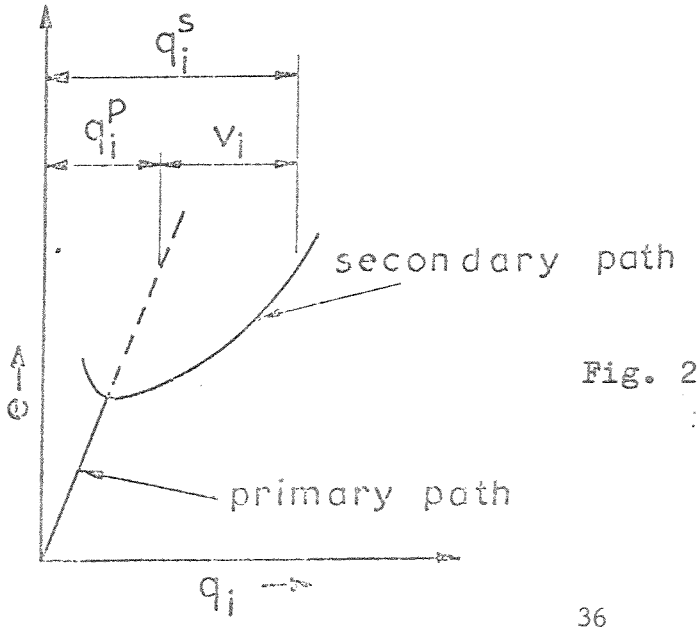

Fig. 2.3 Primary (Prebuckling) and Secondary (Postbuckling) Equilibrium Paths.

state to the more physically realistic situation of constant end displacement across the entire plate assembly.

It is however possible to stipulate the condition of constant end displacement, and this indeed is the basis of the post-local-buckling analysis presented in the next chapter. But the present approach based on the prescription of stress rather than of displacement offers some computational advantages over the latter formulation especially for the initial buckling analysis and these will be pointed out later in this section.

In further discussion it will be convenient to work in terms of dimensionless quantities in order to make possible one treatment for all strips. The following dimensionless variables are therefore introduced:

$$\xi = x/a \quad , \quad \eta = y/b$$

$$\bar{u} = u/h \quad , \quad \bar{v} = v/h \quad , \quad \bar{w} = w/h \quad , \quad \theta = \frac{\partial \bar{w}}{\partial \eta}$$

In this notation the displacement functions satisfying the boundary conditions 3.1(a-d) take the form:

$$\bar{u} = f_{1m} \cos m\pi\xi + e\alpha(\tfrac{1}{2} - \xi)$$

$$\bar{v} = f_{2m} \sin m\pi\xi$$

$$\bar{w} = f_{3m} \sin m\pi\xi$$

$$(m = 1,2 \ldots N) \qquad \ldots 2.2(a\text{-}c)$$

where

$$f_{1m} = (1-\eta)u_{1m} + \eta\, u_{2m}$$

$$f_{2m} = (1-\eta)v_{1m} + \eta\, v_{2m}$$

$$f_{3m} = (1-3\eta^2 + 2\eta^3)w_{1m} + (\eta-2\eta^2+\eta^3)\theta_{1m}$$
$$+ (3\eta^2-2\eta^3)w_{2m} + (-\eta^2+\eta^3)\theta_{2m} \qquad \ldots 2.3(a\text{-}c)$$

u_{1m}, v_{1m}, w_{1m}, θ_{1m} and u_{2m}, v_{2m}, w_{2m}, θ_{2m} are the coefficients of trigonometric terms in the expressions of displacements and rotation along the edges $\eta = 0$ and $\eta = 1$ respectively. For example if $\bar{w}_1$ is the dimensionless normal displacement along the edge $\eta = 0$, then

$$\bar{w}_1 = w_{1m} \sin m\pi\xi$$

The expressions f_{1m}, f_{2m} and f_{3m} which describe the variation of displacements u, v and w across the strip contain just the sufficient number of degrees of freedom to ensure compatibility of deformation between adjacent strips along the common edge. These expressions have been successfully used in the analysis of folded plates[99] and vibration and stability problems[12] of plate assemblies.

The expression for the longitudinal displacement consists of two parts, the second part giving a state of uniform strain 'e' in the longitudinal direction; since the strain in the transverse direction vanishes at the ends by 2.2(b), the applied longitudinal stress works out to $Ee/(1-\nu^2)$ for the plate strip.

2.2.2 Strain Displacement Relations

The middle surface strains ε_x, ε_y and γ_{xy} are related to u, v and w as follows[16]:

$$\varepsilon_x = \frac{\partial u}{\partial x} + \frac{1}{2}\left\{\left(\frac{\partial u}{\partial x}\right)^2 + \left(\frac{\partial v}{\partial x}\right)^2 + \left(\frac{\partial w}{\partial x}\right)^2\right\}$$

$$\varepsilon_y = \frac{\partial v}{\partial y} + \frac{1}{2}\left\{\left(\frac{\partial u}{\partial y}\right)^2 + \left(\frac{\partial v}{\partial y}\right)^2 + \left(\frac{\partial w}{\partial y}\right)^2\right\}$$

$$\gamma_{xy} = \frac{\partial u}{\partial y} + \frac{\partial v}{\partial x} + \frac{\partial u}{\partial x}\cdot\frac{\partial u}{\partial y} + \frac{\partial v}{\partial x}\cdot\frac{\partial v}{\partial y} + \frac{\partial w}{\partial x}\cdot\frac{\partial w}{\partial y}$$

. . . 2.4(a-c)

It is essential to take the strain displacement relations in their nonlinear form, in order to obtain the destabilising effects of inplane stresses in the buckling problem. The nonlinear terms in 'w' are essential in the formulation whether the buckling mode is "local" or "overall", while those in 'v' are important in the context of overall buckling modes only. But the nonlinear terms in 'u' appear to have no significance in the present problem and have been neglected.

2.2.3 Potential Energy Expression

The potential energy of the plate strip (W) is the sum of the elastic strain energy stored in the strip (U) and the potential energy of the applied compressive force (V).

The strain energy in the strip is the sum of the energy of inplane deformation (U_p) and the energy of bending (U_b). The former can be expressed in terms of middle surface strains and the latter in terms of normal displacement 'w' as follows[1]:

$$U_p = \frac{Eh}{2(1-\nu^2)} \int_0^a \int_0^b \{\varepsilon_x^2 + \varepsilon_y^2 + 2\nu\varepsilon_x\varepsilon_y + \tfrac{1}{2}(1-\nu)\gamma_{xy}^2\}dxdy$$

$$U_b = \frac{Eh^3}{24(1-\nu^2)} \int_0^a \int_0^b \left\{(\nabla^2 w)^2 - 2(1-\nu)\left[\frac{\partial^2 w}{\partial x^2}\cdot\frac{\partial^2 w}{\partial y^2} - \left(\frac{\partial^2 w}{\partial x \partial y}\right)^2\right]\right\} dxdy$$

. . . 2.5(a-b)

The loss of potential of the applied compressive forces at both ends is given by

$$\sigma h \int_0^b \left[(u)_{x=a} - (u)_{x=o}\right]dy \qquad \ldots 2.6$$

where σ stands for the applied compression $Ee/(1-\nu^2)$.

Using the strain displacement relations (2.4) and displacement functions (2.2), the total potential energy of the strip (W) can now be

expressed in terms of u_{im}, v_{im} ... etc. in the form given in Appendix II. For convenience in further discussion this expression is written in the form:

$$W = -\nu\, eA_i q_i + \frac{1}{2!}\{A_{ij} - e(B_{ij} + \nu\, C_{ij})\}q_i q_j$$

$$+ \frac{1}{3!} A_{ijk}\, q_i q_j q_k + \frac{1}{4!} A_{ijk\ell}\, q_i q_j q_k q_\ell$$

$$i,j,k,\ell = 1, \ldots N$$

. . . 2.7

where q_i stands for a typical local degree of freedom of the strip i.e. one of the set u_{im}, u_{2m} . .. θ_{2m} ; 'N' is the total number of local degrees of freedom, equal to 8n where 'n' stands for the number of harmonics considered in the solution; and A_i, A_{ij}, B_{ij}, C_{ij}, A_{ijk} and $A_{ijk\ell}$ are coefficients which have the dimensions of FL (Force × length). The coefficients A_{ij}, A_{ijk} etc. are symmetric with respect to each of their subscripts.

The significance of each of these terms will become clear as the analysis proceeds, but a few preliminary remarks are probably necessary; especially so as it is felt necessary to place the expression 2.7 in the context of previous studies of Cheung and Turvey.

1. Firstly, the quartic terms in the expression 2.7 do not play any part in the analysis, as will be shown in further discussion, if as in the present analysis, the prebuckling path is assumed to be linear.

2. The presence of the linear term in the expression, even in the absence of loads prescribed along the junctions ensures that, in general, the prebuckling equilibrium path of a plate assembly is nontrivial i.e. there occur nonzero displacements (apart from the uniform axial com-

pression due to the applied loads at the ends) in the prebuckling stage. These displacements are the result of each plate tending to expand in the transverse direction due to Poisson's effect.

3. If the constituent plates are fully restrained against inplane movement in the transverse direction, all the prebuckling displacements will vanish by virtue of boundary conditions and the plates will carry stresses σ and $\nu\sigma$ in the longitudinal and transverse directions respectively. The destabilising effects of the transverse stresses are given by the underlined quadratic term of 2.7. In this case the cubic terms will be seen to play no part in the buckling analysis.

4. If on the other hand, the constituent plates are not all fully restrained against inplane movement, they will tend to expand in the transverse direction and the prebuckling stress distribution in 3. will be modified by the nonzero transverse displacements. In this case, the cubic terms will be seen to play a significant role in the analysis as they counteract the effect of underlined quadratic term which corresponds to the destabilising effect of a stress $\nu\sigma$ in the transverse direction.

5. In the absence of end compression and in the presence of loads prescribed along the edges of the plate strips, all terms associated with 'e' will vanish; but the prebuckling stress distribution will be nontrivial and the remaining quadratic and cubic terms determine the buckling load.

6. The energy expression corresponding to the finite strip approach for the longitudinally compressed plate assemblies developed by Turvey[11] and Cheung[12], can be derived in a similar manner with the displacement functions 2.2 modified as follows:

$$\bar{u} = f_{1m} \cos m\pi\xi + e\alpha(\tfrac{1}{2} - \xi)$$

$$\bar{v} = f_{2m} \sin m\pi\xi + \nu e\beta\eta + C$$

$$\bar{w} = f_{3m} \sin m\pi\xi$$

. . . 2.8(a-c)

In the foregoing, 'C' is an arbitrary constant whose value is immaterial in the determination of buckling load. These displacement functions give rise to the energy function in the form

$$W = \frac{1}{2!}\left[A_{ij} - e(1-\nu^2)B_{ij}\right]q_i q_j + \text{Higher order terms} \quad . \; . \; . \quad 2.9(a\text{-}c)$$

Note that in this function, the linear terms do not appear, and thus all the prebuckling displacements (u_{im} ... θ_{im}) vanish, so that the prebuckling state of stress is one of uniaxial compression and buckling occurs as bifurcation from a "trivial" equilibrium path. In this case the cubic terms do not play any part in the determination of buckling load.

2.2.4 Generation of prebuckling equilibrium path

In this section the steps involved in obtaining the solution for the prebuckling equilibrium path are described briefly. In the analysis that follows in this and next section, we make use of the perturbation technique, the treatment and notation closely following the discussion by Croll and Walker[13].

Differentiating the expression 2.7 for the total potential energy with respect to a certain local degree of freedom q_i, we obtain

$$E_i = \frac{\partial W}{\partial q_i} = - \nu e\, A_i + \{A_{ij} - e(B_{ij} + \nu\, C_{ij})\}\, q_j$$

$$+ \frac{1}{2!} A_{ijk}\, q_j q_k + \frac{1}{3!} A_{ijk\ell}\, q_j q_k q_\ell \qquad \ldots 2.10$$

$$(j,k,\ell = 1, \ldots N)$$

$$i = 1, \ldots N$$

In physical terms, E_i stands for a force component (or a couple) in the direction of q_i at an edge of the strip, as can be demonstrated using the principle of virtual work. Expression 2.10 is nonlinear and can be used to generate a nonlinear solution to the prebuckling path. However, in many problems of plate assemblies the prebuckling displacements are small in comparison to the thickness of plates, so that it may be justified to treat the prebuckling equilibrium path as linear.

We therefore employ a perturbation technique to generate a linearised version of the expression for edge forces given by 2.10 .

Differentiating E_i in 2.10 with respect to a certain path parameter 'ε',

$$\frac{\partial E_i}{\partial \varepsilon} = - \nu e_1 A_i + \{A_{ij} - e(B_{ij} + \nu\, C_{ij})\} q_{j1}$$

$$+ \{ \quad - e_1 (B_{ij} + \nu\, C_{ij})\} q_j + A_{ijk}\, q_j q_{k1}$$

$$+ \frac{1}{2!} A_{ijk\ell}\, q_j q_k q_{\ell 1}$$

$$(j,k,\ell = 1, \ldots N)$$

$$i = 1, \ldots N$$

where $q_{j1} = \frac{\partial q_j}{\partial \varepsilon}$ and $e_1 = \frac{\partial e}{\partial \varepsilon}$.

Now identifying the path parameter 'ε' with 'e', we obtain $e_1 = 1$.

Applying the above equations to the unloaded state i.e. at e = 0, $q_i = 0$ (i = 1, ... N)

$$\left.\frac{\partial E_i}{\partial \varepsilon}\right|_{q_i=o} = A_{ij}\, q_{j_1} - \nu\, A_i \qquad \text{. . . 2.11}$$

(i = 1, ... N)

Since the prebuckling path is approximated as linear the higher order derivatives E_i with respect to the path parameter are deemed to vanish.

In the above equation q_{j_1} is the increment in the magnitude of the local degree of freedom v_j for a unit increment in 'e' from the unloaded state.

The coefficient matrix A_{ij} is the element stiffness matrix for the linear problem; and A_i plays the part of the vector of applied loads in the local coordinate system.

Equilibrium equations for each edge can now be generated by

(a) resolving each of the edge forces in the directions of global coordinate axes for all the strips meeting at the edge, as indicated in Fig. 2.2.

(b) expressing the local degrees of freedom in terms of global degrees of freedom

and (c) summing up all the resolved components of the edge forces in the direction of each global coordinate axis and equating them to the externally applied forces prescribed along the edge, corresponding to unit value of 'e'. The surface loads on the structure are assumed to bear a given ratio to the edge compressive force at any stage in this discussion.

A set of equilibrium equations for the plate assembly can thus be

generated by going through the above steps for all the edges of strips.

The first two steps are achieved with the aid of transformation matrices and the last one by a systematic assembly of the transformed element stiffness matrices to form the global stiffness matrix. The details of such a procedure are set forth in standard treatises on the finite element method and therefore will not be discussed any further.

Solution of these equations yields the global displacement parameters for unit increment in 'e', from which the local displacement parameters for each strip can be computed. The primary equilibrium path is now defined by $q_i^p = eq_{i_1}$ (i = 1, ... N) in each of the strips for any given 'e'.

2.2.4.1 Merits of the displacement functions used.

Due to the orthogonality of the trigonometric functions describing the displacements (2.2), the unknowns corresponding to each harmonic are uncoupled from those corresponding to other harmonics, in the system of equations generated from 2.9. Therefore it is possible for the degrees of freedom corresponding to any given harmonic to be solved separately. This is an advantage associated with the displacement functions which prescribe the end stresses over those specifying end displacements for simply supported plate assemblies. In comparison with a formulation based on prescription of uniform end displacement, the present formulation has another advantage for the case of simply supported plate assemblies carrying axial compression. It is the ease with which the overall buckling mode can be described in the present case by a single harmonic. This is illustrated in Fig. 2.4 with the example of a stiffened plate. A disadvantage associated with these functions, however, is that they are unsuitable for use in a

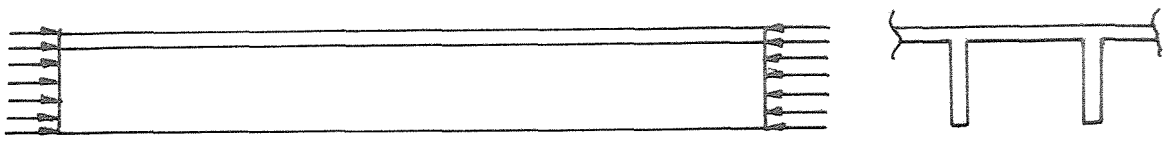

(a) Side View (b) Section

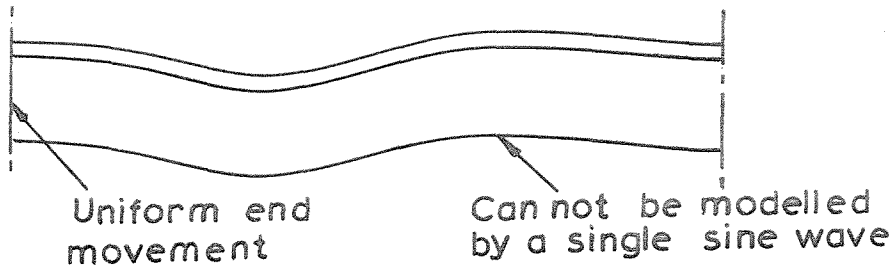

(c) The case of Uniform End Compression.

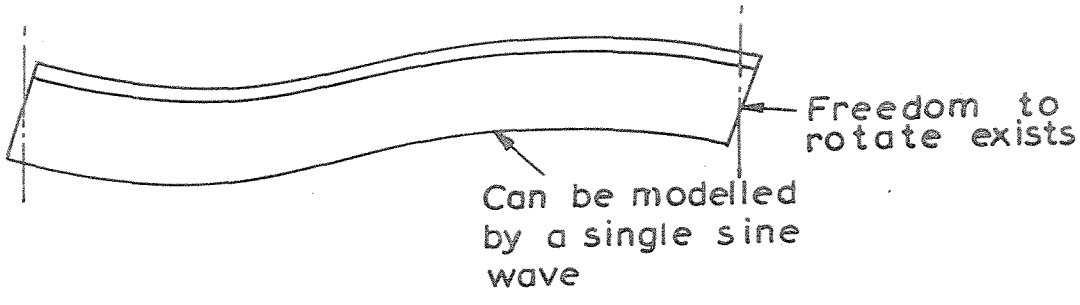

(d) The case of Uniform End Stress.

Fig. 2.4 Overall Buckling Mode of a Stiffened Plate.

postbuckling analysis, as in that case they can model neither the condition of prescribed end stress or end displacement.

2.2.5 Bifurcation from the primary path

In this section, the technique of finding the bifurcation point at which the primary path loses its stability and buckling occurs, is outlined.

In further discussion the displacements along the primary path are denoted by q_i^p ($i = 1, \ldots N$) and the incremental displacement to the secondary path branching off from the primary path are denoted by v_i so that the displacements on the secondary path q_i^s for the same 'e' are given by

$$q_i^s = q_i^p + v_i \qquad (i = 1,2, \ldots N) \qquad \ldots 2.12$$

as shown in Fig. 2.3.

Substituting 2.12 in 2.10 to obtain the set of edge forces, we have

$$E_i^s = - \nu e A_i + \{A_{ij} - e(B_{ij} + \nu C_{ij})\}\{q_j^p + v_j\} + \frac{1}{2!} A_{ijk}(q_j^p + v_j)(q_k^p + v_k) + \frac{1}{3!} A_{ijk\ell}(q_j^p + v_j)(q_k^p + v_k)(q_\ell^p + v_\ell)$$

$$(j,k,\ell = 1, \ldots N)$$

$$i = 1, \ldots N \qquad \ldots 2.13$$

where the superscript 's' denotes that the edge force corresponds to the secondary path. Invoking a similar expression for the primary path and subtracting the same from 2.13, and substituting eq_{i_1} for q_i^p, we obtain

$$E_i^s - E_i^p = \{A_{ij} - e[B_{ij} + \nu C_{ij} - A_{ijk} q_{k_1}] + \underline{\frac{e^2}{2!} A_{ijk\ell}\, q_{k_1} q_{\ell_1}}\}\, v_j$$

$$+ \frac{1}{2!} A_{ijk}\, v_j v_k + \frac{1}{3!} A_{ijk\ell}\, v_j v_k v_\ell$$

$$(j,k, = 1, \ldots N)$$

$$i = 1, \ldots N. \qquad \ldots 2.14$$

In physical terms this represents the "sliding" increment in the edge force corresponding to q_i as the structure moves from the primary to the secondary equilibrium path; and expression 2.14 is the genesis of nonlinear equations of equilibrium for the secondary path in terms of incremental displacements v_i. But here we shall be concerned only with obtaining the bifurcation point and the buckling mode.

In view of our assumption of smallness of prebuckling displacements, we may neglect the underlined term in 2.14 which is nonlinear in the prebuckling displacements, in comparison to the rest and write

$$E_i^s - E_i^p = [A_{ij} - e(B_{ij} + \nu C_{ij} - A_{ijk}\, q_{k_1})]\, v_j$$

$$+ \frac{1}{2!} A_{ijk}\, v_j v_k + \frac{1}{3!} A_{ijk\ell}\, v_j v_k v_\ell \qquad \ldots 2.15$$

Employing the perturbation technique at the bifurcation point, i.e. with $v_i = 0$, the first order perturbation equation takes the form

$$\frac{\partial}{\partial \varepsilon} \{E_i^s - E_i^p\}\Big|_{v_i=o} = \{A_{ij} - e[B_{ij} + \nu C_{ij} - A_{ijk} q_{k_1}]\} v_{j_1}$$

$$(j,k = 1, \ldots N)$$

$$i = 1, \ldots N. \qquad \ldots 2.16$$

Higher order perturbation equations can similarly be written down, but for the purpose of obtaining the buckling load they are of no interest. Note at this stage the quartic terms in the energy expression 2.7 have vanished, thus proving our earlier statement that they play no part in the determination of buckling load.

A set of equilibrium equations can now be generated for the first order perturbation of incremental edge force and they take the form

$$\{[A] - e[B]\}\ \{\theta\} = \{0\}$$

where $\{\theta\}$ represents the vector of global degrees of freedom corresponding to the incremental (or buckling) displacements of the structure. The eigenvalues and vectors for the case where both $[A]$ and $[B]$ are symmetric, can be determined by employing a standard procedure [100]. The lowest eigenvalue e_{cr} and the corresponding eigenvector give the buckling load and mode respectively.

The foregoing analytical treatment has been phrased in general terms and allows for coupling of all harmonics in the buckling mode. This has been done with a view to simplifying the presentation and highlighting the more important aspects of the theory. In actual computation, it is possible to specify the number of harmonics required in the description of the prebuckling state differently from those depicting the buckling mode. For example, for the axially loaded plate assemblies, where normal stresses play a predominant role, it is sufficient to describe the buckling mode by just one harmonic whereas for plates carrying inplane lateral loading more than one harmonic may be required as the buckling mode is, in general, localised in character.

2.2.6 Computer Programme

Based on the formulation described in sec. 2.2.5, a computer

programme in Fortran has been developed. The programme can handle combinations of axial and lateral loads. The number of harmonics describing the prebuckling state can be specified differently from those entering into the buckling mode. The details of the programme are described in Appendix III.

2.3 Worked examples and discussion of results

A few worked examples are now presented to illustrate the application of the theory to specific problems of plate structures. Two sets of examples are considered, one involving end compression and the other inplane patch loading.

2.3.1 Plate assemblies under uniform end compression

These examples are presented with a view to illustrate the influence of prebuckling stresses induced due to Poisson's effect on the buckling load of plate assemblies.

It is proposed to present the results in the form of plots of nondimensional buckling stress σ_{cr}/E against the half wave length λ of buckling. The boundary conditions at the ends of the plate assembly have a local influence on the distribution of transverse stresses in the prebuckling stage and this, in turn, can have an influence, albeit small, on the buckling load for the plate assembly if it is short. In order to suppress this effect the length 'a' was set equal to 3λ in all the calculations.

2.3.1.1 Stiffened plate

The first example presented is that of an 'infinitely' wide plate reinforced with stiffeners at equal intervals shown in Fig. 2.5. The following two cases are considered:

Case (i) The exterior edges of the end panels are free to move in the plane of the plate (Fig. 2.5(a))

Case (ii) They are fully restrained against movement in the plane of the plate. (Fig. 2.5(b))

Since the plate is infinitely wide, it is sufficient to consider the action of a typical panel ABC in Fig. 2.5(c). In both cases (i) and (ii) the edge 'A' of the panel ABC can be assumed as restrained against rotation while for (ii) it is also restrained against inplane movement in the direction AA.

With a view to study the convergence of the solution, case (i) is solved with an increasing number of degrees of freedom, each part AB and BC, subdivided into two, three and four strips and with an increasing number of harmonics to describe the prebuckling displacements. Some typical results are shown in Table 2.1. From a study of this table, it may be concluded that

(i) it is sufficient to subdivide each plate into three strips in order to be assured of convergence within an error of 0.1% and

(ii) the number of harmonics required to describe the prebuckling state (m) to achieve the required accuracy tends to increase with the ratio of wavelengths of buckling in the longitudinal to that in the transverse direction.

In view of the above observations all the examples of axially loaded plate structures discussed in this section have been solved with each of the plates divided into three strips, the value of 'm' incremented till the buckling stresses did not differ by 0.1% in two successive calculations.

The variation of buckling stress with the wavelength for both cases

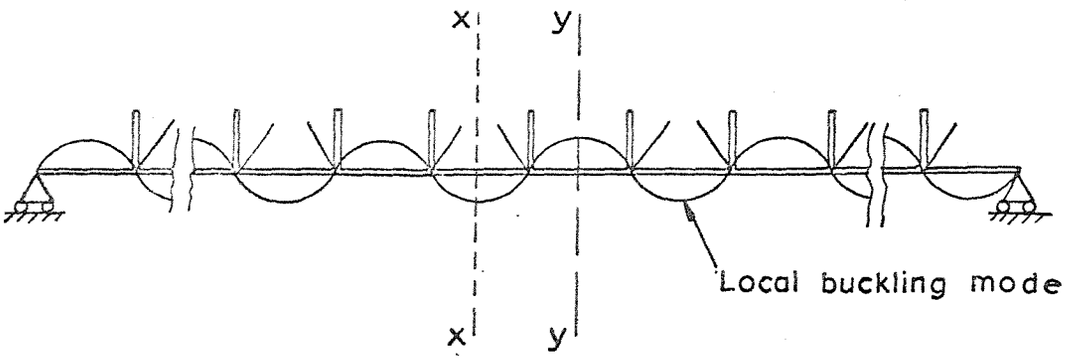

(a)

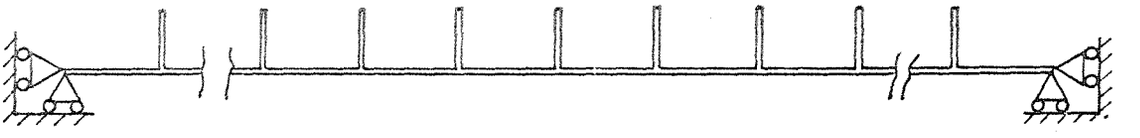

(b)

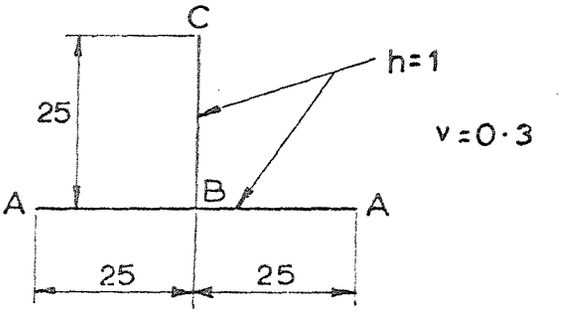

(c)

Fig. 2.5 Details of the example of a panel of an Infinitely wide Stiffened Plate.

Table 2.1

	Number of strips in each plate	Number of harmonics (m = 1,3,...M)	$\frac{\sigma_{cr}}{E} \times 10^3$	
1	2	4	1.34553	
2	3	4	1.34504	λ = 40
3	3	8	1.34319	
4	4	8	1.34310	
5	2	4	1.25295	
6	3	4	1.25315	λ = 80
7	3	8	1.24216	
8	4	8	1.24221	
9	2	4	1.73412	
10	3	4	1.73456	λ = 120
11	3	8	1.69421	
12	4	8	1.69427	

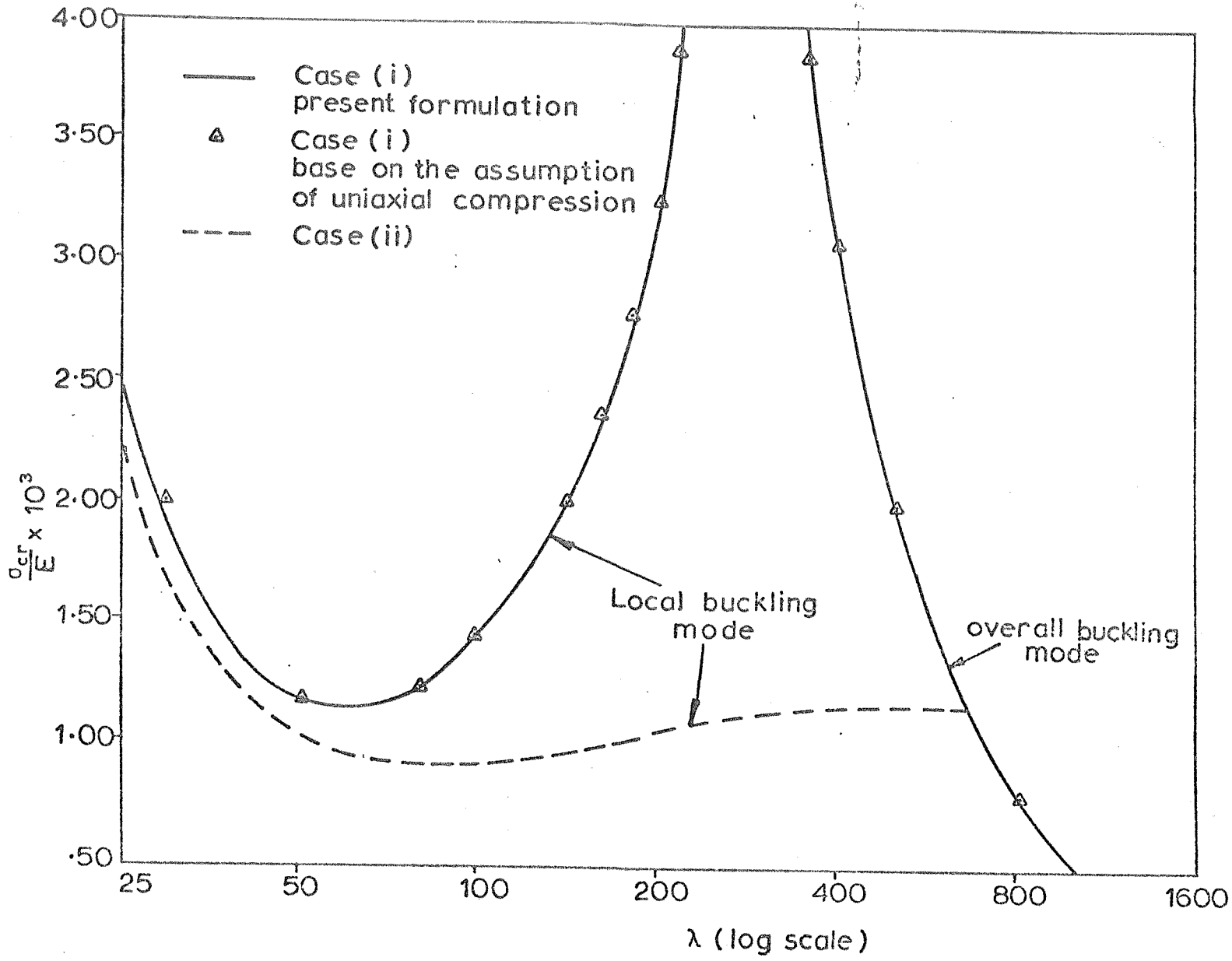

Fig. 2.6 Critical Stress plotted against Half Wave Length of Buckling of the Stiffened Plate in Fig.2.5

(Fig. 2.5(a-b)) of the stiffened plate is shown in Fig. 2.6. A study of these characteristics shows several interesting features which shall now be discussed.

First of all, we note that for the case (i), the results obtained using the present formulation are in very close agreement with the results obtained making an assumption of uniform uniaxial compression in each of the plates in the prebuckling stage. This is as it should be for the platers are fully free to expand in the transverse direction.

The effects of inplane constraints are illustrated by comparison of the curves (i) and (ii). A significant reduction in the local buckling stress occurs when the plate is restrained in the transverse direction. The minimum nondimensional local buckling stress for the case (i) is 1.15×10^{-3} while for the case (ii) is 0.92×10^{-3}. Thus there occurs a reduction of about 20% due to the presence of lateral constraints. Further the wavelengths for which the minimum local buckling stress occurs are also significantly different. Note that as the half wave length of buckling (λ) increases, the difference in the buckling stresses widens at an increasing rate. For the case (ii), the buckling stress remains sensibly constant over a wide range of values of λ. This indicates that the buckling modes for such a panel are nearly coincident and therefore the postbuckling behaviour will generally be characterised by changes of wave form.

In general, the effect of transverse stresses on the buckling load is governed by the ratio of the half wave length of buckling in the longitudinal direction to that in the transverse. The greater this ratio, the more pronounced the effect. For the overall buckling mode, however, this ratio is zero, as the wave length in the transverse direction is infinity. It is not surprising, therefore, that the overall

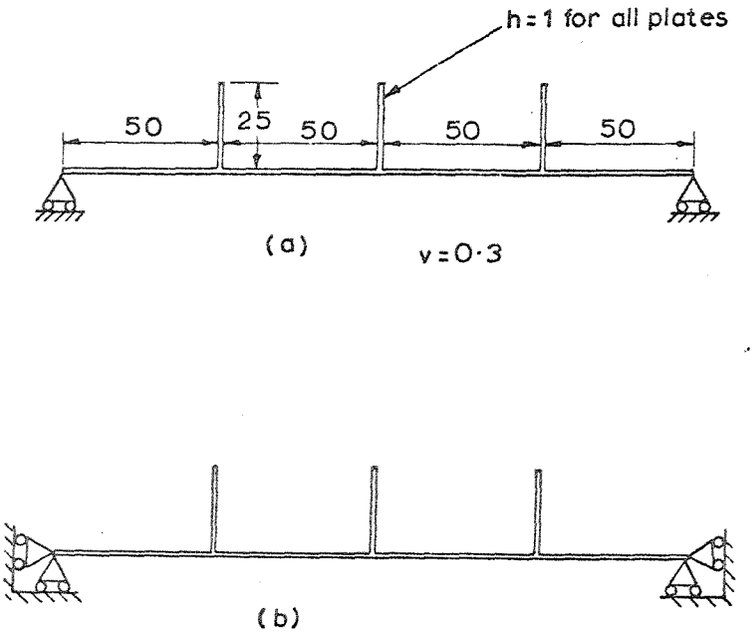

Fig. 2.7 Details of the example of the Stiffened Plate of finite width.

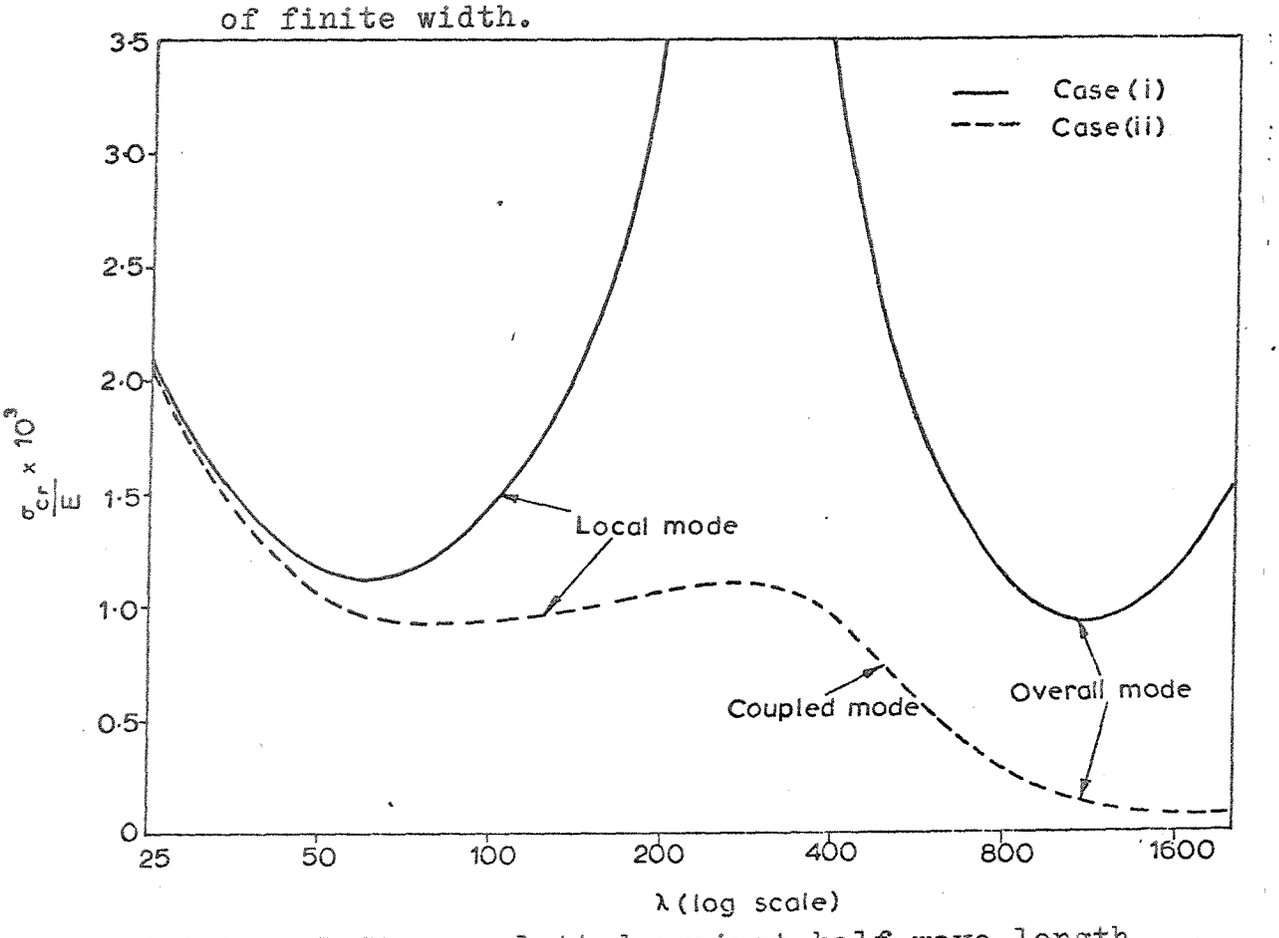

Fig. 2.8 Critical Stress plotted against half wave length of buckling for the Stiffened Plate in Fig. 2.7.

buckling load for the two cases is identical.

A comparison example of a stiffened plate of finite width with three stiffeners shown in Fig. 2.7 is considered next. Here the exterior edges A are simply supported. Two cases are considered again:
Case (i) The plate is laterally unrestrained along the edges (Fig. 2.7(a))
Case (ii) The plate is subject to constraints against inplane movement along the edges A. (Fig. 2.7(b))

The buckling stresses for the two cases have been plotted in Fig. 2.8 . It is seen that the introduction of lateral constraints changes the buckling behaviour profoundly. Not only is the minimum local buckling stress for the case (ii) about 17% lower, but the minimum overall buckling stress falls dramatically to a value which is less than 10% of the corresponding value for the case (i). This is consistent with our earlier observation that the difference in the buckling stresses gets accentuated with increase in the ratio of buckling wave lengths in the longitudinal to transverse direction.

2.3.1.2 Corrugated plate:

The next example is that of a corrugated plate shown in Fig. 2.9 . Here again two cases are considered:

Case (i) : The exterior edges 'A' resting on simple supports (Fig. 2.9 (a)).
Case (ii): The exterior edges 'A' resting on simple supports and restrained against inplane movement. (Fig. 2.9 (b)).

The buckling stresses for various values of 'λ' have been plotted in Fig. 2.10.

The corrugated plate of the same dimensions as in Fig. 2.9 has been investigated by Williams[101] and the results obtained using the present formulation are in good agreement with those published by Williams. It

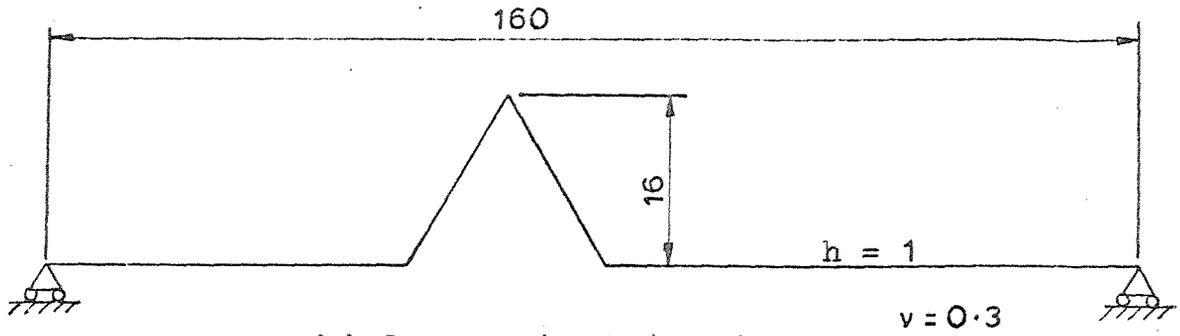

(a) Cross sectional dimensions

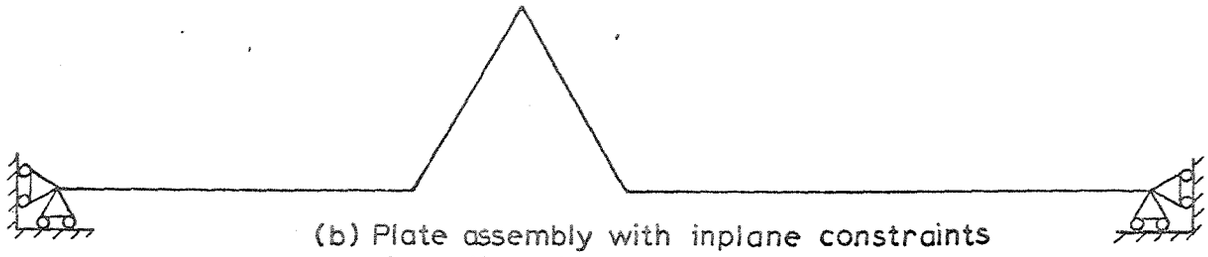

(b) Plate assembly with inplane constraints along the edges

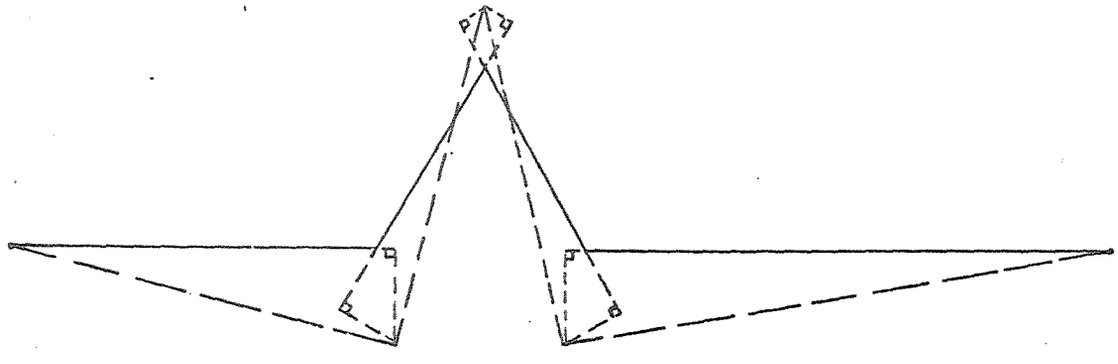

(c) Prebuckling displacements (with bending neglected)

Fig. 2.9 Details of example of a Corrugated Plate.

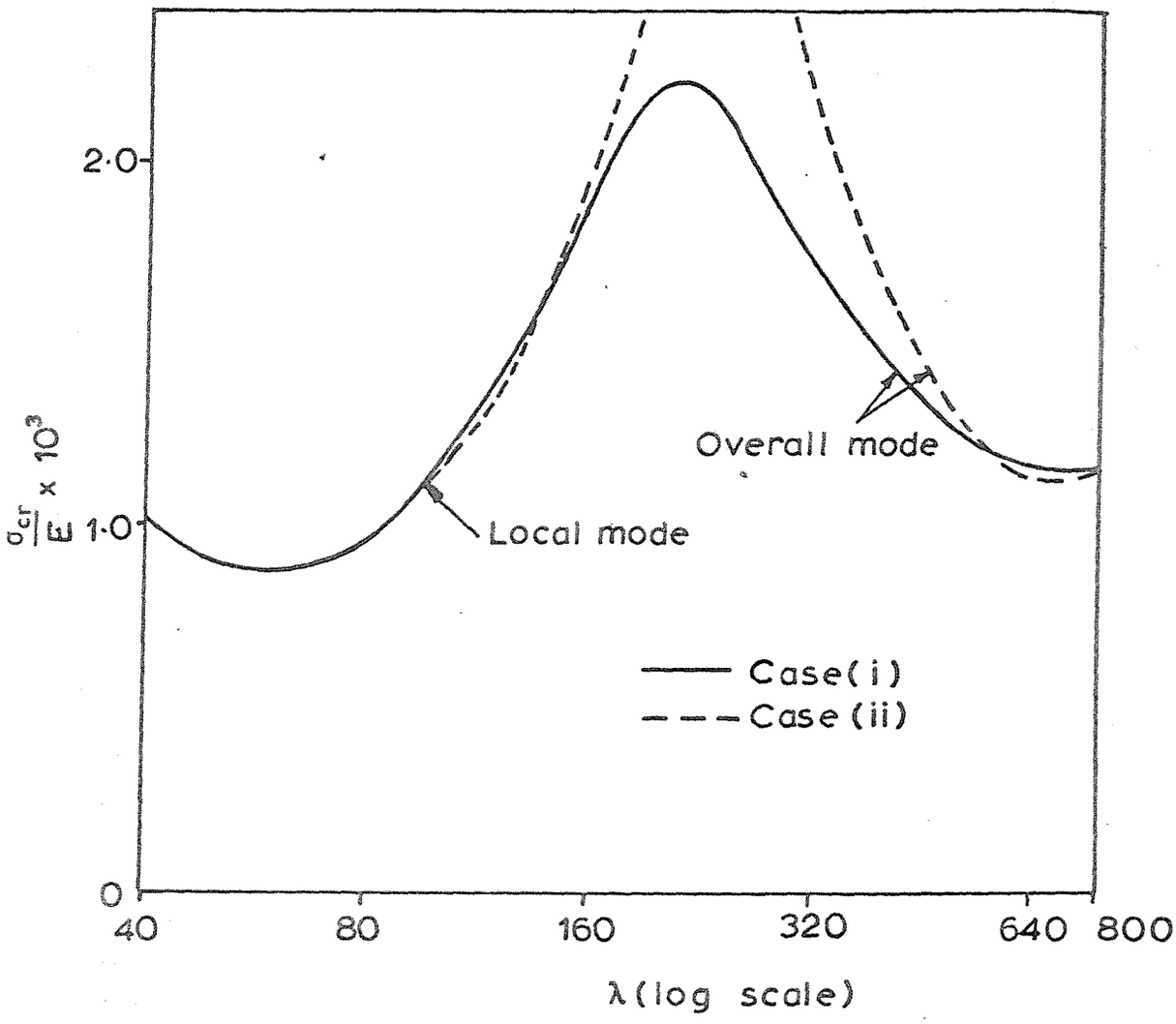

Fig. 2.10 Critical Stress plotted against half wave length of buckling for the Corrugated Plate in Fig.2.9.

may be seen that the minimum local and overall buckling for both the cases (i) and (ii) do not differ significantly. The prebuckling analysis in both the cases shows that the constituent plates are virtually free from transverse normal stresses, thus demonstrating that the restraints offered by flexural rigidities of adjacent plates for the lateral expansion of the plates are negligible. The presence of constraints against inplane movement at the exterior edges in case (ii) does not prevent the plates from stratching inwards thus becoming free of transverse stresses as shown in Fig. 2.9 (c).

However there are significant differences in the buckling stresses as obtained for the two cases in the region between the two minima (corresponding to local and overall buckling modes). These must be attributed in the main to the influence of inplane boundary conditions in the buckling problem.

2.3.1.3 Square box structure with external diagonal members:

Fig. 2.11 shows a configuration of a box column with each junction connected externally to a member, the remote end of which is fully restrained against movement in the plane of the cross-section of the column.

The buckling stresses obtained using the present approach for various values of λ are plotted in Fig. 2.12. In the same figure , are plotted the buckling stresses making the assumption of uniaxial compression in the prebuckling state. The latter approach gives a value of the minimum buckling stress which is in error of about 27%. It is apparent that the configuration does not allow enough degrees of freedom for each mamber to expand freely in the transverse direction. As a result transverse compressive stresses due to Poisson's effect cause

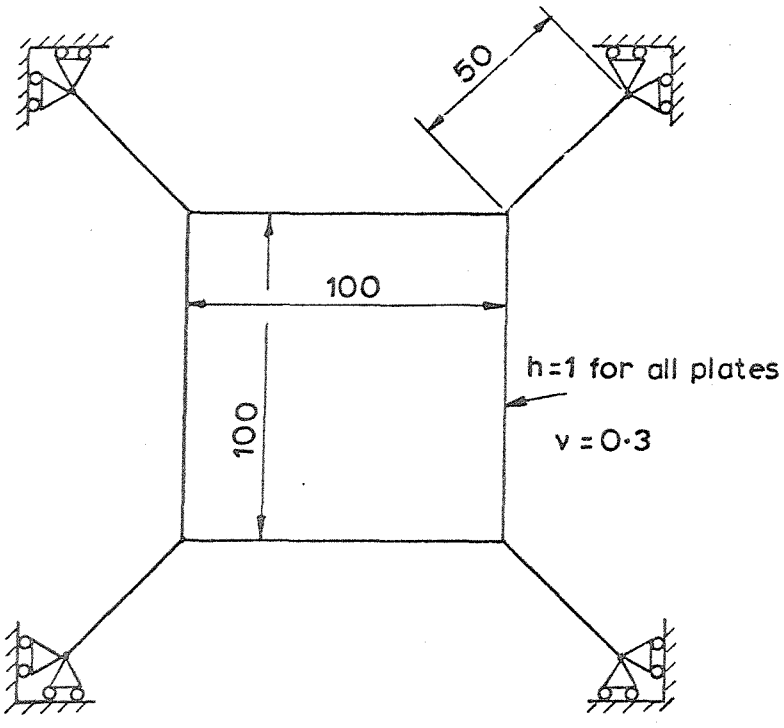

Fig. 2.11 Square Box Column with External Diagonals.

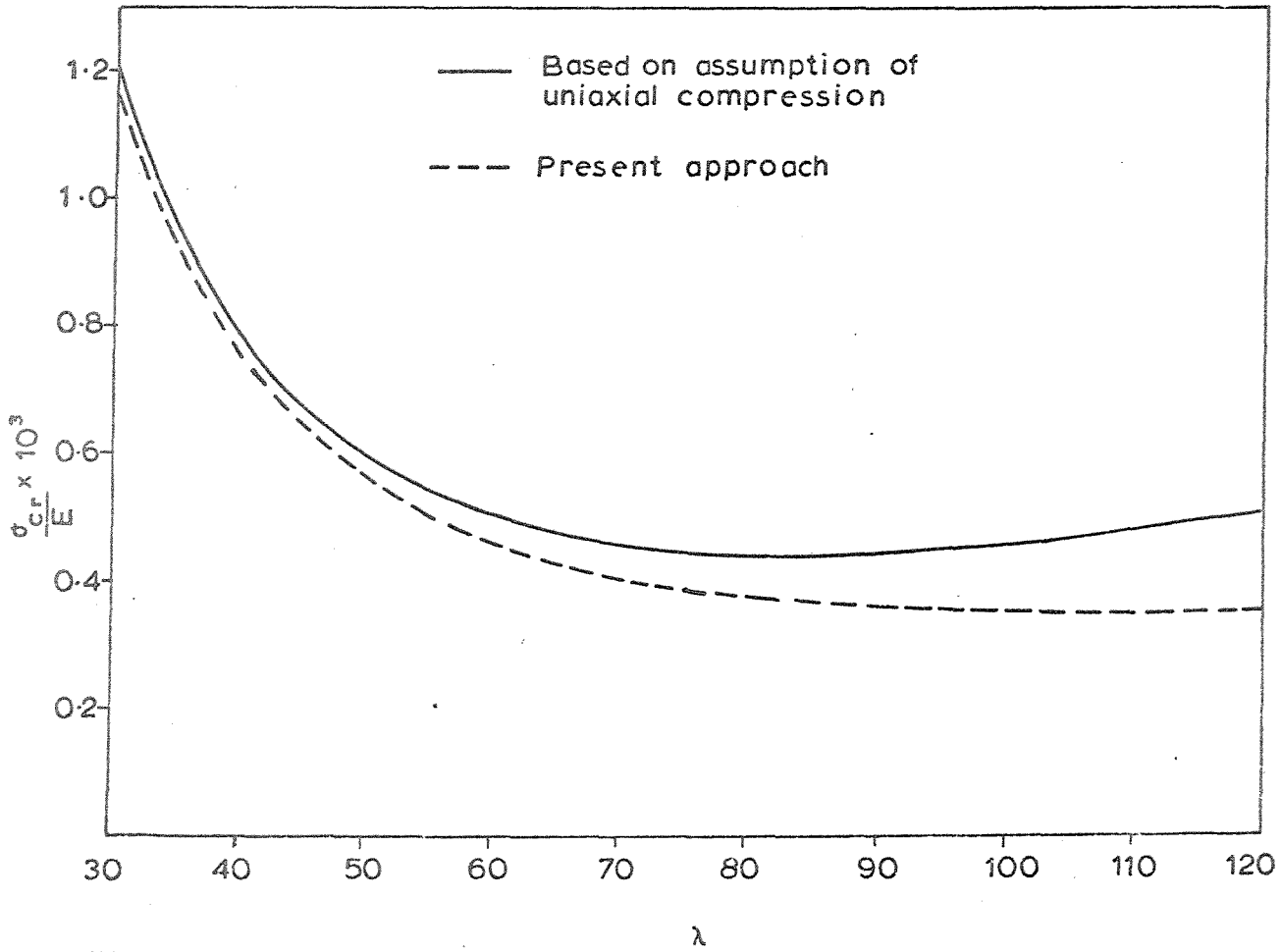

Fig. 2.12 Buckling Stress of the structure in Fig.2.11 plotted against half wave length of buckling.

the plate assembly to buckle at a smaller load.

A general deduction is possible from the significant reduction in the buckling stress noticed in this case as against the case of the corrugated plate for which there was observed no reduction. It appears that provided the plates are long and have small flexural rigidities, the problem of transverse stress distribution prior to buckling in the plate assembly is analogous to the problem of a plane framework with hinged joints, subjected to temperature increase. In this analogy, the transverse strain $\nu\sigma/E$ of the plate corresponds to unit expansion ρt due to a temperature increase of 't' degrees. (ρ is the coefficient of linear expansion of the material). In either case, the prevention of lateral expansion results in a stress of $\nu\sigma$ (or $E\rho t$). A mechanism of the type shown in Fig. 2.13(a) or statically determinate framework of the type shown in Fig. 2.13(b) allows the constituent members to freely expand and thus there develop no stresses due to variation of temperature. In the case of a plate assembly with an 'indeterminate' configuration, such as the one considered in this section, therefore, it may, in general, be expected that the transverse compression would develop in the constituent plates due to Poisson's effect by the application of longitudinal compression; and as a consequence there can be a reduction in the buckling strength.

2.3.1.4 Double box column with internal diagonal members:

As a final example, the case of a double box column with internal diagonal members. The plate is subjected to no external constraints (Fig. 2.14(a)).

The buckling stresses using the present approach for various values of λ have been plotted in Fig. 2.15(a) These have been compared with those

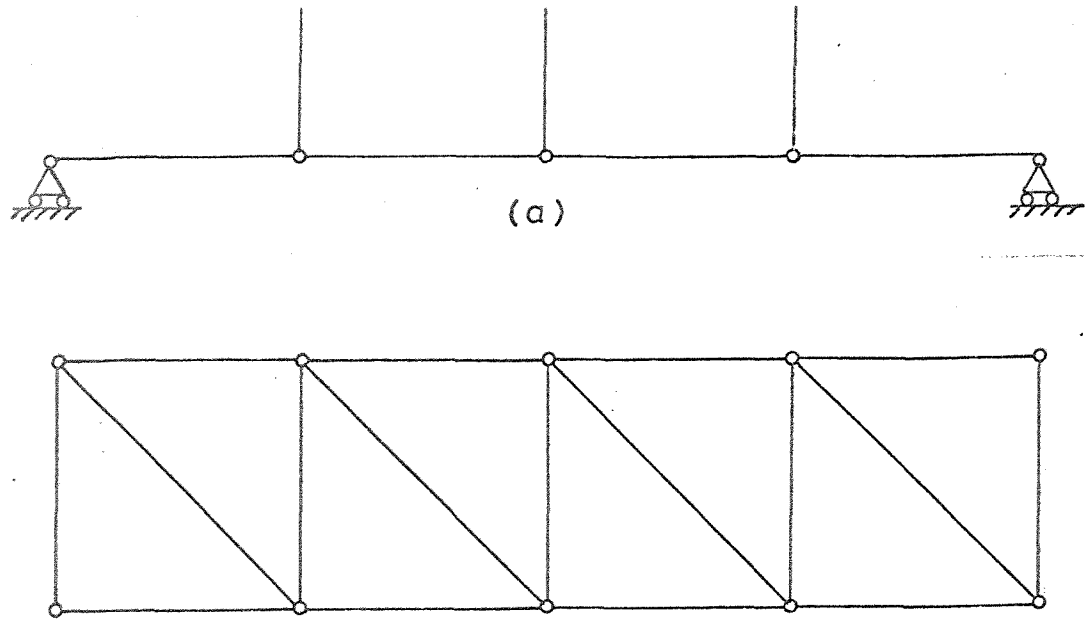

Fig. 2.13 Examples of Plane Frameworks which allow their members to expand freely.

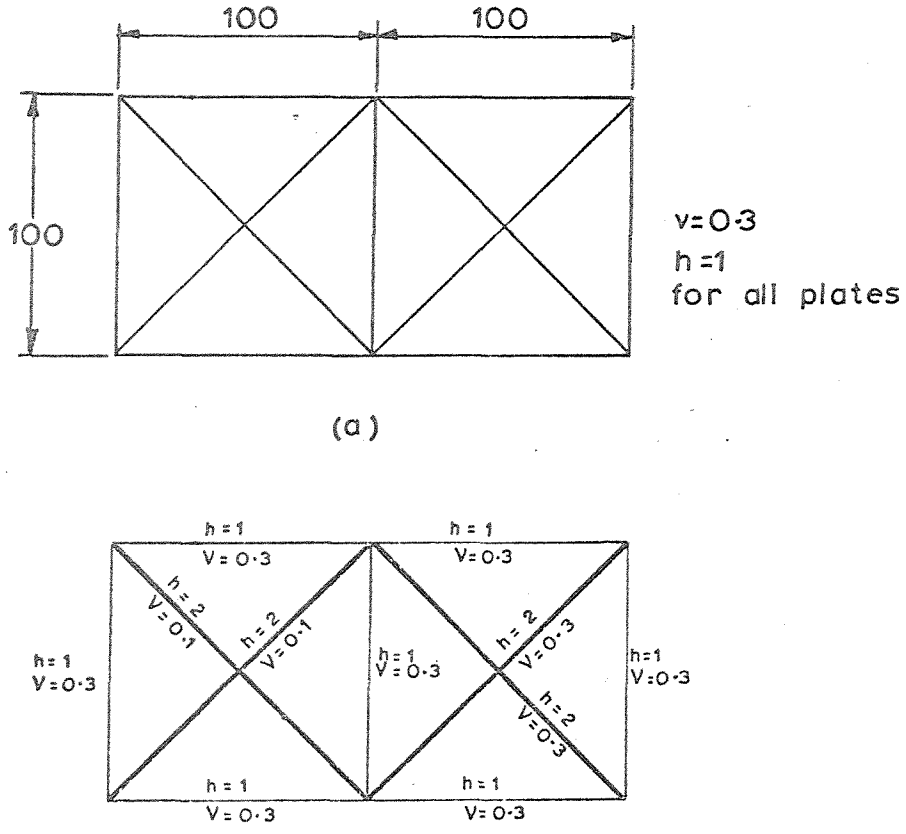

Fig. 2.14 Details of examples on Double Box Columns with internal diagonal members.

obtained making the assumption of uniaxial compression in the prebuckling stage. The two sets of results are in good agreement within 2-3% of each other.

It can be readily established with the aid of a Williot-Mohr diagram[99] that a plane framework of the type shown in Fig. 2.14 when subjected to uniform temperature increase, will remain stress-free (providing 'ρ' for all the members is the same). This explains the remarkably accurate results obtained using the assumption of uniaxial compression for the plates.

The same example is worked again with the following changes (Fig. 2.14(b)) in the data:

(i) The Poisson's ratio of the material of the diagonal members is now assumed as 0.1 while that for the remaining plates is kept at 0.3.

(ii) The diagonal members are assumed to be twice as thick as the other members.

The buckling stresses for this case have been plotted in Fig. 2.15(b). It is seen that the assumption of uniaxial compression is no longer true and results in an overestimate of buckling stresses by about 17%. The prebuckling stress distribution shows that significant intensities of transverse compressive stresses while the diagonals carry smaller tensile stresses. It must be noted in this case, however, the applied stress distribution in the plates is no longer uniform for a given 'e' but proportional to $1/(1-\nu^2)$.

2.3.1.5 Concluding remarks on the worked examples on longitudinally compressed plate assemblies

The worked examples presented in this section illustrate

(i) the effects on the buckling behaviour, of the introduction of in-plane lateral constraints on the constituent plates of the structure and (ii) the error that may be involved in making the assumption of

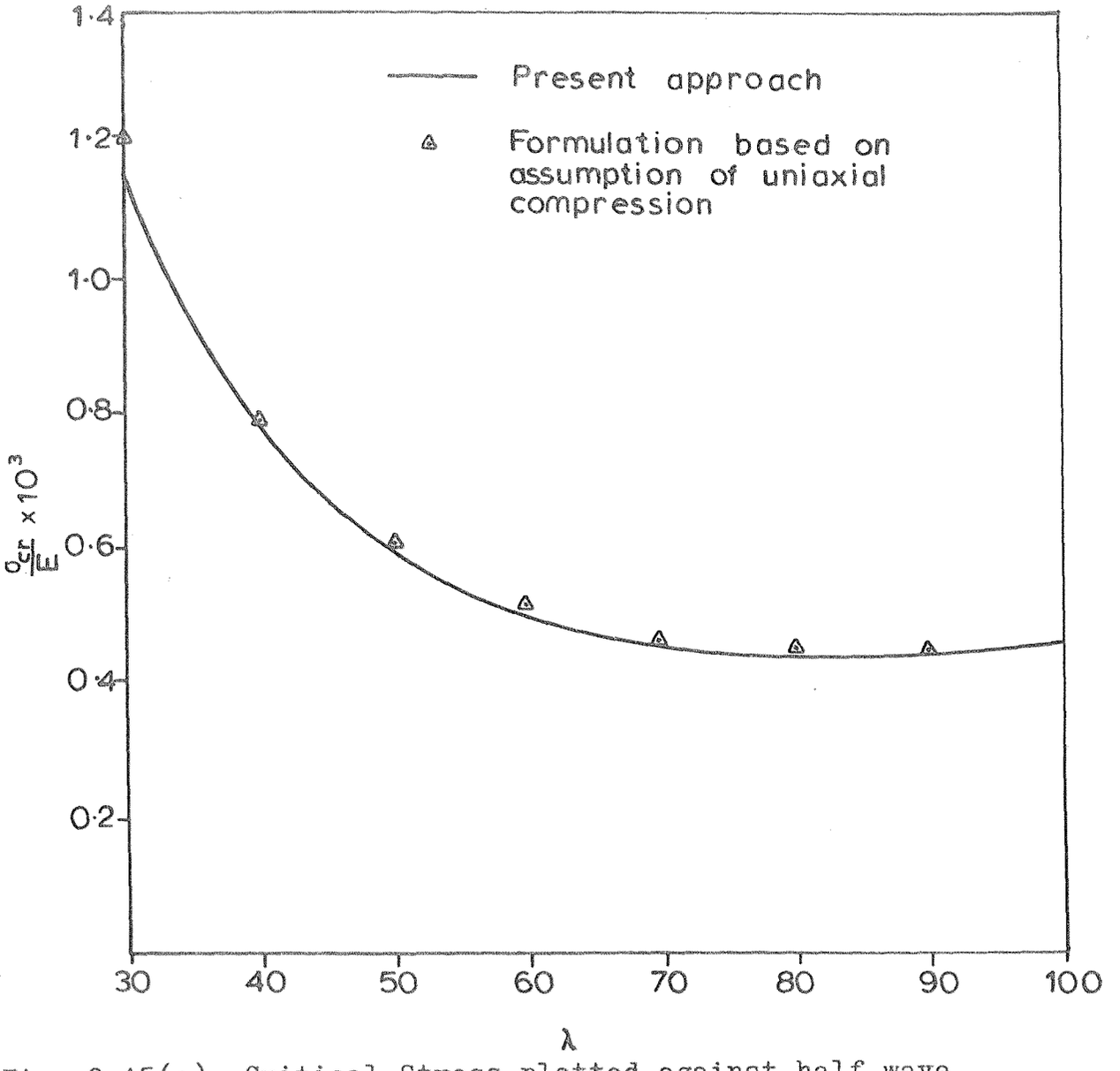

Fig. 2.15(a) Critical Stress plotted against half wave length of buckling for the example in Fig.2.14(a)

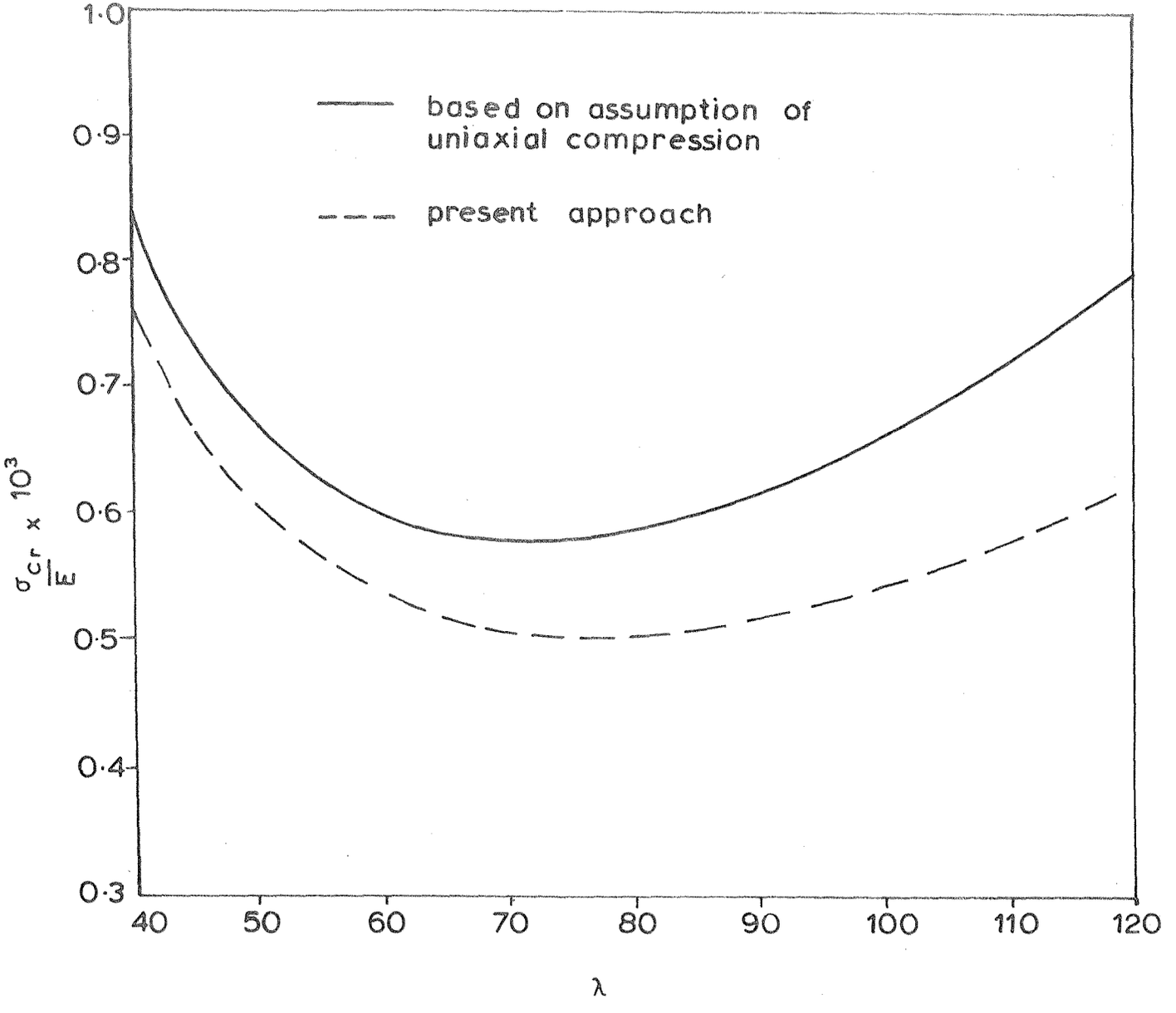

Fig 2.15(b) Critical Stress plotted against half wave length of buckling for the example in Fig.2.14(b)

uniform uniaxial compression in the constituent plates prior to buckling in an 'indeterminate' configuration.

A plane framework analogy suggested herein, is found to be helpful in the interpretation of results.

2.3.2 Plate structures carrying inplane patch loading

The buckling of plates carrying inplane patch loading has been a subject of study by several authors. This problem has been studied with the aid of the finite strip technique developed in this chapter and a few results are now presented with the following objects in view:

(i) To study the accuracy and convergence of the solution

(ii) To illustrate the greater efficiency of the method over the finite element solution in respect of computing effort.

An example of a box girder carrying patch loading along a pair of its junctions is also presented to illustrate the influence of the flanges on the buckling behaviour.

2.3.3 Studies on convergence of the solution: Simply supported rectangular plates

The geometric parameters controlling the problem are defined in Fig. 2.16. The buckling coefficient 'K' may be defined as

$$P_{cr} = \frac{K\pi^2 D}{B}$$

where P_{cr} is the critical value of the applied load. The accuracy of the final result 'K' of a computation depends upon the accuracy with which

(i) the prebuckling stress distribution and

(ii) the buckling mode

are described in the solution procedure. The former depends upon the

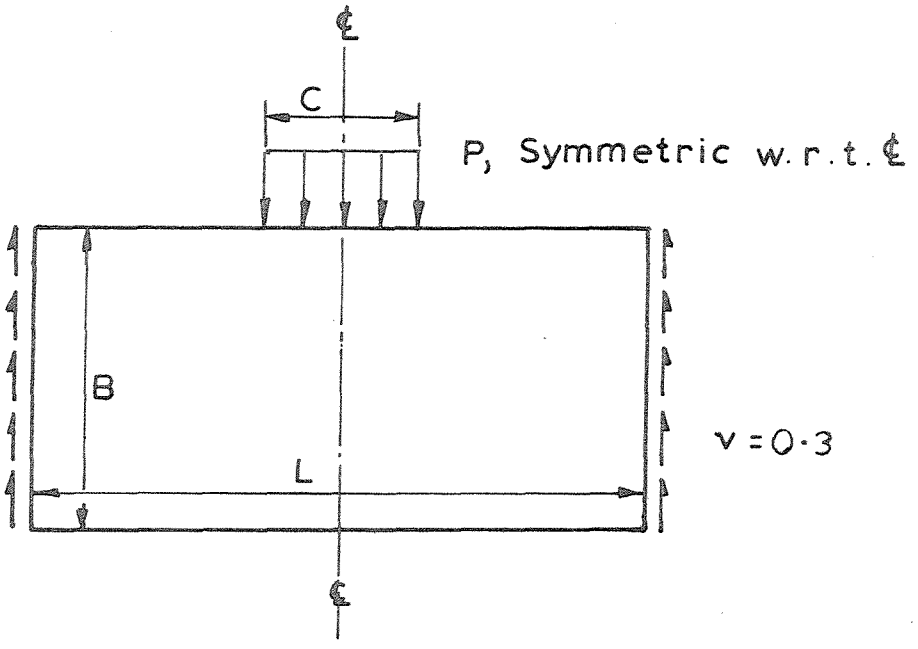

Fig. 2.16 Dimensions of the patch loaded plate.

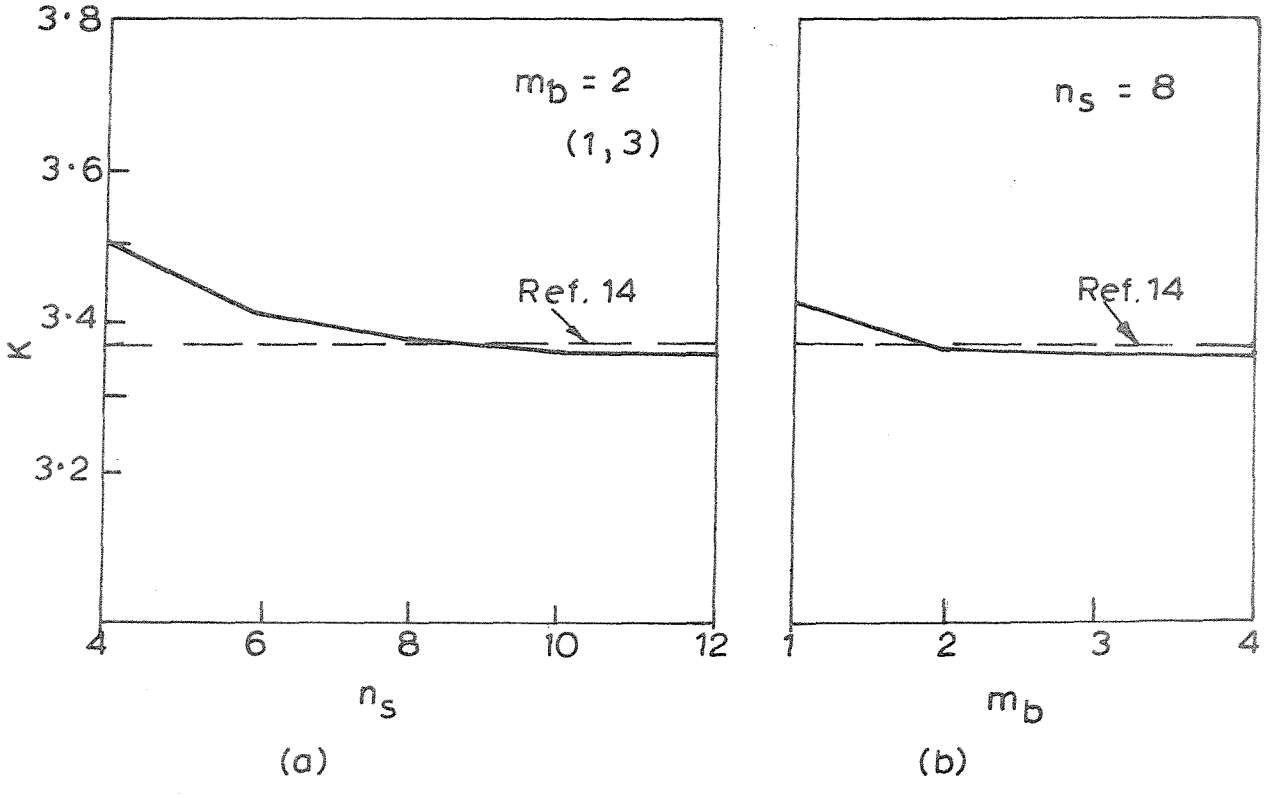

Fig. 2.17 Convergence Studies on a plate with L/B = 1.0 , C/B = 0.20.

number of harmonics considered in the prebuckling analysis (m_p) as well as the number of strips (n_s) representing the plate. The accuracy with which the buckling mode is described depends upon the number of harmonics describing it(m_b)and the number of strips n_s. In view of the fact that the harmonics are uncoupled in the prebuckling analysis, the computing time for the same is a small fraction of the rest of the analysis involving the determination of eigenvalues and vectors. Thus it is possible to include as many harmonics (m_p) as may be desired in this part of the analysis without any significant effect on the total computing time required for the problem. In the problems considered here, it was found that it is unnecessary to include more than 15 nontrivial harmonics (m_p) in order to obtain the value of 'K' within 0.01%. Thus n_s and m_b are the more important factors in convergence study.

The first problem studied is the same as the one studied exhaustively by Rockey and Bagchi. The results of the present convergence study are given in Fig. 2.17(a-b). The value of 'K' (3.356) obtained with 12 strips across the plate and 2 harmonics describing the buckling mode is in very close agreement with Rockey's result as well as can be judged from his graphical plot. For the square plate problem, it is seen that it is sufficient to describe the buckling mode just by one harmonic to obtain the value of 'K' within an error of about 2%, for a given number of strips. This observation is confirmed by other examples of square plates which are presented in Table 2.2. These results are compared with those of Khan et al.[94,95] and Rockey[14], and the agreement is found to be very good.

In Table 2.3, brief convergence studies on long rectangular plates (L/B = 4) are presented. In view of the localised nature of the buckling mode, it is found necessary to employ at least 4 harmonics (m_b = 4) in

Table 2.2(a)

Convergence studies for the case L/B = 1.0, C/B = 0.0

n_s	m_b (1,3...)	K	Remarks
4	2	3.40	Convergence w.r.t. n_s
6	2	3.30	
8	2	3.27	
10	2	3.25	
12	2	3.24	
14	2	3.24	
8	1	3.34	Convergence w.r.t. m_b
8	2	3.27	
8	3	3.27	
8	4	3.27	

Note: 'K' as obtained by Rockey & Bagchi (Ref. 14) = 3.25

Table 2.2(b)

Convergence studies for the case L/B = 1.0, C/B = 0.25

n_s	m_b (1,3...)	K	Remarks
4	2	3.56	Convergence w.r.t. n_s
6	2	3.47	
8	2	3.44	
10	2	3.43	
12	2	3.42	
14	2	3.42	
8	1	3.49	Convergence w.r.t. m_b
8	2	3.44	
8	3	3.44	
8	4	3.44	

Note: { 'K' as obtained by Ref. 95 3.42
'K' as obtained by Ref. 94 3.5

Table 2.3

Convergence studies on a plate with L/B = 4.0

C/B	n_s	m_b (1,3 ...)	K	Remarks
1.0	4	2	2.82	Convergence w.r.t. n_s
	6	2	2.91	
	8	2	2.93	'K' as given by ref. 95 = 2.80
	6	2	2.91	
	6	3	2.74	Convergence w.r.t m_b
	6	4	2.72	
0.25	4	2	2.46	Convergence w.r.t. n_s
	6	2	2.52	
	8	2	2.54	'K' as obtained by Ref. 95 = 2.21
	6	2	2.52	
	6	3	2.23	Convergence w.r.t. m_b
	6	4	2.15	
	6	5	2.13	

order to obtain results with an estimated error of 1%. This is especially true of the case with smaller C/B ratio. Further refinement of the results is not attempted in these cases, in view of the relatively greater computing effort involved.

It may be noted that the solutions of K obtained are not necessarily upperbound for a given value of n_s as may be seen from Table 2.3. This may be attributed to the fact that the solution of the prebuckling stresses as given by the displacement method is not bounded.

The final example is that of a box girder shown in Fig. 2.18, carrying inplane patch loading on the web plate. The dimensions of the web plate and the width of patch loading are the same as in the case (2) in Table 2.3, thus making it possible to study the influence of flanges by comparison. Table 2.4 gives the results obtained for various values of n_s and m_b. It also shows that the buckling mode corresponding to the lowest buckling stress is symmetric with respect to both the planes of symmetry. From a comparison with case (2) in Table 2.3, it is seen that buckling load for the box structure is about 50% higher. This is mainly due to the reduction in the intensities of longitudinal stresses in the latter case, for a given load on the structure. The buckling mode is shown in Fig. 2.19 (a-b). It is seen that the buckling deflections are concentrated in the central portion of the girder of length equal to 0.4 of the span of the girder, in the compression zone.

2.3.4 Comparison of the computing effort involved in the finite strip and the finite element solutions

As stated earlier, the example shown in Fig. 2.17 has been studied by Rockey and Bagchi[14] and from a study of their results, it is seen that at least 48 elements are required to obtain the buckling coefficient to the same order of accuracy as in the present method with $n_s = 8$ and $m_b = 2$. A comparison of the computing efforts is made on this basis in

Table 2.4

Convergence studies on the box girder in Fig. 2.18

n_s	m_b	K	Remarks
8*	3(1,3,5)	3.34	Convergence w.r.t. n_s
12*	3(1,3,5)	3.33	
16*	3(1,3,5)	3.32	
12*	3(1,3,5)	3.33	Convergence w.r.t. m_b
12*	4(1,3,5,7)	3.23	
12*	5(1,3,5,7,9)	3.21	
8*	3(2,4,6)	5.17	Additional checks
8**	3(1,3,5)	4.83	
8**	3(2,4,6)	11.96	

* Mode assumed symmetric w.r.t. plane AADD.

** Mode antisymmetric w.r.t. plane AADD.

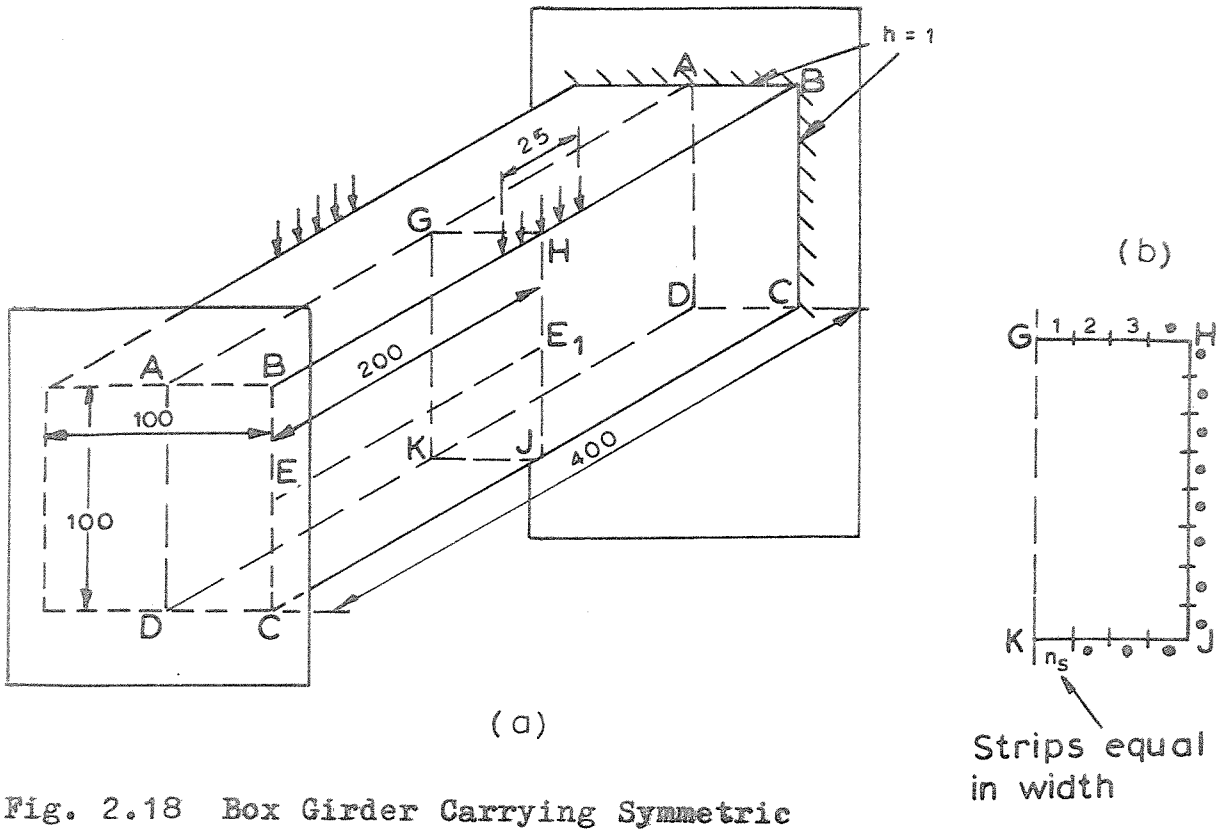

Fig. 2.18 Box Girder Carrying Symmetric Patch Loads at its Top Junctions.

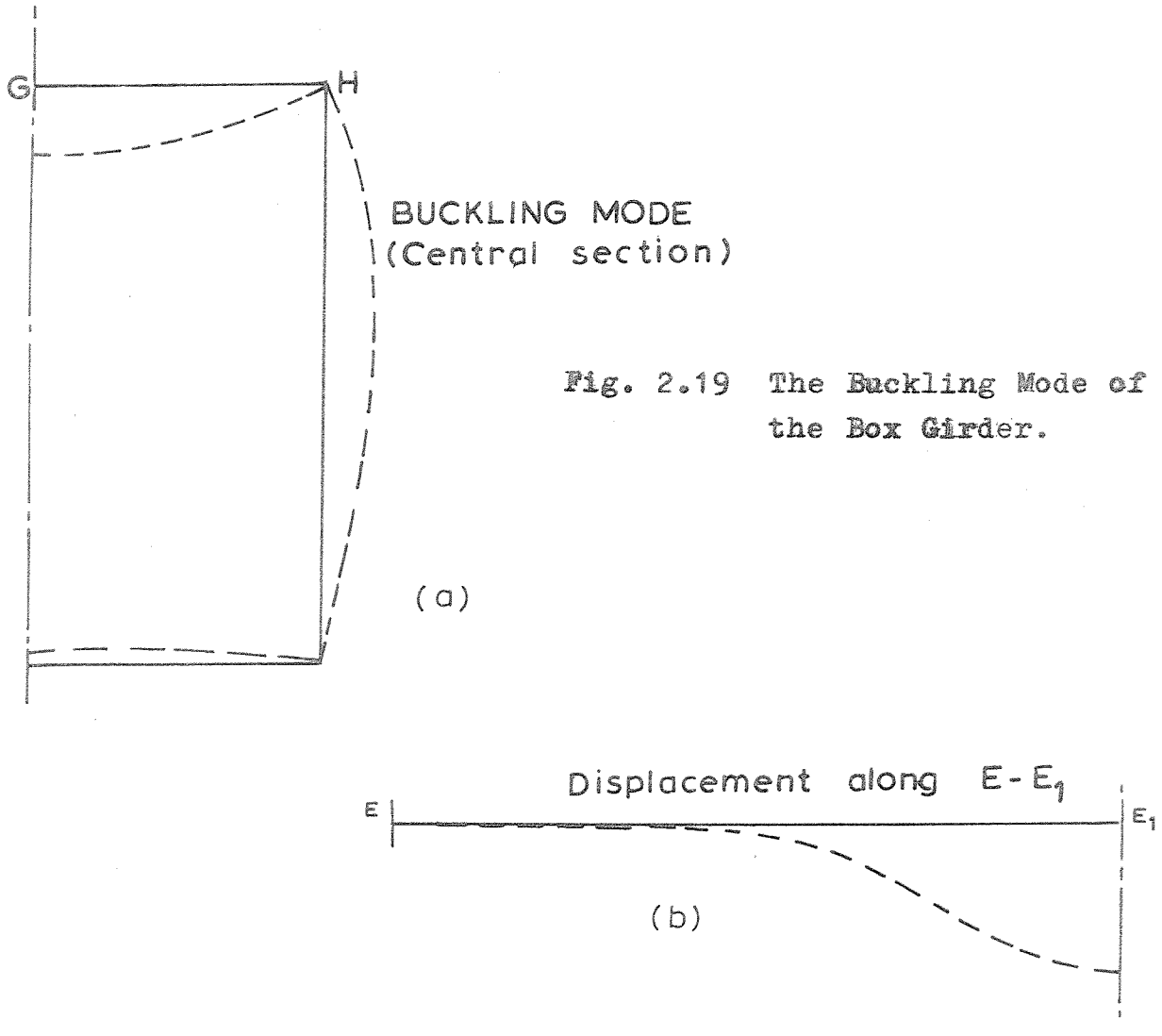

Fig. 2.19 The Buckling Mode of the Box Girder.

Appendix IV where it is shown that the finite strip solution takes about only 1% of the computing time required by the finite element solution.

2.4 Conclusions

An initial buckling analysis which takes into account the effects of prebuckling stress distribution and capable of modelling localised buckling modes has been presented. Examples of plate structures carrying axial and lateral loads are presented. A comparison with an existing finite element solution of a patch loaded plate problem shows that the method presented requires only one percent of the computing effort required by the former.

CHAPTER 3

POST-LOCAL-BUCKLING ANALYSIS

3.1 Introduction

In this chapter, the general theory of post-local-buckling analysis of plate assemblies using the finite strip method is discussed. Two versions of this method are described, each suitable in different contexts. This is followed by a number of worked examples which illustrate the convergence, scope and power of the technique. The chapter opens with a summary of the inadequacies of the earlier methods of post-buckling analysis which provide the motivation for developing the present approach.

3.1.1 Inadequacies of existing methods of postbuckling analysis:

As mentioned in Art 1.2.2 (Chapter 1) most of the earlier work on post-local-buckling analysis of plate assemblies has been based on the solution of the von Karman compatibility equation together with the use of a variational technique. These solutions though of considerable interest in themselves have the following limitations:

1. The boundary conditions have been approximated in order to uncouple 'w' and 'ϕ'; this makes it possible to describe 'w' without reference to 'ϕ' and simplifies the determination of 'ϕ' from the compatibility equation. However, as already stated,these approximations are not always valid, especially where the inplane displacements along the junctions assume such magnitudes as to make the normal displacements along the junction no longer negligible. Since, one of the aims of the present investigation is to study the phenomenon of crinkly collapse of the plate junctions, an approach which neglects the inward movement

of the junctions can hardly be adequate.

2. The solutions are based on the assumption of a buckling mode represented by a single harmonic in the longitudinal direction over the entire length of the plate structure. This assumption has been made with a view to simplifying the algebraic work which would become intractable if more harmonics are taken into account. However with increase in applied compression the wave form in the longitudinal direction undergoes modification and this must be taken into account especially if the applied load exceeds about twice the critical.

3. The other major disadvantage of these solutions is that they do not lend themselves for a formulation of a generalised computational approach. In practical situations one comes across a variety of configurations and some of these are quite complex. In order to be able to deal with these a generalised computational approach is a necessity.

3.1.2 Finite strip method

Most of these limitations can be overcome by the adoption of a finite element approach for the problem, but the excessive computational expense involved has probably remained a deterrent for its application to a study of postbuckling behaviour of plate assemblies. In the present chapter, the finite element technique has been considerably simplified by incorporating in it the information that the buckling and postbuckling normal displacement can be described by a sine wave or by a superposition of a small number of harmonics - and the result is the finite strip method with its variations. A comparison of the computational expense for the finite element method with that of the finite strip method is made taking specific examples later in this chapter.

The finite strip method has not so far, been extensively used for the nonlinear problems. The most serious difficulty associated with this method as evidenced by its application[47-51] to the nonlinear analysis of rotational shells, has been the coupling of harmonics which make for a large number of degrees of freedom and consequently a very large number of coefficients of nonlinear terms. This has necessitated some simplifications being made in the analysis as for instance, the quartic terms being neglected[49] or the coupling between the harmonics assumed to be nonexistent[51]. It is indeed difficult to justify these assumptions in general, especially in problems where the nonlinearities are severe. However these difficulties do not arise in the case of post-buckling analysis of plates. Here, as mentioned earlier, the buckling mode can be accurately described in terms of a few harmonics and for the initial post local buckling analysis, even one harmonic may be sufficient. In order to tackle the problem of computing the large number of coefficients required in the analysis - which increase rapidly with each additional harmonic taken into account, a special algorithm has been developed which will be discussed later in the chapter.

3.1.3 Different versions of the method

In this chapter, two versions of the finite strip method will be presented - one in which certain simplifying approximations are made to deal with boundary conditions along junctions of plates and the other in which no such assumptions are made. Naturally the former approach involves much less computational effort than the latter and must be used if the approximations are appropriate for the problem. The two versions will now be briefly introduced.

3.1.3.1 Version I

In this version, the boundary conditions at the ends and along the longitudinal edges of the constituent plates are specified in the same manner as in Ref. 58-62. The essential feature of this version is the manner in which the boundary conditions along the junctions are approximated. The approximations have the effect of uncoupling the inplane displacements (and forces) of one, with the out of plane displacements (and forces) of the other, of two plates meeting along a common junction at an angle to each other. The implications of this statement will be made more explicit in the next paragraph, but it may be noted here, that this assumption makes it possible to characterise the variation of 'w' and 'v' in the longitudinal direction in independent forms, chosen from the point of view of their mutual compatibility in satisfying the von Karman compatibility equation. Further each plate will be assumed to be in a state of uniaxial (with the plates allowed to freely expand in the transverse direction) or biaxial compression (caused as a result of the plates being fully restrained in the transverse direction) prior to buckling and thus no analysis of the prebuckling state of equilibrium is necessary.

The assumptions made regarding the boundary conditions restrict the application of this version of the method to plate assemblies having certain types of configurations only. The plate assemblies must consist of junctions, each of which fall in one or the other of the following categories:

(i) A "corner"[58] (Fig. 3.1(a)) where two plates meet at a sharp angle. In this case, the normal displacements of each of the plates along the junction are assumed to vanish separately and the plates free to wave in their plane along the junction.

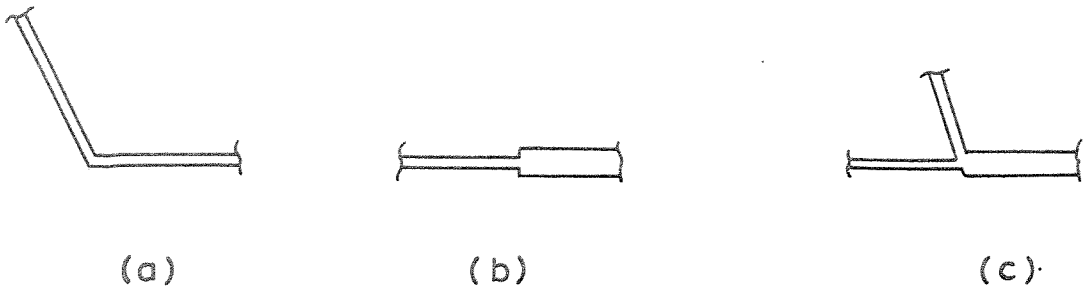

Fig. 3.1 Different types of plate junctions mentioned in Sec.3.1.3.1

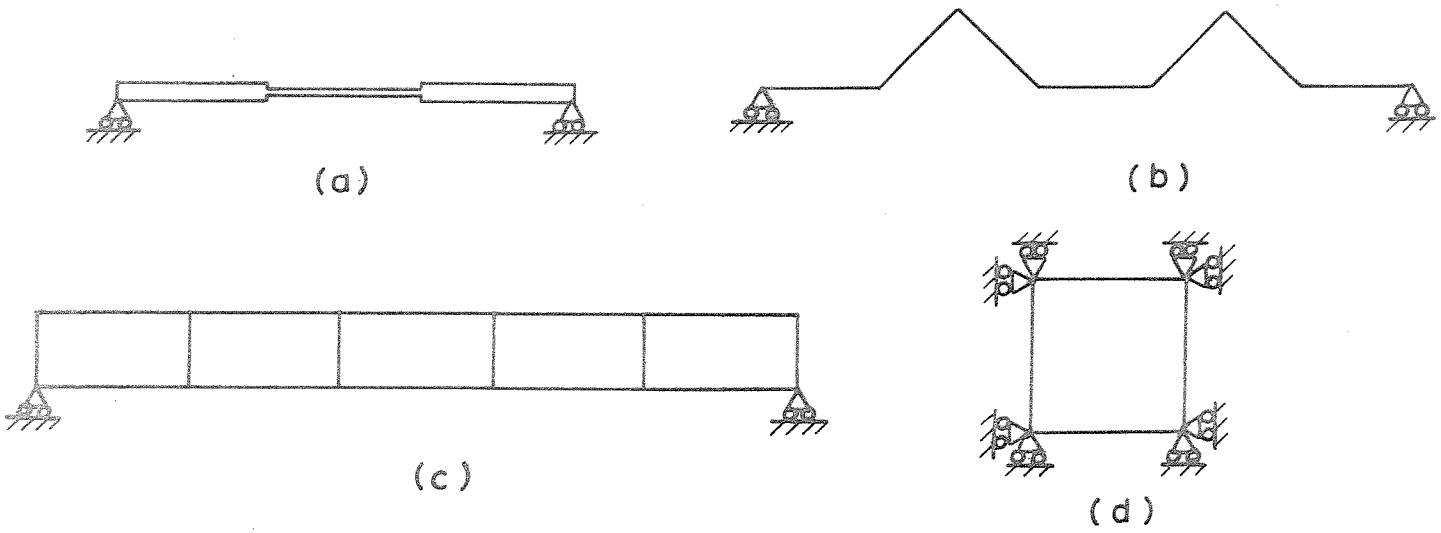

Fig. 3.2 Examples of Plate Assemblies which can be analysed with Version I.

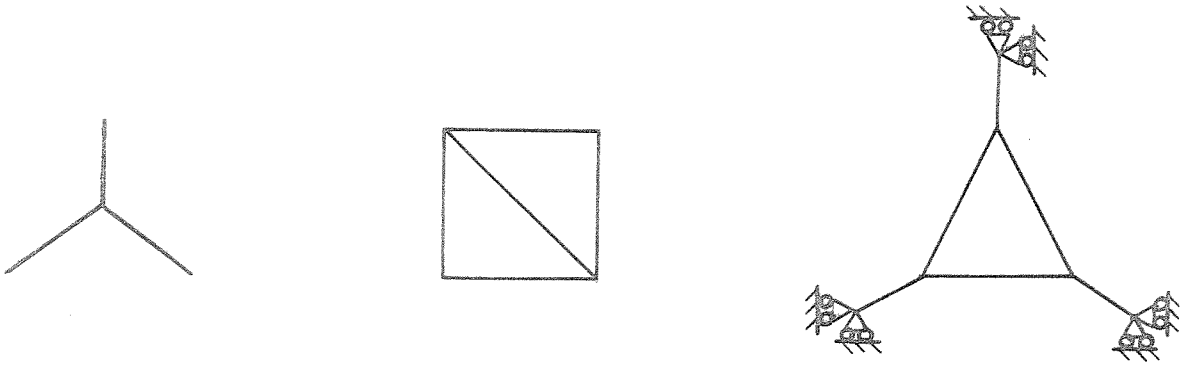

Fig. 3.3 Examples of Junctions and plate assemblies for which Version I is not applicable.

(ii) A "Transition", where two plates which lie in the same plane, have a common edge (Fig. 3.1(b)). Here, the boundary conditions do not involve any coupling between 'v' and 'w' of the plates and the assumptions mirror the reality.

(iii) A "Branch point" where a third plate joins a junction along a common edge of two plates lying in the same plane (Fig. 3.1(c). Here there exists no coupling between plates I and II, and the normal displacement of plate III is assumed to vanish along the junction and the plate free to wave in its plane.

Most of the structures used in practice consist of junctions,all of which fall in one or the other of these categories. Some examples are shown in Fig. 3.1.

Note that the version can not deal with structures with junctions where three or more plates meet at an angle to each other (Fig. 3.3).

3.1.3.2 Version II

In this version, the variations of 'w' and 'v' in the longitudinal direction are described by the same type of functions, so that compatibility of displacements in the transverse plane along the junctions of the plates can be achieved. This version is more expensive in computation as generally several terms are found to be necessary for the description of inplane displacements, but can deal with plate assembly of any complexity and carrying loads far in excess of the critical.

In many cases, some simplification of this version is possible. While it is possible to describe 'w' in the postbuckling stage by a relatively small number of harmonics, the series for 'v' is but slowly convergent. The efficiency of the procedure can be enhanced by allowing 'w' and 'v' to be described by different number of terms. This would

result in the boundary conditions along the junctions not being satisfied for each of the terms by which the series for 'v' exceeds that for 'w'. For these terms, the boundary conditions would be treated in the same menner as for version I. This modification of version II will be called version IIA in further discussion.

3.2 Theory

In this section is outlined the finite strip approach to the post-local-buckling analysis of plate assemblies. The basic reatures of the analysis remain the same as in Chapter 2 i.e. the Lagrangian description of displacements and the systematic use of perturbation technique[97,98]. In the following description, therefore, greater attention is given to the sections where there arise concepts not discussed earlier. The analysis involves the following steps:

1. A set of displacement functions satisfying the boundary conditions at the ends of the plates is chosen.

2. With the aid of strain displacement relations, the strain energy function is built up.

3. Invoking the principle of stationary strain energy, a set of nonlinear algebraic equations of equilibrium is generated.

4. The linearised prebuckling equilibrium path is generated. This step can be skipped for version I.

5. "A sliding incremental displacement" technique is employed in conjunction with the perturbation technique to obtain the buckling load and characteristics of the post buckling path in the immediate vicinity of the bifurcation.

6. The nonlinear postbuckling path can now be traced using a combination of incremental and iterative techniques of solution of nonlinear equations.

Each of these steps is described in some detail in the following. For the sake of clarity the versions I and II are treated separately as these differ in a few significant details.

3.2.1 Version I.

3.2.1.1 Boundary conditions at the ends of the plates

The boundary conditions at the ends of each plate must be considered first before choosing the displacement functions. At the ends, the plates are assumed to be simply supported, to carry no inplane shear stresses and to undergo constant (or linearly varying) longitudinal displacement. These conditions may be stated in the form (referring to Fig. 2.1)

$$w = 0 \ ,$$

$$\frac{\partial^2 w}{\partial x^2} = 0 \ ,$$

$$\tau_{xy} = 0$$

$$u = u_o + u_1 y$$

at $x = 0$ and $x = a$ . . . 3.1(a-d)

In the foregoing u_o and u_1 are constants. Since the present investigation will be mainly concerned with uniformly compressed plates u_1 may be taken as zero.

It must be noted that these boundary conditions involve a contradiction. Condition 3.1(c) implies that the plates are free to expand in the transverse direction at the ends. Consider the case of two plates meeting at right angles as shown in Fig. 3.4. For each of the plates at $x = 0$ and $x = a$

$$v \neq 0 \ , \quad w = 0 \ .$$

Since the normal displacement of plate (I) w^I is the same as the

transverse displacement of plate (II) v^{II} and vice versa, the conditions 3.1(a) and (c) are mutually incompatible. However, conditions 3.1 may be viewed as approximations which are justified in view of the smallness of bending rigidities of the plates and the fact that the inplane displacements are of a lower order of magnitude in comparison to normal displacements in the postbuckling range.

For a plate assembly which buckles into a mode in the form of a sine wave with several nodal lines across the structure, the nodal lines may be assumed to remain straight and free from inplane shear stresses, due to symmetry. For the portion of the plate assembly contained between two successive nodal lines the conditions 3.1 can be applied, and for the post-local-buckling analysis of the plate assembly, it is sufficient to consider one such portion. Thus it would appear that boundary conditions 3.1 are valid approximations especially for an initial postbuckling analysis.

3.2.1.2 Displacement functions

As stated earlier, in this version of the finite strip method, we make the assumption that the prebuckling state of equilibrium is a "trivial" one, either a state of uniaxial or biaxial compression constant along the length of the plate and specified by a single parameter.

Case (i):

We first take up the case of uniform uniaxial compression. The prebuckling equilibrium in this case can be characterised by

$$\varepsilon_x = -e$$

$$\varepsilon_y = \nu e$$

and therefore the prebuckling displacements take the form

$$u = e(\frac{a}{2} - x)$$

$$v = \nu e y + c$$

$$w = 0 \qquad \ldots 3.2(a\text{-}c)$$

In the above 'c' is an arbitrary constant and can be determined from the inplane boundary conditions. However its value is immaterial for the postbuckling analysis.

The displacement functions must be chosen to accommodate these prebuckling displacements as well as to satisfy the boundary conditions. In the notation introduced earlier (Chapter 2), these may be expressed in their dimensionless form as follows:

$$\bar{u} = f_{1m} \sin m\pi\xi + e\alpha(\tfrac{1}{2} - \xi)$$

$$\bar{v} = f_{2m} \cos m\pi\xi + \nu e\beta\eta + c$$

$$\bar{w} = f_{3m} \sin m\pi\xi \qquad \ldots 3.3(a\text{-}c)$$

In the above f_{1m}, f_{2m} and f_{3m} are functions of η which describe the variation of the displacements across the plate strip in terms of displacement parameters u_{im}, ... θ_{im} corresponding to the edges $\eta = 0$ and $\eta = 1$ of the plate, as given by 2.3(a-c). These displacement parameters represent the incremental displacements from an equilibrium state on the primary path (which is the prebuckling equilibrium path extended) corresponding to a certain value of 'e' to an equilibrium state on the secondary path (which is the postbuckling equilibrium path) with the same value of 'e' as illustrated in Fig. 2.3 . These displacements are called "the buckling displacements" in further discussion.

The values of 'm', in each term of the expansions given by the first part of the expressions 3.3(a-c) must be chosen in the following

manner. Let 'm' take the values of i_1, i_2, i_3 ... i_n in the expression for $\bar{w}$, where i_1 ... i_n are integers. Then the values which 'm' must assume in the expressions for $\bar{u}$ and $\bar{v}$ must include all the integers in the expansions

$$\sum_k \sum_\ell i_k + i_\ell \qquad \text{and} \qquad \sum_k \sum_\ell i_k - i_\ell$$

The necessity of considering precisely these terms arises from the nature of strain displacement relations (3-4(a-c)) and the inplane equilibrium equation of the plate. The precise mathematical reasoning involved in this statement is discussed in Appendix V.

The general statement made in the previous paragraph may be made clearer by reference to specific situations.

Let the buckling mode be composed of 'n' half waves along the length of the plate assembly. If it is assumed that the buckling mode undergoes no change in the longitudinal direction, it is sufficient to describe the normal displacement 'w' just by one harmonic given by 'n'. In this case, the functions describing the buckling displacements in 3.3(a-b) take the form

$$\left.\begin{aligned} \bar{u}_b &= f_{1,2n} \sin 2n\pi\xi \\ \bar{v}_b &= f_{2,o} + f_{2,2n} \cos 2n\pi\xi \end{aligned}\right\} \quad \text{(no sum of 'n')}$$

Here the subscript b refers to the contribution to displacements $\bar{u}$ and $\bar{v}$ due to buckling.

If in the above case, it is desired to study the effects of a modification of longitudinal wave form, while the nodal lines remain straight, the normal displacement 'w' must be described by harmonics given by n, 3n, 5n ... etc.

If

$$\bar{w}_b = f_{3,n} \sin n\pi\xi + f_{3,3n} \sin 3n\pi\xi \quad ,$$

then $$\bar{u}_b = f_{1,2n} \sin 2n\pi\xi + f_{1,4n} \sin 4n\pi\xi + f_{1,6n} \sin 6n\pi\xi$$

and $$\bar{v}_b = f_{2,o} + f_{2,2n} \cos 2n\pi\xi + f_{2,4n} \cos 4n\pi\xi + f_{1,6n} \cos 6n\pi\xi$$

[no sum on 'n'].

If the nodal lines are allowed to distort so that the buckling mode is allowed greater freedom, the description of 'w' must take the form

$$\bar{w}_b = f_{3,m} \sin m\pi\xi$$

(m = 1,3,5 ... n ...r); or (m = 2,4,6 ... n ... r)

Here 'm' assumes odd values for a buckling mode which is symmetric with respect to the central cross-section and even values for a mode which is antisymmetric. In either case $\bar{u}_b$ and $\bar{v}_b$ must be taken in the form

$$\bar{u}_b = f_{1,2m} \sin 2m\pi\xi$$

(m = 1,2, ... r)

and $$\bar{v}_b = f_{2,2m} \cos 2m\pi\xi$$

(m = 0,1,2, ... r)

In order to get an idea of the computational labour that may be involved in the use of these displacement functions, it is important to know the number of degrees of freedom associated with the finite strip . With 'w' represented by a single harmonic, say the n^{th}, the vector of degrees of freedom (i.e. the edge displacement parameters) associated with a strip is as follows:

$$\{ u_{1,2n} \quad v_{1,o} \quad v_{1,2n} \quad w_{1,n} \quad \theta_{1,n} \quad u_{2,2n} \quad v_{2,o} \quad v_{2,2n} \quad w_{2,n} \quad \theta_{2,n} \}$$

thus giving 10 degrees of freedom. This is a very small number for an entire strip end to end in comparison to the 20 degrees of freedom of the simplest rectangular plate bending element. However the strip developed here is a specialised one being applicable only for the post-local-buckling analysis.

Case (ii)

The case of plates and plate structures with the longitudinal edges fully restrained in the transverse direction will be considered next. The prebuckling equilibrium in this case can be characterised by

$$\varepsilon_x = -e$$

$$\varepsilon_y = 0$$

and therefore the prebuckling displacements take the form

$$u = e(\frac{a}{2} - x)$$

$$v = w = 0 \ .$$

The displacement functions for this case may be stated in the form

$$\bar{u} = f_{1m} \sin m\pi\xi + e\alpha(\tfrac{1}{2} - \xi)$$

$$\bar{v} = f_{2m} \cos m\pi\xi$$

$$\bar{w} = f_{3m} \sin m\pi\xi$$

The choice of the values which 'm' may take in each of the above expressions must be made in the same manner as explained for case (i).

3.2.1.3 Strain energy expression

In order to generate the equilibrium equations governing the problem, it is necessary to have recourse to a variational principle. For a plate structure under a prescribed uniform end compression, application of the virtual work theorem leads to the principle of

stationary strain energy.

The strain energy can be expressed as a sum of energy of inplane deformation and the energy of bending, each of which is given by 2.5(a-b). The expression for the strain energy can be built up with these expressions together with the strain displacement relations and the displacement functions 3.3(a-c). The strain displacement relations to be used for the post-local-buckling studies are:

$$\varepsilon_x = \frac{\partial u}{\partial x} + \frac{1}{2}\left(\frac{\partial w}{\partial x}\right)^2$$

$$\varepsilon_y = \frac{\partial v}{\partial y} + \frac{1}{2}\left(\frac{\partial w}{\partial y}\right)^2$$

$$\gamma_{xy} = \frac{\partial u}{\partial y} + \frac{\partial v}{\partial x} + \left(\frac{\partial w}{\partial x}\right)\left(\frac{\partial w}{\partial y}\right) \qquad \ldots 3.4(a\text{-}c)$$

The strain energy expression for the cases (i) and (ii) have been given in Appendix VI in full detail. For the case (i) this expression can be expressed in the same format as equation 2.7 in the following manner:

$$U = \frac{1}{2!}\left[A_{ij} - e(1-\nu^2)B_{ij}\right]q_i q_j + \frac{1}{3!}A_{ijk}\, q_i q_j q_k + \frac{1}{4!}A_{ijk\ell}\, q_i q_j q_k q_\ell \qquad \ldots 3.5\ (a\text{-}c)$$

$$(i,j,k,\ell = 1, \ldots N)$$

For the case (ii) it takes the form

$$U = -\nu e\, A_i q_i + \frac{1}{2!}\left[A_{ij} - e(B_{ij} + \nu C_{ij})\right] q_i q_j + \frac{1}{3!}A_{ijk}\, q_i q_j q_k + \frac{1}{4!}A_{ijk\ell}\, q_i q_j q_k q_\ell \qquad \ldots 3.6(a\text{-}c)$$

$$(i,j,k,\ell = 1, \ldots N)$$

As in eq. 2.7, q_i stand for the local degrees of freedom (u_{1m}, u_{2m} $\ldots\theta_{2m}$) which number 'N'; and the coefficients A_{ij}, A_{ijk}, $A_{ijk\ell}$ etc. are

symmetric with respect to each of their subscripts.

3.1.2.4 Expression for a typical edge force:

As a first step towards generating the equilibrium equations governing the problem, the expression for strain energy is differentiated with respect to a typical degree of freedom q_i, thus obtaining an expression for the corresponding edge force. For the case (i) this takes the form

$$E_i = \frac{\partial U}{\partial q_i} = \left[A_{ij} - e(1-\nu^2)B_{ij}\right]q_j + \frac{1}{2!} A_{ijk}\, q_j q_k + \frac{1}{3!} A_{ijk\ell}\, q_j q_k q_\ell \qquad \ldots 3.7$$

$$(j,k,\ell = 1, \ldots N);\ i = 1, \ldots N.$$

For the case (ii), the corresponding expression takes the form:

$$E_i = -\nu e A_i + \left[A_{ij} - e(B_{ij} + \nu C_{ij})\right]q_j + \frac{1}{2!} A_{ijk}\, q_j q_k + \frac{1}{3!} A_{ijk\ell}\, q_j q_k q_\ell \qquad \ldots 3.8$$

The expression 3.8 has the same form as 2.10 but in this case, the linear term does not lead to any nontrivial prebuckling displacements, as it is cancelled out when equilibrium equations are written for interior common edges of the strips and nonexistent in the equations for the junctions of the plates due to the presence of inplane constraints. Thus the linear term does not play any role in the analysis except to indicate that the plate will be subjected to a uniform compression in the transverse direction when all the buckling displacements vanish. In further discussion case (i) alone will be considered as the procedure for case (ii) is exactly alike.

3.2.1.5 Perturbation technique applied to buckling and initial postbuckling analysis

In order to generate a system of sequentially linear equations from the nonlinear expression of edge forces 3.7, it is necessary to differentiate it successively with respect to a suitably chosen parameter 'ε'. In the resulting expressions, we set $q_i = 0$ in order to obtain the bifurcation point and the characteristics of the secondary (postbuckling) path in the immediate vicinity of bifurcation. The result of these operations is a set of expressions; the first three of which are presented below:

$$E_{i_1} = \left.\frac{\partial E_i}{\partial \varepsilon}\right|_{\substack{q_i=o \\ \varepsilon=o}} = \{A_{ij} - e(1-\nu^2)B_{ij}\}q_{j1}$$

$$E_{i_2} = \left.\frac{\partial^2 E}{\partial \varepsilon^2}\right|_{\substack{q_i=o \\ \varepsilon=o}} = \{A_{ij} - e(1-\nu^2)B_{ij}\}q_{j2} - 2e_1(1-\nu^2)B_{ij}q_{j1} + A_{ijk}\, q_{j1}q_{k1}$$

$$E_{i_3} = \left.\frac{\partial^2 E}{\partial \varepsilon^2}\right|_{\substack{q_i=o \\ \varepsilon=o}} = \{A_{ij} - e(1-\nu^2)B_{ij}\}\, q_{j3} - 3e_2\,(1-\nu^2)B_{ij}q_{j1}$$
$$-3e_1(1-\nu^2)\,B_{ij}q_{j2} + 3A_{ijk}\, q_{j1}q_{k2} + A_{ijk\ell}\, q_{j1}q_{k1}q_{\ell 1}$$

. . . 3.9(a-c)

The meaning of these expressions may be seen from the Taylor's expansion for E_i at the bifurcation point, which is

$$E_i = E_{i_1}\varepsilon + \frac{1}{2!}E_{i_2}\varepsilon^2 + \frac{1}{3!}E_{i_3}\varepsilon^3 \qquad \ldots 3.10$$

An ordered set of equilibrium equations can be generated in the same manner as described in chapter 2 corresponding to each of these expressions.

The first of these equations leads to a set of homogeneous equations and constitutes an eigenvalue problem. The lowest eigenvalue gives the critical value of e, e_{cr} at which buckling occurs. Keeping in mind that the plate is under uniaxial compression prior to buckling, the buckling stress is Ee_{cr}. (For case (ii) the buckling stress will be $Ee_{cr}/(1-\nu^2)$).

Note that the coefficient matrix built of the matrices $\{A_{ij} - e(1-\nu^2)B_{ij}\}$ of individual strips remains the same for each of the perturbation equations, a helpful factor in computation. Further the system of equations is banded and symmetric and this must be taken advantage of to economise on the computational effort.

With a proper choice of the perturbation parameters, the buckling mode is obtained with $\varepsilon_1 = 1$. In order to get a meaningful result, this parameter must not be identified with 'e' which plays the role of a loading parameter in this problem[97]. It will be convenient, as is explained in the next paragraph, to identify 'ε' with one of the global degrees of freedom Q_r.

The total number of second order equations which are obtained from 3.9(b) is less than the total number of unknowns they involve, for there is an additional unknown e_1, which appears in these equations. But an additional equation may be written which is $Q_{r_2} = 0$. The existence of the additional unknown and the importation of the extra equation, together, would destroy the symmetric banded structure of the equations and therefore a straightforward solution of these equations is not attempted. Instead the value of e_1 is first extracted using a "contraction mechanism"[97]. Substituting the value of e_1 in these equations and making the use of the information $Q_{r_2} = 0$, (as if it is

a boundary condition) it is possible to solve the remaining global degrees of freedom (Q_{i_2}'s) from the remaining set of banded and symmetrically structured equations. The local degrees of freedom (q_{i_2}'s) are obtained from the Q_{i_2}'s, to be used for further analysis.

The same procedure is employed to calculate e_2 and q_{i_3}'s from the third order equations derived from 3.9(c).

The buckling displacements and the average strain of the entire plate assembly given by 'e', in the immediate vicinity of bifurcation point can be obtained from the Taylor's series:

$$q_i = q_{i_1}\varepsilon + \frac{1}{2!} q_{i_2}\varepsilon^2 + \frac{1}{3!} q_{i_3}\varepsilon^3$$

$$e = e_{cr} + e_1\varepsilon + \frac{1}{2!} e_2\varepsilon^2 \qquad \ldots 3.11(a\text{-}b)$$

It is not proposed to improve the solution by considering the higher order equations, as an iterative procedure will be used to correct this solution.

As has been demonstrated in earlier perturbation solutions[21,25] of plates with 'uncoupled' boundary conditions, it can be seen here also that

(i) 1st order perturbation terms corresponding to inplane displacements vanish i.e. buckling mode is characterised by normal displacements (w) alone.

(ii) 2nd order perturbation terms corresponding to normal displacements vanish and the bifurcation is symmetric, i.e. $e_1 = 0$

(iii) 3rd order perturbation terms corresponding to inplane displacements vanish and so on.

3.2.1.6 Application of boundary conditions

As explained earlier, a special feature of the version I is the manner in which the boundary conditions along the junctions of the plate are stipulated. In this section the manner of implementing the boundary conditions in the computational scheme is described for the case (i) of the version. Similar procedure is applicable for case (ii).

Along a junction 'B' where two plates (1) and (2) meet at an angle as shown in Fig. 3.5(a), no attempt is made to enforce the continuity of displacements in the transverse plane. But instead the normal displacements in each of the strips AB of plate (1) and BC of plate (2) are assumed to be zero; the plates are, in addition, assumed to be free from normal stresses in the transverse direction along the junction. The conventional finite element technique must be modified in the following manner, in order to implement these conditions:-

(i) The global degrees of freedom of the structure are defined in the same sense as the local degrees of freedom of the individual strips. Thus the stiffness matrices of the individual strips can be used straight away to form the global stiffness matrix, without any transformation.

(ii) The transverse displacements along the junction each of the strips AB and BC (Fig. 3.5) are treated as two independent degrees of freedom. This ensures that the forces corresponding to each vanish separately as the strain energy is maintained stationary with respect to each degree of freedom representing the transverse displacements.

(iii) The normal displacements of the strips AB and BC along B are assumed to vanish and eliminated by the application of boundary conditions. These degrees of freedom may be assigned the same number, in order to reduce the total number of degrees of freedom. A possible system of numbering the strips AB and BC is shown in Fig. 3.5 (b).

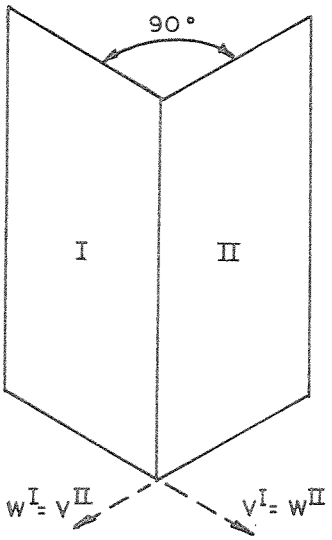

Fig. 3.4 Compatibility of Junction Displacements.

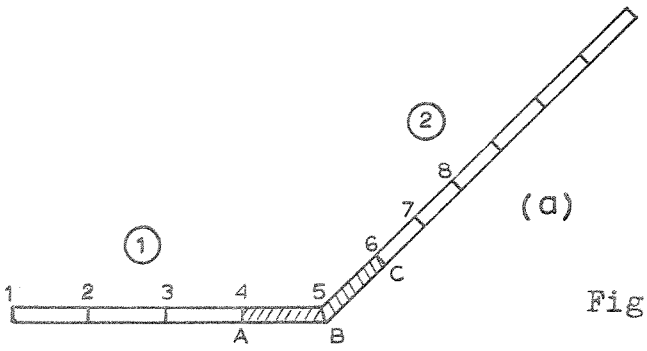

Fig 3.5 Numbering of the Degrees of Freedom along the Junction BB.

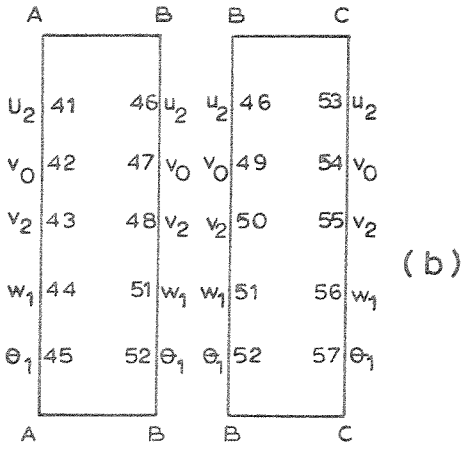

(iv) It is necessary to eliminate the rigid body translation of each of the plates in the transverse direction, in order to prevent the stiffness matrix becoming singular. This can be done by stipulating either $v_{1,o}$ or $v_{2,o}$ of one of the strips constituting the plate to be zero. Note that these represent displacements which are constant all along the edges of the strip.

3.2.1.7 Postbuckling analysis by direct solution of nonlinear equations

The solution generated using the perturbation technique described in the previous section is an approximate one for the nonlinear problem as only a limited number of terms can be considered in the Taylor's series expansion 3.10. Further the accuracy of the solution can be judged only by comparison with the already known accurate solution of the problem and can not be known a priori. An exact solution of the nonlinear equations governing the problem is essential for a complete analysis and the perturbation solution described in the previous section is but a necessary starting point for obtaining the same.

While there are several approaches for the solution of the nonlinear equations[104], what is described in the following is one of the simplest, most commonly used and the most reliable approach. This is based on a prediction of increments in the displacements for a chosen increment in the loading parameter (in our case 'e') and correction of the obtained solution by the Newton-Raphson iterative procedure. This is briefly described here for the sake of completeness.

Perturbation Preidctor

We recall that a typical edge force in the strip is given by the expression

$$E_i = \frac{\partial U}{\partial q_i} = \left[A_{ij} - e(1-\nu^2)B_{ij}\right]q_j + \frac{1}{2!} A_{ijk}\, q_j q_k + \frac{1}{3!} A_{ijk\ell}\, q_j q_k q_\ell$$

. . . 3.7 (repeated)

Let it be assumed that an equilibrium state in the nonlinear solution path is known. Let this be designated as (e_o, q_{i_o}). The rate of change of the edge force E_i, at (e_o, q_{i_o}) with respect to e may be found by differentiating the expression 3.7 by e.

$$\left.\frac{\partial E_i}{\partial e}\right|_{\substack{q_i = q_{i_o} \\ e = e_o}} = \left[A_{ij} - e(1-\nu^2)B_{ij} + A_{ijk}\, q_{ko} + \frac{1}{2!} A_{ijk\ell}\, q_{ko} q_{\ell o}\right] q_{j1} - (1-\nu^2)B_{ij}\, q_{jo}$$

$$(j,k,\ell = 1, \ldots N)$$

$$i = 1, \ldots N$$

. . . 3.12

where q_{i_1} stands for the rate of change of q_i with respect to e.

The matrix $\left[A_{ij} - e(1-\nu^2)B_{ij} + A_{ijk}\, q_{ko} + \frac{1}{2!} A_{ijk\ell}\, q_{ko} q_{\ell o}\right]$ gives the so called incremental stiffness matrix which incorporates within itself

a) The "Linear" stiffness matrix, whose elements are coefficients of linear terms in 3.7, $[A_{ij}]$.

b) The matrix giving the destabilising effects of applied longitudinal compression given by $[B_{ij}]$

and c) the geometric stiffness matrix which gives the geometric effects due to finite displacements given by $\left[A_{ijk}\, q_{ko} + \frac{1}{2!} A_{ijk\ell}\, q_{ko} q_{\ell o}\right]$. The column matrix $\{(1-\nu^2)B_{ij}\, q_{jo}\}$ plays the role of applied loads. The incremental stiffness matrices of the strips are assembled to build the global incremental stiffness matrix. This is the coefficient matrix of the system of equations in terms of the global degrees of

freedom. The column vectors $\{(1-\nu^2)B_{ij}\ q_j\}$ of the strips are assembled to form the right hand side of this system of equations. The boundary conditions are applied and the system of equations solved to obtain q_{i_1}'s.

Let the value of 'e' be incremented by Δe, so that the new value of 'e' is given by $e_o + \Delta e$. An approximate solution q_i^a for the buckling displacements corresponding to this value 'e' is given by

$$q_i^a = q_{i_o} + \Delta e . q_{i_1}$$

This method of prediction outlined above is called the "incremental approach" and can be used as such to trace the nonlinear solution. The major disadvantage with this approach is that the errors in the solution tend to accumulate with increasing number of steps and the magnitude of the errors remains unknown. Therefore it is necessary to employ an iterative correction procedure to eliminate these errors.

Newton-Raphson Correction

Let q_i^c bt the correction to be made to a typical degree of freedom, so that

$$q_i = q_i^a + q_i^c \qquad \ldots 3.13$$

where q_i are the degrees of freedom corresponding to $e = e_o + \Delta e$.

Substituting 3.13 in 3.7, we obtain the edge forces E_i in terms of the unknowns q_i. Linearising this expression with respect to q_i^c in view of its smallness in comparison to q_i^a we obtain

$$E_i = \left[A_{ij} - e(1-\nu^2)B_{ij} + A_{ijk}\, q_k^a + \frac{1}{2!} A_{ijk\ell}\, q_k^a\, q_\ell^a\right] q_j^c + E_i^a \qquad \ldots 3.14$$

where E_i^a stands for the edge force as given by the approximate set of

displacements q_i^a and is given by

$$E_i^a = \left[A_{ij} - e(1-\nu^2)B_{ij}\right]q_j^a + \frac{1}{2!}A_{ijk}\,q_j^a\,q_k^a + \frac{1}{3!}A_{ijk\ell}\,q_j^a\,q_k^a\,q_\ell^a \qquad \ldots 3.15$$

The stiffness matrix as given by the term within the brackets in 3.14 is assembled as before to form the improved global stiffness matrix; as also the column vectors $\{E_i^a\}$ to form the right hand side of the corresponding system of equations. The solution of these equations leads to the corrections to the local degrees of freedom and thus an improved solution vector is obtained. The procedure is repeated till the desired accuracy is achieved. As q_i^a approaches the correct solution q_i, E_i^a in 3.14 approaches the correct value E_i of edge force and each term on the right hand side of the equation tends to zero by virtue of the equilibrium conditions; as a result the corrections q_i^c also tend to zero. This process can be terminated as soon as the corrections become negligibly small.

While there are several convergence criteria used in computations (Ref.46), the one used in the present work is that the sum of the squares of the terms appearing on the right hand side of the equations (which represent unbalanced forces) be less than a small stipulated value. This criterion was found to be simple to use and reliable.

3.2.1.8 Computer programme for Version I

The details of the computer programme based on the procedure outlined in this section (PLAPAV1) are given in Appendix VII.

3.2.2 Version II

In this section we present the formulation of the version II of the finite strip method for the post-local-buckling analysis. The general approach has much in common with version I and therefore the emphasis in the following sections will be on the points of contrast.

3.2.2.1 Boundary conditions at the ends of the plate

In this version the boundary conditions are assumed in the following form:

$$w = 0$$

$$\frac{\partial^2 w}{\partial x^2} = 0$$

$$v = 0$$

$$u = u_o \qquad \ldots 3.16(a\text{-}d)$$

$$\text{at } x = 0 \text{ and } x = a$$

These conditions are the same as those used in version I but for the condition 3.16(c) which prescribes the inplane displacements (and not inplane shear stresses) as zero at the ends. This condition read together with 3.16(a) for each of the strips means that the end cross-sections do not undergo any distortion.

Unlike conditions 3.1, these conditions are logically coherent and are probably realised in practical situations where there is considerable friction between the device applying the load and the ends of the plates.

3.2.2.2 Displacement functions

In this version, no approximations are made in the treatment of boundary conditions along the junctions. Therefore 'w' and 'v' must be

described by expressions which have the same form of variation in the longitudinal direction. To satisfy this condition and the boundary conditions 3.16, the displacement functions may be taken in the form

$$\bar{u} = f_{1m} \sin m\pi\xi + e\alpha(\tfrac{1}{2} - \xi) \qquad (m = 2,4,6 \ldots)$$

$$\bar{v} = f_{2m} \sin m\pi\xi$$

$$w = f_{3m} \sin m\pi\xi \qquad (m = 1,3,5 \ldots)$$

$$\ldots 3.17(a\text{-}c)$$

The prescription of values in the parentheses in the above equations restricts the scope of the displacement functions to problems where the buckling mode is symmetric with respect to the central transverse plane of the structure. This has been done deliberately in order to restrict the terms to a small number. If, on the other hand, the buckling mode is antisymmetric with respect to the centre, the description of u and v must both involve even and odd harmonics. For example, if

$$w = w(y) \sin 2m\pi\xi$$

then $\left(\frac{\partial w}{\partial y}\right)^2 = \left[w'(y)\right]^2 \sin^2 2m\pi\xi$;

Thus $\left(\frac{\partial w}{\partial y}\right)^2$ is an even function with respect to the centre. To pair with this in the strain displacement relations for ε_y, 'v' must contain odd harmonics in its description. But since it must also have the same form of variation as 'w' in the longitudinal directions, it follows that both 'w' and 'v' must be described in terms of odd and even harmonics.

The functions f_{1m}, f_{2m} and f_{3m} which describe the variation of displacements in terms of edge displacement parameters u_{1m}, u_{2m} ... θ_{2m}

have the same meaning as in equations 3.3. The choice of the number of terms in each of the series must be made from considerations of convergence of the solution. In order to ensure compatibility of displacements along the junction, the displacements 'w' and 'v' must each be represented by the same number of terms. A modification of this approach is possible, where the compatibility condition is satisfied but only partially; here 'w' would be described by a smaller number of terms than 'v', thus simplifying the computation a great deal. Such a modification will be discussed in 3.2.2.7.

3.2.2.3 Strain- energy expression

The expression for internal strain energy is built as before using the equations 2.5(a-b) and the strain displacement relations 3.4(a-c) in terms of displacement parameters. This expression is given in Appendix VIII in full detail. For purposes of further discussion, it is taken in the term

$$U = -\nu A_i e\, q_i + \frac{1}{2!}\left[A_{ij} - e(B_{ij} + \nu C_{ij})\right] q_i q_j + \frac{1}{3!} A_{ijk}\, q_i q_j q_k + \frac{1}{4!} A_{ijk\ell}\, q_i q_j q_k q_\ell \quad \ldots 3.18$$

The presence of the linear term (which does not vanish in the equilibrium equations as the edges need, in general, not all carry inplane constraints unlike in case (ii) of version I) plays the same role as in 2.7, of ensuring that the prebuckling path will be nontrivial.

3.2.2.4 Analysis of the prebuckling state of equilibrium

The investigation of the prebuckling state of equilibrium has been found to be necessary in chapter 2 in certain cases of plate assemblies

for a proper buckling analysis. Thus a generalised approach to the problem of post-local-buckling analysis must have built into it as a preliminary, the analysis of prebuckling state of equilibrium. This analysis has already been discussed in section 2.2.4 and will not be repeated here. The prebuckling equilibrium path is assumed to be linear as before and the prebuckling displacement parameters can be expressed as before, in the form

$$q_i^p = e\, q_{i_1}$$

3.2.2.5 Perturbation technique applied to buckling and initial post-buckling analysis

The analysis which follows has many similarities with that discussed in 3.2.1 under version I and the bifurcation analysis in chapter 2. The essential difference between the present analysis and that in version I is that the prebuckling equilibrium path is nontrivial in the present case. Thus it may be viewed as a continuation of the analysis in chapter 2, but with different displacement functions as its starting point. These displacement functions are found to be necessary to depict the more realistic boundary conditions at the ends, which have a great bearing on the behaviour of the plate structure in the postbuckling behaviour.

Let the displacements on the primary path be denoted by q_i and the incremental displacements to the secondary path be denoted by v_i (Fig. 2.5), so that the displacements on the secondary path are denoted, as before by

$$q_i^s = q_i^p + v_i$$

From 3.13, the expression for the "sliding increment" in the edge force,

from an equilibrium state in the primary path to another in the secondary path, both corresponding to the same value of 'e', can be written in the form

$$F_i = E_i^s - E_i^p = \left[A_{ij} - e(B_{ij} + \nu C_{ij} - A_{ijk}\, q_{k_1})\right] v_j + \frac{1}{2!} A_{ijk}\, v_j v_k + \frac{1}{3!} A_{ijk\ell}\, v_j v_k v_\ell$$

This expression for F_i provides the basis for developing equilibrium equations (as does expression 3.7 for version I) for the plate assembly.

The perturbation expressions for the sliding incremental edge force take the form, at the bifurcation point ($v_i = 0$)

$$F_{i,1} = \left.\frac{\partial F_i}{\partial \varepsilon}\right|_{v_i=o} = \{A_{ij} - e(B_{ij} + \nu\, C_{ij} - A_{ijk}\, q_{k_1})\}\, v_{j_1}$$

$$F_{i,2} = \left.\frac{\partial^2 F_i}{\partial \varepsilon^2}\right|_{v_i=o} = \{A_{ij} - e(B_{ij} + \nu\, C_{ij} - A_{ijk}\, q_{k_1})\}\, v_{j_2} - 2e_1\left[B_{ij} + \nu\, C_{ij} - A_{ijk}\, q_{k_1}\right] v_{j_1} + A_{ijk}\, v_{j_1} v_{k_1}$$

$$F_{i,3} = \left.\frac{\partial^3 F_i}{\partial \varepsilon^3}\right|_{v_i=o} = \{A_{ij} - e(B_{ij} + \nu\, C_{ij} - A_{ijk}\, q_{k_1})\}\, v_{j_3} - 3e_2\{B_{ij} + \nu\, C_{ij} - A_{ijk}\, q_{k_1}\}\, v_{j_1} - 3e_1\left[B_{ij} + \nu\, C_{ij} - A_{ijk}\, q_{k_1}\right] v_{j_2} + 3A_{ijk}\, v_{j_1} v_{k_2} + A_{ijk\ell} v_{j_1} v_{k_1} v_{\ell_1}$$

. . . 3. 19(a-c)

As before the set of equilibrium equations built using the first order perturbation expression 3.19(a) leads to an eigenvalue problem, the solution of which gives the critical load. Sequential solution of higher order equations as in 3.2.1.5 leads to a solution of incremental displacement v_i in the form

$$v_i = v_{i_1}\varepsilon + \frac{1}{2!} v_{i_2} \varepsilon^2 + \frac{1}{3!} v_{i_3} \varepsilon^3 \qquad \ldots 3.20$$

$$(i = 1, \ldots N)$$

corresponding to an 'e' given by

$$e = e_{cr} + e_1\varepsilon + \frac{1}{2!} e_2\varepsilon^2$$

The displacements in the postbuckling path with respect to the unloaded state for any 'e' are given by

$$q_i^s = q_i^r + v_i$$

$$= eq_{i_1} + v_i \qquad \ldots 3.21$$

$$(i = 1, \ldots N)$$

These provide approximate solutions for the displacements in the secondary path required for the direct solution of nonlinear equations governing the problem.

3.2.2.6 Postbuckling analysis by the direct solution of nonlinear equations

The procedure for the solution of equations using the perturbation prediction and Newton-Raphson correction is the same as outlined for version I except for the following points of difference:

The solution is sought for the total displacements in the secondary path and not for buckling displacements as in version I. The expression for the edge force in the secondary path is given by

$$E_i^s = - \nu e A_i + \left[A_{ij} - e(B_{ij} + \nu C_{ij})\right] q_j^s$$

$$+ \frac{1}{2!} A_{ijk} q_j^s q_k^s + \frac{1}{3!} A_{ijk\ell} q_j^s q_k^s q_\ell^s$$

as in 2.11. Note that this expression, which is the basis for the solution of the nonlinear problem, includes a constant term absent in the corresponding expression 3.7 of version I.

3.2.2.7 A variation of version II (Version IIA)

As already stated, it is possible in most postbuckling problems to describe 'w' accurately in terms of one or two harmonics, but not 'v'. This is especially the case with longer plate assemblies which buckle with several half waves along the length of the plate. If 'w' is described by a smaller number of terms than 'v', the compatibility of junction displacement will not be satisfied for the set of harmonics which are present in the description of v but absent in that of 'w'. But this may be justified in many situations for reasons already discussed in 3.1.3.1 under version I, where no attempt is made to enforce the compatibility of displacements in the transverse plane along the junctions at all.

The modification of the version II suggested here is a via media between the version I and the more exact version of II discussed earlier in this section, from the point of view satisfying the compatibility of displacements along the junction. Here 'w' is described by a comparatively smaller number of terms say 'm' than 'v' which is described by say 'n' terms. The number of degrees of freedom for the strip is reduced therefore by 4(n-m) and as a consequence there could be significant reductions in the bandwidth of the global stiffness matrix

as well as in the total number of degrees of freedom.

As developed in the present investigation, this modification is applicable only for plate assemblies which consist of junctions which come under the categories of a "corner", "transition" and "branch point" as described in 3.1.3.1. While equilibrium equations are developed in terms of edge forces for the first 'm' harmonics in the usual manner, the plates are assumed to be free from any inplane normal forces corresponding to the remaining 'n-m' harmonics. This is accomplished in the following manner.

(i) The global degrees of freedom along all the edges of the strips are defined as having the same orientation as the local degrees of freedom except along the junctions. Along the junctions the global degrees of freedom corresponding to the 'w' and 'v' of the 'm' common harmonics is defined in the directions of the local degrees of freedom of one of the plates. The degrees of freedom corresponding to 'v' in the remaining n-m harmonics for the strips along the junction are defined as independent global degrees of freedom.

(ii) For the strips with one of their edges coinciding with a junction on the plates, special transformation matrices must be employed which do not transform any but the degrees of freedom occurring in the common 'm' harmonics describing 'w' and 'v' along the junction.

3.2.2.8 Computer Programme

The details of the computer programme (PLAPAV2) using the version II as outlined in sec. 3.2.2 are described in Appendix VII.

3.3 Simplifications of the analysis

The major difficulty in the analysis outlined above is that the number of nonlinear coefficients becomes disproportionately large as increasing number of harmonics are taken into account in the calculation. This is especially true of the coefficients of the quartic term in the strain energy expression (Refer Appendix V) which involves only the normal displacements. In an expansion of the type

$$A_{ijk\ell}\, q_i q_j q_k q_\ell \qquad \ldots 3.22$$

$$(i = 1, \ldots n$$
$$j = 1, \ldots n$$
$$k = 1, \ldots n$$
$$\ell = 1, \ldots n)$$

the total number of $A_{ijk\ell}$'s is n^4. Since 4 degrees of freedom are associated with each harmonic, the total number of nonlinear coefficients in the expansion will be $(4m)^4$ where 'm' is the number of harmonics considered in the solution.

In order to achieve maximum simplicity and efficiency of the computation the following devices can be employed:

1. In the expression 3.22, $A_{ijk\ell}$ is symmetric with respect to each of the subscripts i, j, k and ℓ and therefore most of the terms repeat themselves, in the expansion. A great deal of simplification can be achieved if only the independent terms in the expansion are computed and used in building the stiffness matrices. Table 3.1 gives the total number of terms in the expansion and the total number of independent terms thereof as the number of harmonics is increased from 1 to 5. An algorithm for obtaining an expansion of $A_{ijk\ell}$ and computing the edge forces and elements of stiffness matrix resulting

Table 3.1

No. of harmonics representing 'w'	Corresponding no. of degrees of freedom	Total number of terms in the expansion A_{ijkl}	The number of independent terms
1	4	256	35
2	8	4,094	330
3	12	20,736	1,365
4	16	65,536	3,900
5	20	160,000	8,855

therefrom, using only the independent terms is described in Appendix VIII.

2. In version II, the number of terms representing 'w' are the same as that representing 'v'. However the nonlinear effects of all the harmonics of 'w' may not all be equally significant. These nonlinear effects arise as a result of the nonlinear terms in the strain displacement relations. The strain energy expression, may therefore be built up by considering the nonlinear terms corresponding to a suitably chosen number of harmonics, the rest being neglected.

For example, consider the problem of the plate structure in Fig. 3.15(a). Let 'w' and 'v' both be represented by 5 harmonics, so that

$$w = \sum w_n(n) \sin m\pi\xi$$

$$v = \sum v_m(n) \sin m\pi\xi$$

$$(m = 1,3, \ldots 9).$$

Since the length of the plate is the same as the width of each plate, the harmonic corresponding to m=1 gives the buckling mode and is the most important in the description of 'w'. In order to consider the flattening effect of wave form in the longitudinal direction, it may be necessary to consider the nonlinear effects of one or two additional harmonics, say m=3 and 5. The rest of the harmonics m=7 and 9 may be neglected in building the expressions for ε_x, ε_y and γ_{xy} which involve nonlinear terms in 'w'.

These devices of simplifying the calculations have been built into the computer programmes described in Appendix VII.

3.4 Special problems related to advanced post-local-buckling analysis

In this section reference will be made to two specific problems associated with advanced (elastic) post-local-buckling behaviour of plate assemblies which can be dealt with by the methods described in this chapter, with certain modifications. The first is the problem of change of longitudinal wave form of the buckled plate from one with say 'm' half waves to another with 'n' half waves. The second is the complete loss of stiffness of the locally buckled structure leading to its collapse.

3.4.1 Change of wave form:

Consider a plate which buckles into 'm' half sine waves and let us enquire whether there exists a possibility of a change of this wave form to one with 'n' half waves.

Let 'w' be assumed to have two sets of degrees of freedom corresponding to the two wave forms i.e.

$$\bar{w} = f_{3m} \sin m\pi\xi + f_{3n} \sin n\pi\xi \qquad \ldots 3.23$$

(no sum on 'm' or n)

where f_{3m} and f_{3n} are functions of η defined in 3.3(c).

Some care must be exercised in the choice of displacement functions describing $\bar{u}$ and $\bar{v}$. If for instance, version I is adopted (which is by far the simpler of the two versions) these must be chosen in the manner described in 3.2.1.2. Thus

$$\bar{u}_b = \sum_i \sum_j f_{1,i+j} \sin[(i+j)\pi\xi] + \sum_i \sum_j f_{1,i-j} \sin[(i-j)\pi\xi]$$

$$\bar{v}_b = \sum_i \sum_j f_{2,i+j} \cos[(i+j)\pi\xi] + \sum_i \sum_j f_{2,i-j} \cos[(i-j)\pi\xi]$$

$$\left.\begin{matrix} i = m,n \\ j = m,n \end{matrix}\right\}$$

(The terms which are repetitions of the terms once included may be dropped from the functions; $\bar{u}_b$ and $\bar{v}_b$ represent the buckling displacements).

The solution paths corresponding to each of the buckling modes are traced in steps and at each step the positive definiteness of the second variation of the strain energy expression is investigated. This is done by examining the positive definiteness of the global incremental stiffness matrix for which standard techniques are available. (It can be established by a Taylor's series expansion of the strain energy of the strip, that the incremental stiffness matrix of the strip gives the second variation of the strain energy of strip and therefore the global incremental stiffness matrix represents the second variation of strain energy of the entire structure). If at a step the matrix changes its character i.e. it either ceases to be or becomes positive definite it is an indication of change of stability. With the exclusion of a 'limit point', the change of stability is an indication that there occurs a bifurcation of equilibrium i.e. the equilibrium path corresponding to an uncoupled buckled mode is intersected by one with a coupled mode.

The following possibilities arise:

Case (i): The primary buckling path corresponding to 'm' half waves does not lose stability at all; while the secondary buckling path becomes stable at a certain value of 'e'. (Fig. 3.6(a)).

Case (ii): The primary buckling path loses its stability at a value of e, say e_m, while the secondary path becomes stable at a value of e, say e_n. (Fig. 3.6(b-c)).

Case (iii): The primary buckling path becomes unstable while the secondary path continues to be unstable (Fig. 3.6(d)).

Each of these cases is discussed in the following:

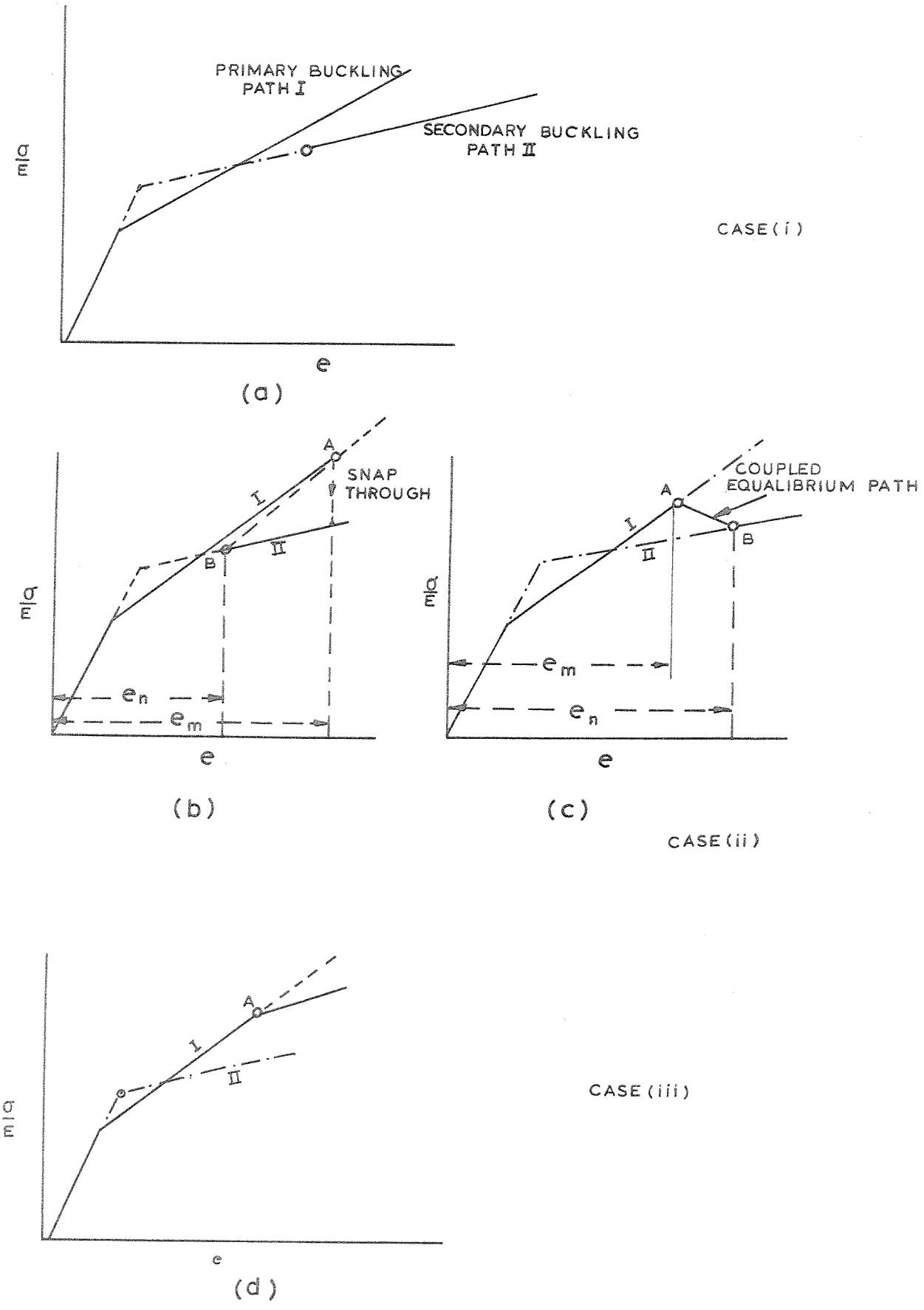

Fig. 3.6 Different Conditions determining the Change of Wave Form.

Taking the case (i), no change of wave form would occur, as the primary path continues to be stable. The fact that there occurs a change of stability for the secondary buckling path indicates the existence of a tertiary coupled equilibrium path, not connected with the primary path. This may have a significance only in the presence of initial imperfections in the shape of the secondary buckling mode.

For the case (ii), the change of wave form does occur at the point where the primary buckling path loses its stability. This change of wave form will be abrupt if $e_m > e_n$ (Fig. 3.6(a)) and will be gradual if $e_m < e_n$ (Fig. 3.6(c)). There exists a coupled tertiary equilibrium path connecting the equilibrium paths at the points A and B where changes of stability occur. This path can be shown to be stable under controlled end shortening[17] if $e_m < e_n$ and unstable if $e_m > e_n$.

For the case (iii) the primary path becomes unstable due to the intersection with a coupled tertiary equilibrium path, not connected with the secondary buckling path. (Fig. 3.6(d)).

The problem is discussed later in the chapter with two numerical examples.

3.4.2 Loss of stiffness of the plate structure due to elastic collapse of the junctions

As the plate assembly is subjected to increasing end compression, much beyond the critical load, the normal displacements continue to grow at a more or less steady rate. This is accompanied by an increasing concentration of longitudinal stresses near the junctions on the one hand and the waving in of the junctions on the other. At a certain stage the inplane displacements in the transverse directions for each plate along the junctions approach such magnitudes as to initiate a column-type collapse of one or more junctions. This further aggravates

the normal deflections in the plate and results in a complete loss of stiffness of the structure and the plate structure starts shedding load, under controlled end compression. At this stage there often occurs a snapthrough type of buckling of the structure resulting in an abrupt drop of the load. The problem of prediction of the collapse load can be tackled using a modification of the version II of the finite strip method developed in this chapter, but further discussion of this subject is postponed until chapter 5.

3.5 Illustrative examples

It is proposed to present a few numerical examples with the following objectives in view:

1. To study the convergence of the solution as given by the two versions and incidentally to check the accuracy of the computer solutions. This is done by comparison with existing solutions.

2. To illustrate the greater efficiency of the finite strip approach in comparison with the finite element method for the postbuckling problems.

3. To illustrate with numerical examples, the procedure to study the changes in wave form outlined in 3.4.1, and to study the influence of coupling in boundary conditions along the longitudinal junction by means of an example.

3.5.1 Study of convergence and accuracy of solutions: Version I

3.5.1.1 Postbuckling stiffness of a simply supported square plate

The first example considered is that of a square plate simply supported on all its edges. In this section we study the convergence of the postbuckling stiffness to the known exact values. The first case studied is that of a plate with unloaded edges free to move but

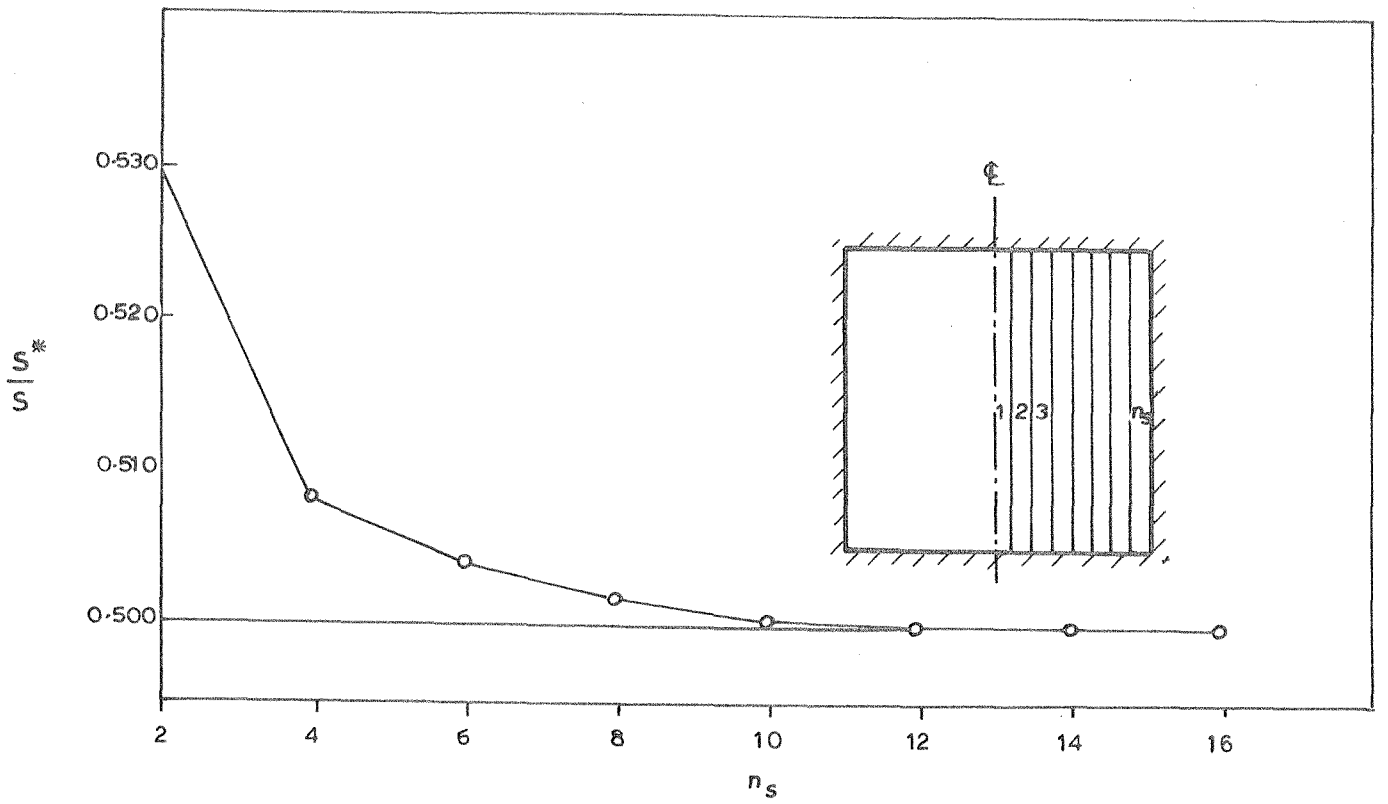

Fig. 3.7 Convergence Study on a Simply Supported Square Plate with the Unloaded Edges Free to move, but held Straight.

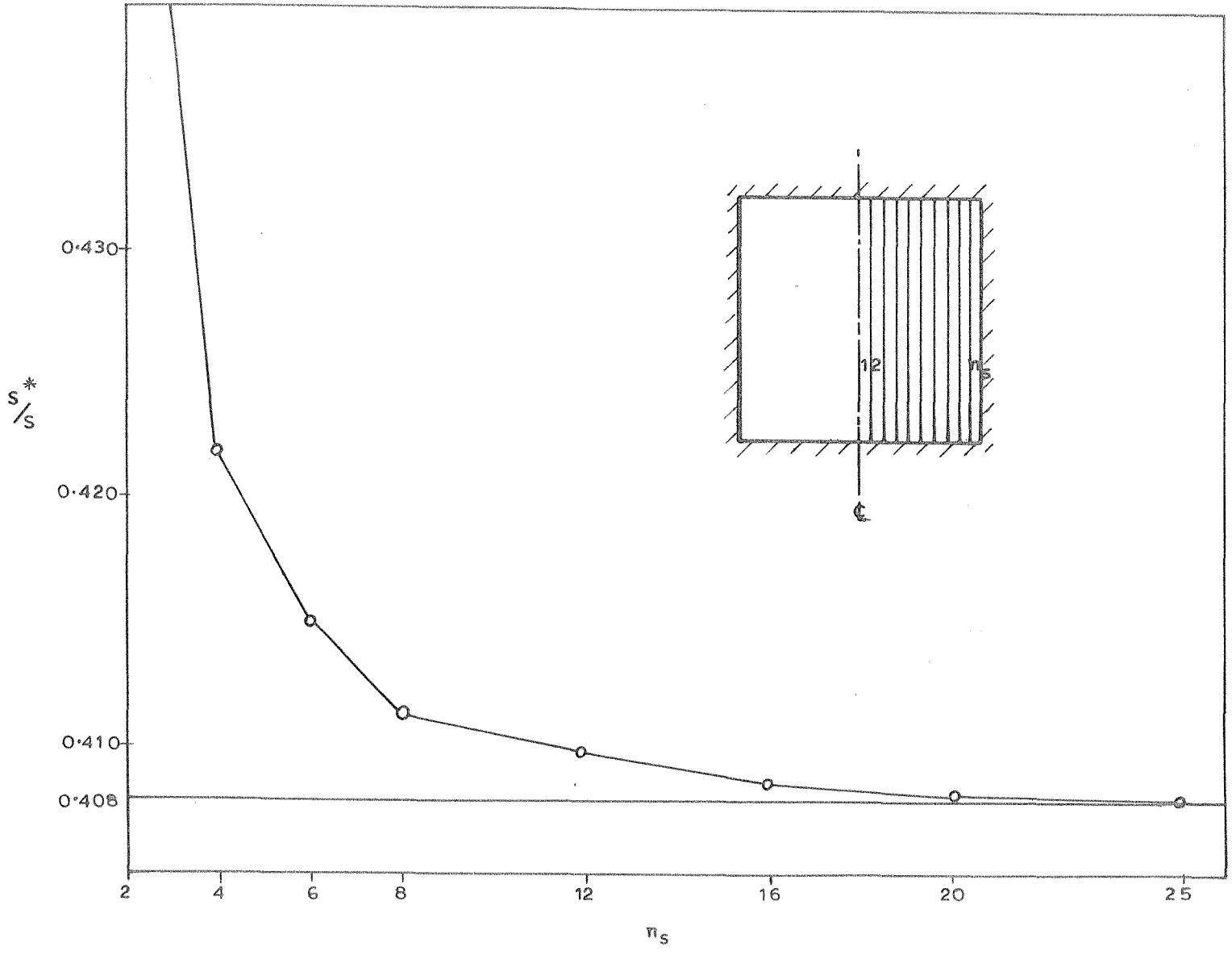

Fig. 3.8 Convergence study on a Simply Supported Square Plate with the Unloaded Edges Free to Wave.

held straight. The ratio of postbuckling stiffness to the prebuckling stiffness (S*/S) obtained with increasing number of elements is shown in Fig. 3.7. The convergence to correct value of 0.5 reported by Cox[26] is rapid and monotonic. With 6 elements in the half plate the value of S*/S is obtained within an error of 1%. The results of a similar convergence study on a simply supported square plate with the unloaded edges free to wave are shown in Fig. 3.8. Here the convergence is found to be slower than in the previous case as a result of the additional force boundary condition this problem involves.

3.5.1.2 Postbuckling behaviour of square plate under different boundary conditions

The square plate problem is next studied under the following sets of boundary conditions in the postbuckling range upto a point where the applied stress exceeds 3 to 4 times the critical. In all the cases the square plate is simply supported along one pair of opposite edges.

Plate I(a): The unloaded edges are simply supported and allowed to move, but held straight.

Plate I(b): The unloaded edges are simply supported and free to wave in the plate of the plate.

Plate II(a): The unloaded edges are clamped and allowed to move but held straight.

Plate II(b): The unloaded edges are clamped and free to wave in the plane of the plate.

The problem was studied with the normal displacement 'w' represented by two terms in the following manner:

$$\bar{w} = f_{3,1} \sin\pi\xi + f_{3,3} \sin 3\pi\xi$$

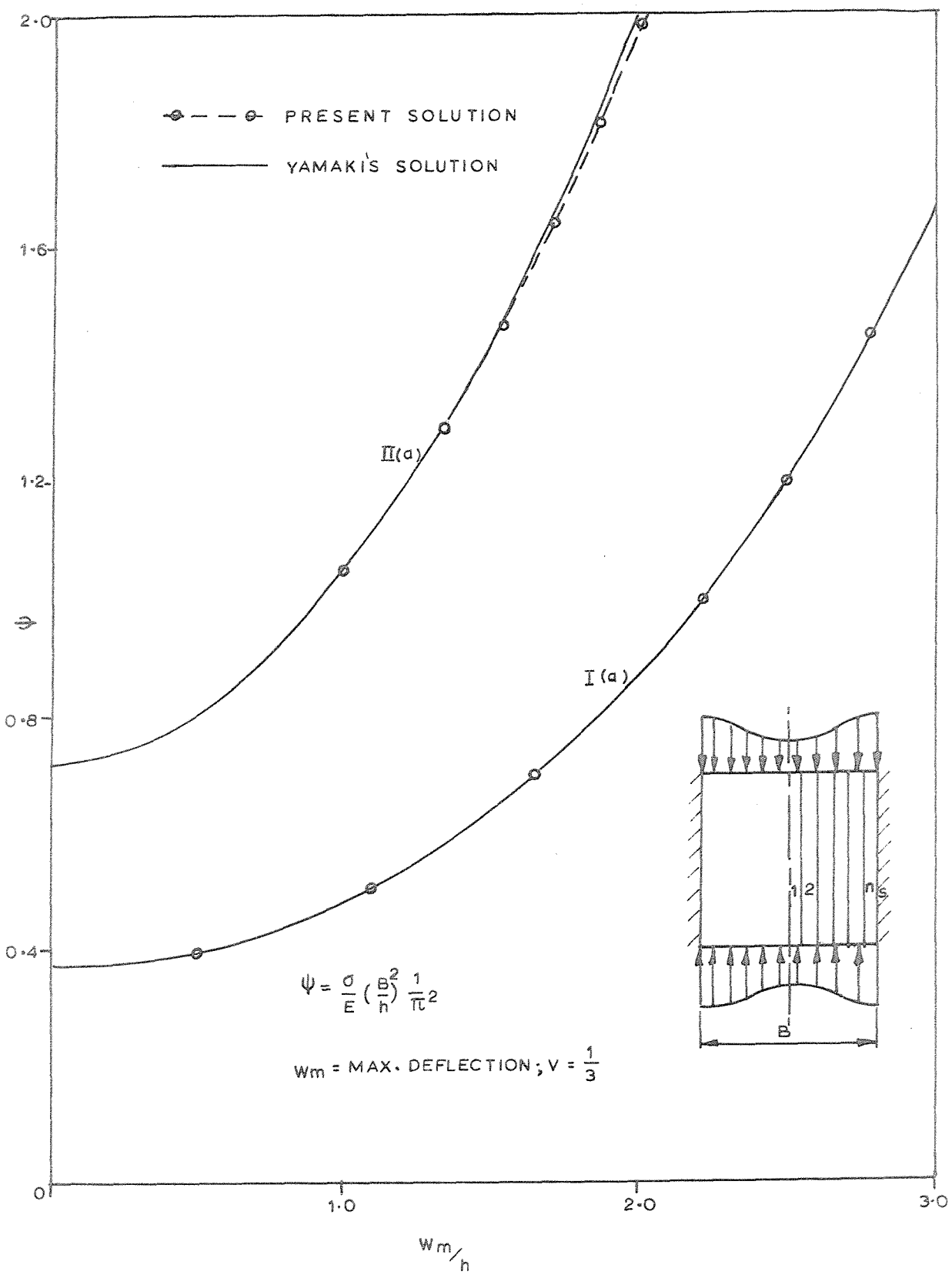

Fig. 3.9 (a) Relation between load and maximum deflection for cases I(a) and II(a).

Fig. 3.9 (b) Relation between load and end-shortening for Cases I(a) and II(a).

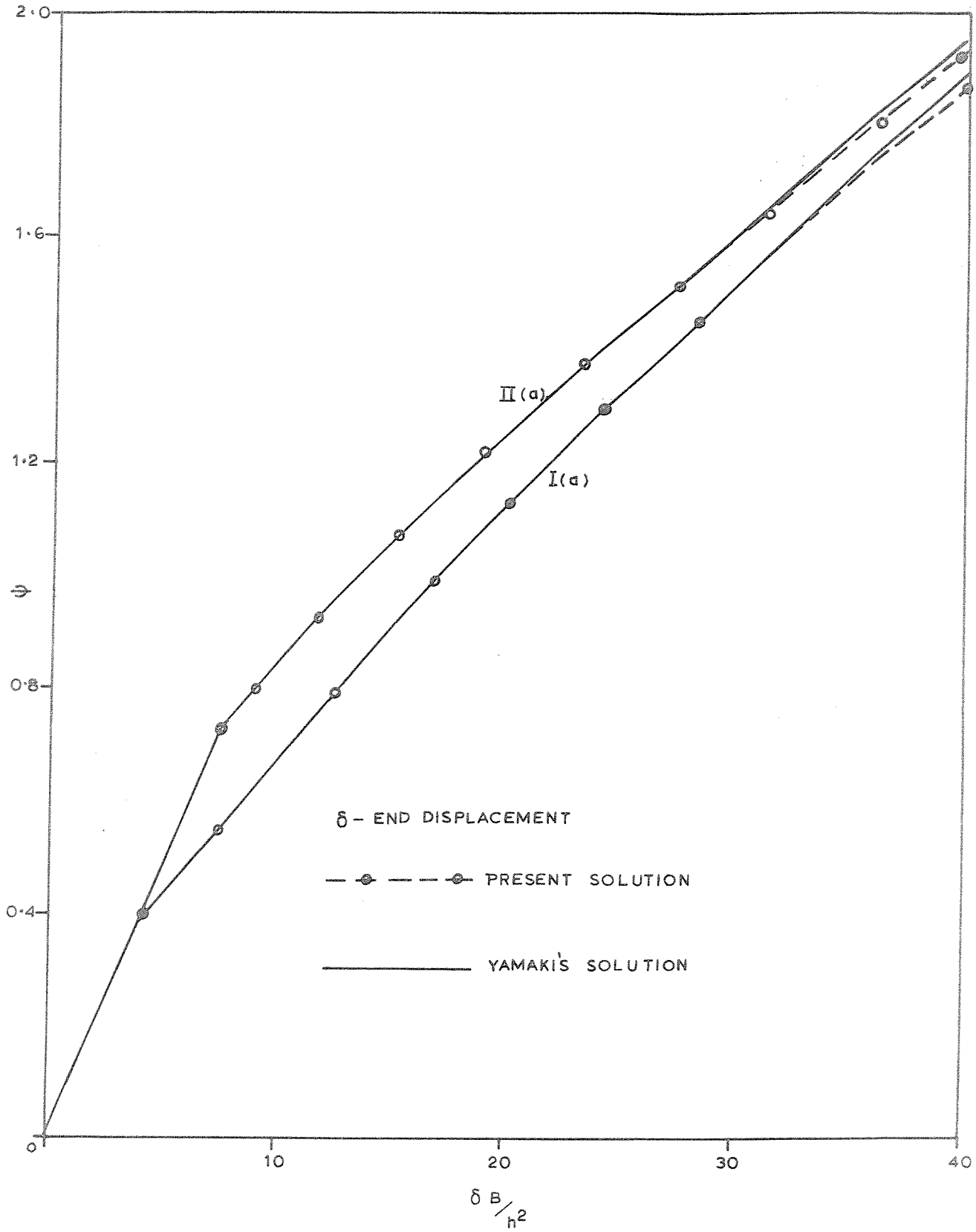

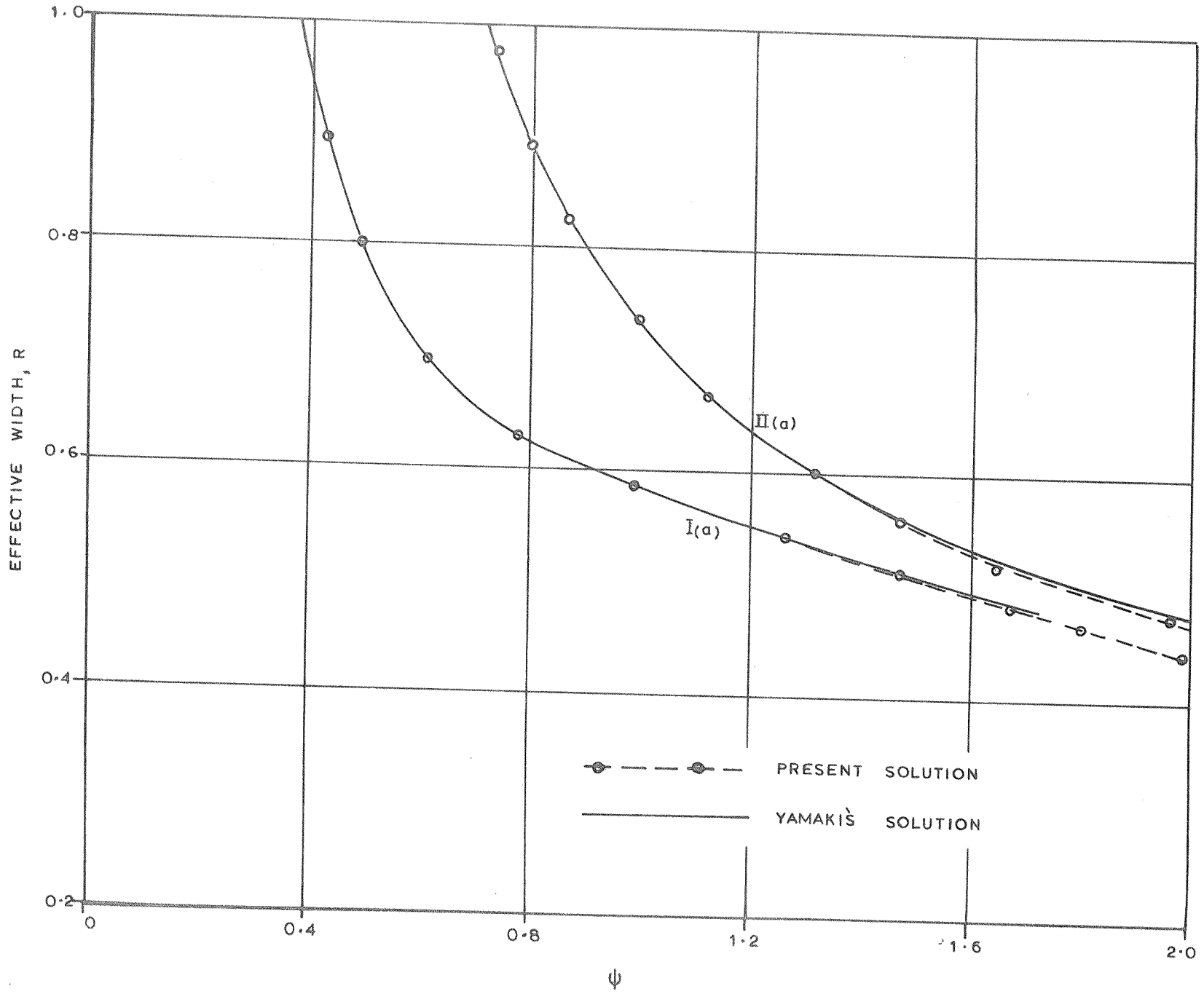

Fig 3.9 (c)
Relation between Load and Effective Width for Cases I(a and II(a).

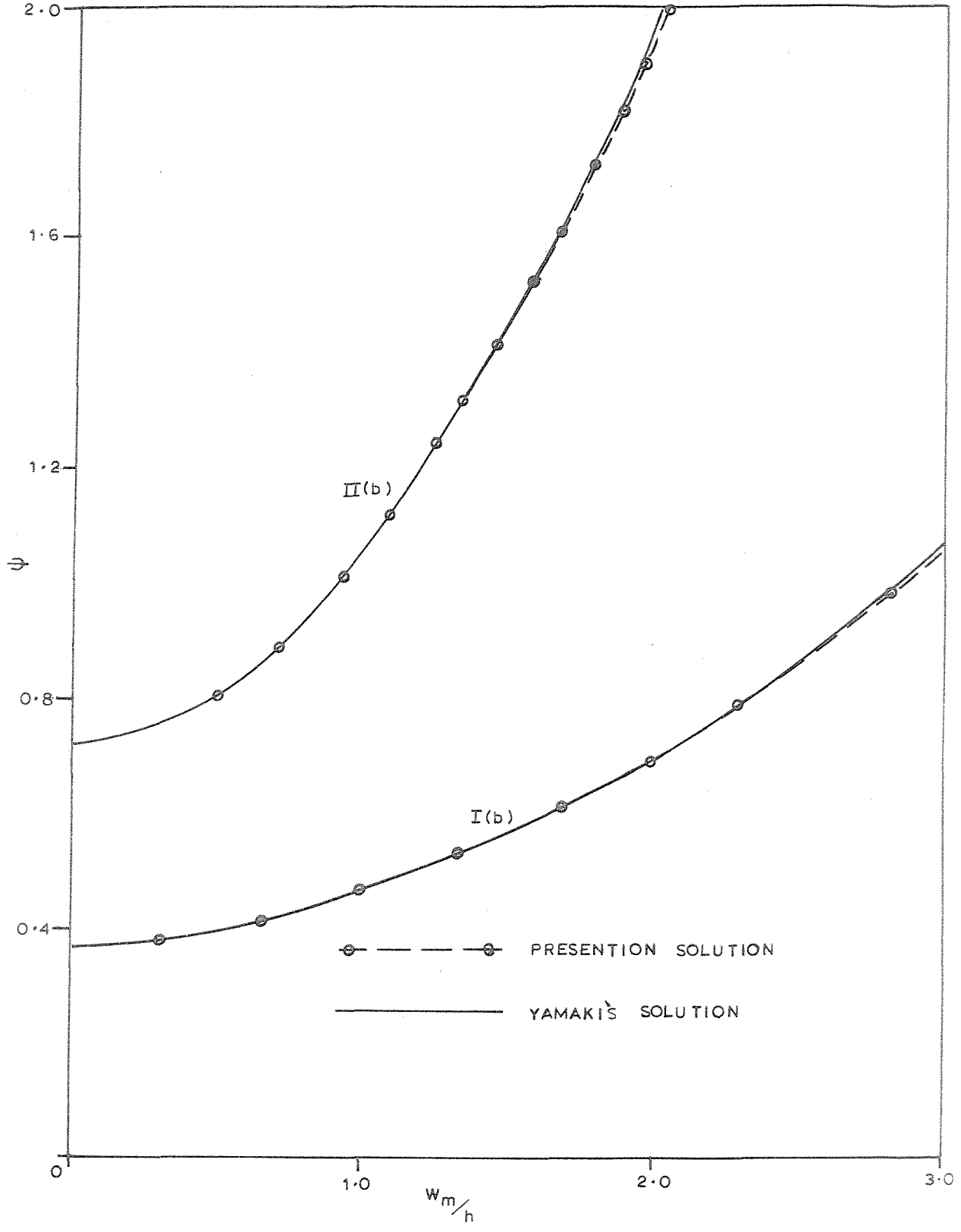

Fig. 3.10(a) Relation between load and maximum deflection for Cases I(b) and II(b).

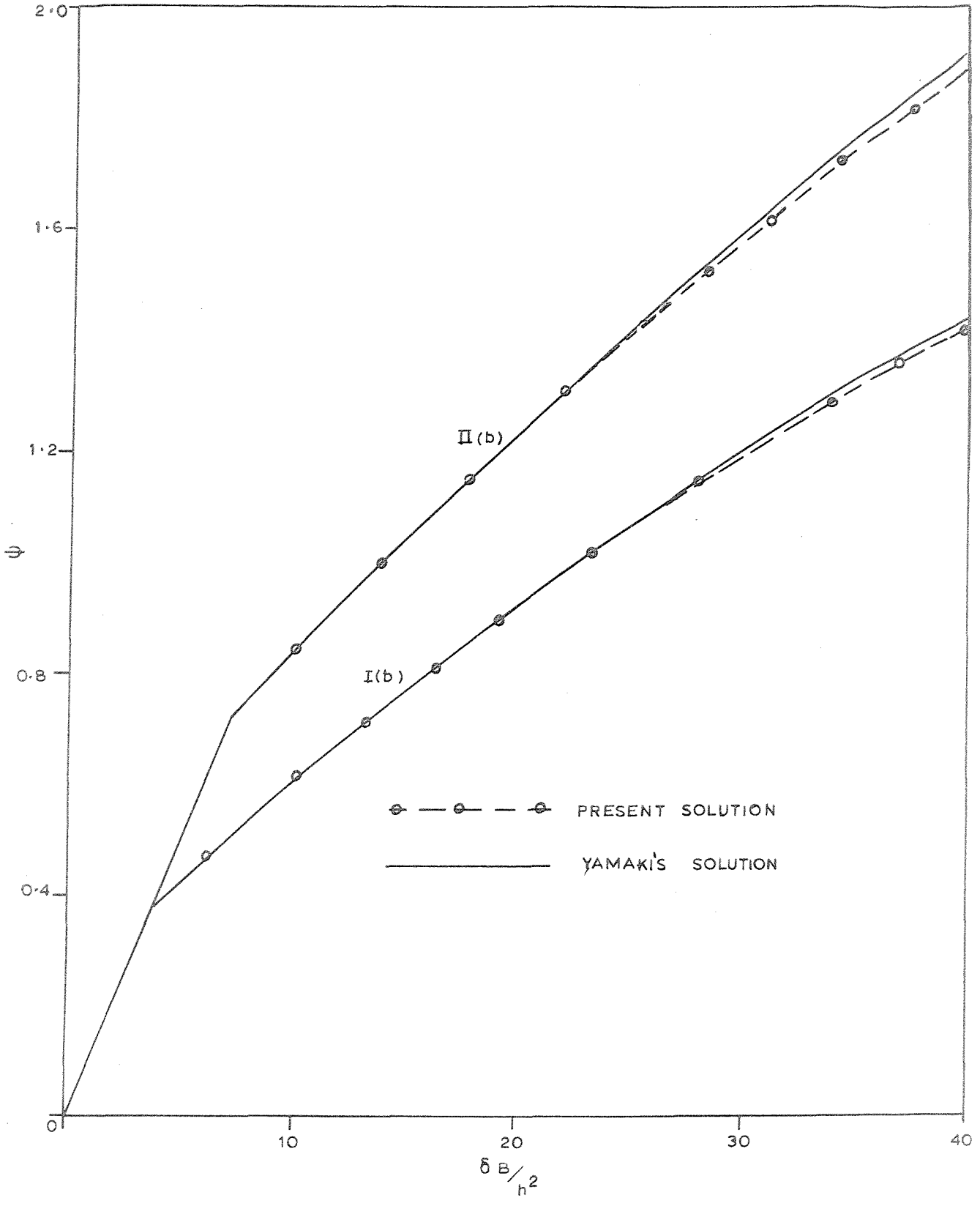

Fig. 3.10(b) Relation between load and end-shortening for Cases I(b) and II(b).

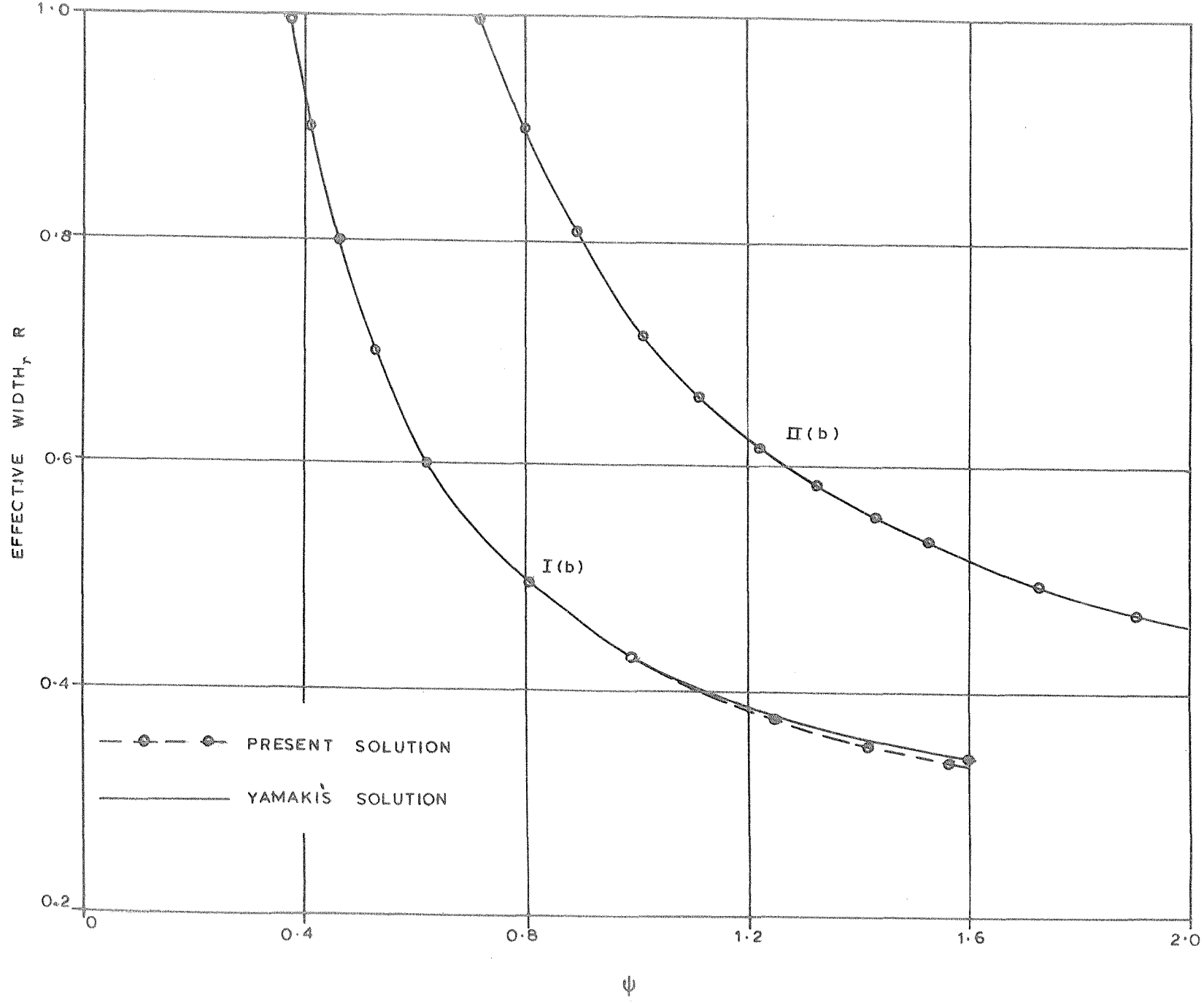

Fig. 3.10(c) Relation between Load and Effective Width for Cases I(b) and II(b).

and the displacement functions for $\bar{u}$ and $\bar{v}$ chosen as explained in 3.2.1.2. The half plate was divided into 12 strips. For the case II, the deflection surface was assumed to be made up of two half waves in the longitudinal direction. The relationships between the load in its nondimensional form on the one hand to maximum deflection, end shortening and effective width (in their dimensionless forms) on the other, have been plotted for cases I(a) and II(a) in Fig. 3.9(a-c) and for cases I(b) and II(b) in Fig. 3.10(a-c). These results are compared with those obtained by Yamaki[24] who employed two terms in the solution to describe the normal displacement in each direction. As can be seen from the plots, the agreement between the two results in all cases over most of the range studied is excellent. It is noticed that at higher loads the present solution indicates a slightly lower stiffness for the plate than Yamaki's. The normal displacement in the present solution is given considerably greater degree of freedom in the transverse direction than in Yamaki's solution, where it is restricted to two terms. In view of the fact that both the solutions give upper bounds for the displacements, the present solution must be considered the more accurate.

3.5.1.3 Postbuckling stiffnesses of rectangular columns with various aspect ratios

The next example considered is that of a rectangular column, composed of plates of same thickness. It is necessary to study only the portion ABC of Fig. 3.11 included between two lines of symmetry OA and OC. The column is considered to be a long one, so that a preliminary investigation of the lowest buckling stress and the corresponding wave length is found to be necessary. A portion between successive nodal lines alone need be considered with the assumption that the deflection

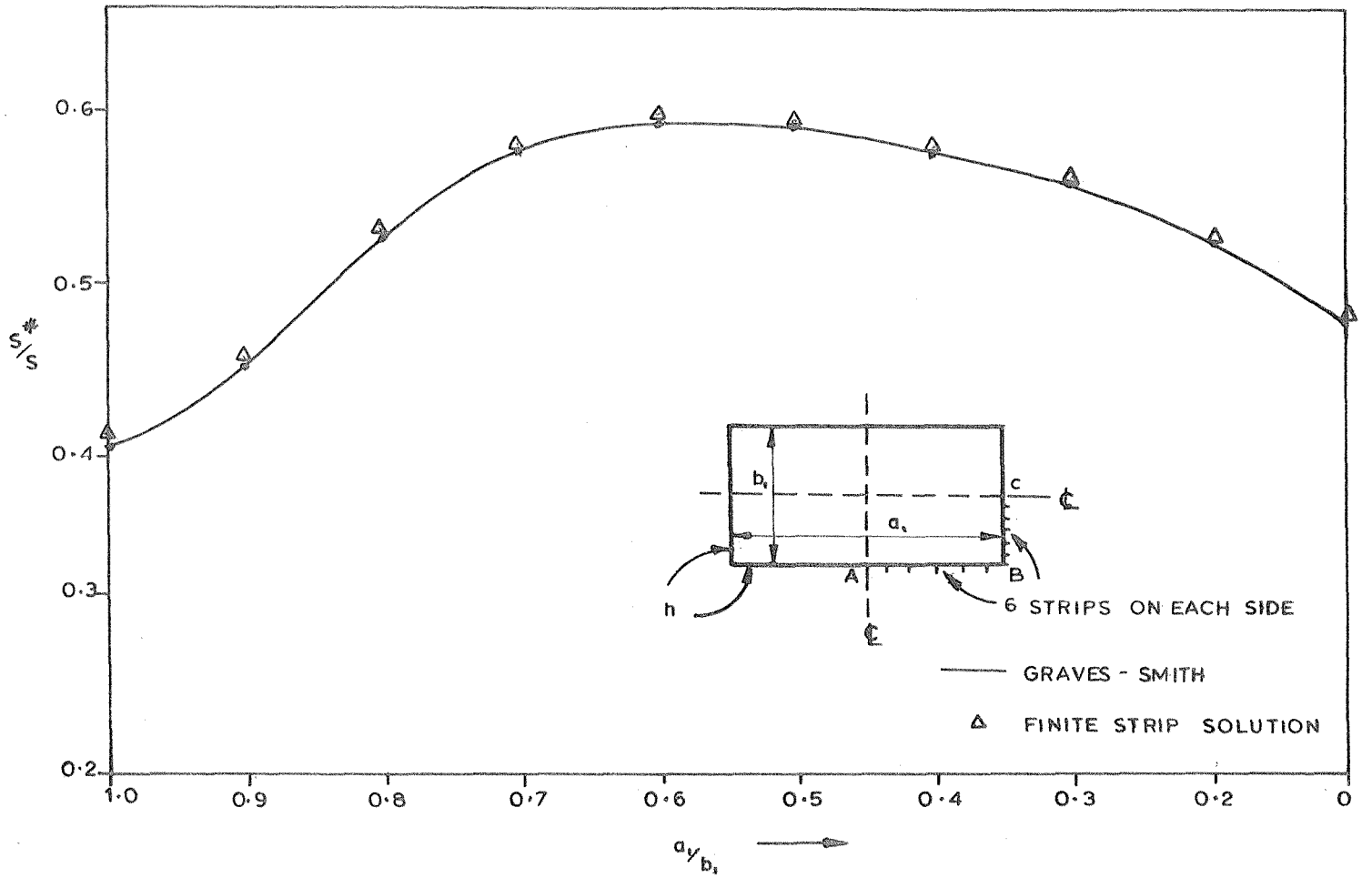

Fig. 3.11 Initial Postbuckling Stiffnesses of Rectangular Columns with Various Aspect Ratios.

surface is made up of single harmonic in the longitudinal direction Here the attention is confined to finding initial postbuckling stiffness in the immediate vicinity of the buckling load.

Columns with ratios of longer to shorter sides (a_1/b_1) varying from 0.1 to 1.0 have been studied. The limiting case of local buckling when b_1 tends to zero can be treated as a plate clamped along its longitudinal edges and free to wave in its plane. The problem was studied with 6 strips on each plate AB and BC. The ratios of postbuckling to pre-buckling sti-fnesses obtained have been compared with those reported by Graves-Smith[60] in Fig. 3.11.

The solution given by Graves-Smith must be considered the more accurate, based as it is on the theoretically exact buckling mode, and the corresponding inplane stress system. It may be noted however that the agreement between the two results is quite close, the finite strip solution overestimating the stiffnesses by 1 to 2%. This is because of the relatively small number of strips employed in the solution. Referring to Fig. 3.8 it can be seen that in order to obtain the postbuckling stiffness within an error of 0.5%, for a plate with longitudinal edges free to wave, it is necessary to employ 12 strips in a half of the plate.

3.5.1.4 Check for equilibrium

In order to check the internal consistency of the solution, the longitudinal stresses were summed up at different sections and agreement in the total values of compression was in complete agreement upto 8 digits. This is mainly due to the mathematically consistent choice of the functions depicting the inplane displacements and the compatibility of displacements along the edges of the strip inherent in the method.

3.5.2 Study of convergence: Version II

In this section a few examples illustrating the convergence of the solution based on version II of the finite strip method will be presented. It is important to note that the set of boundary conditions assumed at the ends of the plate in this version is different from those treated in the literature in one detail. It is the condition that the inplane displacements in the transverse direction at the ends are zero. This rules out comparison with other solutions for short plates. However when the plate buckles into several half waves, the solution would approach that for conditions assumed in version I.

3.5.2.1 The problem of rectangular plate

The ratio S*/S for a square plate and for rectangular plates with length to breadth ratios of 3 and 5 have been obtained taking varying number of strips in the half plate, and the number of harmonics characterising 'u' and 'v'. These are given in the Table 3.2. The plates were assumed to be free to wave in their plane along the longitudinal edges. In order to check the internal consistency of the solution, an equilibrium check was performed by comparing the changes in the total longitudinal compression between two successive steps involving an increment of 'e' equal to 2×10^{-5}, at different sections. Such a procedure is found to be necessary in order to isolate the errors involved in the description of prebuckling stress distribution. The deviation from the mean value as computed by taking 10 equidistant sections across the length of the plate are also given in Table 3.2.

A study of Table 3.2 reveals some interesting features. First of all, for the square plate a higher value of S*/S equal to 0.420 is obtained as against 0.408 reported in 3.5.1.1. This is due to the stiffer inplane boundary conditions at the ends of the plate. However,

the influence of these boundary conditions is not significant for greater aspect ratios whose values of S*/S approach that of the square plate in version I.

An important factor governing the accuracy of the solution is the choice of the number of terms in the functions representing 'u' and 'v'. It was noted that for version I, the number of terms representing u and v can be chosen exactly, once the number of terms characterising 'w' are known. The same can not be said of version II. However, the number and character of terms entering into the description 'u' and 'v' in version I, can be good indicators of the number of terms required in version II.

Consider the case of a plate which buckles with 'n' half waves along the plate. Then the description of 'v' is composed of two terms, one a constant and the other which varies in the form cos $2n\pi\xi$ in the longitudinal direction, according to version I. The number of terms required to represent a term like cos $2n\pi\xi$, in the form of a Fourier series consisting of sine terms increases with 'n'. Thus the greater the length of the plate, the greater the number of terms required to represent inplane displacements.

From the Table 3.2, it is seen that for the case with $a/\lambda = 1$ and 'w' described by the first harmonic, at least four terms are required for describing the inplane displacements; increasing this number will not improve the accuracy of the solution for a given number of strips into which the plate is divided. Smaller number of terms in the description would result not only in the inaccuracies in the prediction of the post-buckling stiffness but also in the errors which become noticeable in the equilibrium check. With the increase in the ratio a/λ to 3 the number of terms required to represent the inplane displacements increases to six;

Table 3.2 Convergence studies on FSM (Version II) as applied to rectangular plate

Aspect ratio (a/B)	No. of strips in half plate	No. of harmonics to represent			S*/S	Mean error in equilibrium check
		w	u	v		
1	4	1(1)	3(2,4,6)	3(1,3,5)	0.437	0.4%
			4(2,4,6,8)	4(1,3,5,7)	0.433	0.3%
			5(2,4,6,8,10)	5(1,3,5,7,9)	0.433	0.1%
	6	1(1)	3(2,4,6)	3(1,3,5)	0.428	0.4%
			4(2,4,6,8)	4(1,3,5,7)	0.426	0.2%
			5(2,4,6,8,10)	5(1,3,5,7,9)	0.426	0.05%
	12	1(1)	5(2,4,6,8,10)	5(1,3,5,7,9)	0.421	0.03%
3	4	1(3)	5(2,4,6,8,10)	5(1,3,5,7,9)	0.428	0.4%
			6(2,4,6,8,10,12)	6(1,3,5,7,9,11)	0.426	0.2%
			7(2,4,6,9,10,12,14)	7(1,3,5,7,9,11,13)	0.426	0.1%
	6	1(3)	5(2,4,6,8,10)	5(1,3,5,7,9)	0.419	0.3%
			6(2,4,6,8,10,12)	6(1,3,5,7,9,11)	0.417	0.2%
			7(2,4,6,8,10,12,14)	7(1,3,5,7,9,11,13)	0.417	0.05%
	12	1(3)	7(2,4,6,8,10,12,14)	7(1,3,5,7,9,11,13)	0.412	0.02%
5	4	1(5)	9(2,4,6,8,10,12,14,16,18)	9(1,3,5,7,9,11,13,15,17)	0.423	0.1%
	6	1(5)	9(2,4,6,8,10,12,14,16,18)	9(1,3,5,7,9,11,13,15,17)	0.417	0.1%
	12	1(5)	9(2,4,6,8,10,12,14,16,18)	9(1,3,5,7,9,11,13,15,17)	0.410	0.05%

and so on. However, the results for a plate with a/λ equal to 3 are sufficiently close approximations to those of the longer plates.

In all the above cases, the normal displacement has been described by a single harmonic. With 'w' represented by greater number of harmonics in order to study the postbuckling behaviour at loads considerably greater than the critical load, more terms will be required to represent the inplane displacements.

3.5.2.2 Effects of extra-buckling harmonics

In the initial postbuckling analysis it is sufficient to describe the normal displacement by a single harmonic and most of the existing solutions are based on such an approach. At higher loads there occurs a gradual deterioration of the accuracy of such a solution.

A simple example is considered to illustrate the influence of harmonics other than the one which constitutes the buckling mode. It is the problem of a square plate simply supported along all the edges, with one pair of opposite edges free to wave in the plane of the plate. The problem was studied with version II of the finite strip method, with 8 strips in half the plate. The ratio of S*/S and the nondimensional central deflection obtained using one (m=1), two (m=1,3) and three harmonics (m=1,3,5) for various levels of applied stress have been plotted in Fig. 3.12(a-b).

It is seen that upto twice the critical load, it is sufficient to consider just one harmonic, to predict accurately the postbuckling stiffness. The agreement in the values of central deflection for the three solutions is closer than for the postbuckling stiffness. Comparing the three solutions, it may be concluded that it is sufficient to consider two harmonics for an accurate solution of the square plate problem.

For plates with greater ratios of length to width, the role of extra

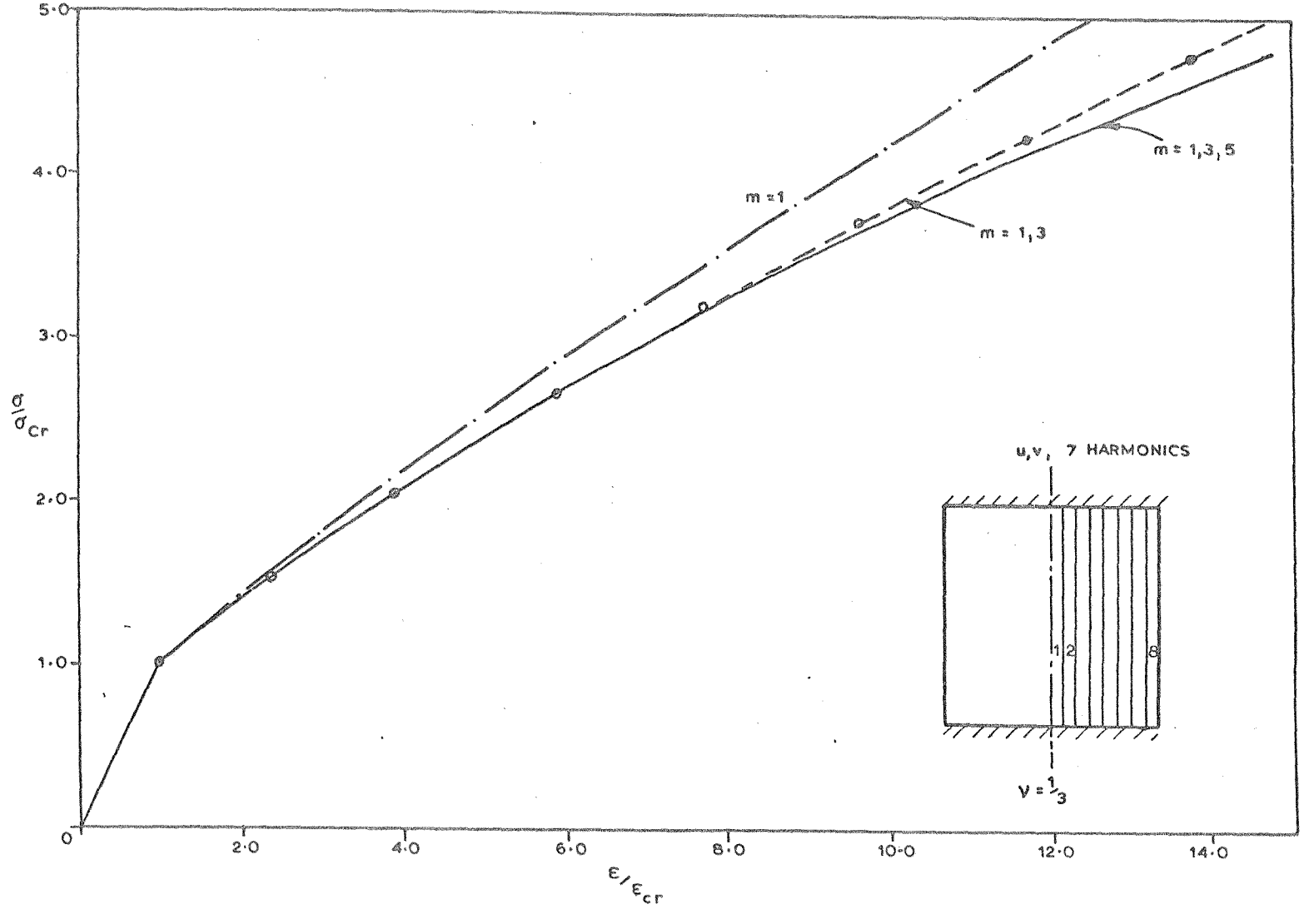

Fig.3.12(a) Influence of Extra-buckling harmonics in the Stress-Strain relationship of a Square Plate.

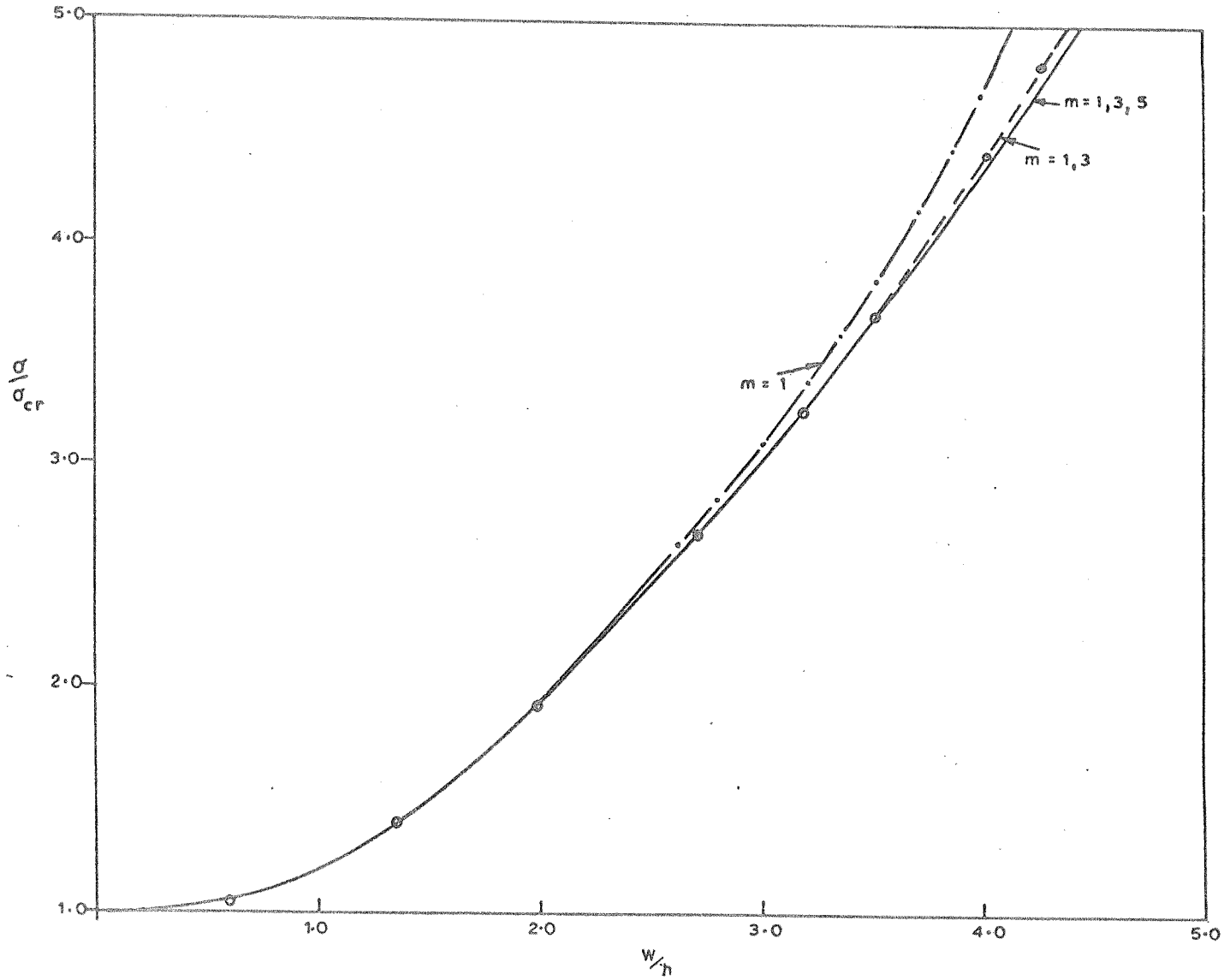

Fig. 3.12(b) Influence of Extra-buckling harmonics in the Load - Maximum Deflection relationship.

buckling harmonics can be even more important due to the freedom of nodal lines to distort - something which does not exist for a square plate.

3.5.3 Computational efficiency of the finite strip method

In this section, an attempt is made to compare the computational efficiencies of the conventional finite element method and the finite strip method for the class of problems considered in this chapter. This is done by considering examples of postbuckling analysis of plates using the finite element method available in the literature. Two examples will be considered, one dealing with the determination of initial post-buckling stiffness of a plate and the other with the postbuckling behaviour upto about thrice the critical load.

The first example is that of a square plate simply supported along all the edges, with the unloaded edges allowed to move but held straight. The results obtained using the finite element approach by Akin Ecer[45] have been plotted in Fig. 3.13. Two patterns built up of triangular elements with five degrees of freedom at each node were considered with one of them giving a better result. This is compared with the result obtained with the version I of the finite strip method. The postbuckling stiffness is correctly predicted with 10 elements across the plate width for the Type II while 10 finite strips are needed across half the plate width in the present method. But this indicates a vastly greater computing effort involved in the finite element method - a fact which becomes evident by a consideration of the total number of unknowns in the equations and the half band width of the stiffness matrix. Considering only a quarter of the plate for the finite element approach, the total number of unknowns and the half band width work out to be 180 and 35

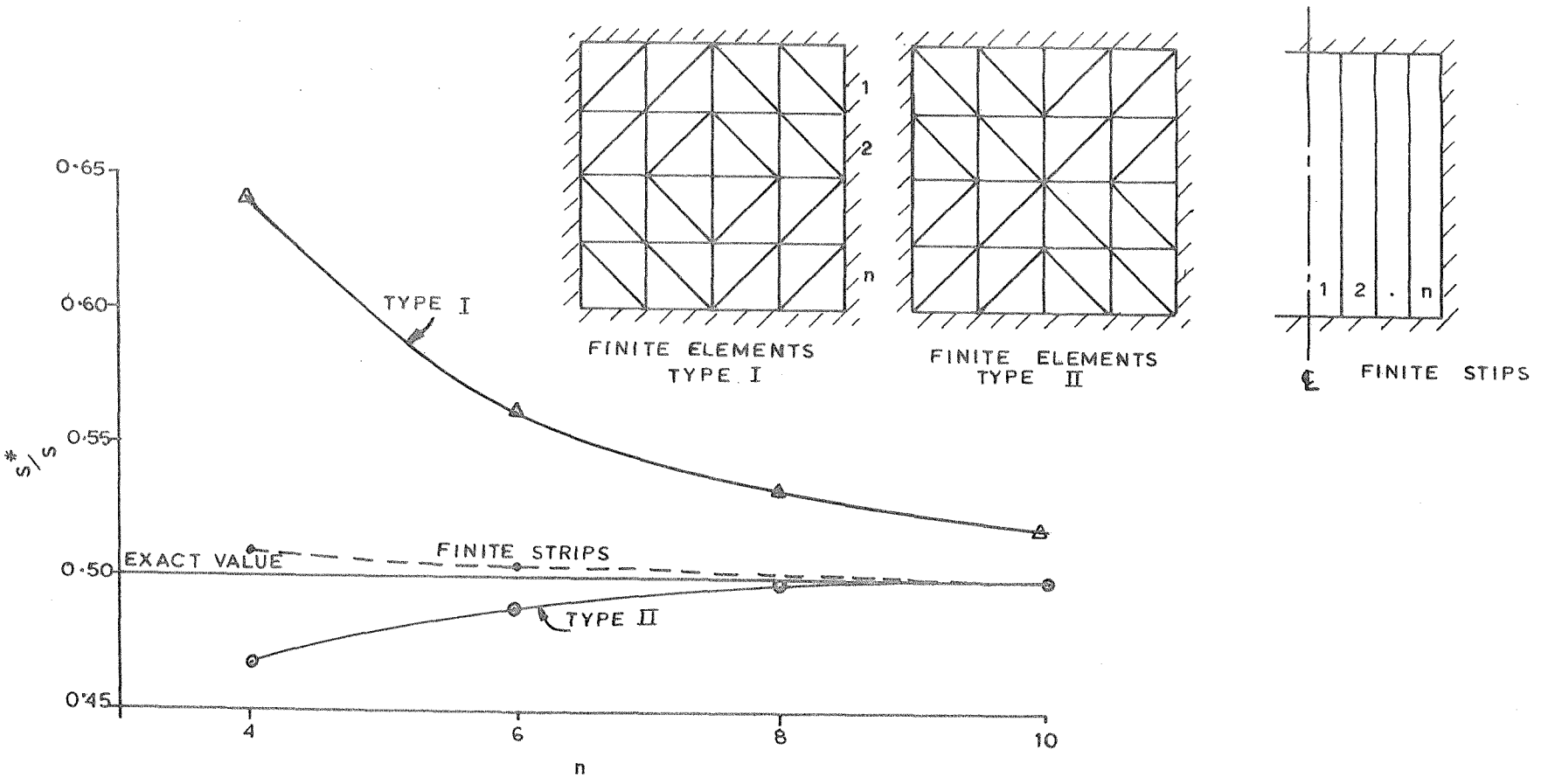

Fig. 3.13 A Comparison between Finite Element (Ref.45) and Finite Strip Solutions.

respectively, (Fig. 3.13) while for the finite strip method these are 55 and 10 respectively. Taking the computing time to be proportional to the square of the band width and directly proportional to the total number of unknowns, the finite strip method will be found to take only about 3% of that taken by the finite element method. In addition, it is seen that the finite strip gives sufficiently accurate results even if only a small number of strips are employed e.g. the value of S*/S is obtained in this problem within an error of 2% with just four strips in the half plate.

The next example considered is that of a simply supported square plate again, considered by Bergan[46]. In this case the unloaded edges are free to wave in the plane of the plate. The finite element mesh used by Bergan together with his results for the central deflection of the plate are shown in Fig. 3.14. Even though there are only five degrees of freedom associated with each node, there are several internal degrees of freedom associated with each element which are eliminated by static condensation. The results obtained using a 3 × 3 mesh in a quarter of the plate are of the same order of accuracy as those obtained with 6 strips in the half plate in the version I of the finite strip method. In the finite element approach, the total number of unknowns involved in the solution (excluding the internal degrees of freedom) are 80 and the half band width of the stiffness matrix 30. In the case of the finite strip method, these work out to be 35 and 10 respectively. By the reasoning employed in the previous case the computing time required for the finite strip method is of the order of 5% of that required for the finite element approach.

The major advantage of the finite strip method is that the band width of the system of equations remains constant once the number of harmonics

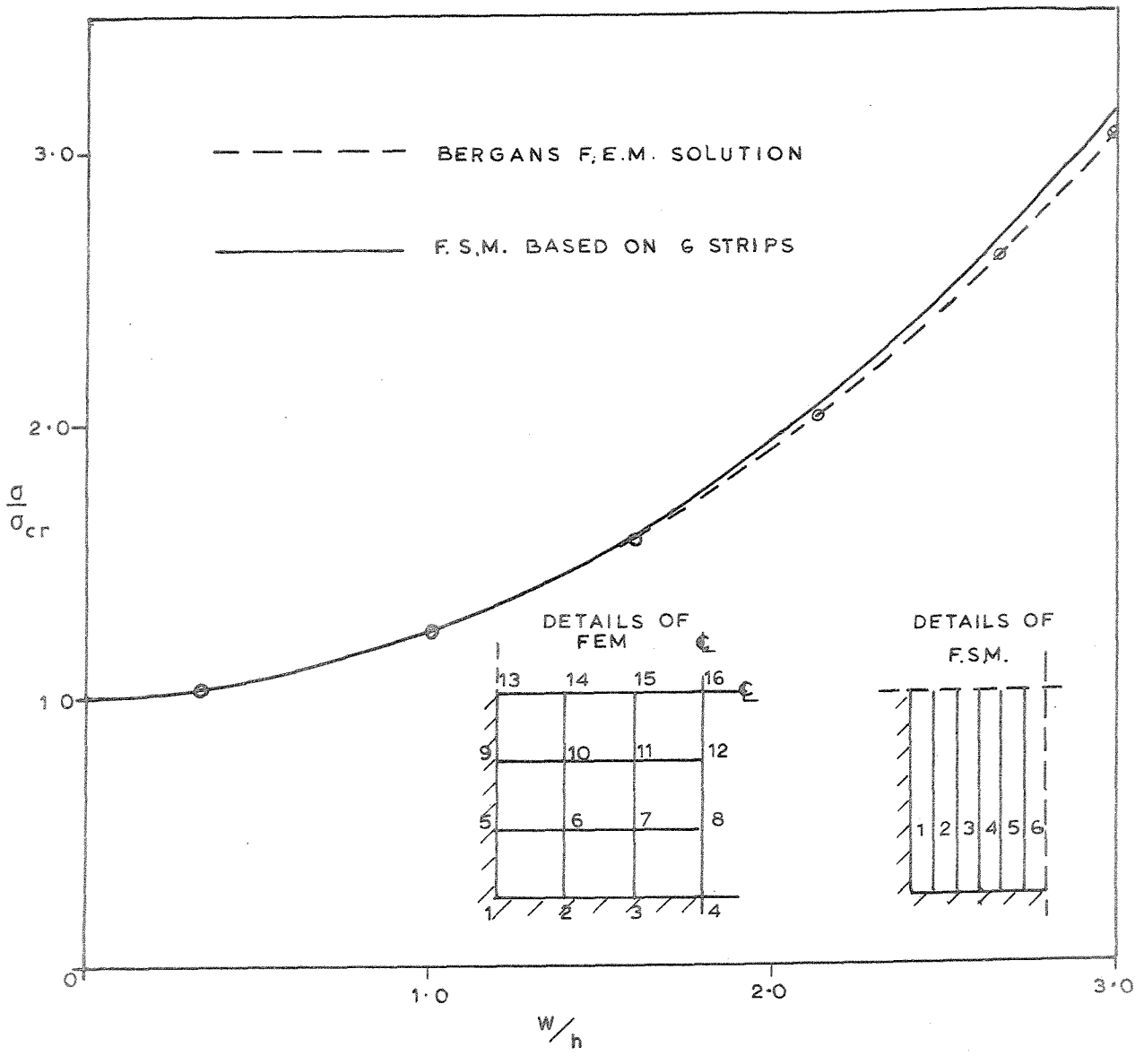

Fig. 3.14 Relationship between average Stress and Central Deflection as given by Finite Element (Ref.46) and Finite Strip Solutions.

representing 'w' have been chosen. For example, in version I, if 'w' is represented by a single harmonic, (say n) the semi-band width in a plate problem is 10; if two harmonics (say n and 3n) are employed, it is 22. In most post local buckling analyses, it may not be necessary to consider more than two harmonics. Thus the semi-band-width would rarely exceed 22. But in the finite element procedure band width depends upon the number of elements in the shorter direction and this can be determined only by a study of the convergence of the solution in a given case and would often be several times greater.

However there are situations where the finite element method may have advantages over the finite strip method. Consider a long plate or a plate structure which buckles locally into a number of half waves, say 5 or more. If it is required to perform a postbuckling analysis giving freedom for each buckle to flatten in both directions and nodal lines to distort, then it may be necessary to consider several harmonics in a solution based on a finite strip method. This will considerably increase the number of local degrees of freedom and therefore the band width of the stiffness matrix. In addition the task of computing the coefficients of nonlinear terms becomes increasingly tedious as more and more number of harmonics are taken into account in the representation of 'w'. In such situations careful consideration must be given to both the methods, before deciding upon one or the other. Such problems are however apt to prove very difficult to tackle by either method. In most practical situations, however, the material would yield before the greater degree of freedom for the displacements envisaged in this situation results in a significant reduction in the postbuckling stiffness of the structure; and to study the elastoplastic problem there appears to be no better method than the finite element method.

3.5.4 Effect of displacements along the edges of the plates

In most analyses of plate assemblies as well as in version I of the finite strip method, certain assumptions have been made regarding the displacements along the edges of the plate. These assumptions have been discussed at some length in 3.2.1.1. Even though these assumptions have been justified by Benthem using a mathematical argument, it will be nevertheless interesting to enquire what order of magnitude of errors may be introduced by these, in actual computations.

In order to study the effects of displacements along the longitudinal edges of the plates, two examples are presented in this section. In Fig. 3.15(a-b) are shown two plate structures made up of two identical plates; in one of them (Fig. 3.15(a)), the plates meet at a very oblique angle of 170^{o} and in the other at a right angle. The outer edges of the plate structure are supported in the vertical direction and therefore not in a direction normal to the plates. Thus the longitudinal edges of each of the plates can undergo displacements normal to the plane of the respective plate.

The post-local-buckling behaviour of the plate assemblies has been studied using version II of the finite strip method which does not make any approximations with regard to boundary conditions along the junctions. In the analysis, both 'w' and 'v' are represented by five harmonics (m=1,2 ... 9) but the nonlinear effects of only the first three harmonics of 'w' are considered in the analysis. The average stress-strain relationship has been plotted for each case in Fig. 3.16. Next the problem was studied using the simplifying approximations, that the normal displacement 'w' is zero for each plate along the junctions and the edges are free to wave. These assumptions reduce the structure into two identical simply supported plates with edges free of all inplane stresses, due to

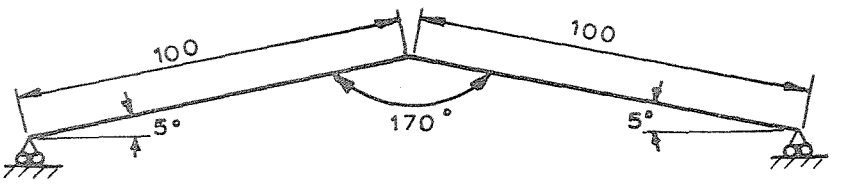

a = 100

(a)

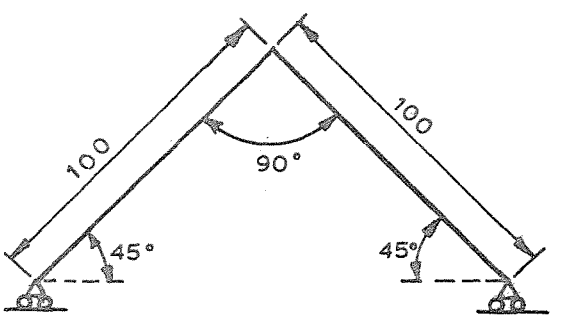

(b)

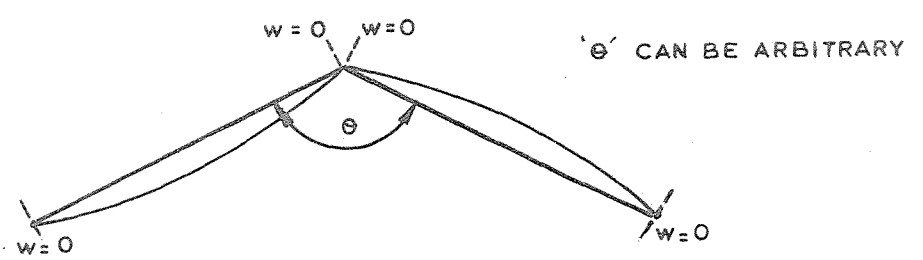

(c) Usual Approximations in the Boundary Conditions, illustrated.

Fig. 3.15 Example chosen to study the effects of approximations in boundary conditions.

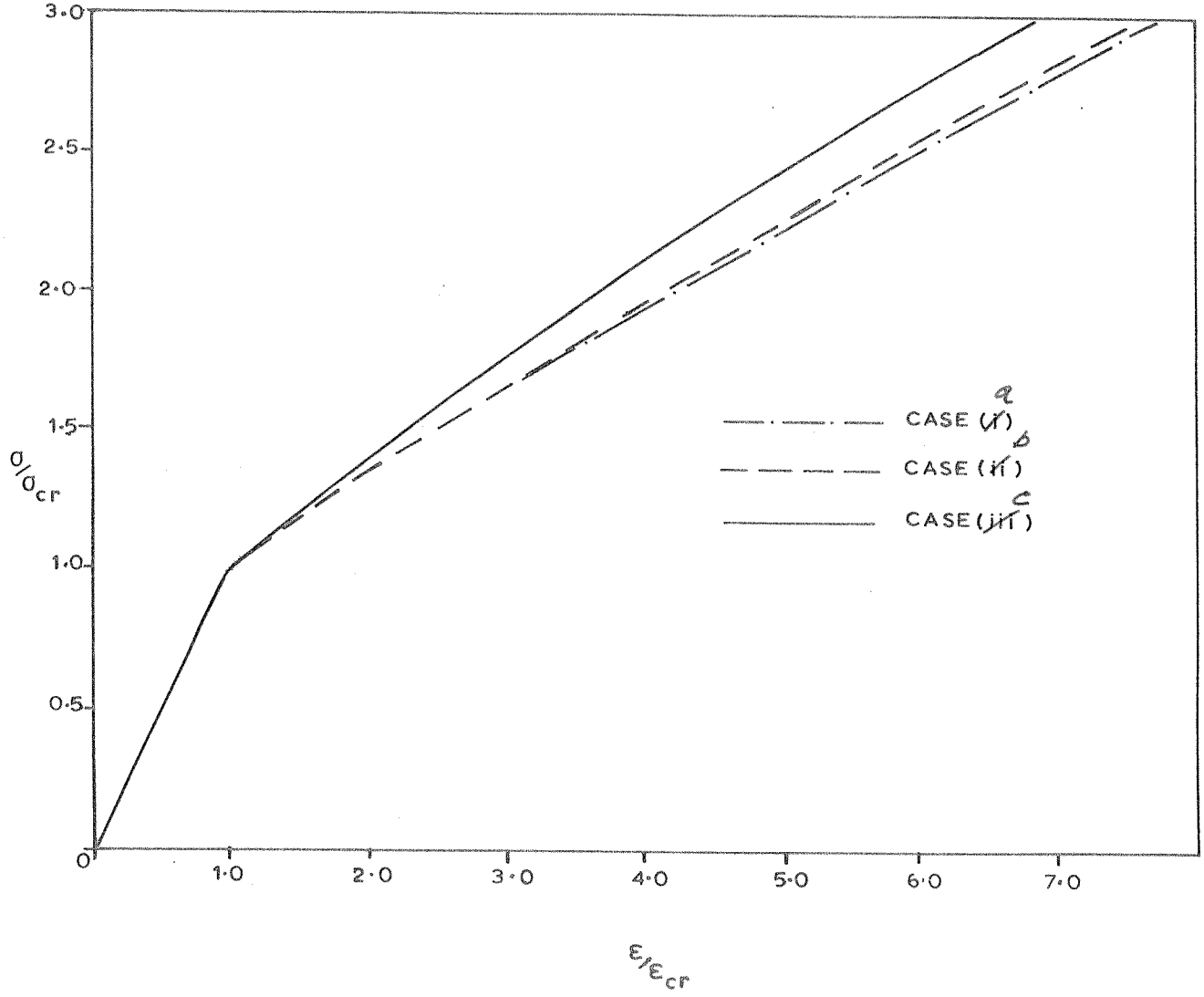

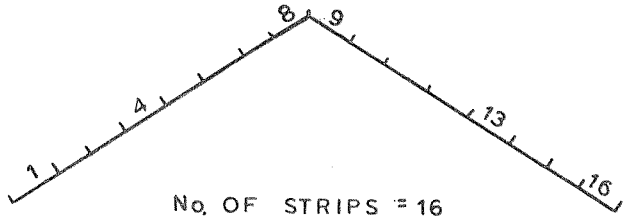

Fig. 3.16 The influence of 'coupled' boundary conditions along the edges of the structure in Fig.3.15.

the antisymmetry of the buckling mode with respect to the common junction. (Fig. 3.15(c)) This problem has been solved for the same degree of accuracy and the results are plotted alongside those of the plate assemblies in Fig. 3.16.

From a study of these results, it is seen that the simplifying approximations have the effect of overestimating the postbuckling stiffness. In the range where the average stress is about twice the critical, the error is about 12%. This is a consequence of displacements along the junctions which make them less stiff and reduce the stresses in their vicinity. Any post-local-buckling analysis, which assumes the normal displacements of the member plates to vanish along the junctions is subject to errors of similar magnitude, and this observation may be helpful in placing the right value on the results of such analyses.

3.5.5 Study of change of wave form

In this section, the procedure outlined in section 3.4.1 for a study of change of longitudinal wave form will be illustrated with examples.

3.5.5.1 Rectangular plate restrained against lateral movement

The first example studied is that of a rectangular plate simply supported on all the edges restrained against inplane movement in the transverse direction and having an aspect ratio of 2. (Fig. 3.17(a)) The problem was studied with version I of the finite strip method.

The lowest buckling stress corresponds to a buckling mode made up of one half wave along the length of the plate; the next higher eigenvalue of the buckling problem corresponds to a buckling mode of two half waves along the length. The primary and secondary modes were traced separately with degrees of freedom corresponding to both the modes

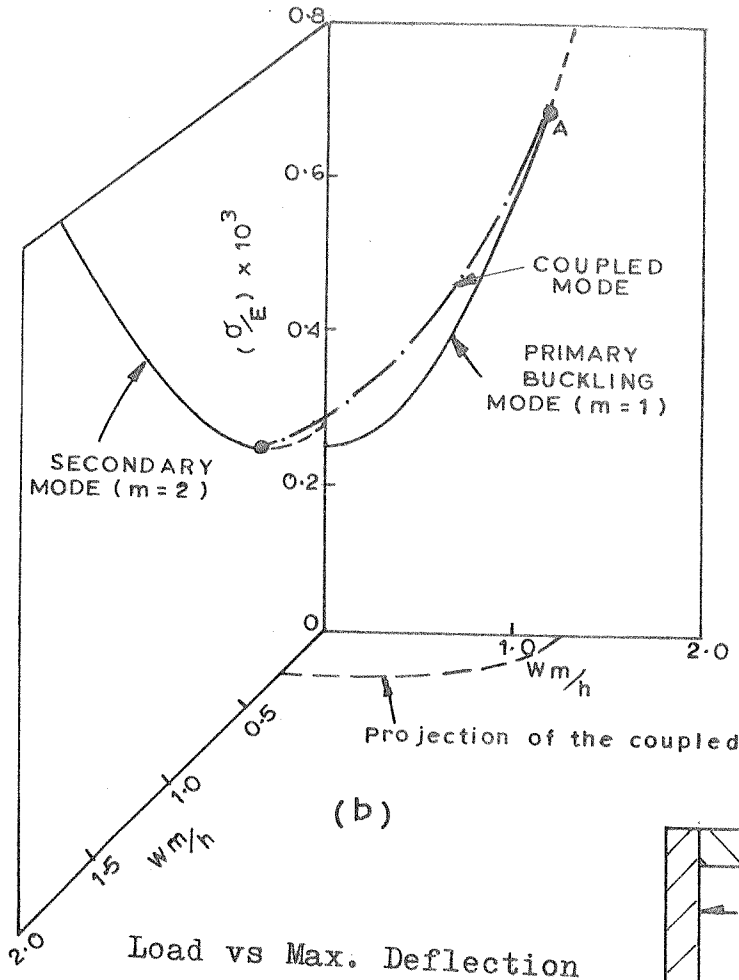

(b)

Load vs Max. Deflection

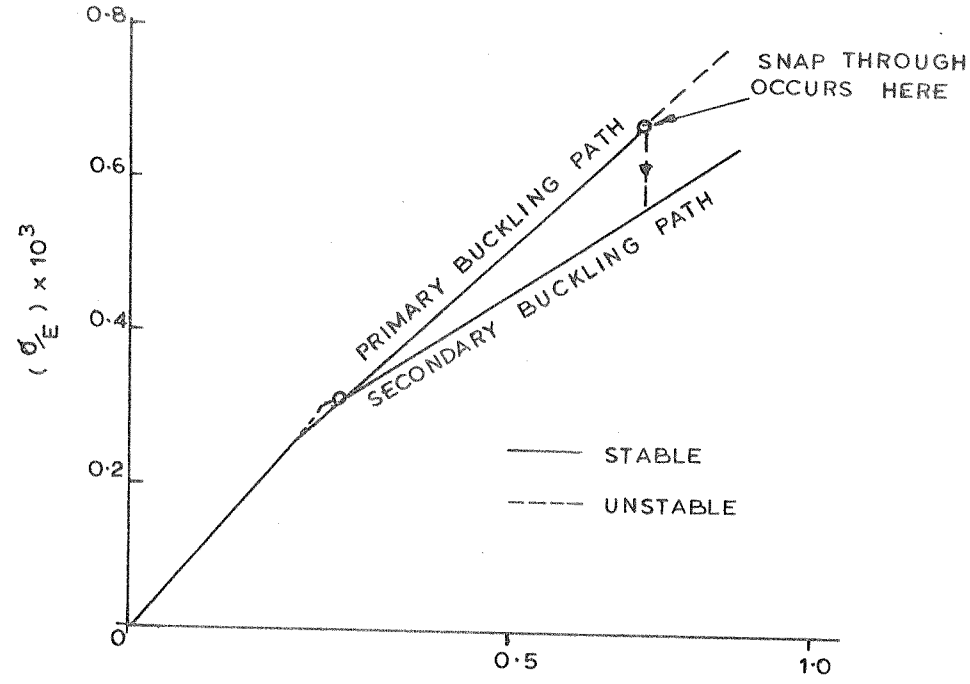

(c)

Average Stress vs Strain.

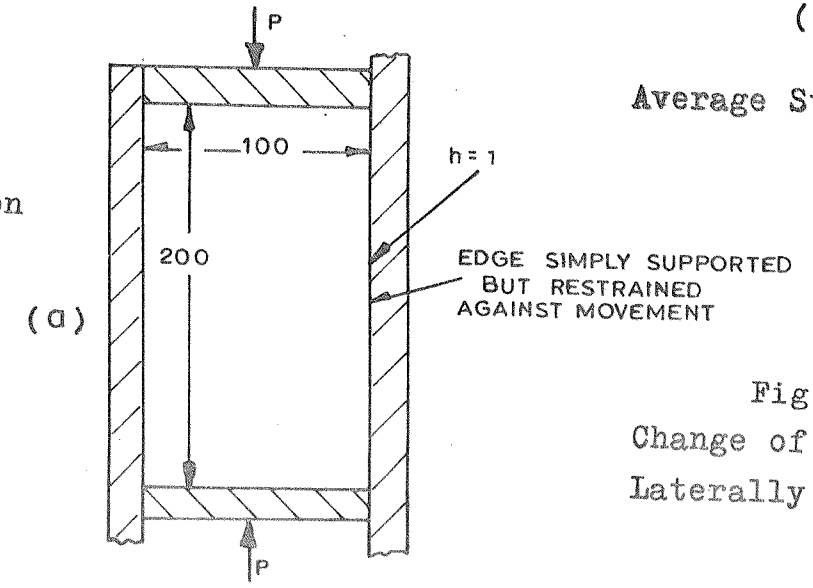

(a)

Fig. 3.17
Change of Wave form of a
Laterally restrained Plate.

represented in the analysis. Thus the displacement functions chosen for 'w' took the form

$$w_b = w_1 \sin\pi\xi + w_2 \sin 2\pi\xi$$

where w_1 and w_2 are appropriate functions of η.
The corresponding functions for the buckling displacements $\bar{u}_b$ and $\bar{v}_b$ therefore were taken in the form

$$u_b = u_n(\eta) \sin n\pi\xi \qquad (n = 1,2,3,4)$$

and

$$v_b = v_n(\eta) \cos n\pi\xi \qquad (n = 0,1,2,3,4)$$

It is seen that the primary buckling mode loses its stability between 2.75 and 2.80 times the critical load, as indicated by the second variation of strain energy ceasing to be positive definite. On the other hand the equilibrium path corresponding to the secondary buckling mode which is unstable at the beginning, becomes stable at a load which is 10% higher than the corresponding critical load. Thus a snap through will occur from the primary buckling path to the secondary path at about a load of 2.8 times the critical as shown in 3.17(a-c). These observations are in close agreement with those of Supple[66] who studied the same problem by a different method, thus confirming the validity of the procedure used.

3.5.5.2 Rectangular plate free to move along the unloaded edges but held straight

The next example considered is that of a plate with the same dimensions and boundary conditions except that in this case the unloaded edges are free to move but held straight. (Fig. 3.18(a)) This change in the boundary conditions can be seen to influence the behaviour of the

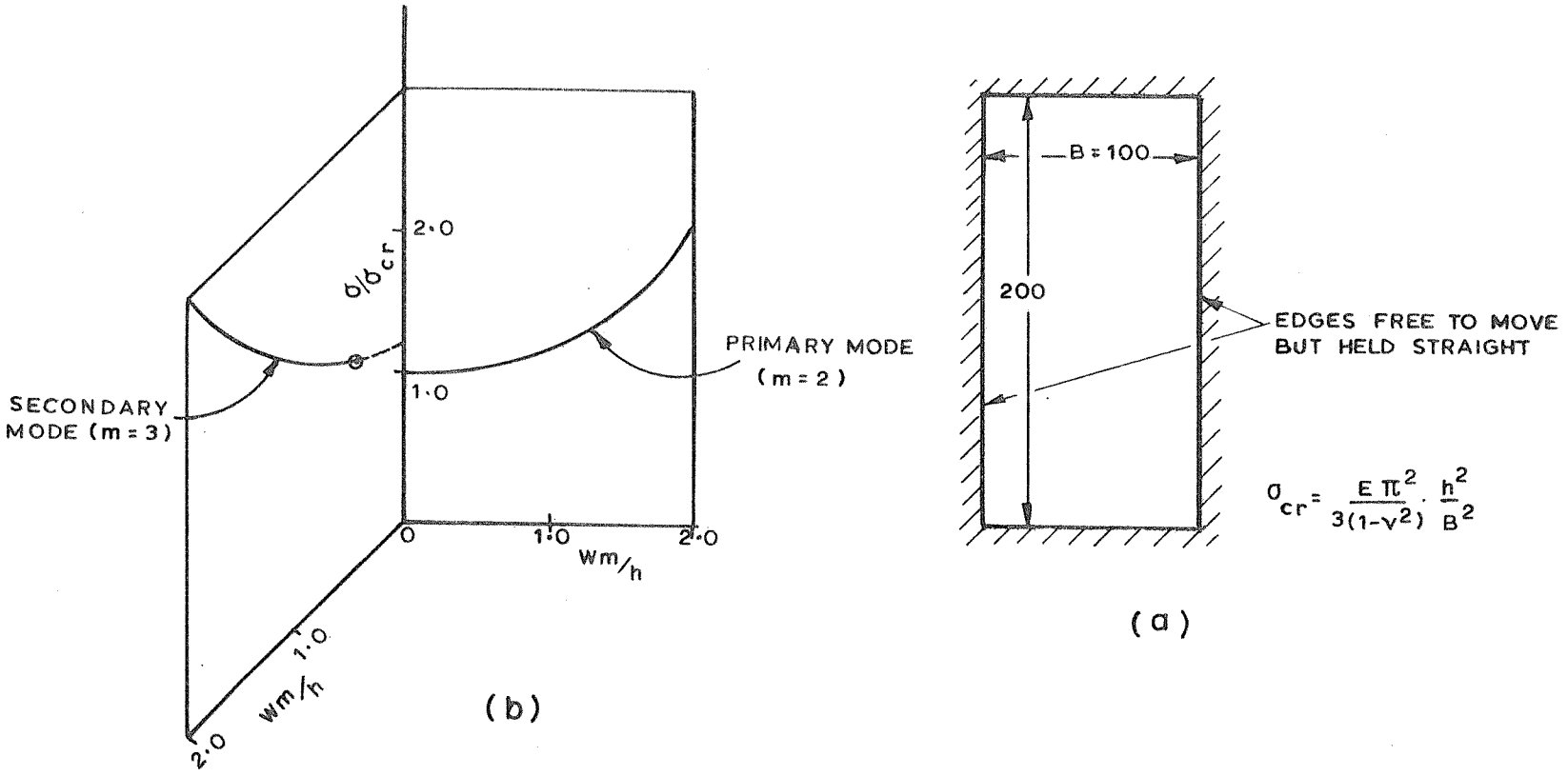

Fig. 3.18 Postbuckling Equilibrium Paths of a Simply Supported Plate with edges held straight.

plate profoundly.

The primary buckling path corresponds to a mode with two half sine waves along the length of the plate. The secondary buckling path which bifurcates from the straight form of equilibrium from the next higher eigenvalue corresponds to a buckling mode of three half sine waves. The displacement functions for the buckling displacements were therefore chosen in the form

$$w_b = w_2(\eta) \sin 2\pi\xi + w_3(\eta) \sin 3\pi\xi$$

$$u_b = u_1(\eta) \sin \pi\xi + u_4(\eta) \sin 4\pi\xi + u_5(\eta) \sin 5\pi\xi + u_6(\eta) \sin 6\pi\xi$$

$$v_b = v_o(\eta) + v_1(\eta) \cos\pi\xi + v_4(\eta) \cos 4\pi\xi + v_5(\eta) \cos 5\pi\xi + v_6(\eta) \cos 6\pi\xi$$

It was found that the primary buckling path was found to remain stable to an indefinite extent. The secondary path does become stable at a certain point indicating the existence of a path corresponding to a "coupled" mode branching from the secondary buckling path, but this is of no relevance to the behaviour of the initially perfect plate, which will remain in stable equilibrium along the primary buckling path. (Fig. 3.18(b)) These observations are in agreement again with those of Supple[66].

3.6 Concluding remarks

The finite strip method has been developed for the postbuckling analysis of plates and post-local-buckling analysis of plate assemblies. Two versions of the method have been presented each being suitable in different contexts. Examples have been presented to test the accuracy of the solutions by comparison with earlier solutions. Convergence studies reported indicate the order of magnitude of computational effort involved in obtaining solutions of desired accuracy. The superior

computational efficiency of the method over the conventional finite element method for the class of problems considered here, was illustrated by two case studies. The other examples presented relate to the effects of extra-buckling harmonics in the solution, the influence of 'coupled' boundary conditions and the study of change of wave form using the method presented.

The analytical tools and programmes discussed in this chapter form the basis for the theoretical studies reported in the chapters that follow.

CHAPTER 4

STUDIES ON POST-LOCAL-BUCKLING BEHAVIOUR OF SOME TYPICAL PLATE ASSEMBLIES

4.1 Introduction

The last chapter was devoted to the discussion of the analytical techniques developed as part of the present investigation. In the present chapter, the post-local-buckling behaviour of a few typical combinations of plates is examined. The aim has been to study the effects of varying the geometric parameters of the structure on the postbuckling behaviour. It must be emphasised that the present studies are concerned exclusively with local buckling (vide Art 1.2.2 (Chapter 1)) i.e. the junctions of plates are assumed to remain essentially straight and in each plate $w >> u,v$. Thus the conclusions are applicable to relatively short structures composed of thin walls so that the possibility of interaction of overall buckling is excluded.

The types of plate structures investigated are plain channel section struts, corrugated plates and stiffened panels. The results presented have been produced using version I of the finite strip method discussed in chapter 3. This means that the 'coupled' nature of the boundary conditions has been ignored. In addition, the nodal lines have been assumed to be straight in the solutions. Unless mentioned, the solution employs a single harmonic in the description of normal displacement. The results presented are based on a wave length corresponding to the minimum buckling stress in each case.

4.2 Studies on plain channel section columns

The problem of post-local-buckling behaviour of channel section columns has been studied by Rhodes and Harvey[62] whose analysis is based on the assumption that the buckling mode does not undergo any changes in the post buckling range. In the present study, the buckling mode is allowed freedom to change both in the longitudinal and transverse directions and as a result it has been possible to obtain the reductions in the postbuckling stiffnesses which are quite significant in most cases.

Fig. 4.1 shows the geometry of the cross-section. Since the local buckling mode is symmetric with respect to the line xx, it is sufficient to consider one half of the cross-section ABC for the analysis. Convergence studies in chapter 3 have shown that it is sufficient to subdivide it into 12 strips in order to obtain an accurate description of the post-buckling behaviour. Thus the portions AB and BC, have each been divided into 12 strips for the purposes of the study. Only a single harmonic has been used in the description of 'w' in the study, except for a chosen number of cases for which two harmonics (n and 3n in general) were employed in order to study the effect of changes in buckling wave form in the longitudinal direction.

Fig. 4.2(a) gives the minimum critical stresses and the corresponding wavelengths for various values of b_2/b_1 varying from 0 to 1. The critical stresses are expressed in terms of K which is defined in the form

$$K = \frac{\sigma_{cr}}{\frac{\pi^2}{12(1-\nu^2)} \cdot \frac{h^2}{b_1^2}}$$

[Thus for a simply supported plate of width 'b_1' the value of K is 4.]
The values of K as well as those of S*/S (the ratio of the postbuckling to prebuckling stiffness) at the onset of buckling given in Fig. 4.2(b)

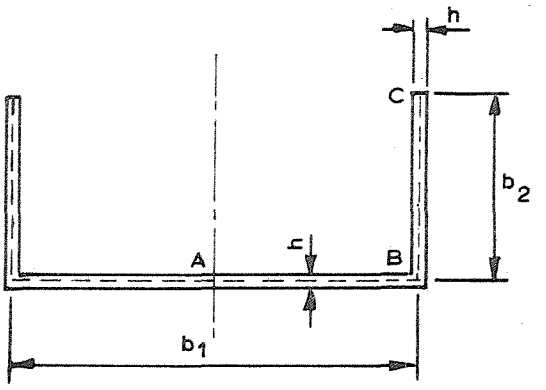

(a) PROPORTIONS

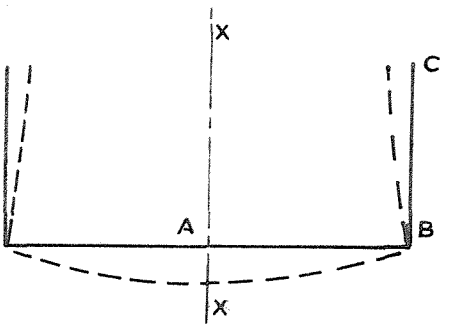

(b) BUCKLING MODE

Fig. 4.1 Cross-section and Buckling mode of the Channel Strut.

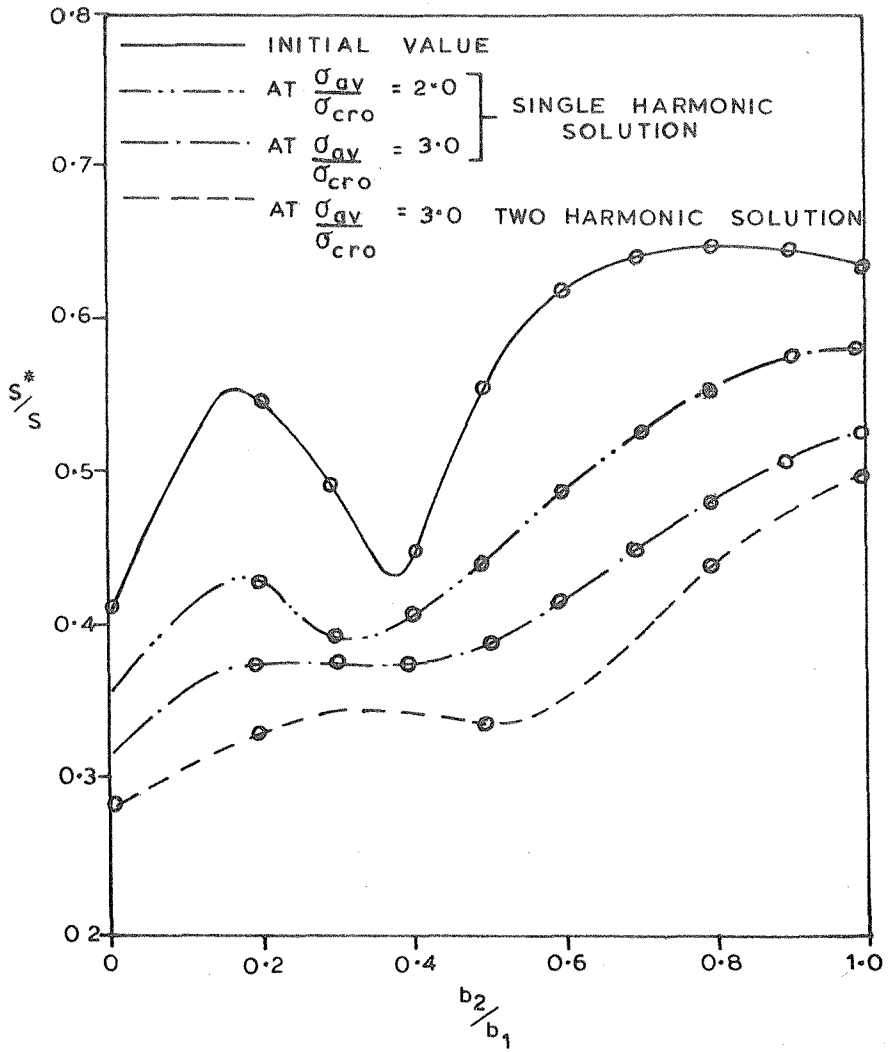

Fig. 4.2(b) Post-Local-Buckling Stiffnesses of Channel Struts.

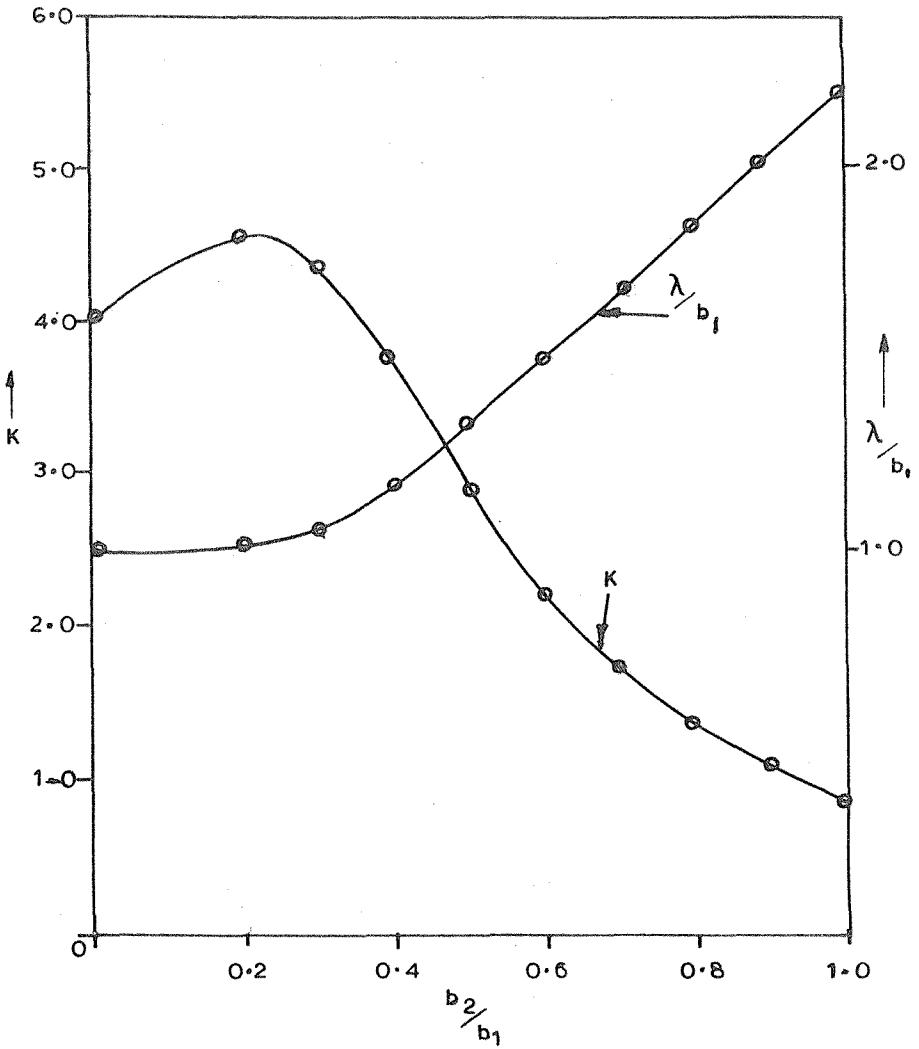

Fig. 4.2(a) Minimum Buckling Stresses and and corresponding Half Wave Lengths of Channel Struts.

are in complete agreement with those obtained by Rhodes and Harvey[62].

In Fig. 4.1(b) are also plotted the values of S*/S at twice and thrice the values of the critical loads. In addition the values obtained using two harmonics in the solution are also shown in the figure. On an average, the reduction in stiffness at thrice the critical load is about 30%.

As the ratio b_2/b_1 increases, there occurs a rapid fall in the value of the critical stress but the postbuckling stiffness increases in the region $b_2/b_1 > 0.4$. In order to compare the structural performance of two cross-sections it is necessary to obtain the ultimate stress. In the absence of an elastoplastic analysis, an indicator of the ultimate load is the average stress at which the maximum membrane stress (i.e. the stress at the middle surface of the plate) first exceeds the yield stress of the material. Such a criterion of ultimate stress has been used by certain authors in the past[25,26]. Fig. 4.3 shows the average stress and the maximum membrane stress σ_{max} (which occurs at the junction) plotted against the average strain for two cases, one with $b_2/b_1 = 0.5$ and the other with $b_2/b_1 = 1.0$. Both the stresses and strains have been divided by $\frac{\sigma}{E}_{cro} = \varepsilon_{cro} = \frac{\pi^2}{3(1-\nu^2)} \cdot \frac{h^2}{b_1^2}$, the critical stress or strain for a plate of width b_1 simply supported along its longitudinal edges. Taking $b_1/h = 50$ and the σ_y/E for the material to be 2×10^{-3}, yielding will occur when $\sigma_{max}/\sigma_{cro}$ reaches a value of 1.383. Reading the corresponding values of average stresses on the graphs, it is seen that the channel section with $b_2/b_1 = 0.5$ is capable of carrying 20% more average stress than the one with $b_2/b_1 = 1.0$. It would appear, therefore, that it is best to proportion the channel sections such that b_2/b_1 lies between 0.4 to 0.6; with $b_2/b_1 < 0.4$, the overall buckling is an important considera-

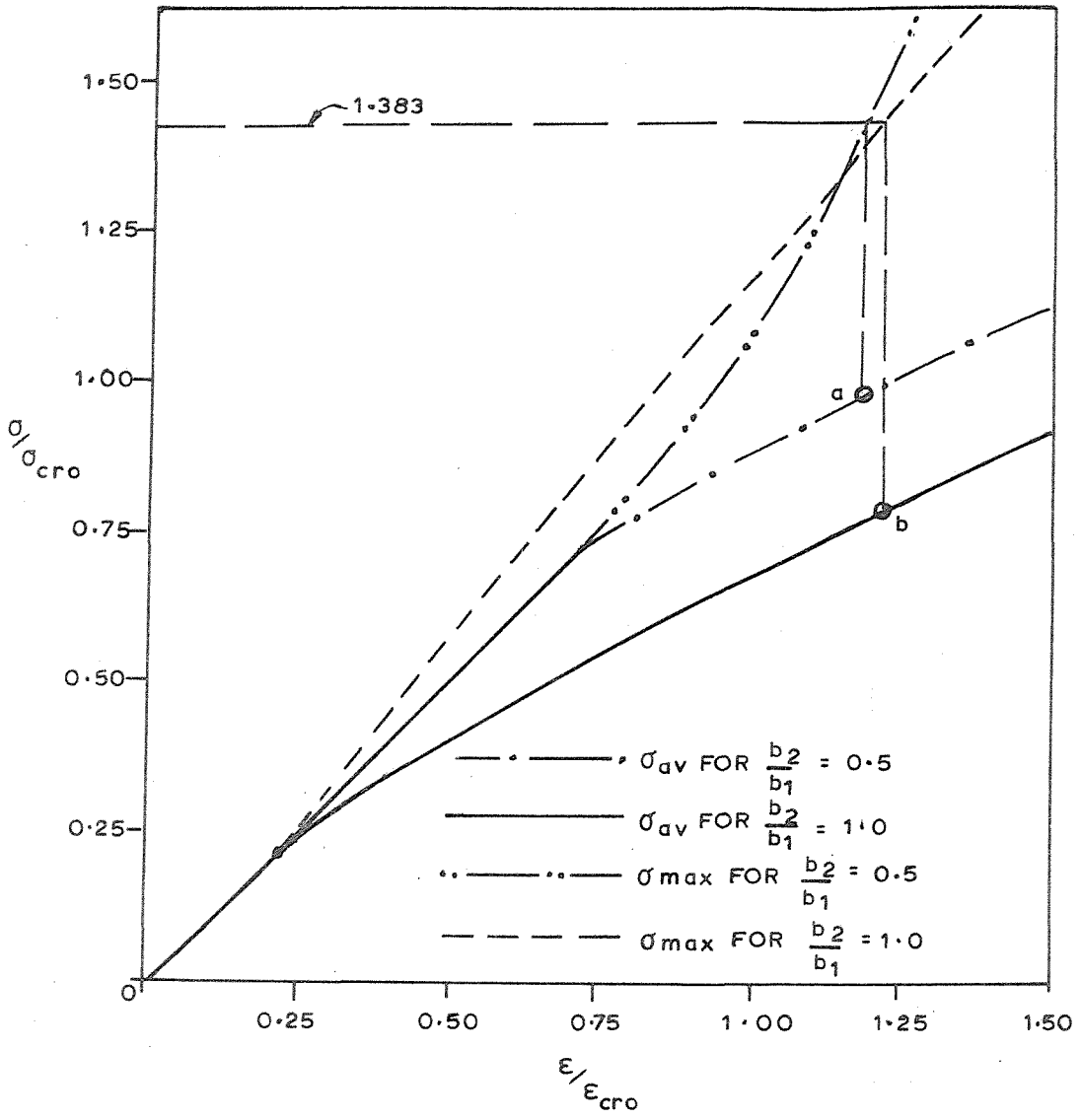

Fig 4.3 Relations of average and maximum membrane stresses with average strain for the Channel Struts with b_2/b_1 ratios of 0.5 and 1.0.

tion except for very short columns as shown by Williams and Wittrick[105]. With $b_2/b_1 > 0.6$, the local buckling stresses are considerably lower (Fig. 4.2). As a result, the longitudinal stresses begin to get concentrated near the junctions quite early on in the load displacement history thus leading to an early failure. If a higher b_2/b_1 ratio must be had, it will be advantageous to make the outstands stiffer in comparison to the main plate.

4.3 Studies on corrugated plates

The load carrying capacity of the plates can be improved by introducing one or more V-shaped corrugations in them (Fig. 4.4(a)). The problem of initial buckling of corrugated plates with a single corrugation has been studied by Williams[101]. In the present section, the results of studies on post-local-buckling analysis of plates with a central V-shaped corrugation, are presented.

The analysis is based on an assumed buckling mode which is anti-symmetric with respect to the line of symmetry of the cross-section xx as shown in Fig. 4.4; this together with the approximation that the normal displacements of the plates BC and CD at C vanish, inherent in Version I of the finite strip method, makes it possible to treat the plate BC as being simply supported at C and the longitudinal edge C free to wave in the plane BC. Thus the problem is reduced to that of a plate structure consisting of two plates AB and BC, meeting along a common junction B and simply supported along their respective remote ends as shown in Fig. 4.4(c).

The results of a parametric study using 12 strips in each plate AB and BC are presented in Table 4.1. Since in the context of assumptions in Version I the behaviour is governed only by the ratio of the widths

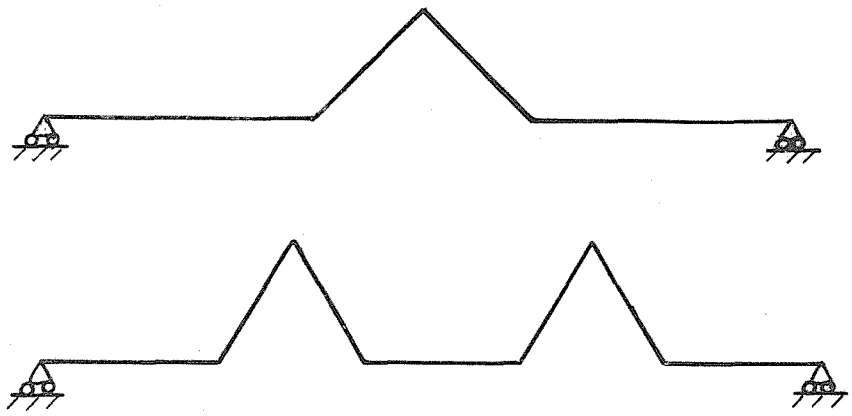

(a) Examples of Plates with V-shaped Corrugations.

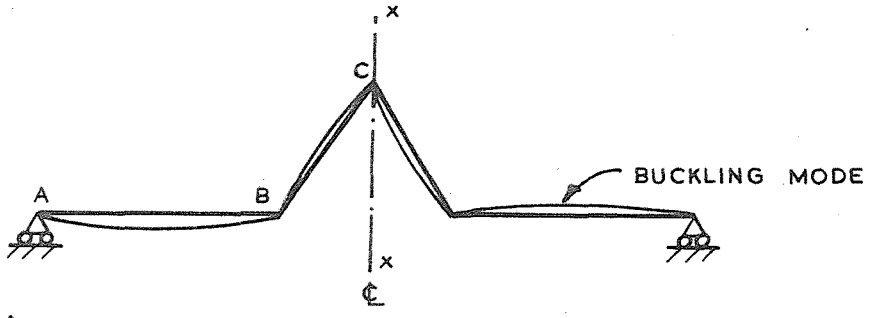

(b) Buckling Modelof a Plate with a Single V-Corrugations.

(c) Equivalent Structure for analysis.

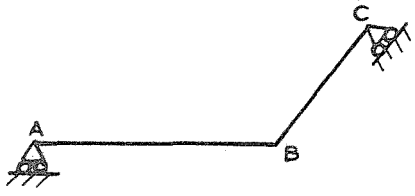

Fig. 4.4 Plates with V-shaped Corrugations.

Table 4.1 Initial buckling data for the corrugated plates investigated

NO.	C/L	θ	λ/L	$K = \frac{\sigma_{cr}}{\left\{\frac{\pi^2}{12(1-\nu^2)} \cdot \frac{h^2}{L^2}\right\}}$	S*/S
1	0.5	60°	0.880	4.71	0.61
2		30°	0.545	13.18	0.55
3	0.6	60°	0.730	7.11	0.62
4		30°	0.550	12.59	0.61
5	0.7	60°	0.660	8.96	0.56
6		45°	0.625	9.48	0.62
7		30°	0.620	9.61	0.61
8	0.8	60°	0.705	7.36	0.61
9		45°	0.690	7.51	0.57
10		30°	0.685	7.60	0.55
11	0.9	60°	0.765	6.09	0.53
12		30°	0.750	6.27	0.50

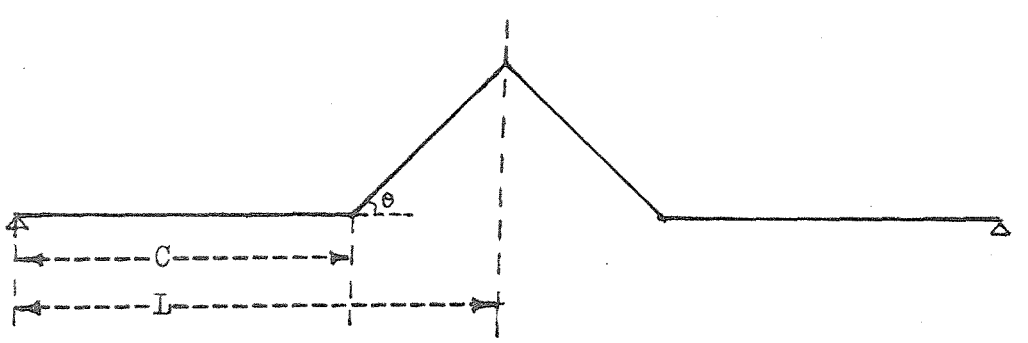

of the plates, it is appropriate to plot S*/S against b_1/b_2 (the ratio of shorter to the longer plate) and this has been done in Fig. 4.5. As 'b_1' approaches zero, the problem becomes one of a plate of width b_2 simply supported along one of its longitudinal edges and clamped along the other. At the other end of the spectrum, with b_1/b_2 equal to unity, each plate behaves as if simply supported along the longitudinal edges.

In order to illustrate the effects of change in b_1/b_2, we consider cases 2 and 11 in Table 4.1. The cross-sections of the corresponding corrugated plates are shown in Fig. 4.6(a-b) where the length 'L' is assumed to be 100 and thickness unity. The total cross-sectional area works out to be 107.74 and 110.00 in case 2 and 11 respectively. Thus the total quantity of the material is roughly the same. This provides the basis for enquiring which of the two configurations works out to be economical for supporting a given total load. It is seen that the case 11 with a b_1/b_2 ratio of 0.22 buckles at a considerably smaller load than the case 2, with a b_1/b_2 ratio of 0.866. This is due to the fact that the buckling stress is controlled mainly by the ratio b_2/h, the ratio of width to thickness of the wider plate. Fig. 4.7 shows the stress-strain curves for the two cases. There occurs a significant reduction of postbuckling stiffness for the case 2, but because of the higher buckling stress, continues to carry a higher load in comparison to case 11. In the figure are also shown the values of maximum membrane stress (in their nondimensional form viz. σ_{max}/E) on the stress-strain characteristics, at discrete values, such as 2.0×10^{-3}, 2.5×10^{-3} and so on. From the figure, it is possible to obtain the first yield loads for given values of σ_y/E. If, for example, this is equal to 2×10^{-3}, the first yield load for case 2 exceeds that of case 11 by about 30%. The difference in the average stress carried by the plate structures for

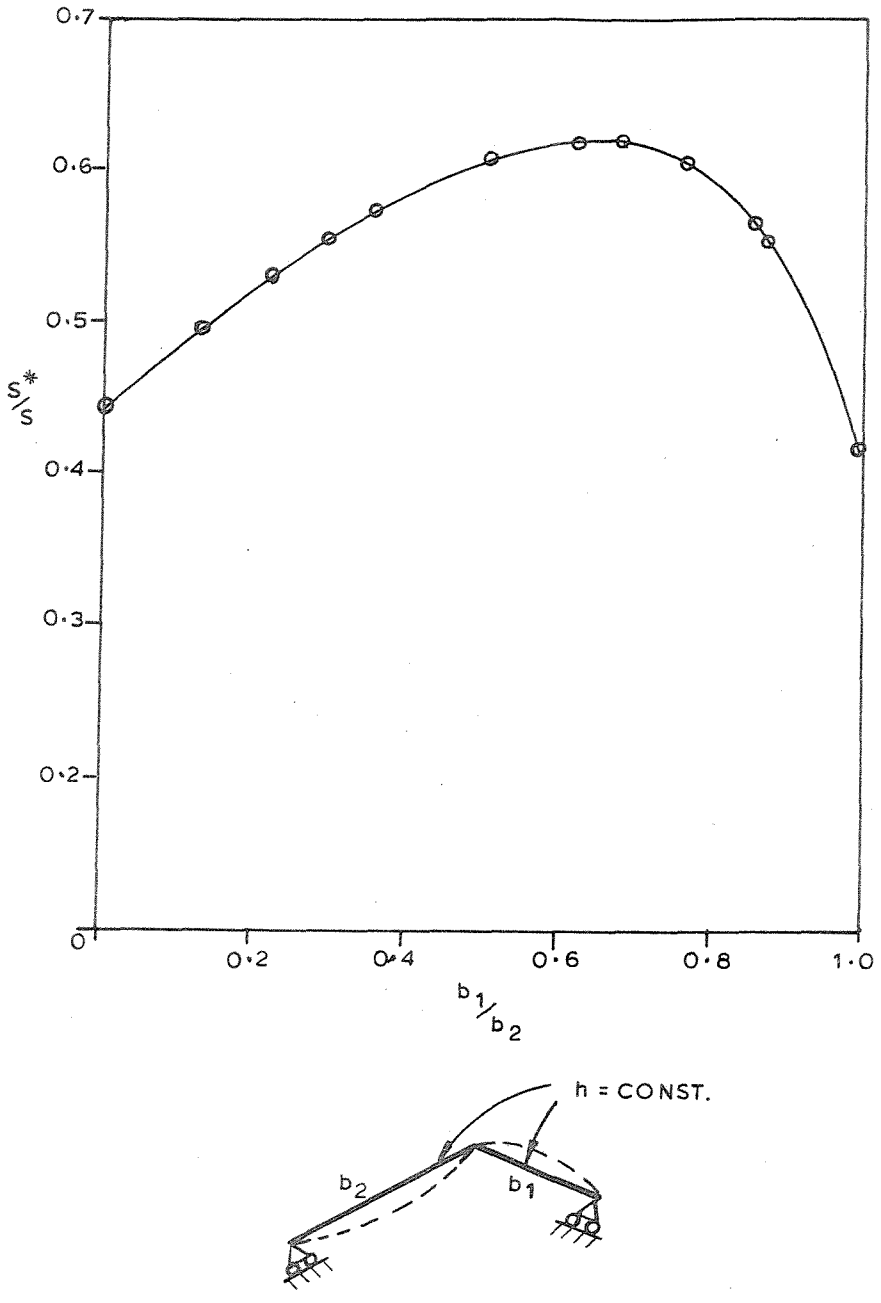

Fig 4.5 Postbuckling Stiffnesses of the Two Plate Assembly with its Outer Edges Simply Supported.

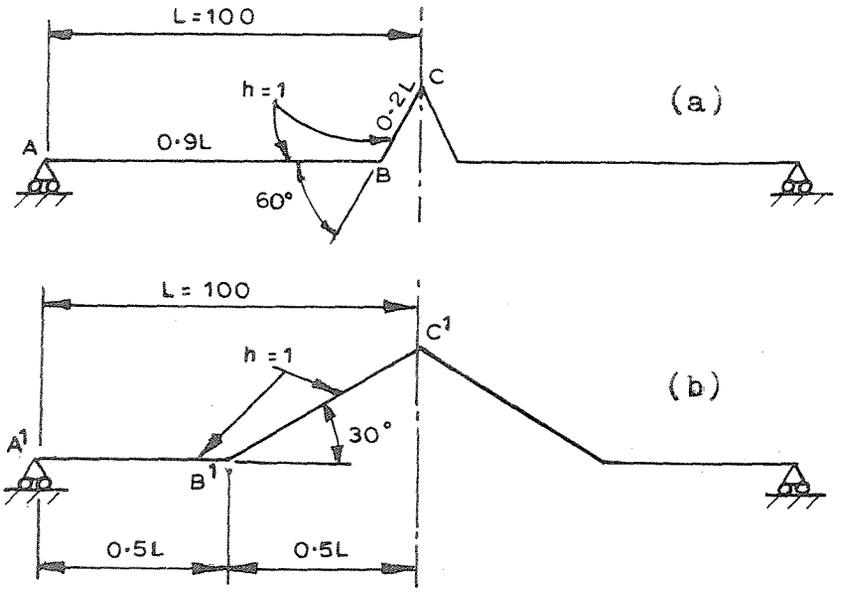

Fig.4.6 Dimensions of Corrugated Plates designated as Cases 11. & 2. in Table 4.1

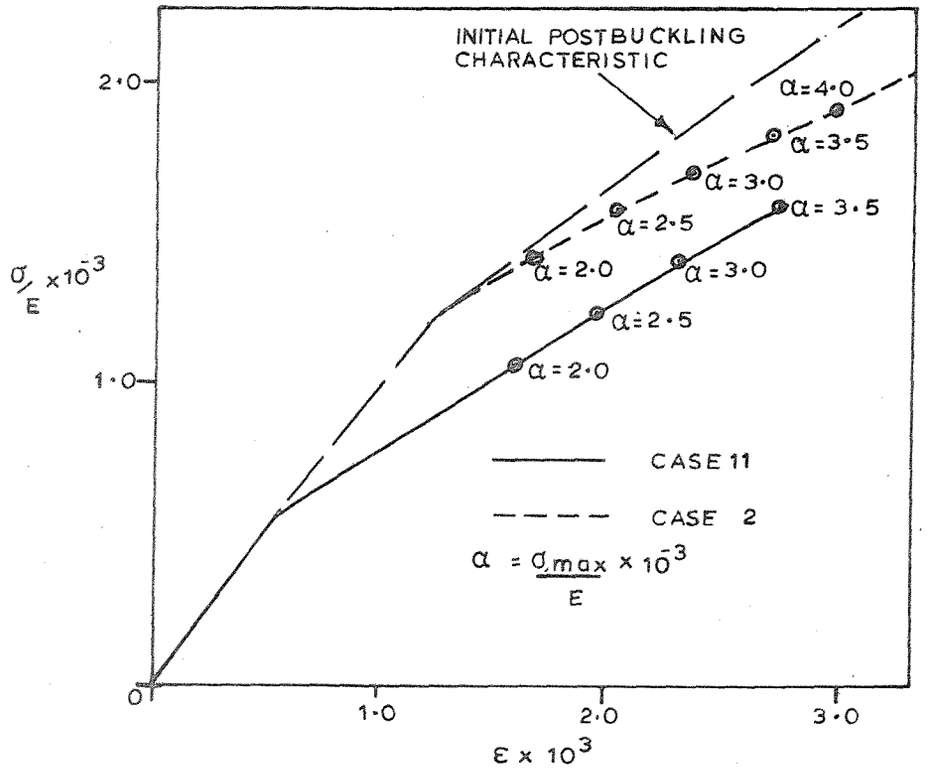

Stress- Strain relations for Cases 2. and 11. of Table 4.1.

Fig. 4.7 A Comparative Study of Corrugated Plates.

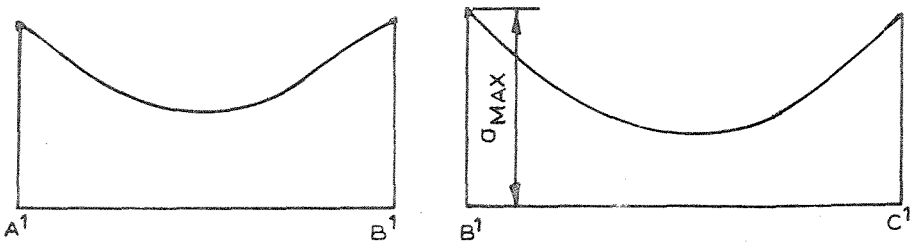

(a) Case 2. in Table 4.1

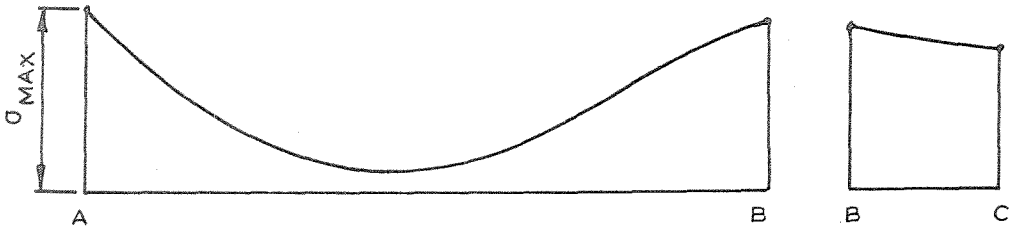

(b) Case 11. in Table 4.1

Fig 4.8. Longitudinal Stress distribution at the Centre for the Corrugated Plates when $\sigma_{max} \equiv 2.5 \times 10^{-3}$

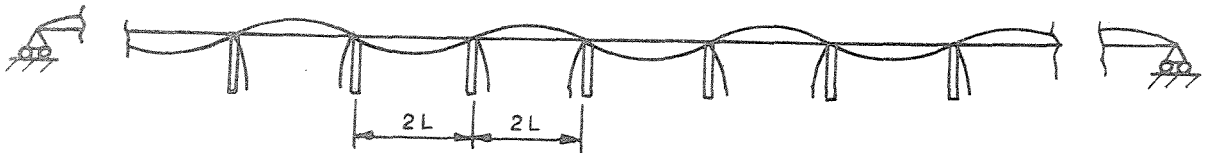

Fig. 4.9 (a) Infinitely Wide Stiffened Plate with equispaced stiffeners and the Local Buckling Mode.

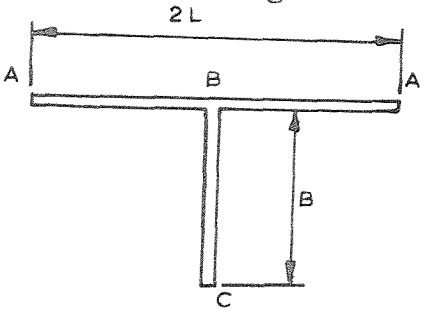

Fig. 4.9 (b) A Typical Panel ABC.

the same value of the maximum stress is explained by Fig. 4.8(a-b). It is seen that for the same value of maximum stress given by $\sigma_{max}/E = 2.5 \times 10^{-3}$ at one of the edges of the constituent plates, the stresses for the case 2 are more equitably distributed whereas there is a wide range of variation of stress for the case 11.

If the thickness of the plates is changed from h to h_1, the characteristics in Fig. 4.7 can still be used provided all the stresses and the strain are scaled by a factor $(h_1/h)^2$. For very thin plates, which have a large elastic range of behaviour after buckling, the differences in the first yield loads, for the two cases, would tend to become smaller as the stress-strain characteristic for case 11 catches up with that of case 2.

The example presented in Fig. 4.7 illustrates the greater structural efficiency of corrugated plates with b_2/b_1 in the vicinity of unity in comparison to those with plates having widely different widths.

4.4. Studies on stiffened panels

One of the structural elements most frequently met with in practice is the plate stiffened with a number of equispaced stiffeners. If the plate is sufficiently wide and carries a large number of stiffeners, it is sufficient to consider the action of a typical panel shown in Fig. 4.9. In this section, the results of a study on the post-local-buckling behaviour of stiffened panels are presented. Effects of changes in the width and thicknesses of the stiffeners are investigated. Note that the problems involving buckling of the plate as a whole, are beyond the scope of the present study.

Fig. 4.9(a) shows an infinitely wide plate stiffened by equispaced stiffeners, together with the buckling mode assumed in the investigation.

A typical panel is shown in Fig. 4.9(b). The boundary conditions at the edges A are as follows:

1) The edges 'A' are free to move in the transverse direction, but remain straight

2) The shear stresses along the longitudinal edges vanish

3) The rotation in the transverse plane vanishes

4) The longitudinal edges are free from transverse shearing forces.

These conditions are the result of the symmetry of the local buckling mode of the plate between the stiffeners with respect to the longitudinal edges A. The analysis employed 8 strips in each leg AB, BA and BC of the panel.

Fig. 4.10(a-c) shows the proportions of the panels investigated. Table 4.2 gives the minimum critical load, the corresponding wave length and the ratio of the postbuckling to the prebuckling stiffness of the panel. The critical load expressed in terms of K where

$$K = \frac{\sigma_{cr}/E}{\frac{\pi^2}{12(1-\nu^2)} \cdot \left(\frac{h}{2L}\right)^2} \quad .$$

(Thus if K = 4, the critical stress equals that of a plate simply supported over a width of 2L). The load displacement characteristics are shown in Fig. 4.11(a-c), where those of panels having the same widths of member plates (but varying thicknesses of stiffeners) are shown along side each other. All the stresses and strains have been divided by a factor $\frac{\sigma}{E}_{cro} = \varepsilon_{cro} = \frac{1}{3(1-\nu^2)} \left(\frac{h}{2L}\right)^2$ for ready comparison with the behaviour of a simply supported plate of width 2L; the maximum values of membrane stresses are also plotted in the figure so that the first yield loads can be obtained once a certain ratio of σ_y/E is specified.

The behaviour of panels ST4, ST5 and ST6 which carry thinner stiffeners is of particular interest. From Table 4.2, it is seen that these panels buckle at very low stresses in comparison to the other panels.

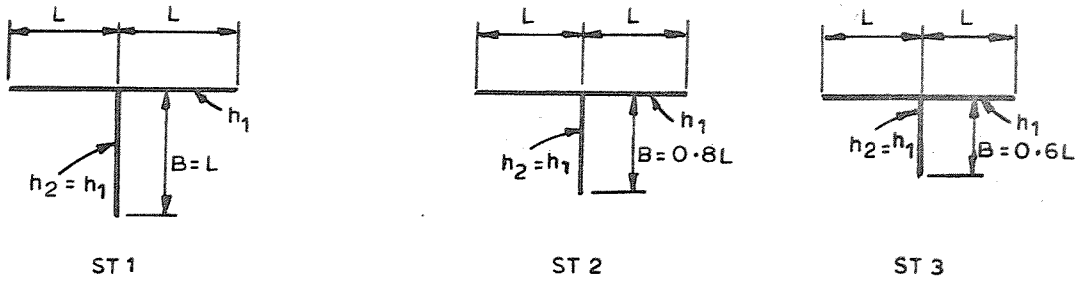

ST 1 ST 2 ST 3

(a) Group I

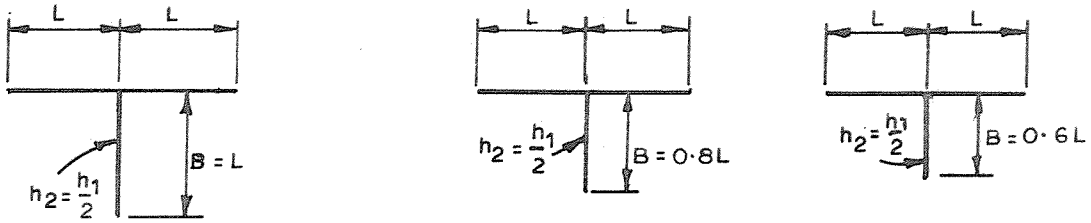

ST 4 ST 5 ST 6

(b) Group II

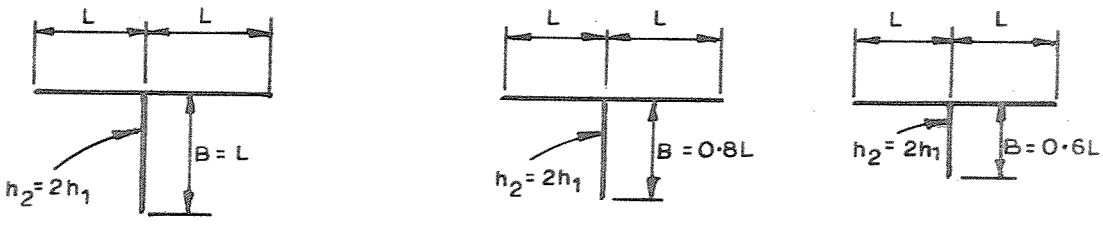

ST 7 ST 8 ST 9

(c) Group III

Fig 4.10 Proportions of Panels investigated.

Table 4.2 Initial buckling data for the stiffened panels investigated

Group	Identification	$\lambda/2L$	K	S*/S
I	ST1	1.21	3.20	0.64
	ST2	1.10	3.86	0.52
	ST3	1.02	4.22	0.55
II	ST4	0.86	1.23	0.91
	ST5	0.69	1.92	0.92
	ST6	0.53	3.41	0.94
III	ST7	0.78	6.17	0.72
	ST8	0.78	6.15	0.68
	ST9	0.79	6.06	0.66

This is due to the buckling of the stiffener almost independently of the main plate as illustrated by the buckling mode for the panel ST4 in Fig. 4.12. This also accounts for the very high initial stiffness of buckled structure. Thus, in this case, buckling stress bears no relationship to the structural capacity of the panel, except as a starting point of the nonlinear behaviour. From 4.11(a-c) it is seen that the high initial stiffnesses of these panels gradually decrease and approach the values of those of ST1, ST2 and ST3 at their respective critical loads. This shows the importance of studying higher ranges of postbuckling behaviour and obtaining the accompanying reductions in stiffness.

From Fig. 4.11(a), it is seen that for a given yield stress, the panel ST7 takes up the highest average stress, ST1 the next higher and ST4 the least. Thus the structural efficiency (as measured by load carried per unit area) of panel ST7, which carries a stiffener twice as thick as the plate, is the highest. This demonstrates the key role played by the stiffener which must be made stiffer than the plate it supports. The boundary conditions of the stiffeners are a little weaker as one of their longitudinal edges is free. If they are slender (i.e. if the ratio thickness to breadth is relatively small) they are liable to buckle independently of the main plate,undergo increasing deflections and thus transfer some of their load to the plates. This would in turn weaken the plates and increase the rate at which the junction stresses build up with respect to a given increase in the average stress.

It is not obvious from Fig. 4.11(a-c) what actual increase, in the load carrying capacity, if any, is associated with panels belonging to Group 3 (which have heavier stiffeners) over other panels, for a given quantity of material used. In order to explore this the panels ST7 and

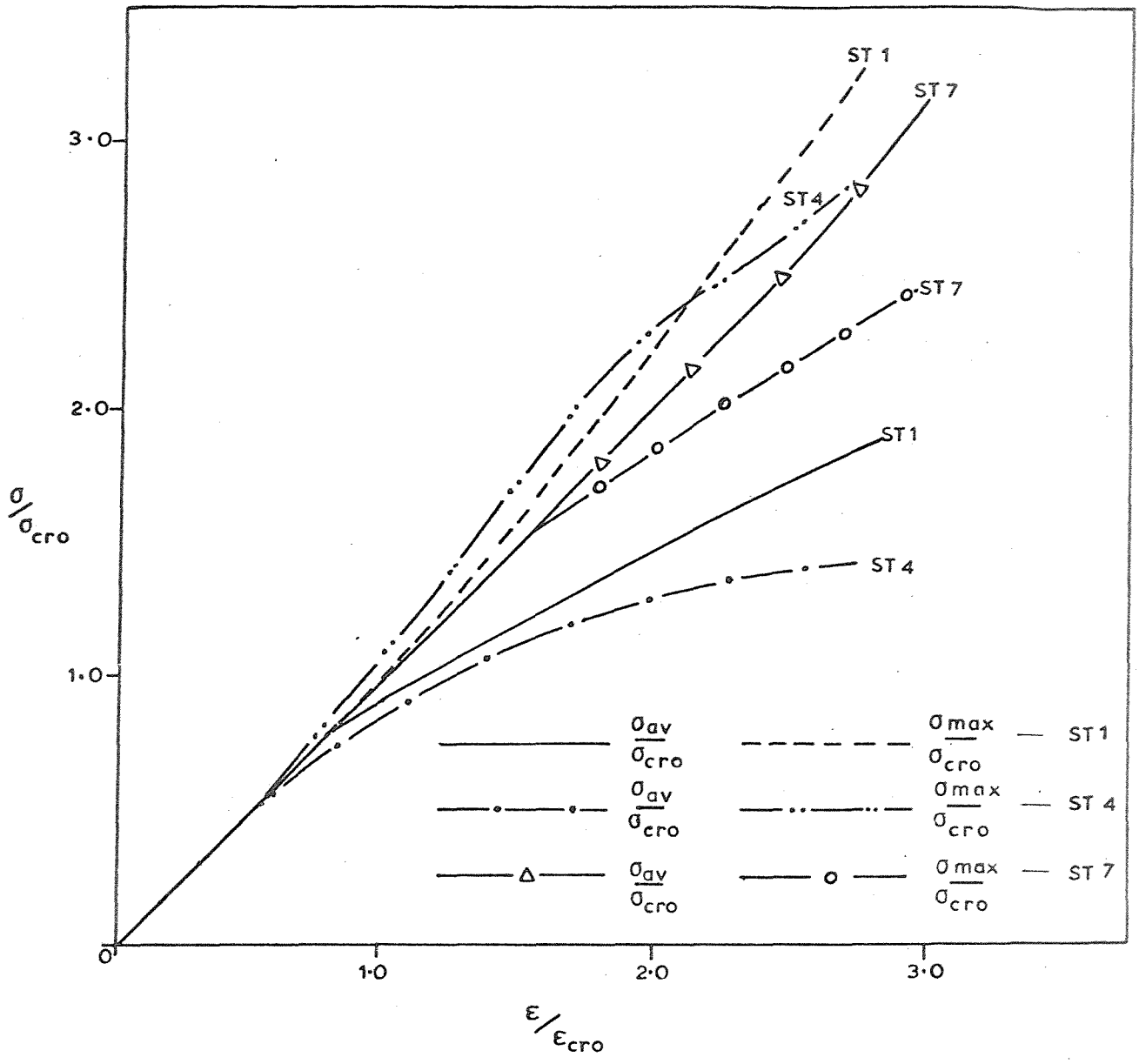

Fig. 4.11 (a) Stress-Strain relations for the panels ST1, ST4 & ST7.

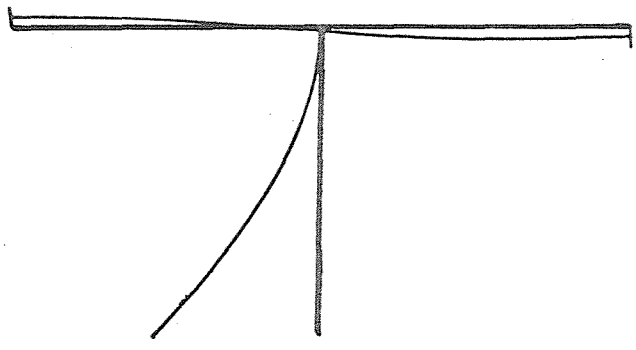

Fig. 4.12 Initial Buckling Mode of the Panel ST4.

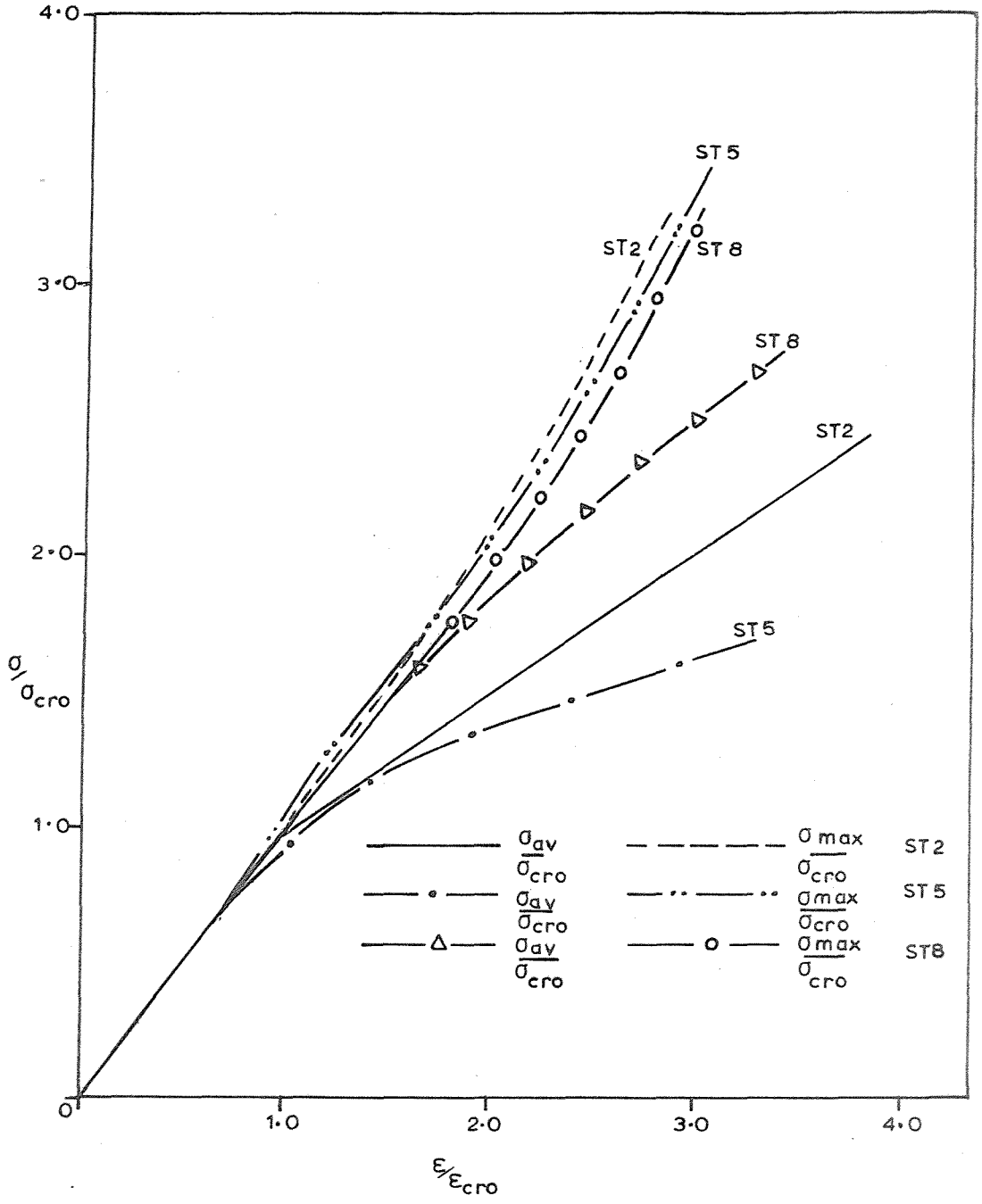

Fig. 4.11(b) Stress-Strain relations for the panels ST2, ST5 and ST8.

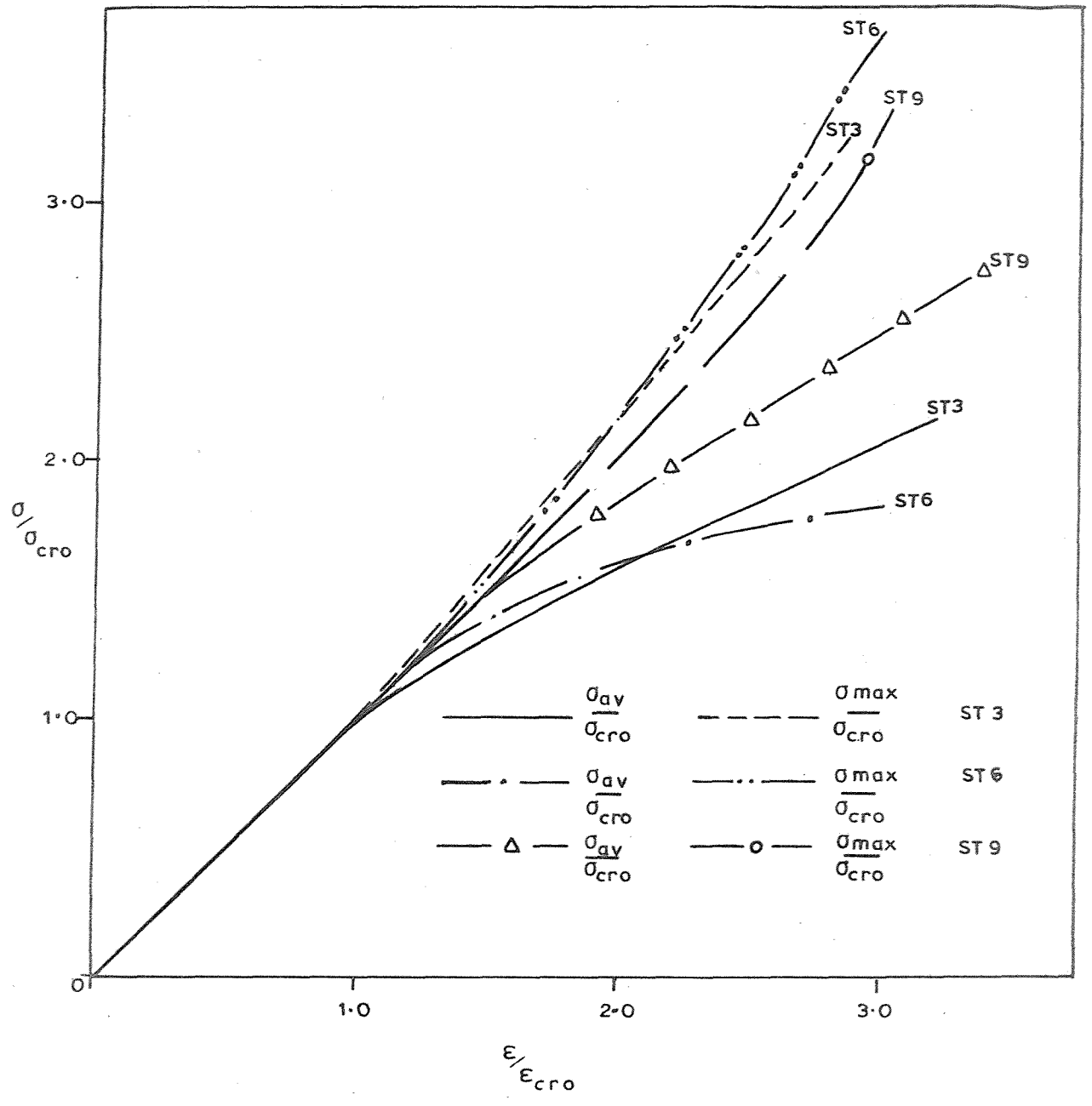

Fig. 4.11(c) Stress-Strain relations for the panels ST3, ST6 & ST9.

ST4 are reproportioned in the manner indicated in Fig. 4.13 (and re-designated as ST7* and ST4*) such that the ratios of the thicknesses of the plates are maintained but the area of cross section works out in each case to be $3h_1L$ - the same as that of ST1. The relationships between average and maximum membrane stresses and strain for the panels are shown in Fig. 4.14. These can be obtained for the cases ST7* and ST4* from the characteristics plotted in Fig. 4.11(a) by using a scaling factor equal to $(h_1/h_1^*)^2$ both for the stresses and strain.

It can be shown with the aid of Fig. 4.14, that the proportions of the panel ST7* are the most economical. In order to demonstrate this, we consider a specific example. Let h/L = 50, and E = 2×10^6 kg/cm^2, ν = 0.3 then σ_{cro} = 723 kg/cm^2. Assuming $\sigma_y/\sigma_{cro} = 3$ (corresponding to a yield stress of 2169 kg/cm^2), the corresponding nondimensional average stresses are given by points P, Q and R in Fig. 4.14 for the panels ST7*, ST1 and ST4* respectively. It is seen that the panel ST7* is capable of taking 10% greater load than the panel ST4* - an indication of the advantage of making the stiffeners heavier.

Comparison of stress-strain relationships for the panels in each of the groups in Table 4.2, from Fig. 4.11(a-c) shows that panels with stiffeners of smaller width take up higher average stresses at the first yield. This is especially true of the panels in the first two groups.

Thus there appears to be a case for proportioning the stiffener BC (Fig. 4.9(b)) such that it has a h/B ratio of at least 4 times the corresponding value for the main plate AA. It is possible to achieve this by reducing the value of 'B', but this will reduce the resistance of the structure to overall buckling. Finally it must be noted that as the stiffeners are made increasingly stiffer, at a certain stage the local buckling mode will change, the plate behaving as if clamped at the stiffeners.

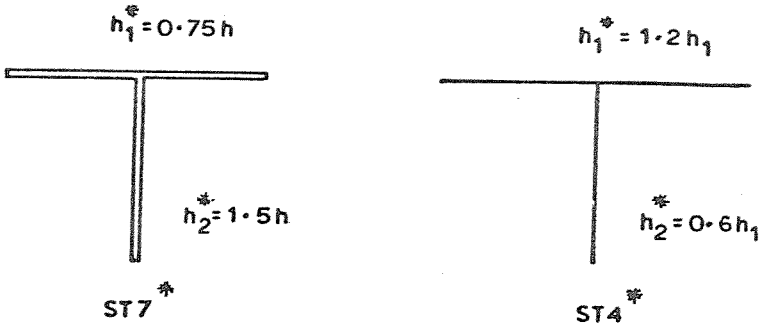

Fig.4.13 Proportioning of the panels ST4* and ST7*.

Fig.4.14 Stress-Strain relations for the panels ST1, ST4* & ST7*.

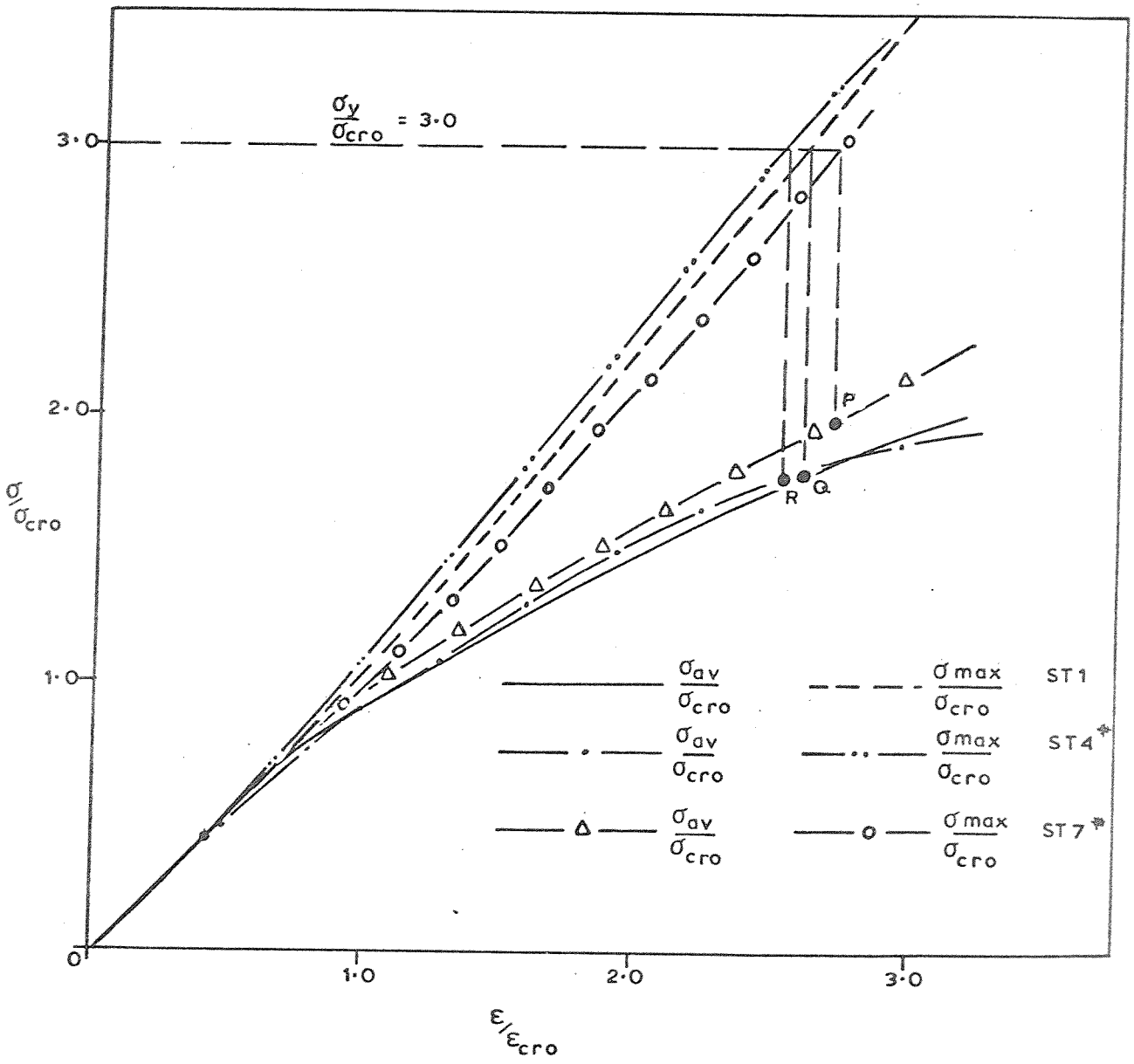

4.5 Examples of panels with box type stiffeners

The disadvantage associated with the stiffened plates discussed in the previous section, is that the stiffener happens to be the weakest member of the structure, being completely unsupported along one of its edges. In order to maximise the structural efficiency of the system, the stiffener must be made stiffer, as demonstrated in the last section. It is possible to improve their performance in other ways, as for example by providing additional supporting members as shown in Fig. 4.15(a-c). In the present section, it is proposed to consider the performance of box type stiffeners shown in Fig. 4.15(c); these improve considerably the resistance of the structure against overall buckling,with the result it would fail often exclusively by local buckling. Thus the post-local-buckling behaviour of such structures is of special interest; and the subject is discussed in this section by considering a few worked examples.

Fig. 4.16(a-d) shows the configurations of the plates in the examples studied. The panels fall into two groups identified by A and B; the preferred buckling mode in each case is also shown in the figure. The panels belonging to Group A have the same proportions as the panel ST1 in Table 4.2 except for the introduction of a plate parallel to the main plate connecting the adjacent stiffeners, thus providing a basis for comparison with the panel studied earlier. In the second group of panels, the spacing between the boxes has been doubled. The effects of changes in thickness of the plates constituting the stiffeners in each group are studied.

Fig. 4.17(a-b) gives details of the panels of each group investigated. The stress-strain characteristics are plotted in Fig. 4.18(a-b).

Considering the stress-strain relations of the panels in Group I (Fig. 4.18(a)), it is seen that the panel identified by A3 buckles at a

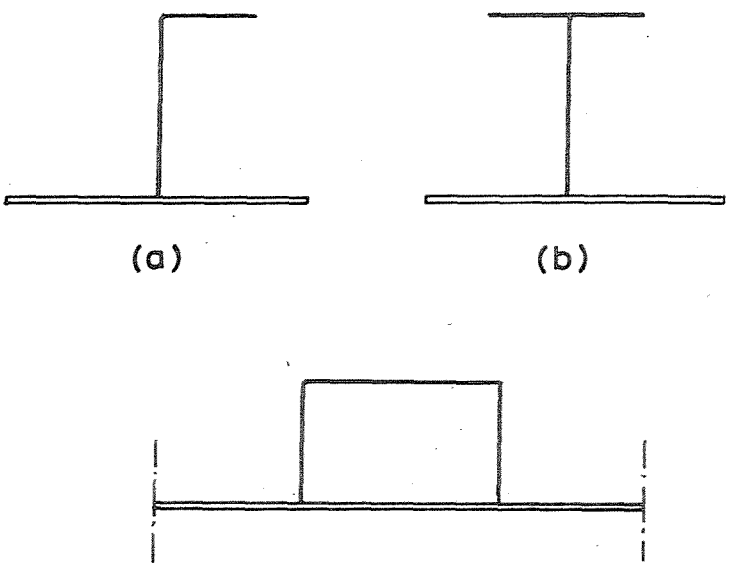

Fig.4.15 Different Types of Stiffeners.

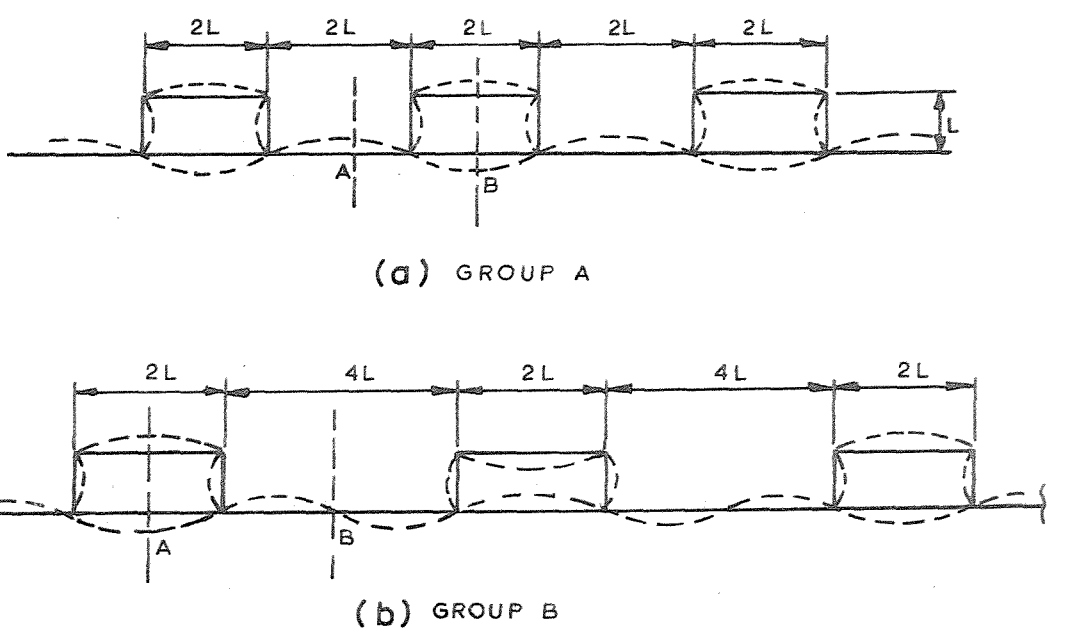

Fig.4.16 Box type Stiffened Panels studied and their buckling modes.

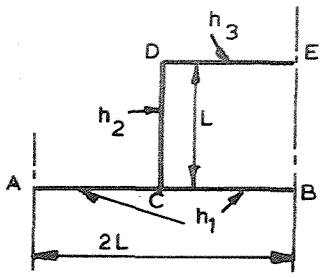

(a)

Group A

A_1 : $h_1 = h_2 = h_3 = h$.

A_2 : $h_1 = h_2 = h$; $h_3 = h/2$

A_3 : $h_1 = h$; $h_2 = h_3 = h/2$

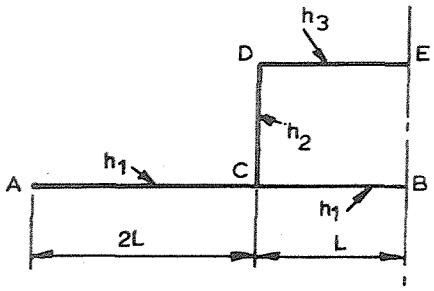

(b)

Group B

B_1 : $h_1 = h_2 = h_3 = h$

B_2 : $h_1 = h_2 = h$; $h_3 = h/2$

B_3 : $h_1 = h$; $h_2 = h_3 = h/2$

Fig.4.17 Details of the panels

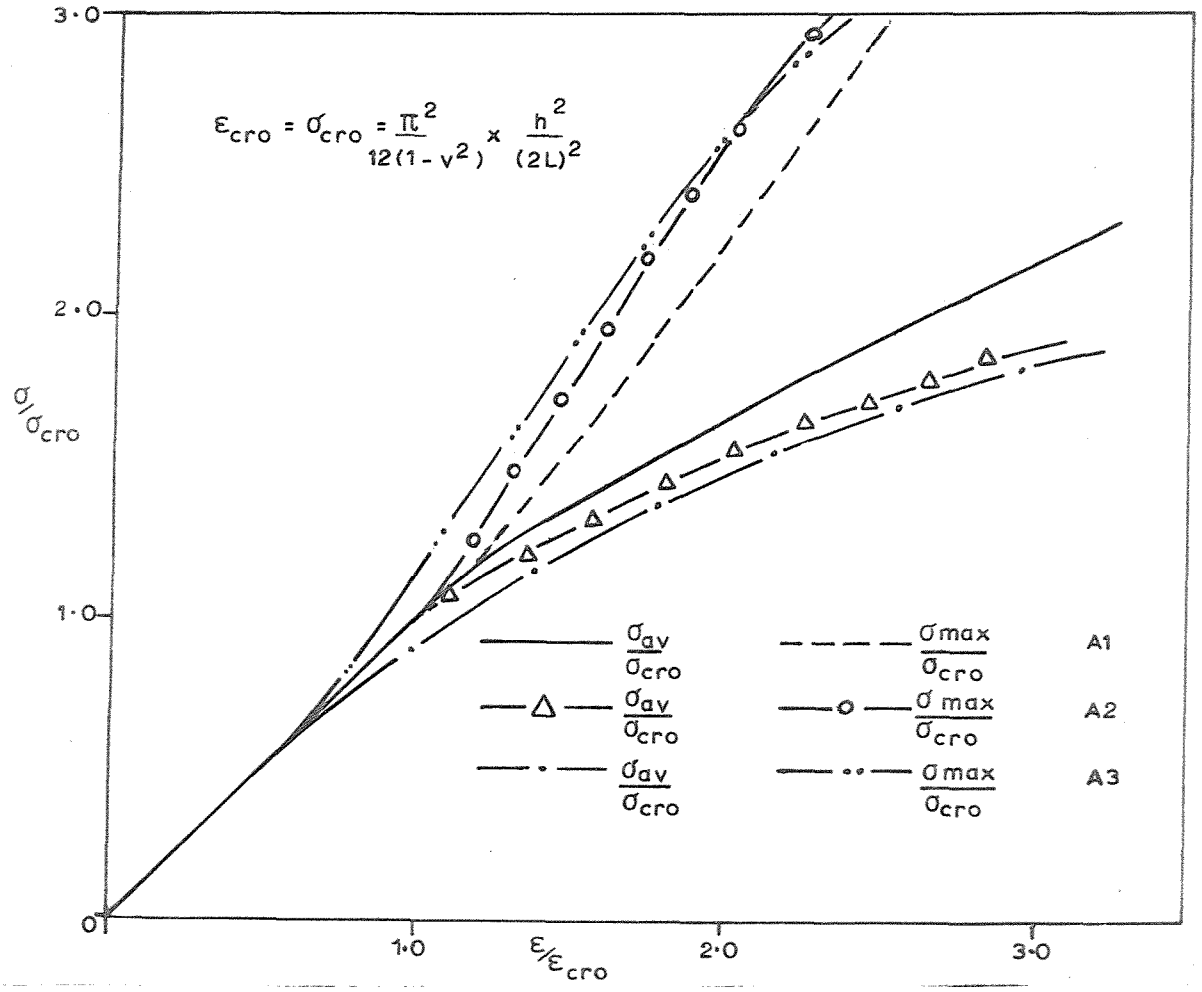

Fig.4.18(a) Stress-Strain relations of the panels of Group A.

considerably lower stress in comparison to A1 or A2. This is due to the buckling of the stiffening plates CD and DE and in particular, the latter, with other plates developing comparatively very small displacements in the vicinity of the critical load. Therefore the postbuckling stiffness remains high; thus the panel carries the same average stress as the panel A2 in the initial postbuckling range of the latter. Comparison of the relationships between the average and maximum stresses on one hand to the average strain on the other for the three cases shows that panel A1 carries the highest average stress for a given yield stress of the material. But this does not in itself imply that the manner of proportioning of A1 is the most economical. In order to examine this aspect, it is necessary as before, to obtain loads carried by the panels for a given total area of cross section at incipient yield. This is done by reproportioning A2 and A3 such that the cross sectional area of each of these is the same as that of A1, as shown in Fig. 4.19. The stress-strain relations for the panels A1, A2* A3* (Fig. 4.19) are shown in Fig. 4.20. Assuming $\sigma_y/\sigma_{cro} = 3$ as in the previous section, the corresponding nondimensional average stresses are given by the points P, Q and R for the panels A1, A2* and A3* respectively. It is seen that the panel A3* carries the maximum load and thus is the most economical of the three. But the difference between the loads taken by the panel A1 and A3* is not significant, being within 4%. Bearing in mind the low buckling stress of the panel A3* and the smaller thicknesses of the plates constituting the stiffener, the panel is particularly vulnerable to the effects of initial imperfections and the extra load carrying capacity can easily be lost thereby. In addition the panel would buckle even at working loads and this may not always be allowed.

The stress-strain relations of the second group of panels B1, B2 and B3 are shown in Fig. 4.18(b). These follow the same trends as the

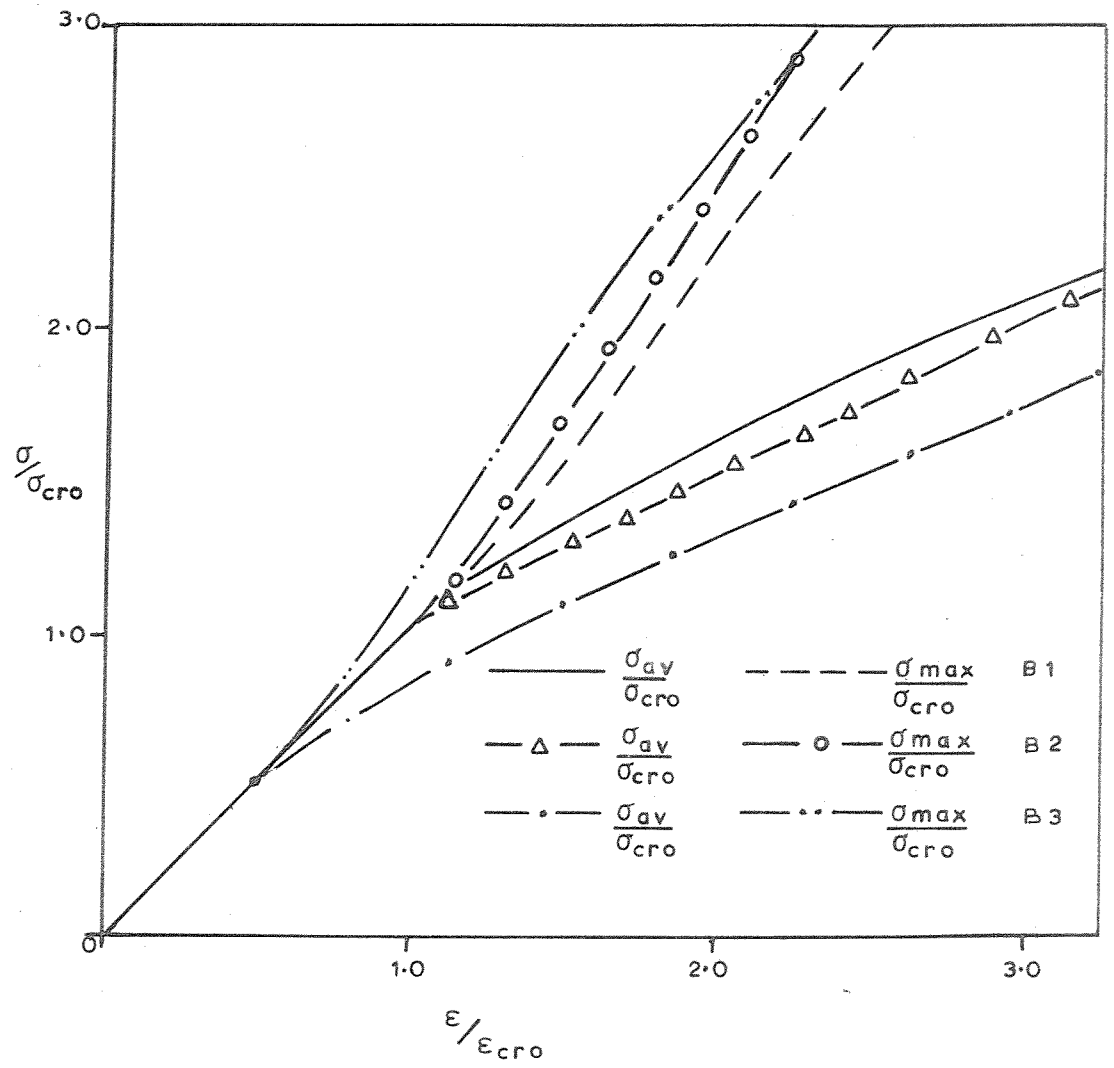

Fig.4.18(b) Stress-Strain relations of the panels of Group B.

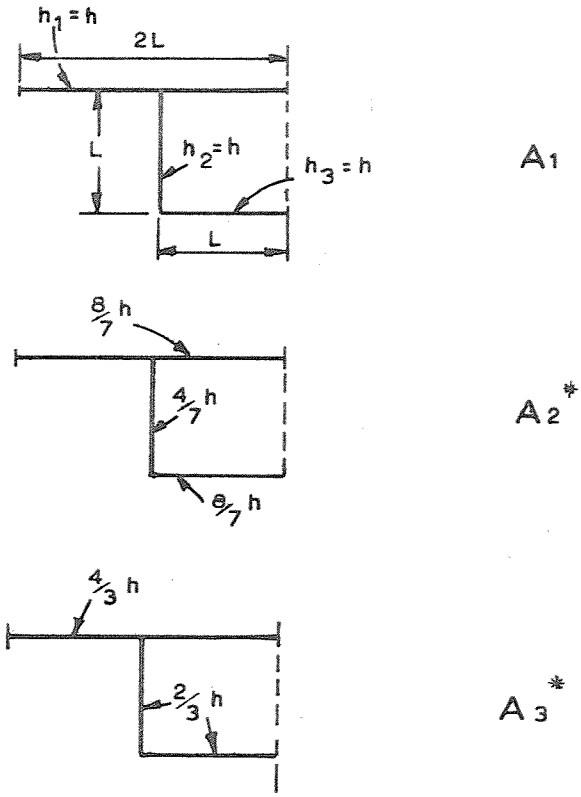

Fig. 4.19 Proportioning of A_2^* and A_3^*

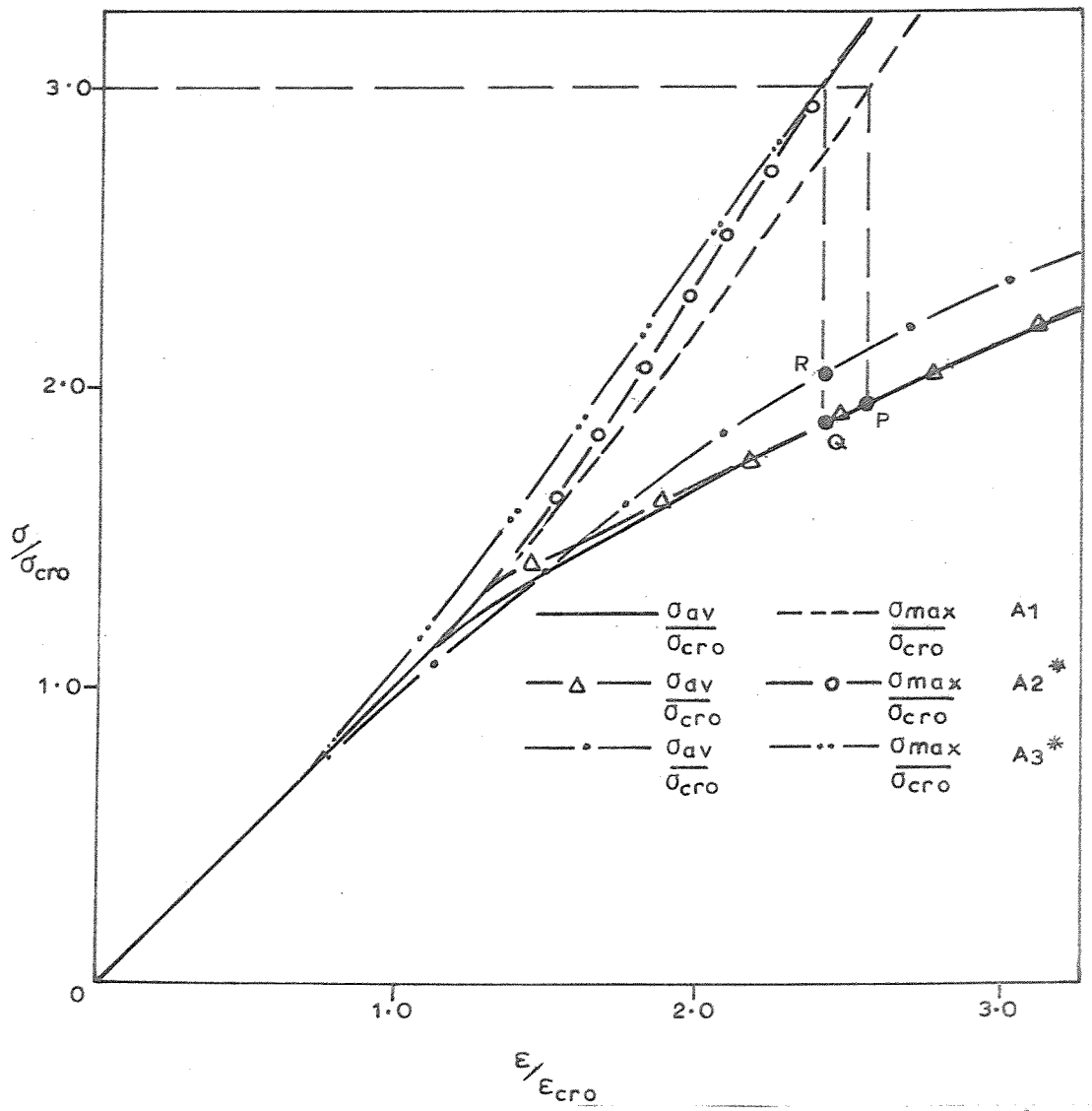

Fig. 4.20 Stress-Strain relations of panels A_1, A_2^* & A_3^*

group A. Comparison of the two groups of stiffened panels (A and B) shows that the load carrying capacity per unit area of cross-section is higher for the group A. However, if comparison of the two groups is made on the basis of the same cross-sectional area over a length of the main plate, the group B would be found to be more efficient. Taking for example, the panels A1 and B1, it can be seen that the thickness of each member of the latter must be increased by 20%, to obtain the same cross-sectional area as panel A1. This is responsible for the higher efficiency of B1 over A1.

Similarly it can be shown that the panel ST1 considered in the previous section has a greater efficiency than the panel A1. But the panel A1 has an advantage over the panels ST1 and B1, in that it has a greater resistance to overall buckling.

4.6 Concluding Remarks

Numerical studies on post local buckling behaviour of a few typical combinations of plate assemblies often met with in structural work are presented. By a comparative study of the characteristics relating the average strain of the plate structure to the average and maximum membrane stresses, relative merits of various ways of proportioning the members have been examined. The conclusions arrived at may be summarised as follows:

(i) In the case of channel section struts made up of plates of uniform thickness, the width of the outstands must be kept as small as possible taking into account the risk of overall buckling. The structural efficiency decreases rapidly with increasing value of b_2/b_1. (Fig. 4.1) The structural performance of the section for higher values of b_2/b_1 can be improved by provision of extra thickness for the outstands. This conclusion follows, in retrospect, from the study of stiffened panels

(ii) In the case of corrugated plates (Fig. 4.4) built up of plates of the same thickness, the width of the constituent plates must be made as nearly equal to each other as possible.

(iii) In the case of stiffened panels which are prone to local buckling, it is important to make stiffener (BC in Fig. 4.9(b)) sufficiently stiff by increasing its h/B ratio to at least 4 times the corresponding value for the main plate (AA in Fig. 4.9(b)). In the case of box type stiffeners, however, there appears to be no advantage in making the stiffener plates stronger than the main plate. On the other hand, the structural efficiency can be marginally improved by making the main plate slightly thicker than the plates constituting the stiffener.

CHAPTER 5

ELASTIC COLLAPSE OF PLATE STRUCTURES

5.1 Introduction

The failure of locally buckled plate structures is often marked by a 'crinkly' collapse of the junctions referred to in 1.2.3.4 (chapter 1). While in practical steel structures, the failure is preceded by plastic yielding of the material, it has been found that the crinkly collapse can be an entirely elastic phenomenon[92]. Therefore, it appears, that a complete elastic analysis would in itself provide an insight into the mechanics of this type of collapse. The high reproducibility of this phenomenon (chapter 6) observed in the tests indicates that

(i) it is a well defined inherent feature of nonlinear behaviour of plate structures

and (ii) mathematically, it would constitute a well conditioned problem. On these grounds, the problem of elastic collapse of plate structures appears eminently worth investigating.

Consider a plate assembly subjected to axial compression, which exceeds its initial buckling stress. With increasing compression, the normal displacements continue to grow at a steady rate. This is accompanied by an increasing concentration of the longitudinal stresses near the junctions on the one hand and the waving in of the junctions on the other. At a certain stage, the inplane displacements in the transverse directions for each plate along the junctions approach such magnitudes as to make them behave like columns with initial imperfections. As a consequence, there begins a column-type collapse of the junctions - aggravating further the normal deflections of the plates and resulting in

a complete loss of stiffness of the structure. In an experimental set up where the end displacements are controlled, the structure would now start shedding load. However, as will be seen in the next chapter, there often occurs at this stage, a snapthrough type of buckling of the structure with an abrupt drop of the load, to a remote equilibrium state characterised by the 'crinkly' buckling mode.

In the discussion of the elastic collapse of plate structures, which is the subject matter of the present chapter, it is therefore necessary to distinguish between

(i) the advanced post-local-buckling equilibrium states which precede and lead to the exhaustion of the capacity of the structure to carry loads

(ii) the post-collapse states of equilibrium characterised by 'crinkly' modes, and

(iii) the intervening states of equilibrium which are skipped in the snapthrough buckling. (Fig. 5.1)

A comprehensive analytical study of the three states mentioned in the foregoing, leading eventually to a mathematical modelling of the crinkly collapse mechanism offers itself as a fascinating proposition for research. But such a study is bound to prove intractably difficult owing to the fact that the deflections in the equilibrium states (ii) and (iii) in the above, become so large that no simplifying approximations (such as those used in von Karman equations) in the strain-displacement and curvature-displacement relations can be justified; and the exact equations for these must be used. These equations[92] are very complicated indeed and would increase the computational effort by an order of magnitude. In the present investigation, therefore, attention is restricted to the study of post-local-buckling behaviour until the structure takes a

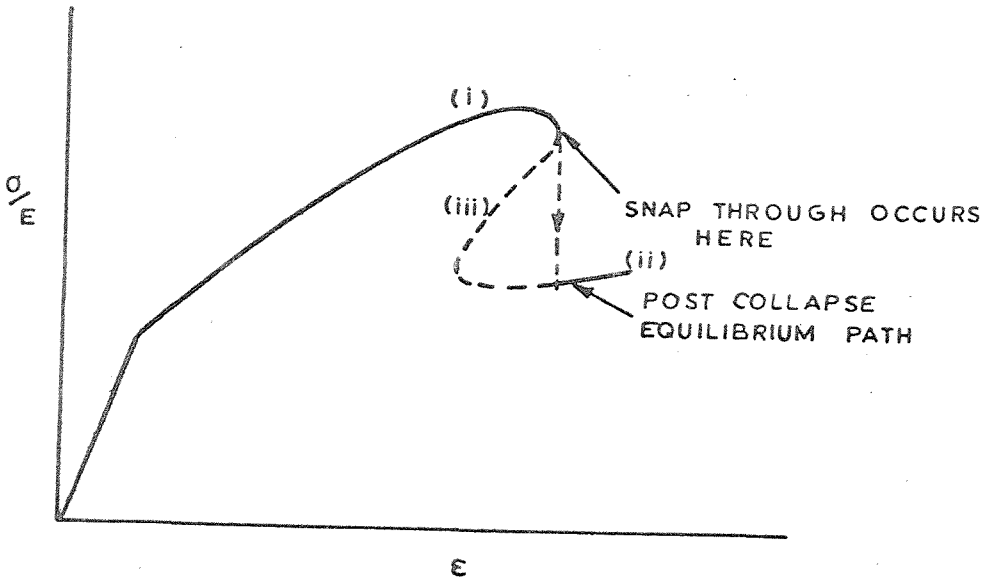

Fig. 5.1 Different States of Postbuckling Equilibrium.

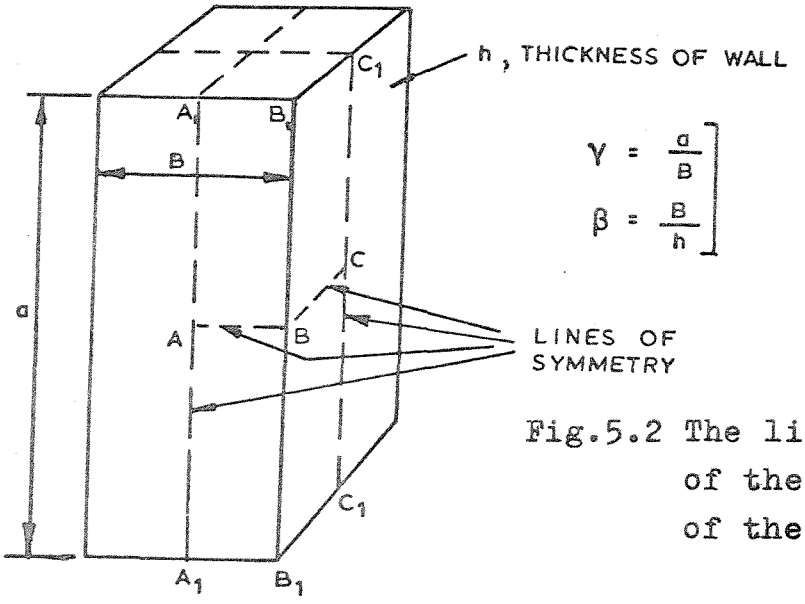

Fig.5.2 The lines of Symmetry of the displacements of the box Column.

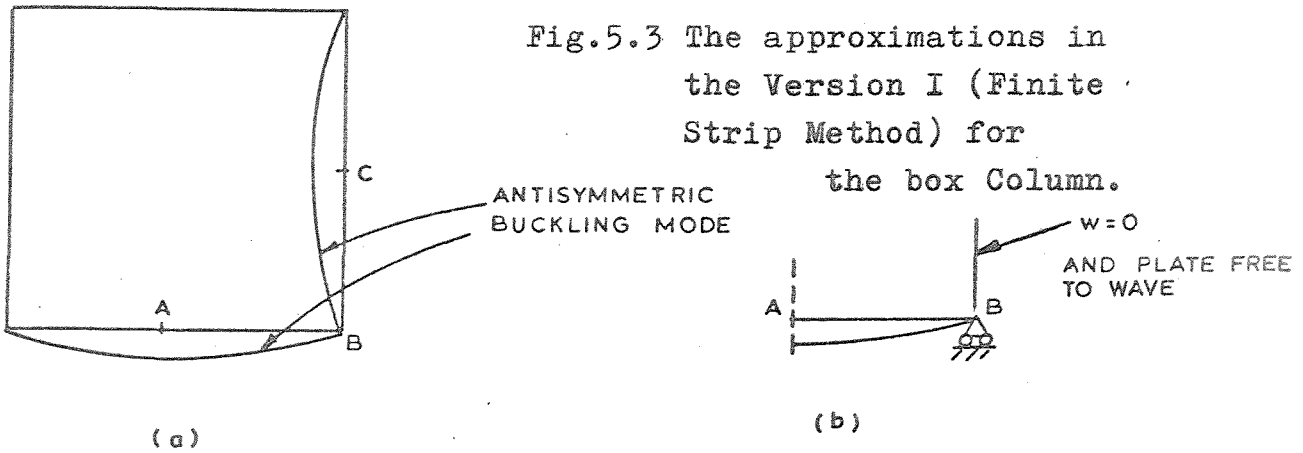

Fig.5.3 The approximations in the Version I (Finite Strip Method) for the box Column.

maximum load and the failure by snapbuckling becomes imminent.

In order to explain simply the phenomenon of crinkly collapse, a mechanical model of a column resting on a nonlinear elastic foundation is proposed in the next chapter.

5.2 Theory

The problem is studied with the aid of the Finite Strip Method developed in chapter 3. Of the two versions of the method discussed therein, Version II is the more accurate in that it satisfies the boundary conditions along the junctions taking into account their 'coupled' nature. This coupling has a significant influence on the structural response in the advanced stages of postbuckling equilibrium for the following reasons.

(i) The normal displacements along the junctions of the plates assume values which can no longer be disregarded; and

(ii) the plates after considerable local buckling tend to behave like interconnected thin shells and the movements of the junction in the plates of the constituent plates are resisted by development of inplane forces.

These effects can not be depicted by Version I of the finite strip method which can not therefore form a reliable basis for the elastic collapse analysis of plate assemblies. But this approach has the merit of simplicity and does not involve any serious approximations as applied to a single plate. It is therefore used in this chapter for, making comparisons with solutions based on Version II.

Since the collapse of the structure is triggered by the growth of inplane displacements in a process of column type buckling of the junctions, it is vitally important to incorporate the destabilising influence of the

inplane displacements 'v' in the analysis. This can be done by including the nonlinear terms in 'v' in the strain displacement relations, i.e. the strain displacement relations must be taken in the form

$$\varepsilon_x = \frac{\partial u}{\partial x} + \frac{1}{2}\left(\frac{\partial w}{\partial x}\right)^2 + \frac{1}{2}\left(\frac{\partial v}{\partial x}\right)^2$$

$$\varepsilon_y = \frac{\partial v}{\partial y} + \frac{1}{2}\left(\frac{\partial w}{\partial y}\right)^2 + \frac{1}{2}\left(\frac{\partial v}{\partial y}\right)^2$$

$$\gamma_{xy} = \frac{\partial u}{\partial y} + \frac{\partial v}{\partial x} + \frac{\partial w}{\partial x} \cdot \frac{\partial w}{\partial y} + \frac{\partial v}{\partial x} \cdot \frac{\partial v}{\partial y}$$

. . . 5.1(a-c)

Introduction of these nonlinear terms in 'v' would result in a large number of additional terms in the energy expression and make the computation considerably more expensive. However it seems possible to introduce simplifying approximations which would enable the prediction of the collapse load without serious loss of accuracy. In the present formulation all the cubic and quartic terms involving the second or higher degrees of 'v' are neglected. Only the quadratic term which results from the interaction of applied compression 'e' (the average strain) and the quadratic term ' $\left(\frac{\partial v}{\partial x}\right)^2$ ', is retained.

The truncation of the energy expression in the manner described above, is capable of a simple physical explanation which will now be given.

The region of the plate in the vicinity of the junctions may be thought of as a column carrying uniaxial compressive stress equal to Ee. This is tantamount to assuming the postbuckled stiffness of the junctions to be equal to that of the plate prior to buckling. Under a prescribed end compression given by 'e', the strain energy stored in the region of the plate during a virtual displacement is given by

$$U^* = -Ee.h \iint_A \delta\epsilon_x \, dxdy$$

$$= -\delta(Ehe \iint \epsilon_x \, dxdy)$$

Now substituting Eq. 5.1(a) for ϵ_x, the strain energy stored in the region of the plate is given by

$$U^* = - Ehe \iint \left[\underline{\frac{\partial u}{\partial x} + \frac{1}{2}\left(\frac{\partial w}{\partial x}\right)^2} + \frac{1}{2}\left(\frac{\partial v}{\partial x}\right)^2 \right] dxdy$$

The underlined terms have already been comprehended in the strain energy expression developed in chapter 3 (and given in Appendix VIII) and therefore the additional terms ΔU^* now sought to be included is

$$\Delta U^* = - \frac{1}{2} Ehe \iint_A \left(\frac{\partial v}{\partial x}\right)^2 dxdy \qquad \ldots 5.2$$

This term has little significance in the regions of the plate where 'v' remains small in comparison to 'w' and there its presence or otherwise would not influence the solution. But in the vicinity of the junctions its influence is significant and must be considered. It must be noted that precisely the same term would occur in the buckling analysis of a column, based on the principle of stationary strain energy on the lines indicated for the plate problem in chapter 3. Such an analysis is based on the principle that 'v' remains so small that the longitudinal stress remains unchanged, but is nevertheless nonzero to make buckling possible.

The strain energy expression including the term 6.1 is given in the last section of Appendix VIII

5.3 Elastic collapse of square box columns

In order to confirm the validity of the approximation discussed in 5.2 and to gain an insight into the mechanics of the phenomenon of elastic collapse of the plate structures, an analytical and experimental investigation into the problem of square box column (being one of the simplest type of plate structure) has been undertaken. The results of the analytical investigation are presented in this chapter. Some of these will be recalled in the next chapter for a comparison with experimental observations.

5.3.1 Details of the theoretical studies

The geometric parameters of the square box columns chosen for the study are given in Table 5.1.

Because of the symmetry of the postbuckling deflections of the column, it is necessary to consider only a quarter of the column contained between the longitudinal lines of symmetry (Fig. 5.2). Table 5.1 gives the number of harmonics in the displacement functions as well as the number of strips into which each half of the plate (AB or BC) is subdivided in the analyses.

The choice of the parameters for the investigation requires an explanation. Firstly, it may be noted that all the studies based on version II are on the columns with $\gamma = 3$. ('γ' represents the ratio of the length to width of the constituent plates). This choice is made obligatory by the following considerations.

(i) Version II of the finite strip method, is primarily intended for cases where the buckling mode is symmetric with respect to the middle of the structure as already noted in 3.2.2.2. An antisymmetric buckling mode will require displacement functions to be described in terms of both even and odd harmonics, thus increasing the number of

degrees of freedom in the problem. Thus it would be an advantage to investigate columns with values of γ = 1,3,5 ... etc.

(ii) The greater the number of half waves into which the structure buckles, the greater will be the number of harmonics in the functions describing 'v'. This would in turn call for an equal number of matching harmonics in 'w' for establishing compatibility along the junctions. The final result of this would be a vastly increased number of degrees of freedom making the computation very expensive.

(iii) In short columns ($\gamma \simeq 1$) the influence of the boundary condition with regard to the transverse displacement i.e. v = 0, will be felt well into the interior of the structure and therefore such a column can not be representative of longer columns which buckle into several half waves.

The choice of γ = 3 appears to be a good compromise between the conflicting requirements of economy in computation in (ii) above on the one hand and a proper modelling of practical situations on the other. If the initial postbuckling stiffness is any indication at all (vide chapter 3), columns with γ = 3 can be sufficiently accurate representation of longer columns for a study of postbuckling phenomena.

A discussion of the nature of the harmonics entering into the description of 'w' is relevant here. The harmonic corresponding to m = 3 represents the buckling mode of the box column and is fundamental to the analysis; the harmonic corresponding to m = 9 gives the flattening effect of the deflection surface between the nodal lines; the remaining harmonics m = 1,5,7 allow the nodal lines to distort and shift and together with other harmonics (m = 3,9) play a part in satisfying the coupled boundary conditions along the junction (by matching with the first five harmonics describing 'v' in the plate at right angles). In order to illustrate quantitatively the influence of each of the harmonics, the contributions of the harmonics in the displacement profile along the

Table 5.1

γ (Ratio of length to width)	β (Ratio of width to thickness)	Harmonics representing			No. of strips in a half of each plate	Version of the FSM used
		w	u	v		
3	20	1,3,5,7,9	2,4,6,8,10...20	1,3,5...19	4,6,8,10 & 12	II
	30,40,50,60,70,80 and 90	"	"	"	12	II
	100	"	"	"	6,8,10,12 & 14	II
Arbitrary 'n'	20	n,3n	2n,4n,6n	0,2n,4n,6n	6,8,10& 12	I
	30,40,50,60,70,80 and 90	"	"	"	12	I
	100	"	"	"	6,8,10,12 & 14	I

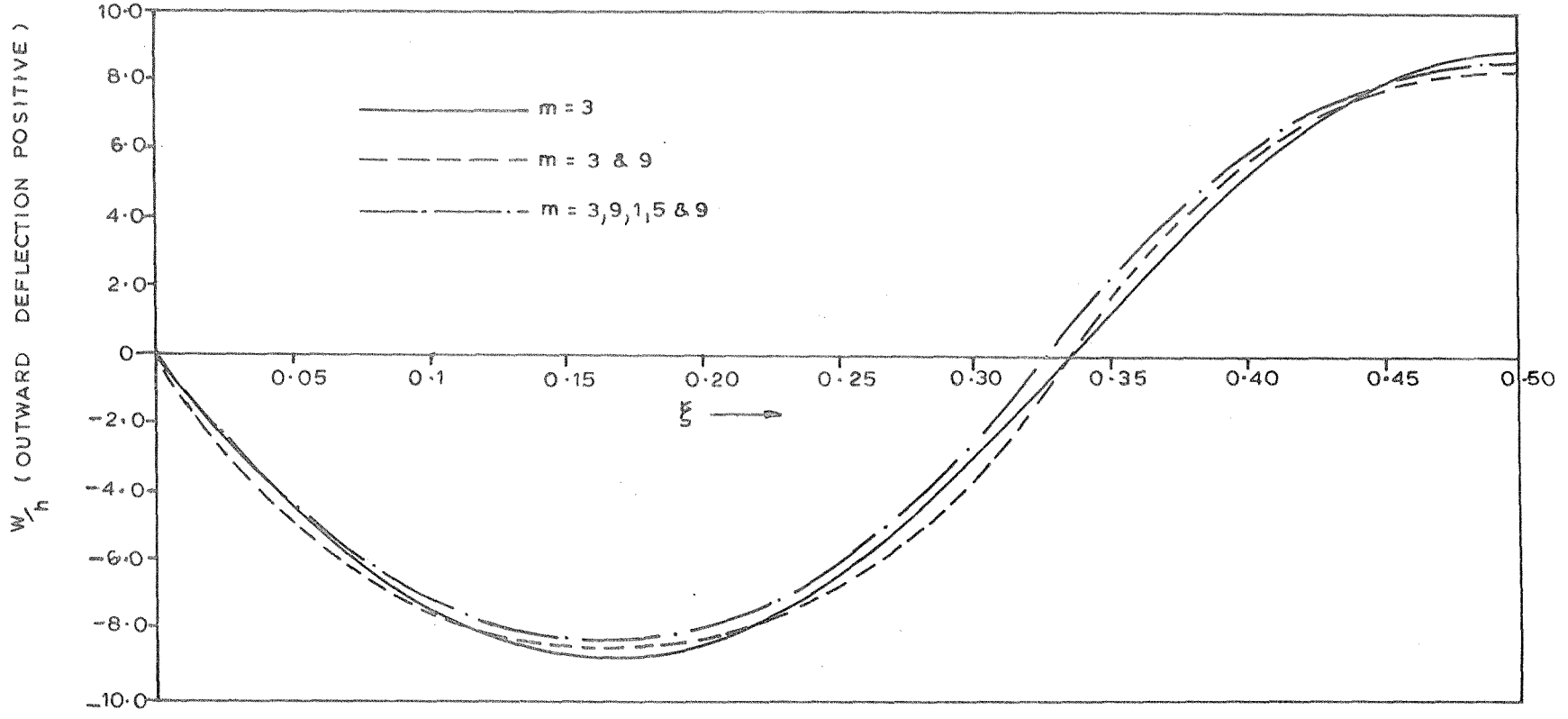

Fig. 5.4 Influence of the different harmonics in the deflection profile along AA for the Column $\gamma = 3$, $\beta = 100$, at $\frac{\sigma}{\sigma_{cr}} = 9.85$.

centre of the column, at a load equal to about 10 times the critical load is shown in Fig. 5.3. It is seen that the harmonics m = 3 and 9 are predominant, but the influence of other harmonics though small is not negligible. Their influence, however, is far more important in the vicinity of the junctions.

The problem is also studied for the same values of the parameter 'β' with the version I of the finite strip method for a column whose length may be an integral multiple of the width say 'n'. Here the buckling mode is represented by two terms 'n' and '3n'. This means that the nodal lines are assumed to remain straight. Since the boundary conditions along the junctions are assumed to be 'uncoupled', the antisymmetry of the buckling mode is preserved in the postbuckling range and therefore it is sufficient to consider one half of either plate A_B or BC (Fig. 5.3). In view of the assumptions involved, the results of this analysis are applicable strictly, to a single plate simply supported on all the edges with the unloaded edges free to wave and are approximations to the behaviour of a square box column.

5.3.2 Convergence of solutions

5.3.2.1 Version II

The convergence of the solution to a sufficiently accurate value depends upon (i) the number of harmonics employed in the displacement functions and (ii) the number of strips which represent the structure.

5.3.2.1.1 Convergence of the solution with respect to the number of harmonics

As already stzted in chapter 3, it is comparatively easy to predetermine the number of harmonics required to describe 'w' in the post local buckling analysis. The significance of each of the harmonics

employed in the present analysis has been discussed in sect. 5.2. As demonstrated in chapter 3, the number of harmonics required for the description of 'u' and 'v' depends on the number of harmonics describing 'w' and must be greater than the latter.

The procedure adopted to check the adequacy of the number of harmonics describing the inplane displacements, employed in the present study is indirect. It is to compare the contribution of each of the harmonics with the actual magnitude of certain key displacements. Since the contribution of the last two harmonics turned out to be, in general, of the order of 1 to 2% of the value of the value of the displacements, the number of harmonics are deemed to be sufficient. Some typical results are shown in Fig. 5.5(a-b).

Fig. 5.5(a) shows the cumulative value of 'v' at the centre of the plate AB, at locations 'E' and 'F' (Fig. 5.5(c)) as each additional harmonic is taken into account. Fig. 5.5(b) shows the cumulative value of $\partial u/\partial x$ (being more significant than 'u' for the longitudinally compressed plates) at the centre of the supported edge of the plate AB (Al Fig. 5.5(c)). It is seen that convergence is oscillatory and that the values of 'v' and $\partial u/\partial x$ for 8 harmonics differ from those 10 harmonics by less than 2% in all the cases. The results given in 5.5(a-b) are typical of the entire range of plates and stresses considered in the present investigation.

5.3.2.1.2 Convergence of the solution with increasing number of strips

In Fig. 5.6(a-b) are plotted the nondimensional load-end displacement relationships of the columns with $\beta = 20$ and $\beta = 100$, with increasing number of strips to represent the plates AB and BC. Convergence is found to be much more rapid in the case with $\beta = 20$ than in the case with $\beta = 100$. In the former case, the difference in the collapse

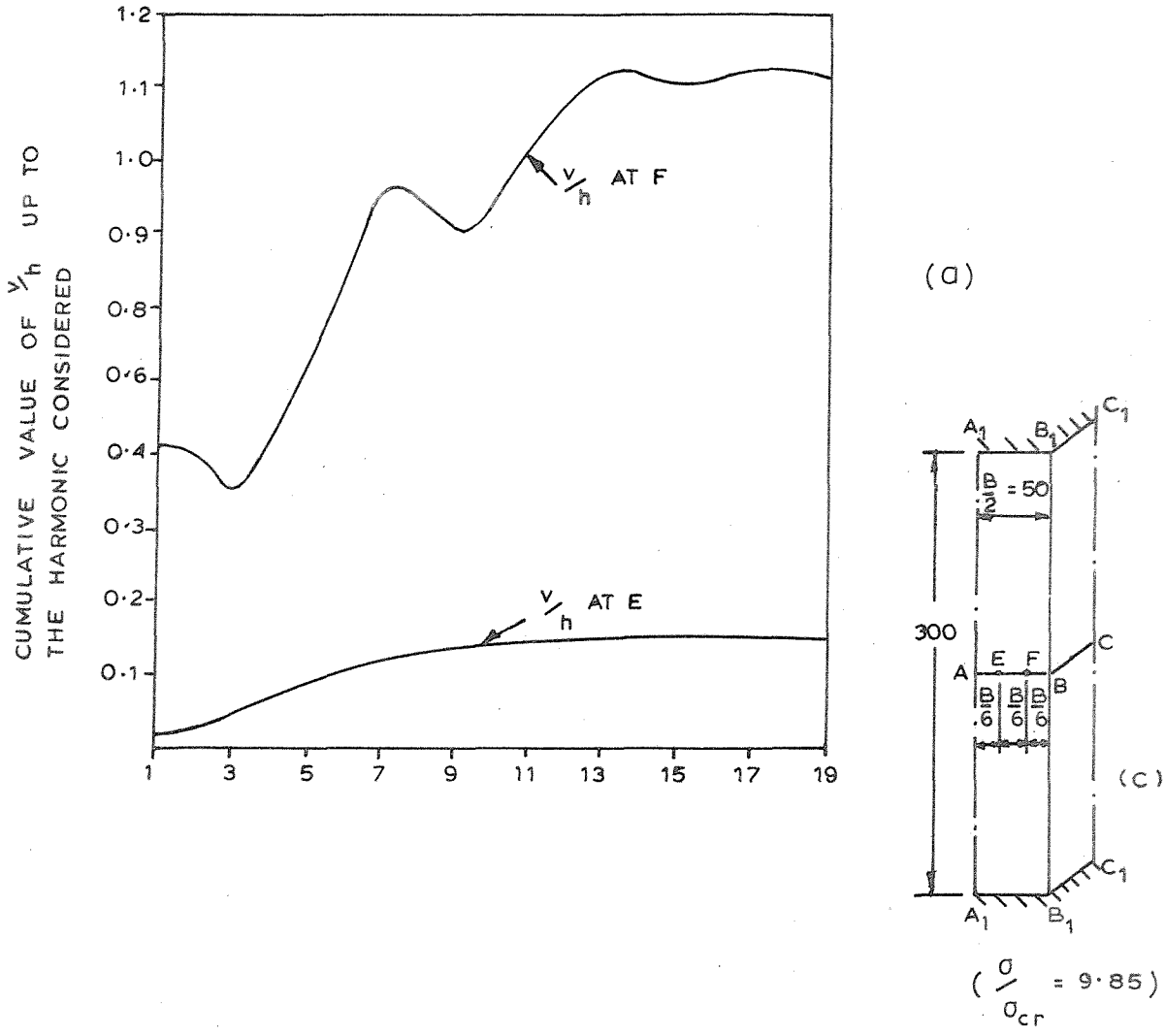

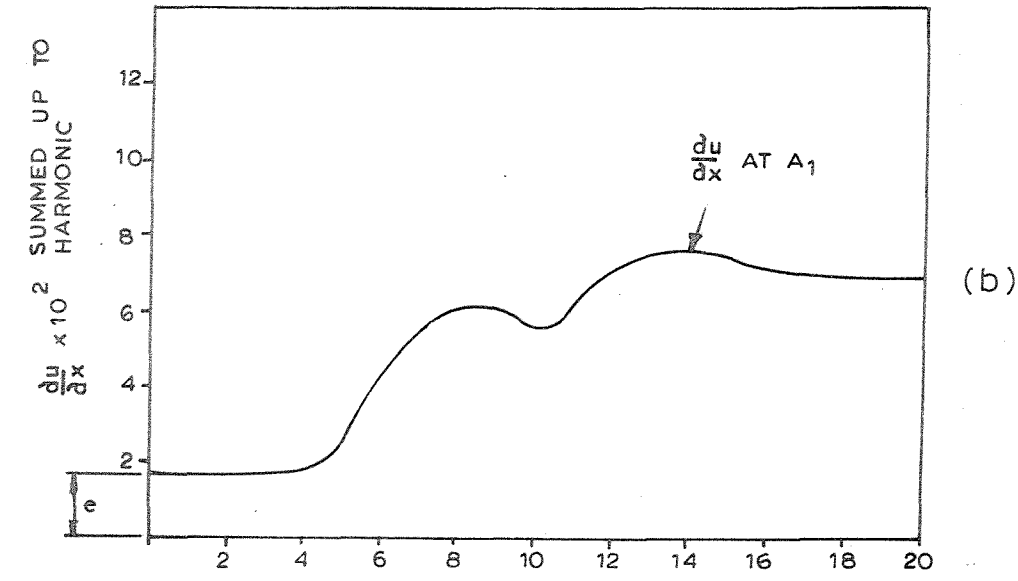

Fig. 5.5 Convergence of the magnitude of the inplane displacements with increasing number of harmonics.

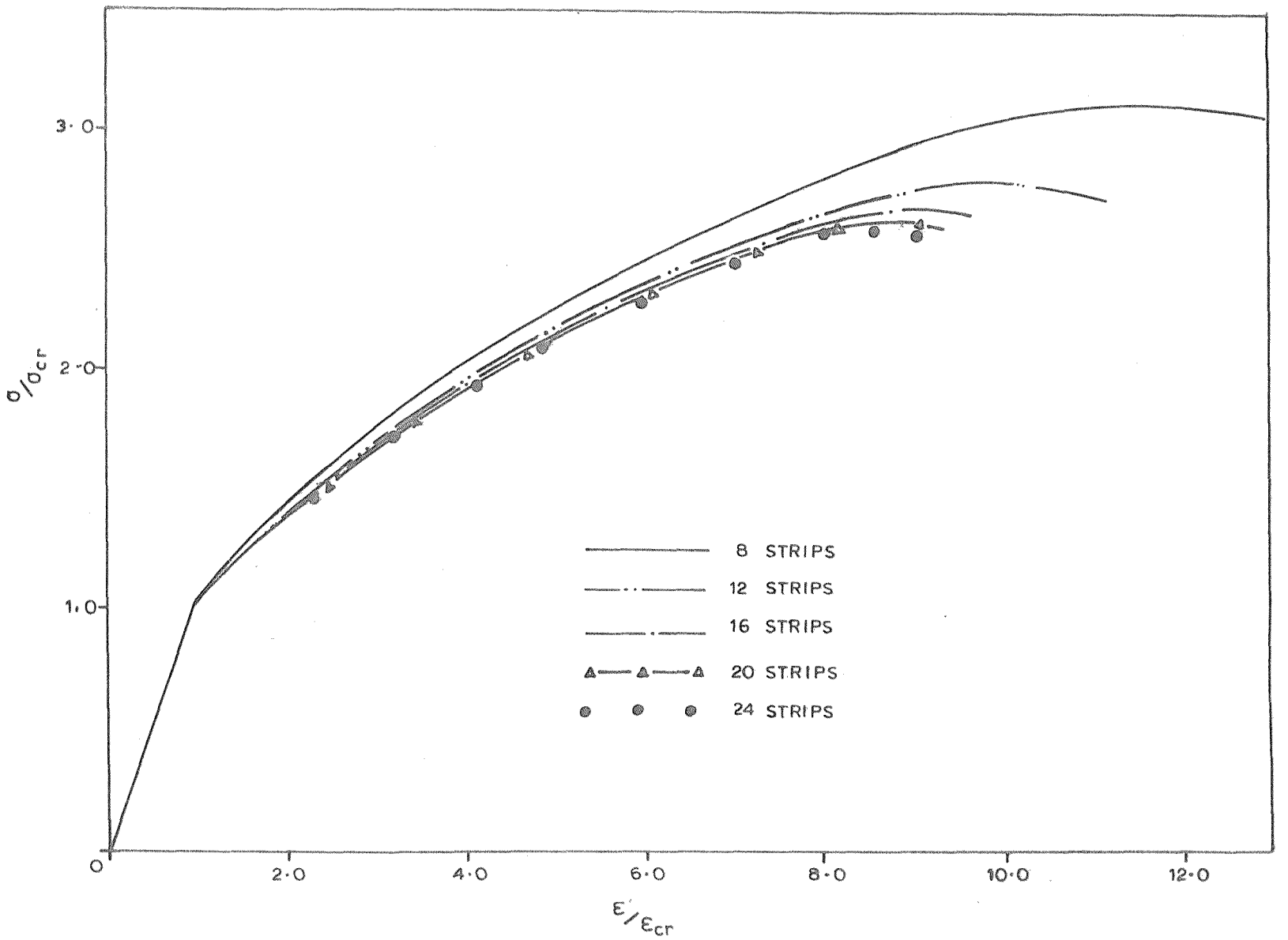

Fig. 5.6(a) Convergence of Version II Solutions for a Column with $\gamma = 3$, and $p = 20$.

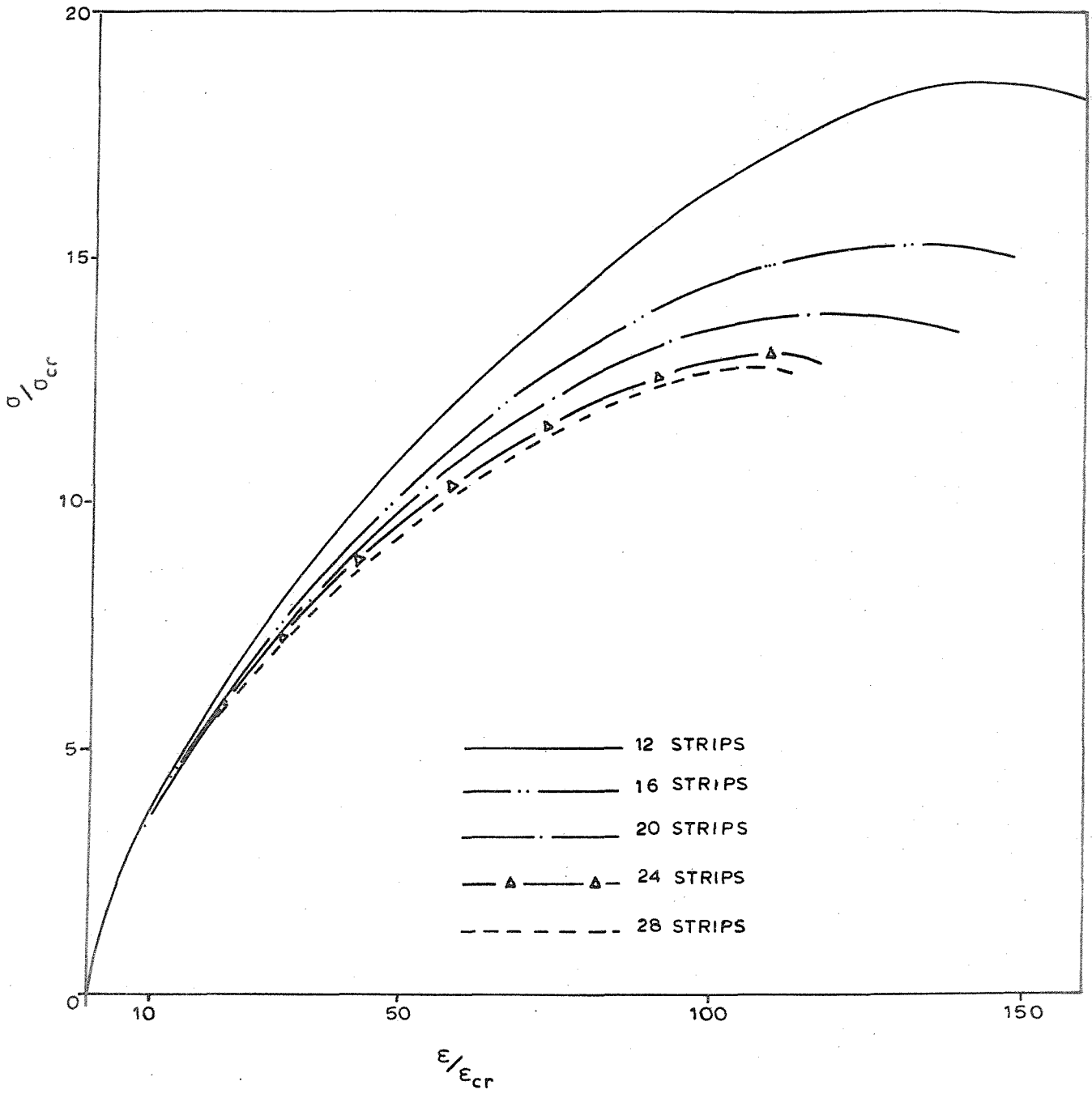

Fig. 5.6(b) Convergence of Version II Solutions for a Column with $\gamma=3$ and $\beta=100$.

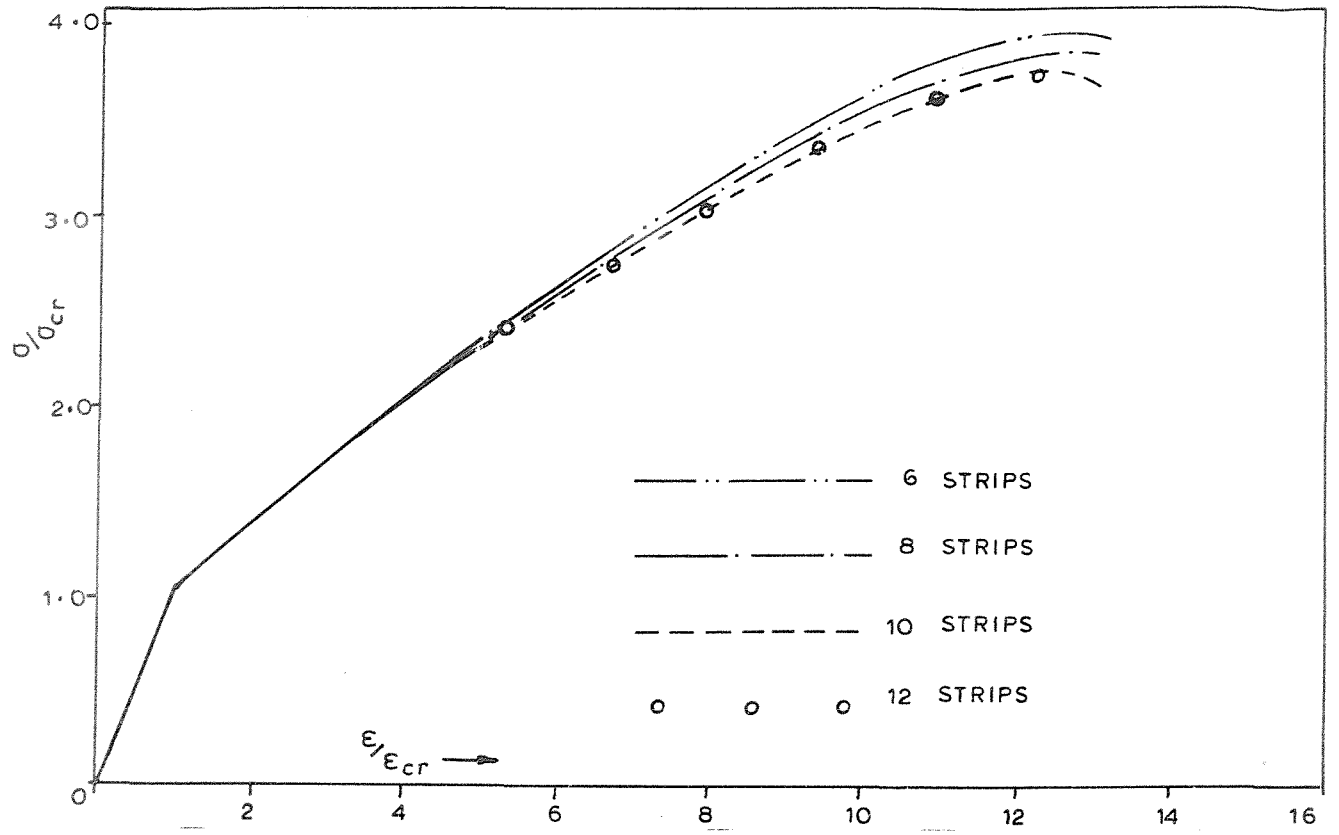

Fig. 5.7(a) Convergence of Version I Solution for a plate with β=20.

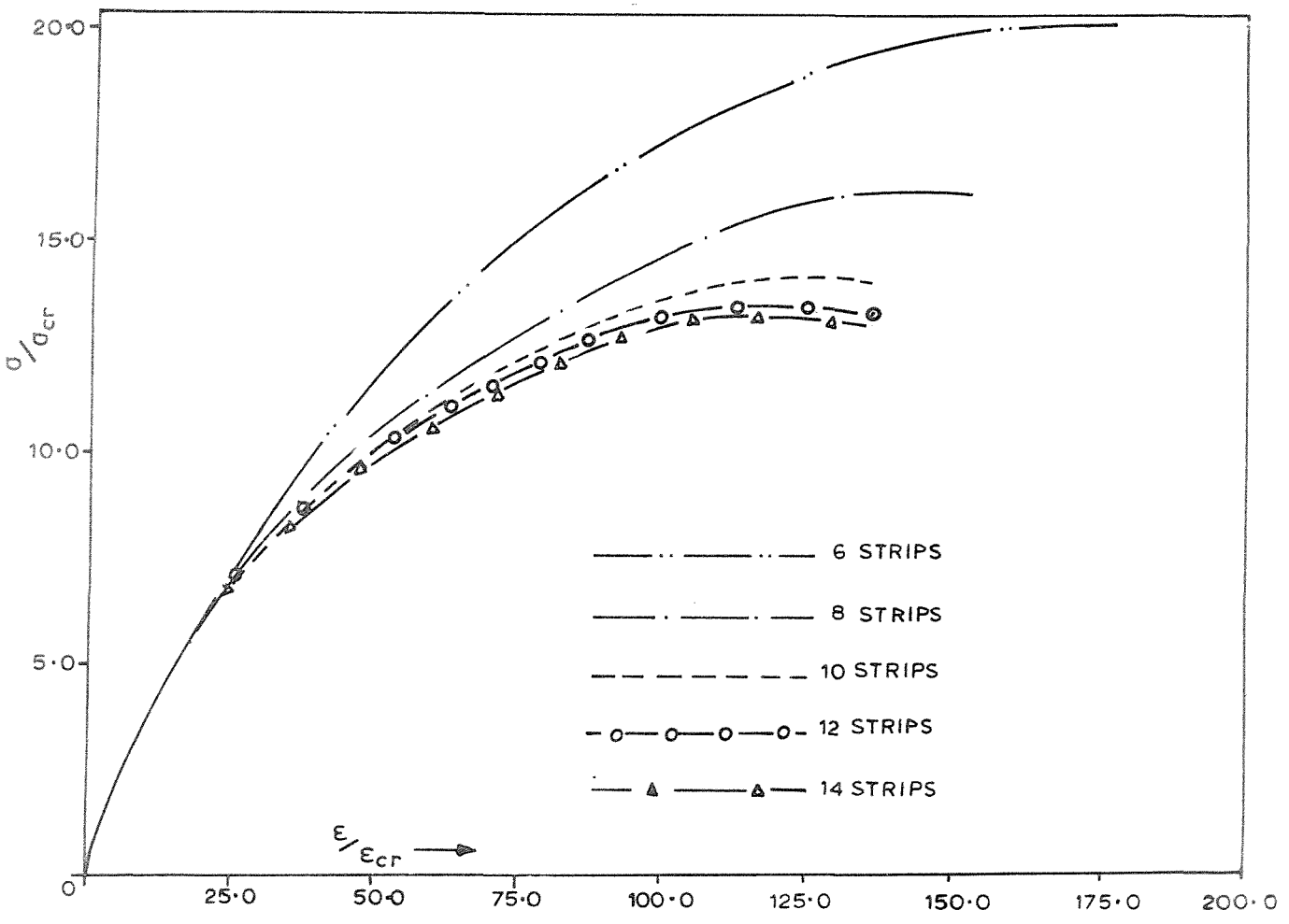

Fig.5.7(b) Convergence of Version I Solution for a plate with β=100.

stress obtained with 10 strips and that with 12 strips is less than 1%. In the latter case, the difference in the collapse stress obtained with 12 strips and that with 14 strips lies between 2 to 3%. The poorer accuracy in this case is due to the larger nonlinear range of precollapse behaviour of the column, made up as it is of thinner walls. In order to obtain solutions of collapse loads within an error of 2% on an average, over the range of values of 'β' considered (from 20 to 100), it appears sufficient to employ 12 strips to represent each of the plates AB and BC.

5.3.2.2 Version I

In Fig. 5.7(a-b) are shown the results of the convergence studie on square plates with $\beta = 20$ and $\beta = 100$, using version I of the finite strip method. The trends are very similar to those observed in the studies on the square box columns using version II.

5.3.3 Discussion of Results

5.3.3.1 General trends

Fig. 5.8(a-c) shows the nondimensional load-end displacement relationships for the nine cases ($\beta = 20, 30 \ldots 100$) of the box columns investigated using version II. It is seen that, with increasing values of β, there occurs a reduction of the collapse stress (σ_u) on the one hand, while the ratio of σ_u/σ_{cr} increases on the other. In the initial postbuckling range, the ratio σ/σ_{cr} of the average stress carried by the column to the initial buckling stress is independent of 'β' i.e. it bears the same relation to the average strain or the nondimensional normal displacement w/h, for any box column whatever its value of β (Fig. 5.8). But once the normal displacements reach such proportions as to initiate the collapse, the stress-strain relationship is no longer

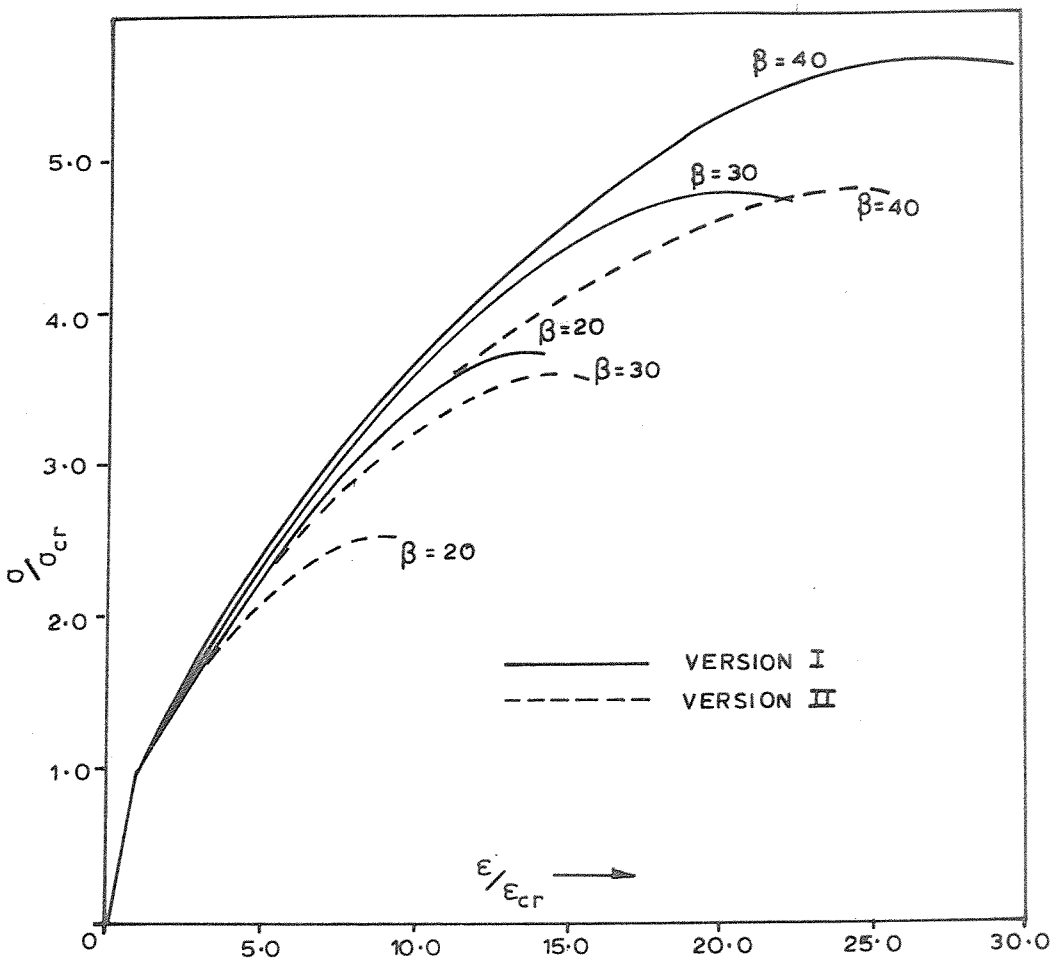
β = 40
β = 30
β=40
β=20
β=30
β = 20
VERSION I
VERSION II
σ/σcr
ε/εcr
5·0
4·0
3·0
2·0
1·0
0
5·0
10·0
15·0
20·0
25·0
30·0

(a)

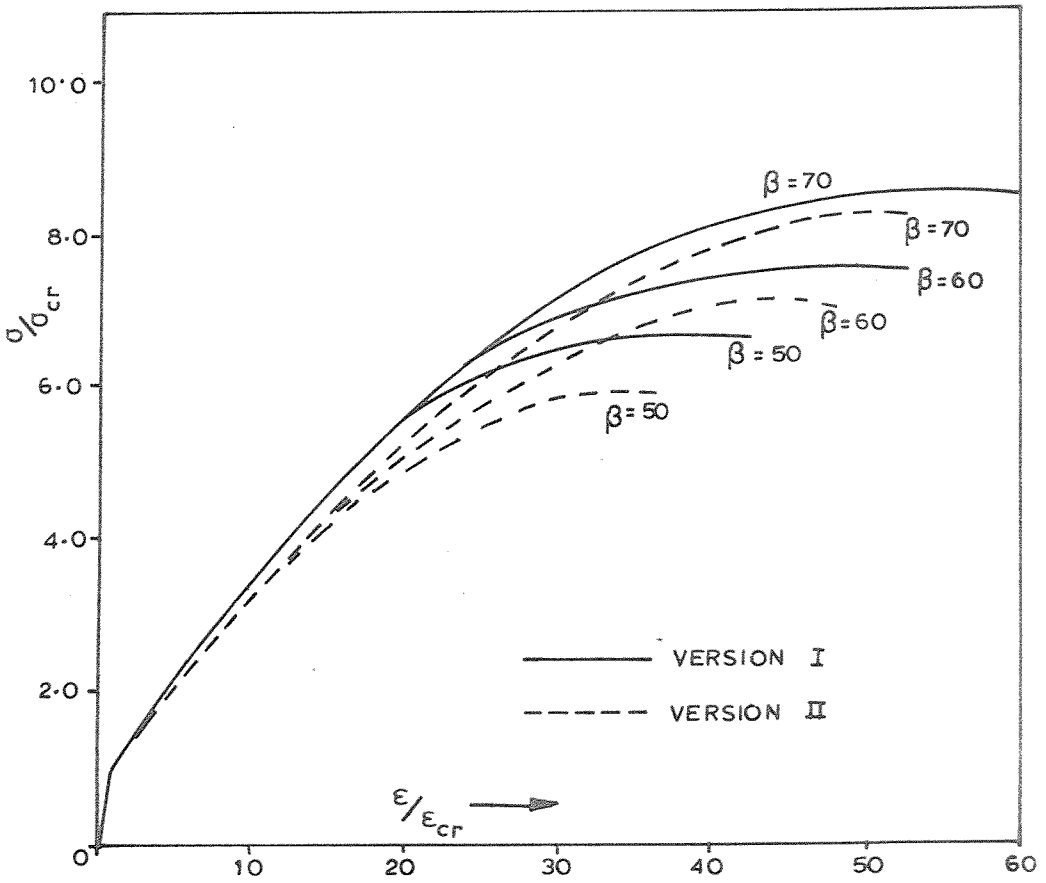
β = 70
β = 70
β=60
β=60
β = 50
β=50
VERSION I
VERSION II
σ/σcr
ε/εcr
10·0
8·0
6·0
4·0
2·0
0
10
20
30
40
50
60

(b)

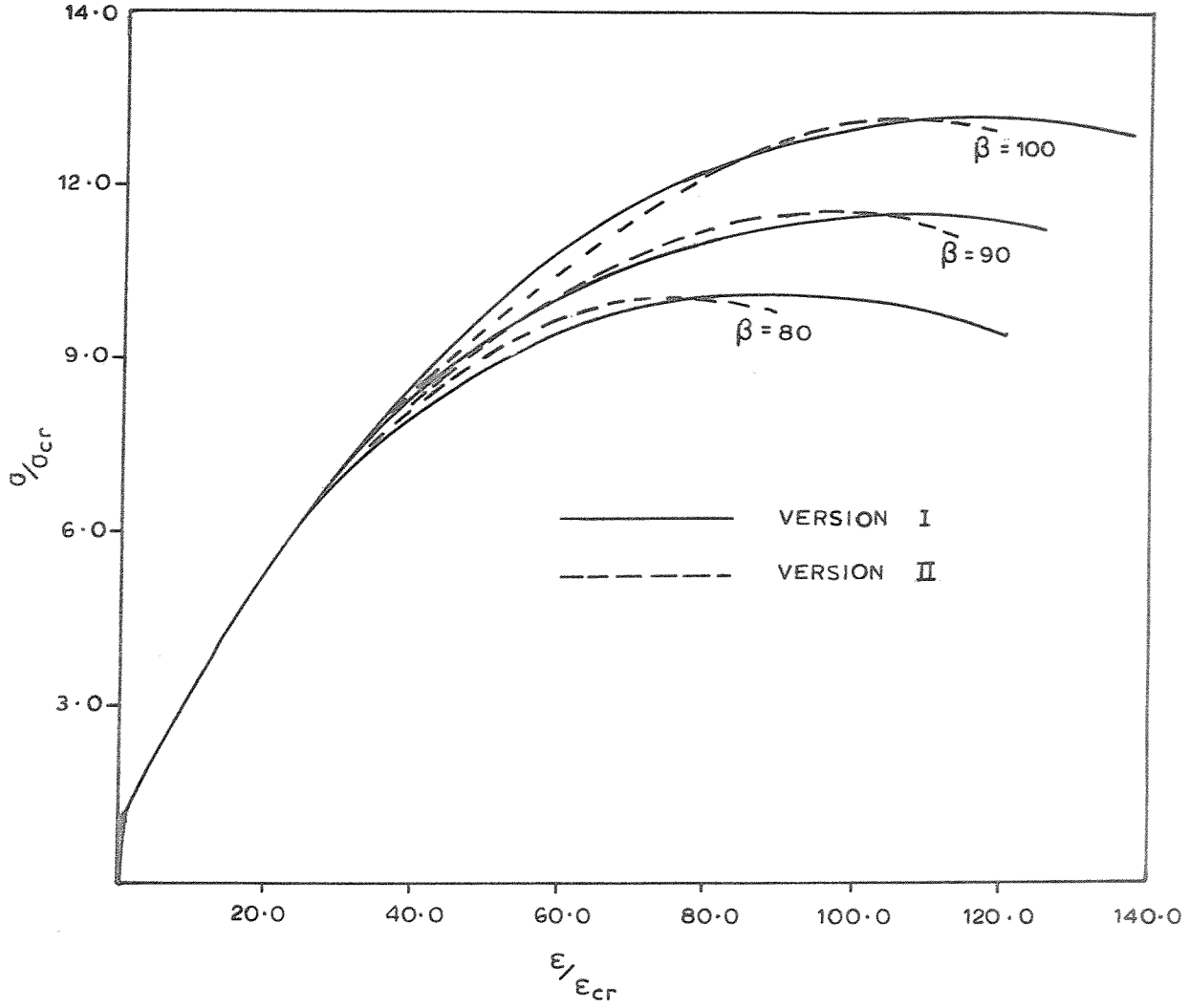

(c)

Fig 5.8 (a-c) Nondimensional Stress-Strain relations for the Columns with β = 20-100.

independent of 'β'. The collapse becomes imminent once the maximum deflection reaches a certain proportion of the width. This observation is supported by Fig. 5.9, where the maximum deflection at collapse in most cases is found to lie in the range of $\frac{1}{5}$ to $\frac{1}{7}$ of the width of the column. For a given value of 'h', a higher value of 'β' means a column of greater width, which collapses at a correspondingly greater deflection. This is illustrated in 5.10 for various values of 'β'.

The same general trend is noticed in the solutions based on version I which are plotted in Fig. 5.8(a-c) alongside the results of version II. The magnitude of errors introduced by the use of approximations in version I for the square box columns are very significant for those with smaller values of 'β'; for example the error involved in the calculation of collapse load for the case $\beta = 20$ is about 50%. However, the error diminishes steadily with increasing 'β' and becomes as small as 3% for the case with $\beta = 70$; for higher values of 'β' the collapse stresses predicted by the two versions are almost the same.

The use of version I for square box columns involves two types of errors:

(i) The normal displacements along the junction are assumed to vanish along the longitudinal edges. As a result, the stiffness of the box column is overestimated. This effect is noticeable in the relatively early stages of the postbuckling behaviour i.e. about twice the critical load.

(ii) For advanced stages of postbuckling behaviour of the box columns, the constituent plates, with their highly accentuated local buckles start functioning like thin shells - the most characteristic feature of these being the capacity to resist forces by developing membrane stresses. Thus they resist the inplane movement of the edges

Fig.5.9 The ratio of maximum deflection at collapse to the width of the plate for various values of 'β'.

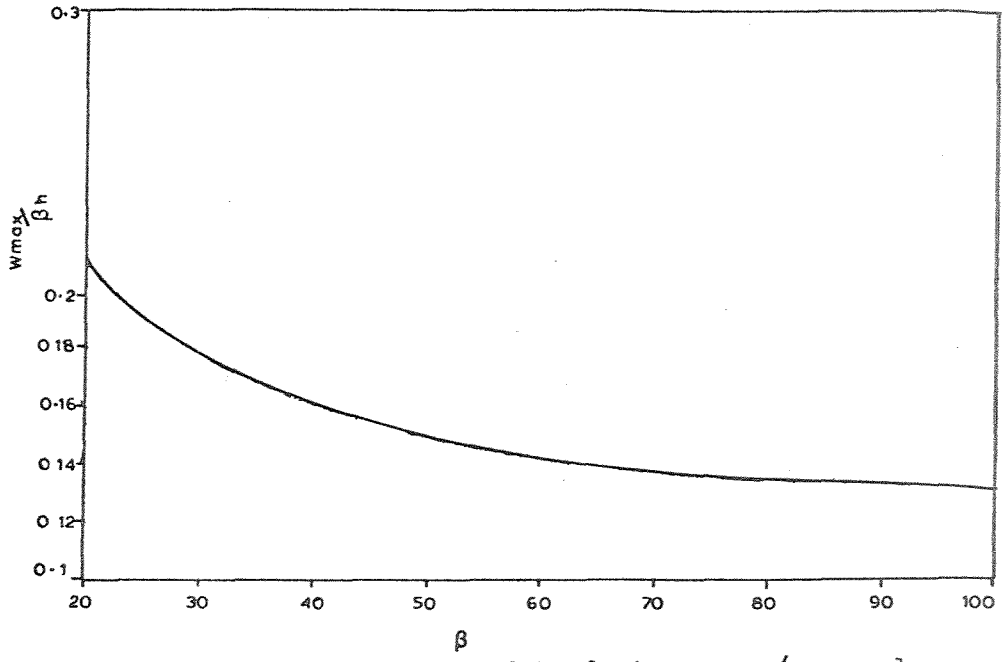

Fig.5.10 The relationship between σ/σ_{cr} and the maximum deflection in the buckle nearest to the ends.

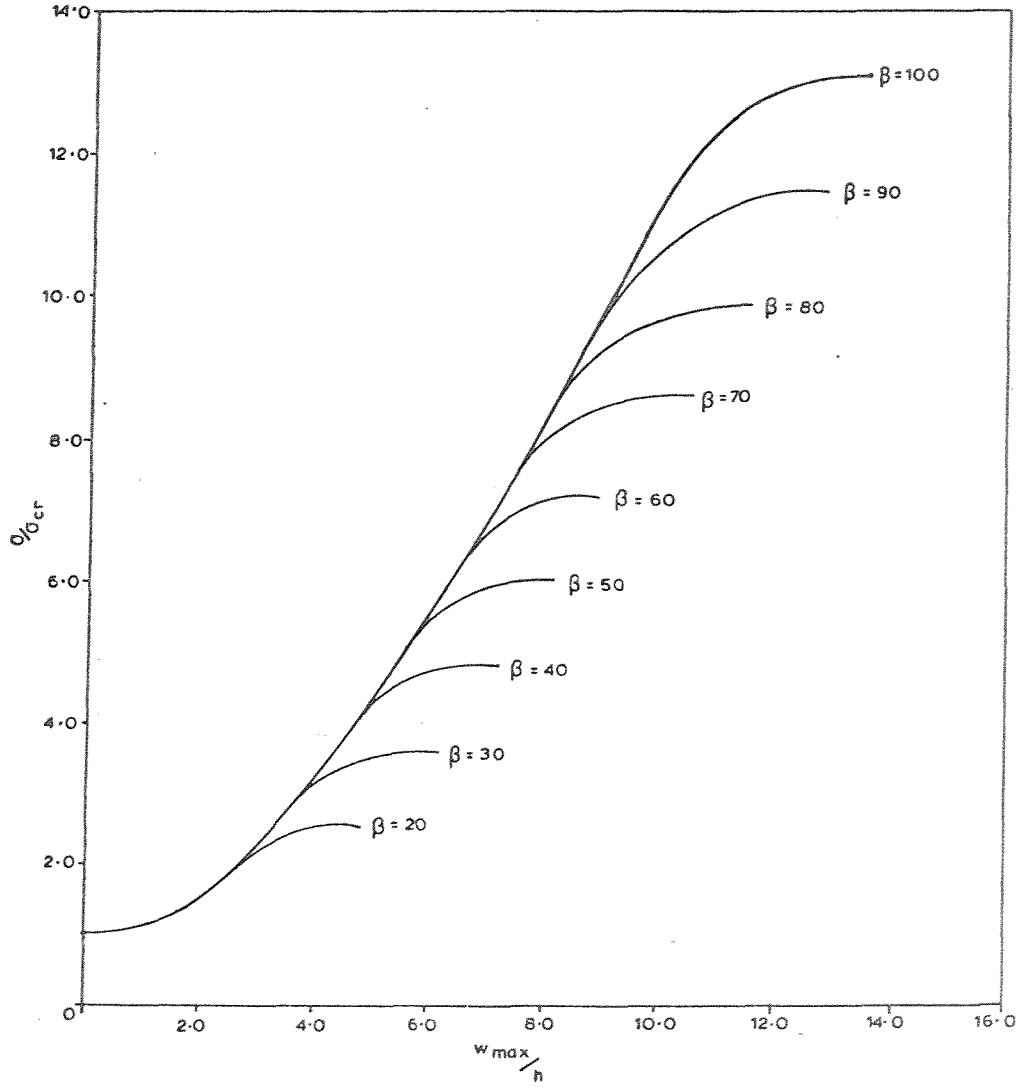

of the plates by developing tensile stresses as shown in Fig. 5.11, across the junctions, thus stiffening up the structure and delaying the collapse. This effect is of importance only after the deflections have become sufficiently large in comparison to the thickness and therefore for box columns with greater values of 'β'. Version I which treats the longitudinal edges free of stresses can not depict this feature.

The error in (i) above, explains why a higher collapse load is given by Version I for columns with smaller values of 'β'. The errors in (i) and (ii) are mutually compensating for columns with relatively larger range of nonlinear behaviour and this explains why the two versions give almost the same collapse loads for columns with higher values of 'β'.

5.3.3.2 Assumptions in the analysis in the light of the results obtained

The inplane displacement 'v' in the middle of the junction 'C' for the plate AC is plotted in Fig. 5.12. It is seen that it increases at a small steady rate in the initial stages of postbuckling equilibrium, but begins to build up rapidly at a load equal to about 80% of the collapse load. The rapid increase in the inplane displacements is apparently caused by the buckling of the strip of the plate adjoining the junctions as a column - an indication of the destabilising influence of the inplane displacement.

In Fig. 5.13 are shown the variations of 'v' and 'w' in the transverse direction along the centre line of the plate AB ($\beta = 100$) at a value of the applied load about 10 times the critical - a value close to the collapse load. It is seen that 'v' remains negligibly small in the interior of the plate but assumes values comparable to 'w' in the vicinity of the junction. This indicates that nonlinear effects of 'v' are of importance in the vicinity of the junctions and not elsewhere.

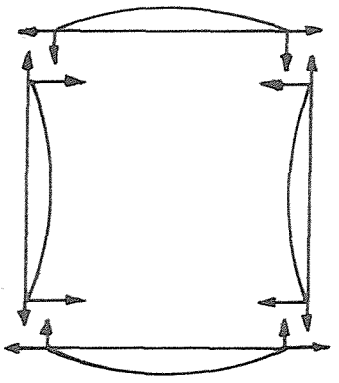

Fig.5.11. Inplane movement of the edges resisted by tensile forces across the junctions.

Fig.5.13.Variation of 'v' and 'w' across the central section AB at $\sigma = 9.85\sigma_{cr}$

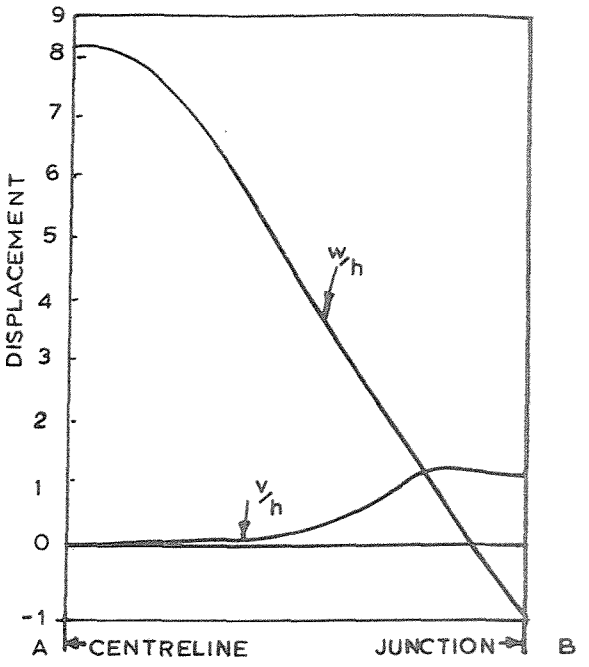

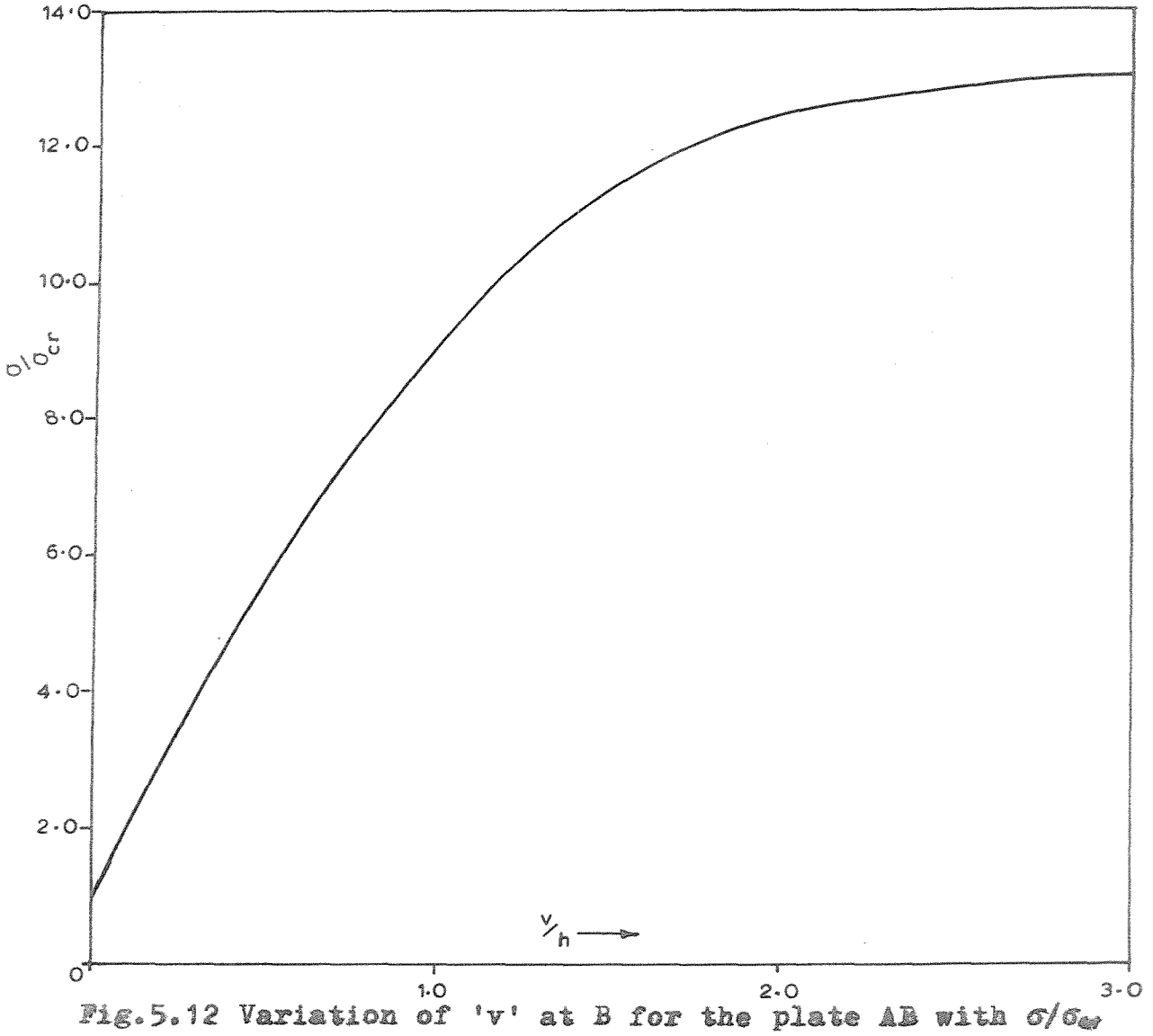

Fig.5.12 Variation of 'v' at B for the plate AB with σ/σ_{cr}

Fig. 5.14(b) shows the distribution of the average longitudinal stress over the two strips on either side of the junction B B_1 of the column (Fig. 5.14(a)) considered in the last illustration and at the same level of load. The stress is found to have only a small range of variation, and the mean value close to 'e'. Thus it appears logical to approximate the longitudinal stress to a value equal to 'Ee', in the assessment of its destabilising influence of its interaction with 'v'.

5.3.3.3 Imperfection sensitivity

In view of the observation that the collapse is associated with the geometric instability of the buckles and occurs at a maximum deflection equal to $\frac{1}{5}$ to $\frac{1}{7}$ of the width, the initial imperfections of the plates - unless they are of comparable magnitude - are not likely to have any influence on the collapse load. This is supported by experimental observations discussed in the next chapter.

5.3.3.4 Implications of the approximation in the elastoplastic analysis

Consider a plate ABCD simply supported on all its edges, loaded along the edges AB and CD and free to wave along AD and BC in the plane of the plate. It has been demonstrated that the collapse is triggered by the column type buckling of strips of the plate in the vicinity of the edges AD and BC in the plane of the plate. In an analysis which takes into account the plastic yielding of the material, the entire section at the middle of the plate along the edges AD and BC would be found to yield once the membrane stress exceeds the yield stress of the material. As a consequence the strips of the plate in the close vicinity of the edges AD and BC would begin to function like columns with a plastic hinge at their centres 'E' and 'F' respectively, resting on the elastic

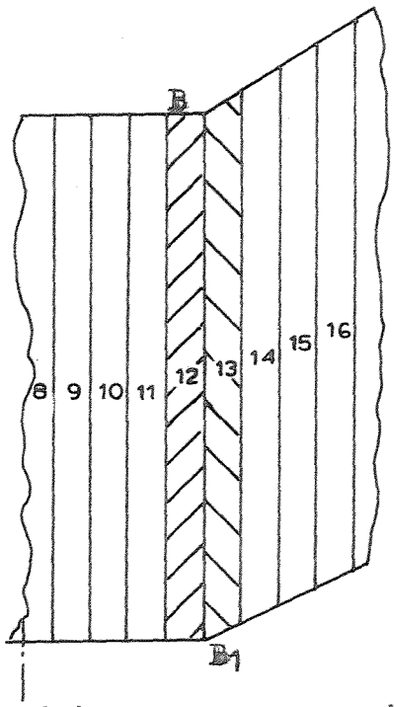

Fig.5.14(a) The Corner region over which the stresses are averaged.

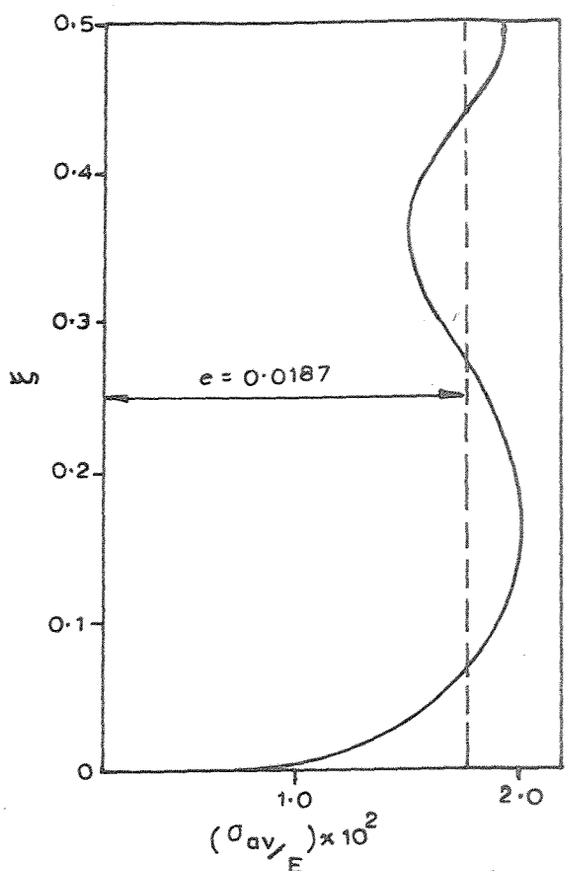

Fig.5.14(b) Variation of the average longitudinal stress in the corner region in Fig.5.14(a).

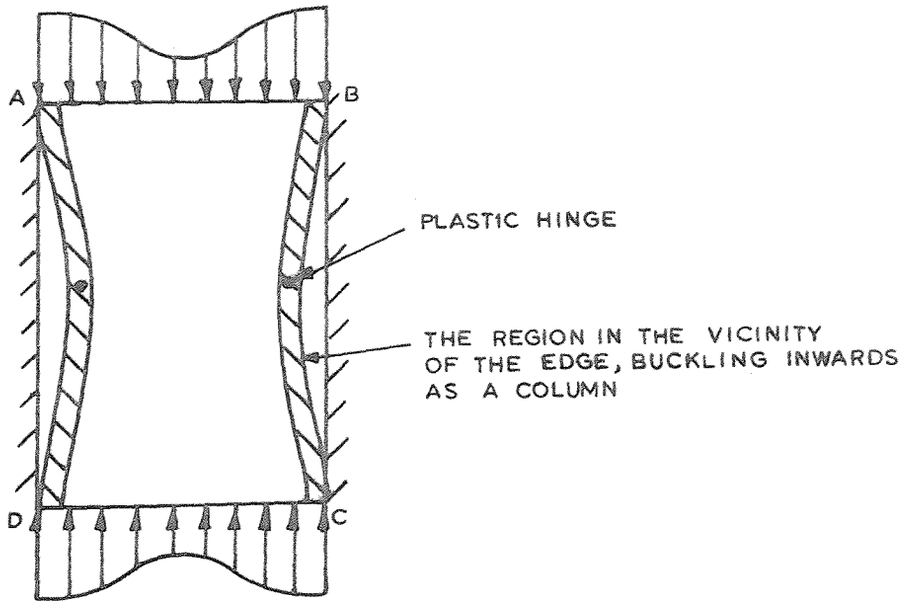

Fig.5.15 The mechanics of collapse of a longitudinally compressed plate, illustrated.

support offered by the buckled plate. Buckling of such a column would be immediate and accompanied by the rapid increase in the deflections of the plate, leading to its collapse. This explains why the failure load is accurately predicted by the criterion of the first yield (i.e. the membrane stress exceeding the yield stress of the material), in the case of plates with edges free to wave[25]. In a complete elastoplastic study of the behaviour of the plates, this phenomenon of inplane buckling of the edges of the plates can be of importance in that it can make the collapse more abrupt than it would be otherwise[60]. However, in order to incorporate this feature in the analysis, it is necessary to take into account either in a rigorous or approximate manner as suggested in this chapter, the destabilising influence of the inplane displacement 'v'.

5.4 Concluding Remarks

In the light of the analytical studies reported in this chapter, the following conclusions may be drawn:

(i) There exists an elastic limit to the capacity of plate structures to carry axial compression, beyond which the structures would start shedding load under controlled compression. This occurs primarily because the junctions start waving in at a rapid rate at a certain stage in the postbuckling equilibrium path. This phenomenon closely resembles the buckling of junctions as columns.

(ii) The collapse appears to be governed by the ratio of the maximum deflection to the width of the column which was found to lie between $\frac{1}{5}$ to $\frac{1}{7}$ for most of the cases investigated. This results in higher values of σ_u/σ_{cr} for columns with greater values of 'β'.

(iii) It is necessary to take into account the destabilising influence of 'v' in the calculations, in order to depict the column-type buckling behaviour of the junctions and the consequent exhaustion of the

capacity of the structure. An approximate method has been proposed to take this into effect in a simple manner; the numerical results obtained are consistent with the assumptions made. The final justification of these assumptions rests on a corroboration by the experimental observations in the next chapter.

(iv) Since the behaviour of the junctions is vitally important in the study of the advanced postbuckling behaviour, it is appropriate to employ version II of the finite strip method for the analysis of plate assemblies. However accurate results for the collapse loads can be obtained using version I provided the plates are sufficiently thin.

(v) In practical situations, however, the collapse is an elasto-plastic phenomenon, but the results presented herein demonstrate the importance of incorporating the destabilising influence of the inplane displacement in the proper modelling of the collapse and the post-collapse behaviour of practical structures.

CHAPTER 6

EXPERIMENTAL INVESTIGATION AND DISCUSSION OF RESULTS

PART I. EXPERIMENTAL INVESTIGATION ON SQUARE BOX COLUMNS

6.1 Introduction

Observation of new phneomena is often the starting point of research. Nowhere is this more true than in the study of behaviour of structures prone to instability, where an exclusive preoccupation with the theory can result in a complete loss of contact with reality. The purpose of the experiments is mainly threefold: To ascertain whether a certain instability phenomenon is imperfection-sensitive, to suggest simplifying approximations to deal with the problem and to corroborate the theoretical predictions, thus confirming the validity of the theoretical approach.

In this chapter, an experimental investigation on the elastic crinkly collapse of the box specimens is reported. The collapse of the specimens exclusively by elastic instability, the constant occurrence of the 'crinkly' buckling modes accompanying the collapse and the high degree of reproducibility of the collapse loads make this phenomenon an appropriate subject of an experimental investigation.

The objectives of the experimental programme are:

(i) To study the reproducibility of the crinkly collapse of the plate structures

(ii) To gain an insight into the mechanics of collapse by direct observation of the behaviour of the specimens under test

and (iii) To compare the results of the theoretical analysis with experimental observations and thus to confirm the validity of the theory.

Since it is proposed to study exclusively the elastic behaviour, silicone rubber is chosen as the model material. This material possesses several merits,the most important of which is that it remains elastic until it fractures.

The plate structure chosen for the present study is the square box column - one of the simplest and the most commonly used plate structure in practice. Because of the high cross-sectional stiffness of the structure, there is a considerable range of length of the structure over which the failure is exclusively by local buckling. This is an advantage because the present investigation is concerned essentially with post-local-buckling behaviour.

The first part of this chapter gives an account of the process of making the specimens of silicone rubber and testing them under axial compression. A recurrent feature of the tests is that the specimens under increasing compression lose their stiffness after buckling at a steady rate, till a maximum load is reached after and closely following which there occurs a snap through type of failure, with the appearance of a localised crinkly buckling mode. The second part of the chapter is devoted to a discussion of the salient features of experimental results which are compared with those of the theoretical analysis up to the point of collapse. The post-collapse behaviour is explained with reference to a theoretical mechanical model of a column resting on discrete nonlinear springs.

6.2 Description of the experimental technique

In this section the technique employed to make the silicone rubber specimens and precautions to be observed in testing them are outlined.

6.2.1 Modelling with silicone rubber

Patterson[10.6] studied the problems involved in manufacturing sheets of silicone rubber of specified thickness and of making structural models therefrom. His report (ref. 106) on the subject is a valuable source of information on the making of structural models with silicone rubber and forms the basis of modelling work in the present investigation. Greater experience in the use of the technique has helped the author to make improvements in details, to produce models of consistently high quality; and these will be specially mentioned in the following description.

6.2.1.1 Silcoset as a modelling material

Silcoset is a commercial brand of silicone rubber manufactured by I.C.I. It is supplied in the form of liquids and pastes that cure to form resilient silicone rubbers on the addition of a curing agent (two-pack system) or simply on exposure to atmospheric moisture (one pack system).

The suitability of silcoset as a modelling material stems from its flexibility, resistance to oxidation, excellent antisticking property, protection from dust and particularly its high elasticity.

6.2.1.2 Manufacture of sheets

After experimenting with various techniques, Patterson found that settling the rubber on a flat plate produced sheets of high quality and accuracy. Of the several grades of Silcoset available, Silcoset 105 which is the least viscous member of the two pack system is chosen for the present work and can be described as a very easily pourable white liquid.

6.2.1.2.1 Casting the sheets:

The procedure used consists of pouring a specified quantity of Silcoset 105 thoroughly mixed with a curing agent on a suitably confined area of a level and polished steel surface and allowing it to settle and cure. The details involved in the above procedure will now be

briefly described.

Preparation of the surface of steel plate:

In principle it is possible to cast rubber on glass or metallic surfaces with the aid of suitable release agents. In order to allow the rubber sufficient time to settle out before it starts curing, it is necessary to use extremely small quantities (say of the order of 0.1 to 0.2%) of the curing agent. With the use of such a small quantity of curing agent, rubber was found to stick to glass surface and it was found not possible to remove the cured rubber sheet from the glass plate. With the steel surface, however, this difficulty does not arise and therefore the latter must be preferred for casting the sheet.

The steel plate is mounted on a steel table each leg of which is resting on levelling screws. With the help of these, it is found possible to level the table to a high degree of precision by using a sensitive spirit level with the least count of 0.1 mm/metre. The surface is next well polished and rubbed with traffic wax to act as a release agent for the rubber sheet.

From the size of the model to be made the size of the sheet required is calculated allowing for estimated wastage. This area can then be marked out directly on to the metal plate surface using a steel rule and rapidograph pen. A certain quantity of plasticene is then rolled into a long thin strip and firmly pressed against the surface all along the line marked out, to prevent the leakage of the Silcoset. The table kept ready for casting the sheets of rubber is shown in Fig. 6.1.

Calculation of the quantity of rubber required by weight:

In order to be able to calculate the weight of the rubber required for a sheet of given dimensions, the density of the rubber fluid must be known. The density of the rubber fluid increases from the surface to

bottom of the vessel in which it is stored and therefore it is necessary to stir the rubber fluid in the vessel in order to obtain a uniform density. In order to eliminate uncertainties, it is found helpful to make a trial casting of a rubber sheet with a known weight of Silcoset and thus obtain the thickness and therefore its density.

Pouring the Silcoset:

In order to transfer a known weight of the rubber fluid on the marked area of the steel plate, the following procedure is found to be necessary.

A paper cup with a spatula is weighed on a balance first. A quantity of Silcoset which exceeds the required amount by a small margin (5 to 10 gms) is weighed out in the cup. The curing agent of about 0.2% by weight is added and thoroughly mixed with the spatula. The contents of the cup are then transferred on to the prepared surface to cover it completely, spreading the same with the spatula in several stages and the cup and spatula weighed at each stage to ensure that just the required amount of rubber and no more is transferred to the surface.

Since the uniformity of thickness of sheet depends upon the settling of the rubber fluid under gravity, the smaller the size of the sheet the better the results. Thus it is expedient to cast each side of the square box column separately i.e. to cast four equal strips rather than one big sheet for a specimen. This has the effect of localising the variations in thickness which may occur due to the viscosity of the rubber fluid, imperfections of the surface and inaccuracies in levelling. Fig. 6.2 shows the rubber cast in nine strips on the prepared steel surface. After the sheet has cured, the best method of removal is to cut the sheet with a sharp knife just inside the plasticene border. The sheet is then easily peeled off.

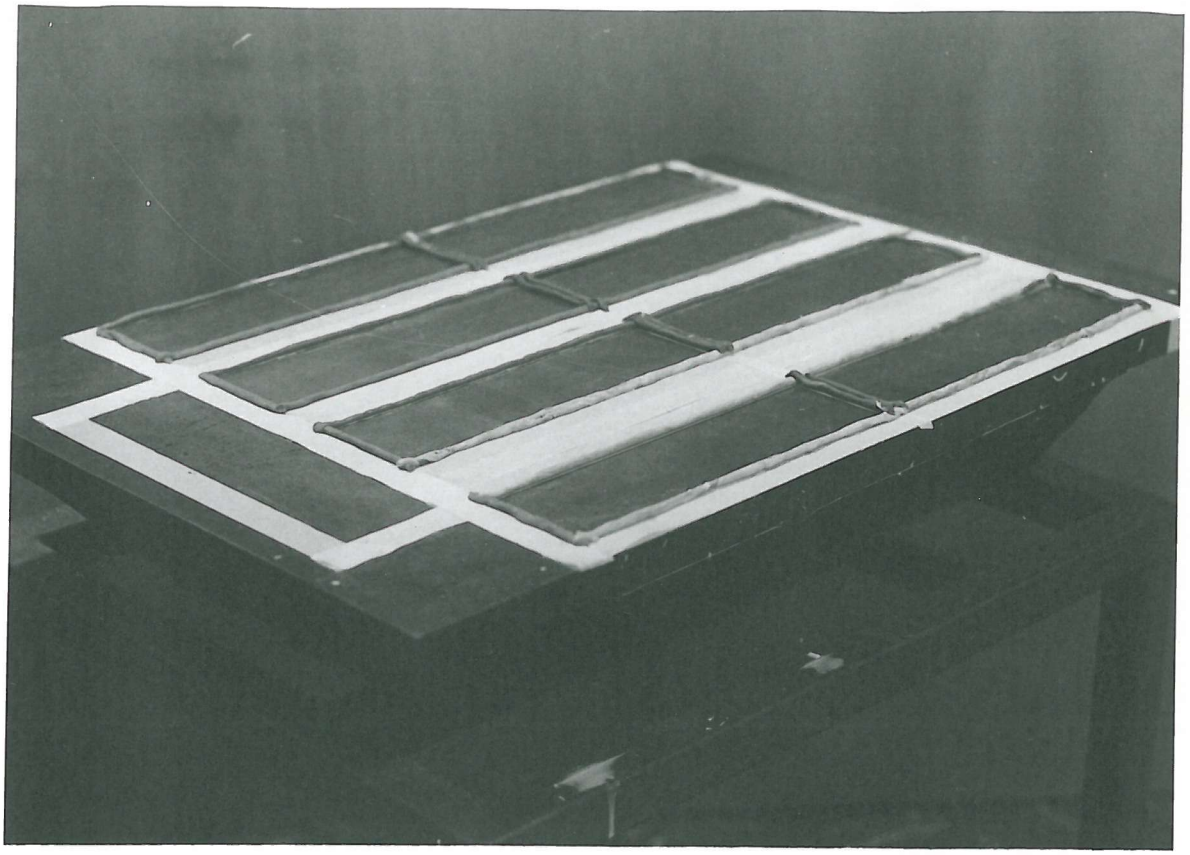

Fig. 6.1 The Table Kept Ready for Casting the Sheets

Fig. 6.2 The Silcoset Sheets Cast on the Table

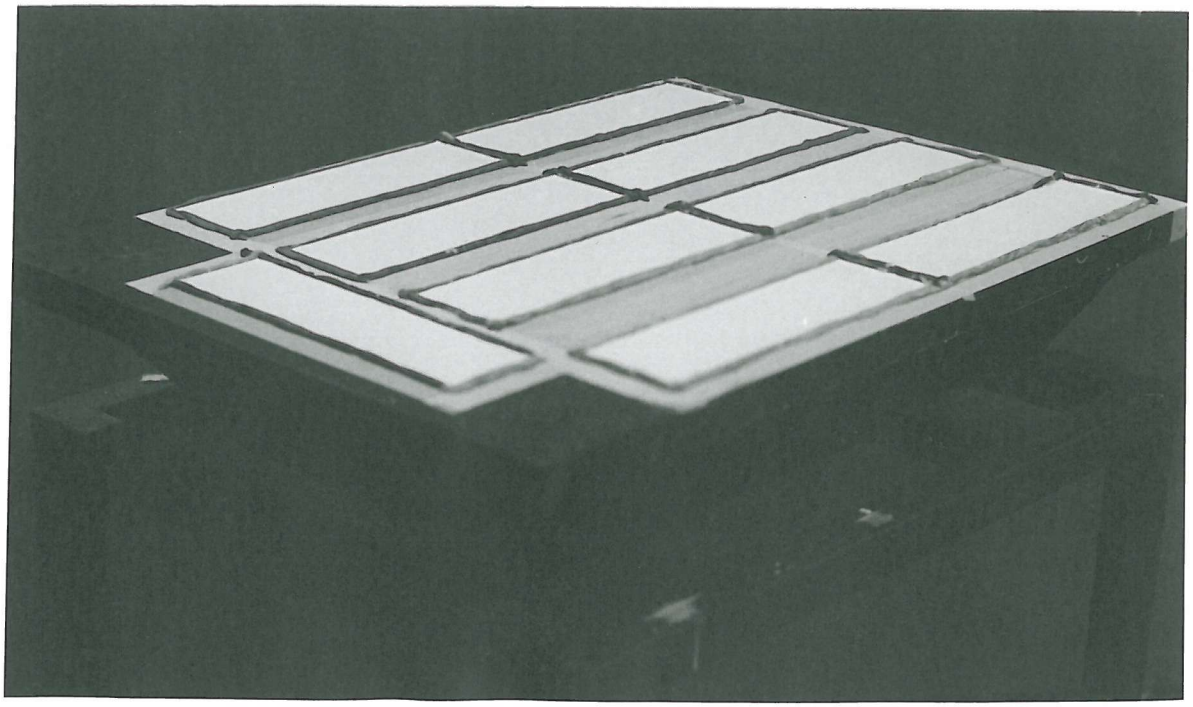

6.2.1.2.2 Quality of the sheet

It is found that the method outlined above produced sheets free of trapped air bubbles as can be checked by holding it up against bright light.

The thickness of the rubber sheet can be measured with the aid of a micrometer screw with the rubber sheet sandwiched between two metal plates, with care taken not to squeeze the rubber when closing. A typical set of readings on a sheet is shown in Appendix X which also gives the standard deviation from the mean thickness. In a great majority of cases the standard deviation was found to be between 2 and 3% of the mean thickness.

6.2.1.3 Making the models

Once the sheets required for making a specimen are available, making the models consists of two steps: cutting the sheets to size and joining the sheets along the edges.

6.2.1.3.1 Cutting the sheets to size:

It was found extremely difficult to cut the rubber along a given line as the sheet stretched and heaved as the blade was run along the line. Another problem was that it is impossible to draw on the rubber with any sort of ink, pencil or crayon. These problems are overcome by sticking strips of masking tape on to the rubber. Then lines can be drawn at required positions on the tape using a rapidograph drawing pen. A metal block of about 1 cm in thickness is placed with its edge on the line to be cut. This is to act as a guide to the cutting blade which can be run along the face of the metal block to cut the rubber along the straight line. The tape prevents the rubber from stretching thus giving a vertical straight cut.

6.2.1.3.2 Joining the sheets

Silcoset sheets can be joined together using Silcoset itself. As a joining material, one pack Silcoset - Silcoset 151 - proved superior to two pack Silcoset 105 because of its greater viscosity and strength.

The technique of joining two sheets A and B is illustrated in Fig. 6.3(a-b). A steel block with a small chamfer along one of its edges is placed on the sheet (B) with a margin equal to the thickness of sheet (A) with the groove facing outward. The joining material is applied along the edge of the sheet (A) and placed hugging the metal block and pressed home. The excess joining material is squeezed out into the tiny space provided by the chamfer, so that the metallic block does not come into contact with the rubber material. The arrangement is left undisturbed for about an hour after which the metal block can be removed. In order to ensure perfect bonding a minute fillet of the joining material is applied with a pen knife all along the joint.

The other edges are then joined in turn, allowing each join to set, before continuing. The final join is illustrated in the Fig. 6.4(a). The finished model is shown in Fig. 6.4(b).

6.2.2 Test set up

The square box column specimens are capped with square wooden blocks at either ends, with their outer surfaces flush with the top and bottom of the specimen. These are bonded to specimen using Silcoset 151, and provide perfectly flat surfaces for loading. In order to correct any errors in the positioning of the wooden blocks at right angles to the axis of the specimen, the specimen is held against the guide of a sanding machine and the ends ground against the wheel with its

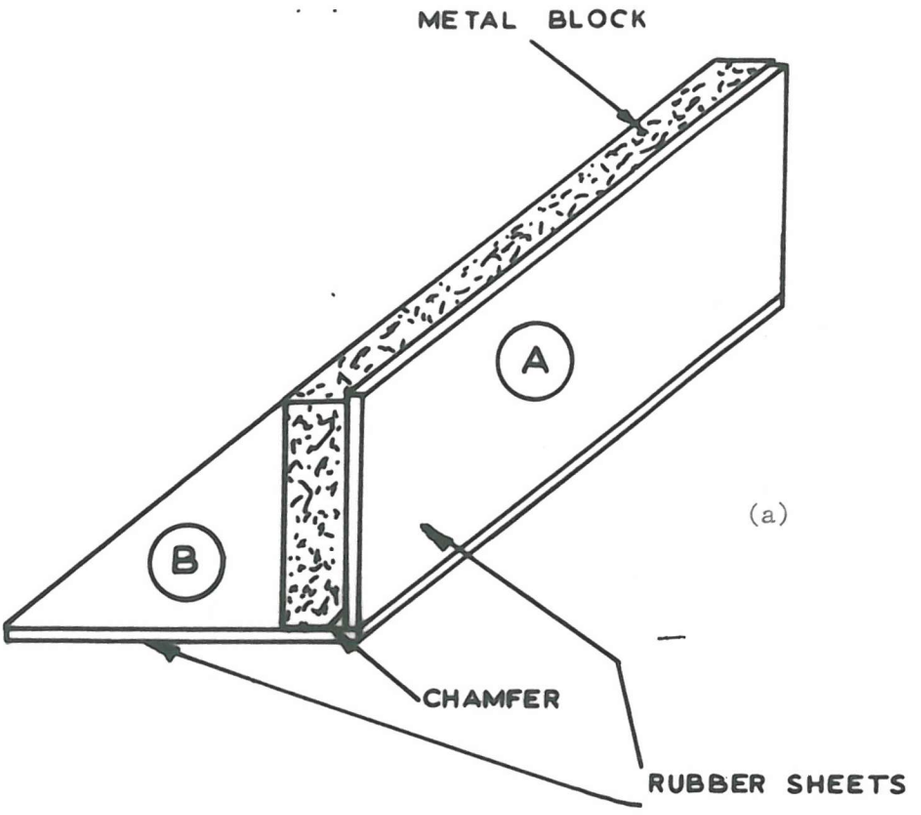

Fig.6.3(a-b) The Technique of Joining the Sheets

(b)

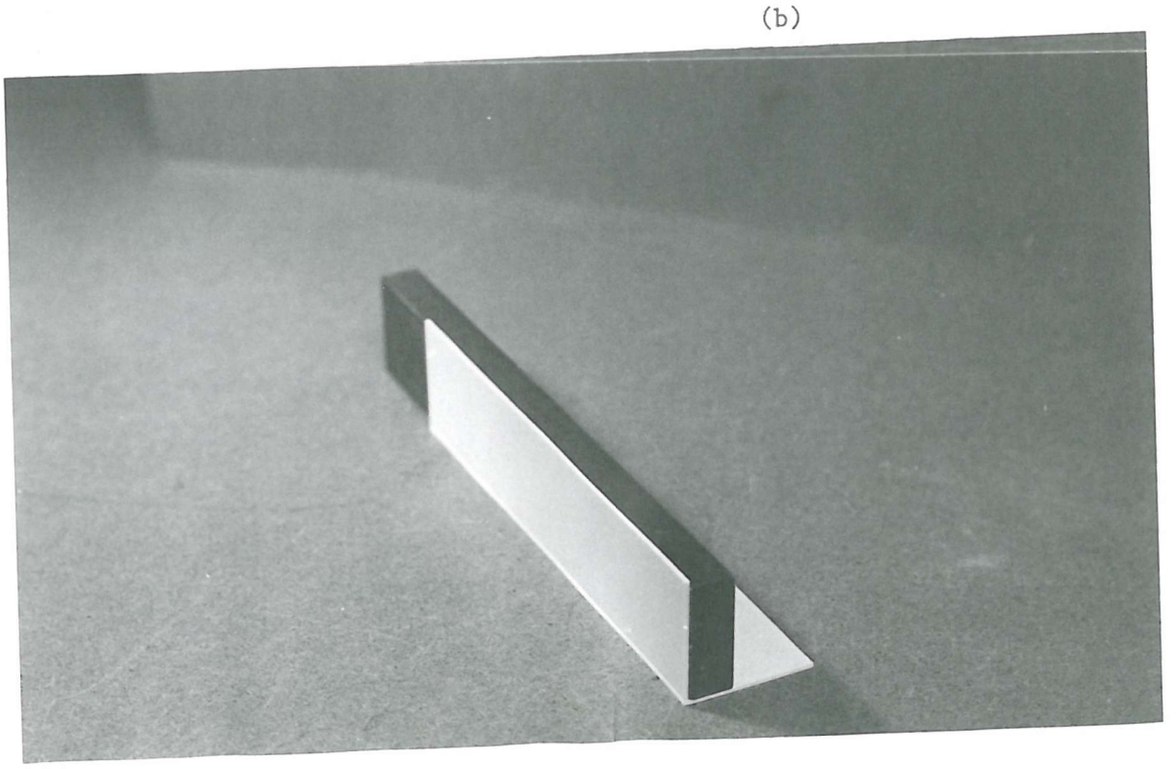

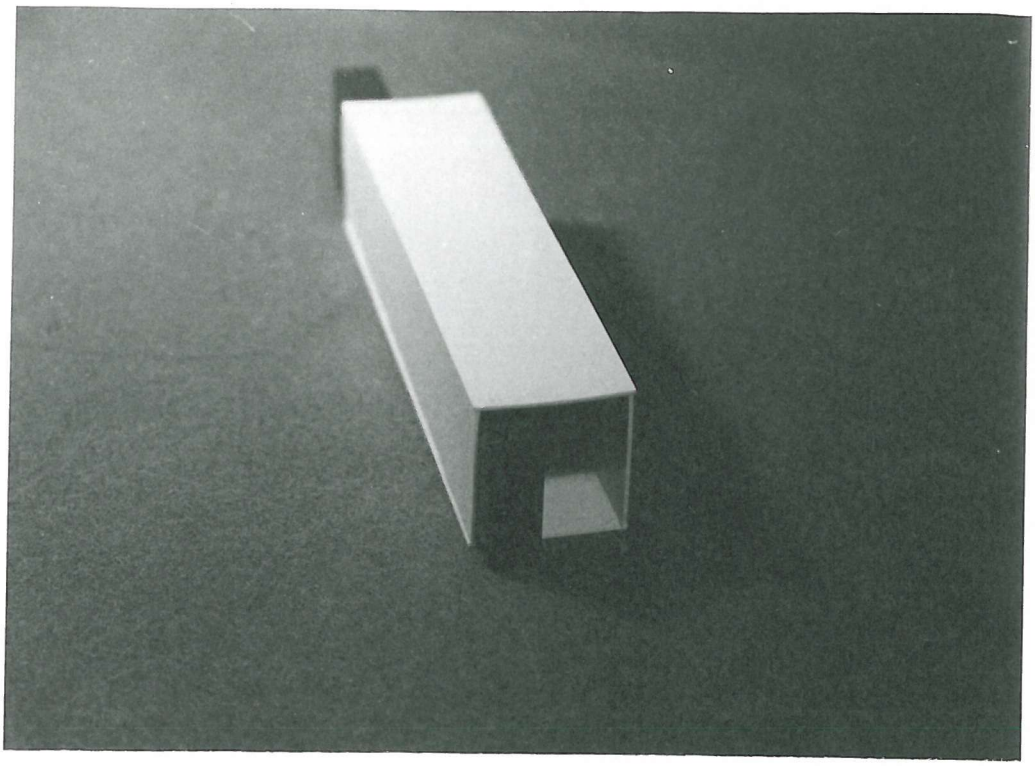

Fig. 6.4(a) The Final Join

Fig. 6.4(b) The Finished Model

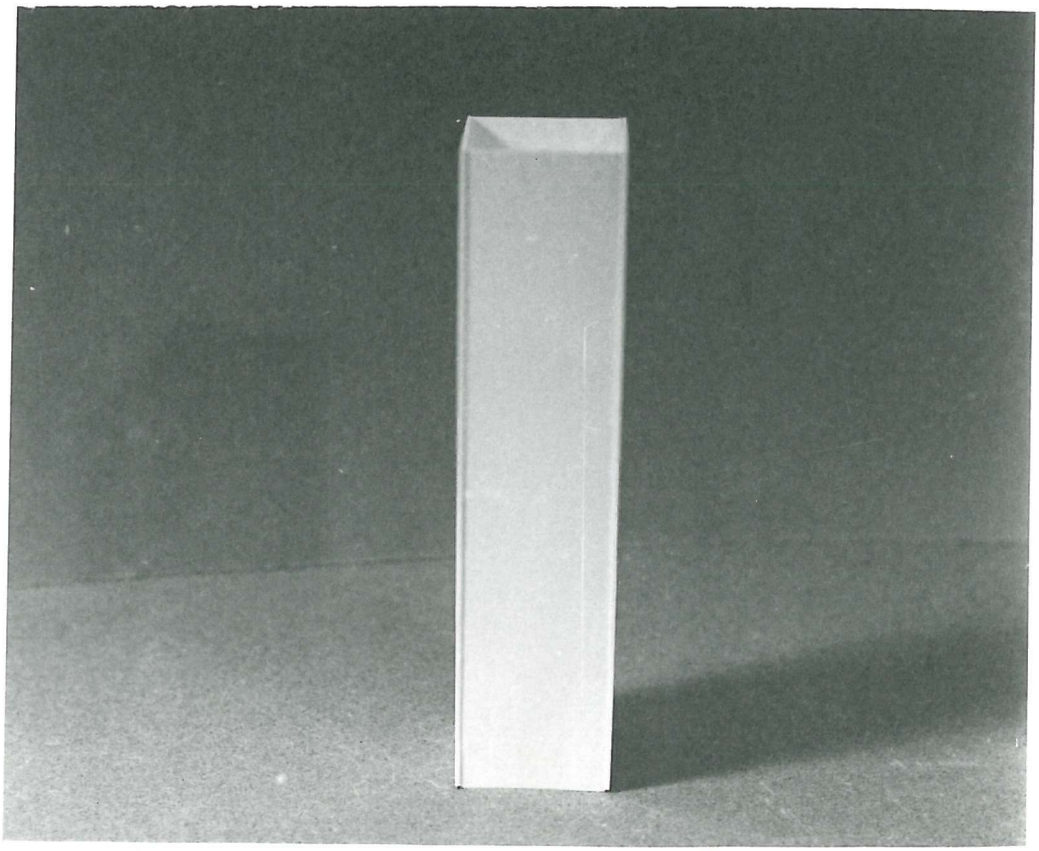

plane at right angles to the guide. The specimen is turned end to end and the procedure repeated.

The specimen is then placed on the fixed cross head of the Instron machine (Fig. 6.5) and the movable cross head of the machine is brought in close proximity to the top of the specimen. In order to ensure uniformity of loading on the top surface, the specimen is held against the movable cross head and the space between the bottom surface and the fixed cross head packed tightly with tin shims.

The specimen is now compressed at a steady rate choosing an appropriate scale and rate of loading and end compression. Since the testing machine is very rigid in comparison with the rubber specimen, it is possible to record the unloading of the specimen which occurs during failure. Since the material continues to be elastic, it is possible to record the load-end compression relationship in the process of decompression of the specimen as well.

6.3 Experimental Programme

Square box specimens with varying values of γ (the ratio of the length to the width) and β (the ratio of the width to the wall thickness) made of Silcoset are tested in compression. The main interest in the programme is to obtain the load-end displacement relationship, the maximum load taken and to study the mechanics of collapse and post-collapse behaviour.

6.3.1 Details of specimens

Table 6.1 gives the values of γ and β of the specimens tested. The actual dimensions and material properties of the specimens are given in Appendix XI. As shown in the table, there are two groups of specimens.

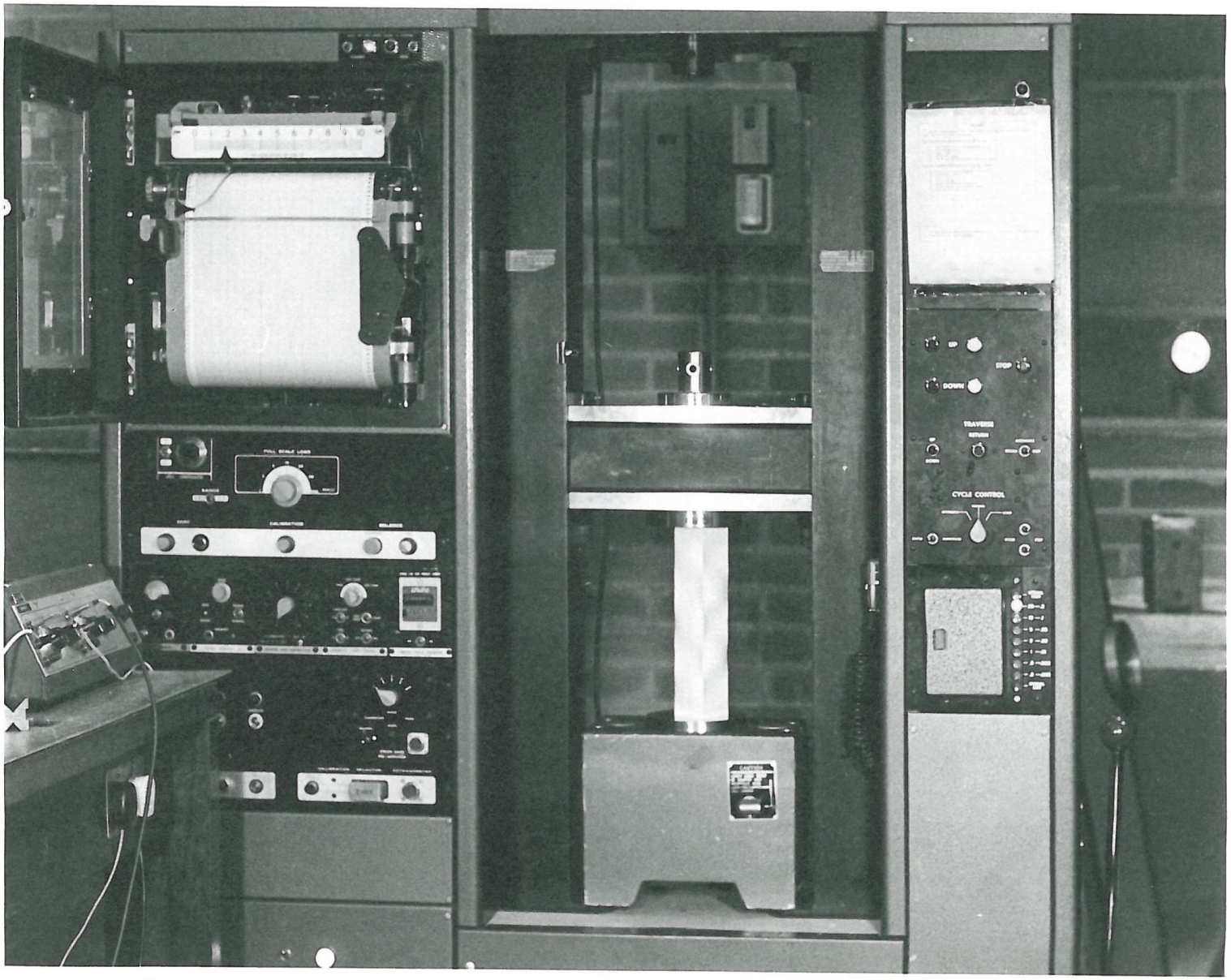

Fig. 6.5 The Test Set-up

Table 6.1 Geometric parameters of the specimens tested

Identification	γ	β	Remarks
A1(1) A1(2) A2(1) A2(2)	4	30	A1(1) and A1(2) have the same nominal dimensions and 'E' [214.0×53.5×1.78 mm; and 292 psi] A2(1) and A2(2) have the same nominal dimensions and 'E' [223.0×56.0×1.86 mm; and 296 psi]
B1(1), B1(2)	3	20	
B2(1),B2(2)	4	20	Actual dimensions and material properties given in Appendix XII
B3(1),B3(2)	5	20	
B4(1),B4(2)	9	20	
B5(1),B5(2)	2	30	
B6(1),B6(2)	3	30	
B7(1),B7(2)	4	30	
B8(1),B8(2)	5	30	
B9(1),B9(2)	9	30	
B10(1),B10(2)	3	40	
B11(1),B11(2)	4	40	
B12(1),B12(2)	5	40	
B13(1),B13(2)	5	50	
B14(1),B14(2)	5	60	

The members of the first group, identified by letter A have all the same values of γ and β and have been used to study the reproducibility of the behaviour of the specimens. The second group of specimens identified by letter B have varying values of γ and β. In this group there are fourteen combinations of γ and β and for each set of γ and β, two specimens are tested. This is found to be sufficient in view of the generally high reproducibility of the test results.

For values of β equal to 50 and 60, the specimens are found not to have adequate structural stiffness to retain their initially straight configurations whilst carrying their own self weight. Therefore it has been decided to restrict the maximum value of 'β' to 60 in the test programme. In view of the difficulties met with in making accurately the longer specimens, the maximum value of 'γ' was restricted to 9. It is believed that sufficient understanding of the phenomena investigated can be obtained within these bounds of γ and β.

6.3.2 Reduction of experimental load-end displacement relations to nondimensional stress-strain plots

For making comparisons between the behaviour of specimens which are not identical, but only geometrically similar and made up of rubber with differing values of E, it is necessary to represent the results in terms of nondimensional parameters. In the post local buckling behaviour of plate structures, the relationship between the average stress and average strain is of main interest, and therefore the experimental results are reduced to plots of σ/E versus 'ε' i.e. nondimensional stress versus average strain. The value of 'E' is obtained from a tension test carried out on a strip of rubber, which was cast along with the sheets out of which the specimen is made. The determination of 'E' in each case is vitally important as its value is found to change with

the age of the material and the density of the rubber fluid. (vide Appendix XI). In view of the very low stresses involved under compression, the initial tangent modulus is used for all the calculations (vide Appendix XI).

In the calculation of 'σ', account must be taken of the self-weight of the specimen. This effect is especially significant for the specimens with higher values of γ and β . Since the selfweight imposes a uniformly varying dead load on the specimen, increasing from zero at the top to a maximum at the bottom, only half the weight is considered in the calculations.

PART II. DISCUSSION OF RESULTS

In this part of the chapter, the salient features of experimental results are presented and discussed.

6.4 Postbuckling behaviour of the specimens

6.4.1 The General Pattern

A typical load-end displacement characteristic as obtained from the tests is shown in Fig. 6.6. There are in general, four distinct stages in the behaviour of the specimens. These are

(i) The initially straight form of equilibrium (Fig. 6.7(a)) corresponding to portion (i) of the characteristic shown in Fig. 6.6.

(ii) The appearance of the local buckles, (Fig. 6.7(b)) corresponding to portion (ii) of the curve in Fig. 6.6.

(iii) The accentuation of local buckles to such an extent that the inward movement of the junctions becomes significant and noticeable, (Fig. 6.7(c)) corresponding to portion (iii) in Fig. 6.6.

(iv) The sudden crinkly collapse of a pair of junctions (most frequently a diagonally opposite pair) with the load abruptly dropping; the specimen regains its stability at a much reduced value of the load, (Fig. 6.7(d)) corresponding to portion (iv) in Fig. 6.6.

At this stage if the applied compression is released at a controlled rate, the specimen takes a slightly increased load along the path DE in Fig. 6.6 and at a certain stage snaps back to the original equilibrium path (at F in Fig. 6.6).

The displacement profile after the collapse is markedly different from that in the postbuckling equilibrium path (iii) in Fig. 6.6 and is a localised buckling mode. The abruptness of unloading is an indication

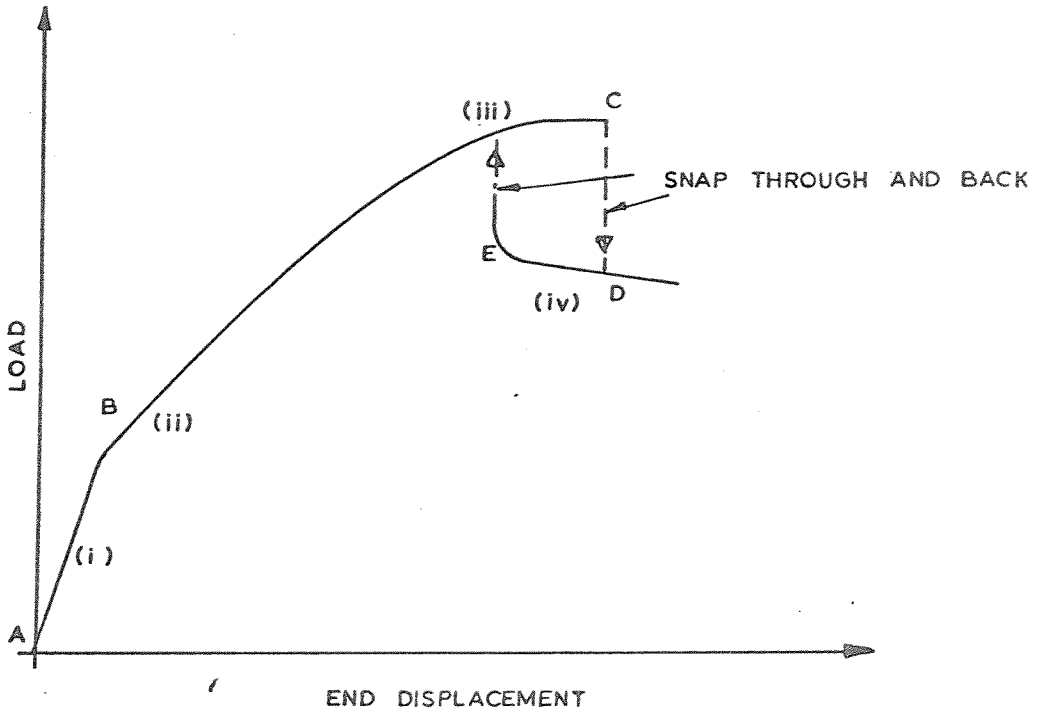

Fig. 6.6. A typical Load - End displacement Characteristic.

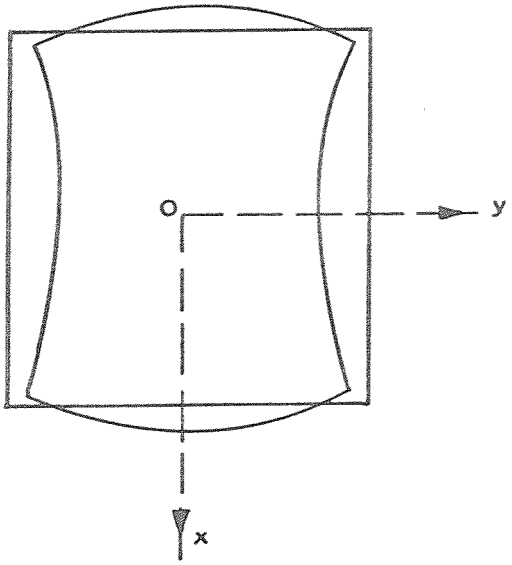

Fig. 6.8 (a) Normal Displacements in a cross-section prior to collapse.

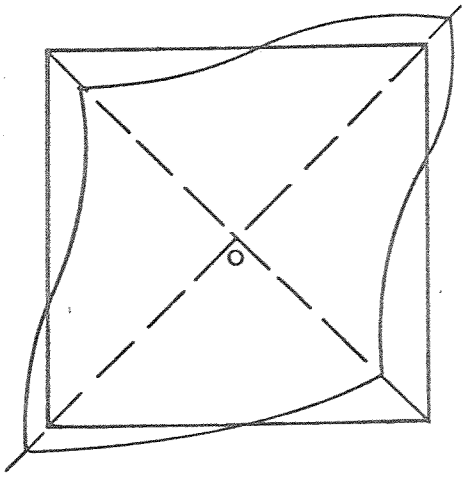

Fig.6.8 (b) A possible Bifurcation mode Symmetric w.r.t. the diagonals.

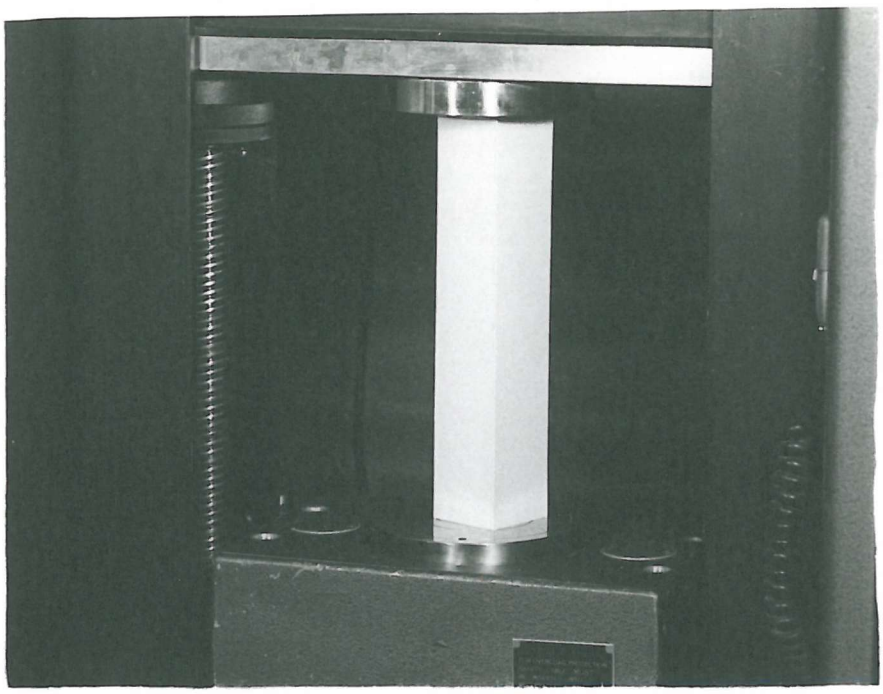

Fig. 6.7(a) The Initial Straight Configuration

Fig. 6.7(b) Occurrence of Local Buckling

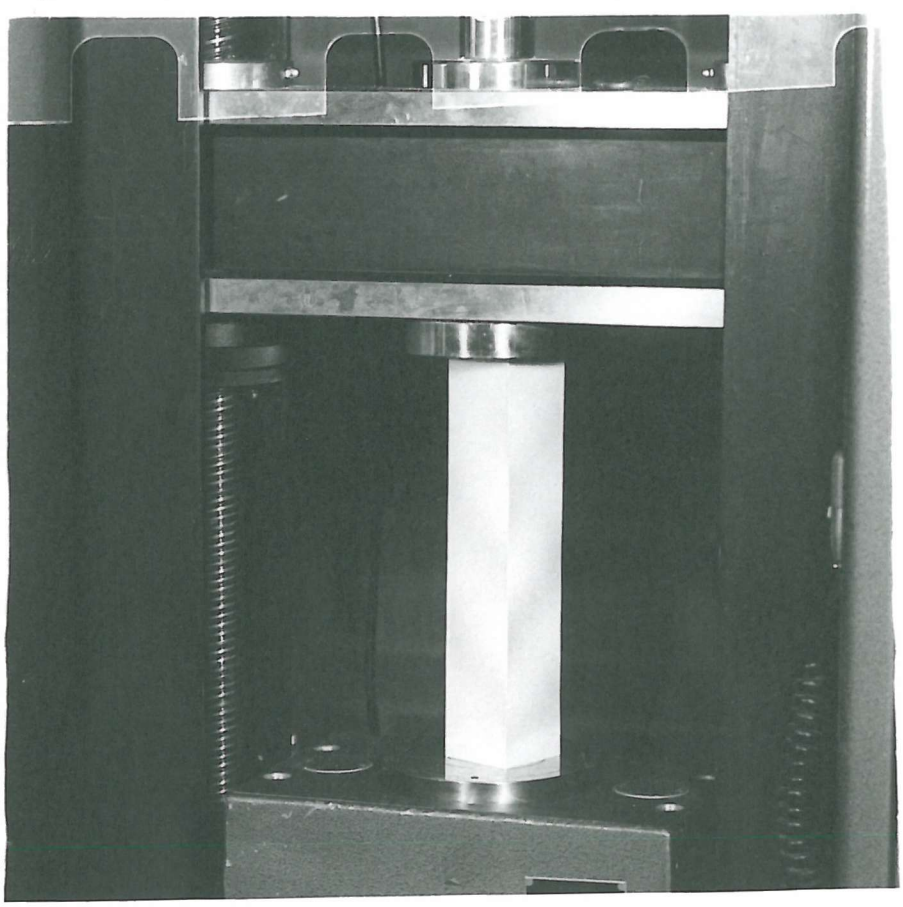

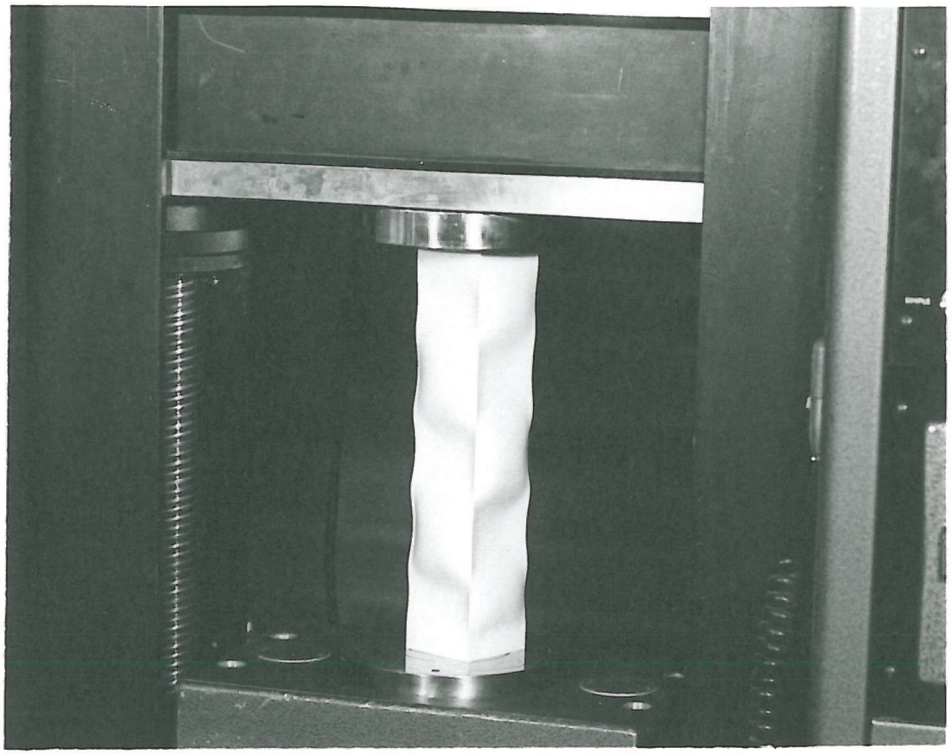

Fig. 6.7(c) Local Buckling at an Advanced Stage

Fig. 6.7(d) Crinkly Buckling of a Pair of Diagonally Opposite Edges

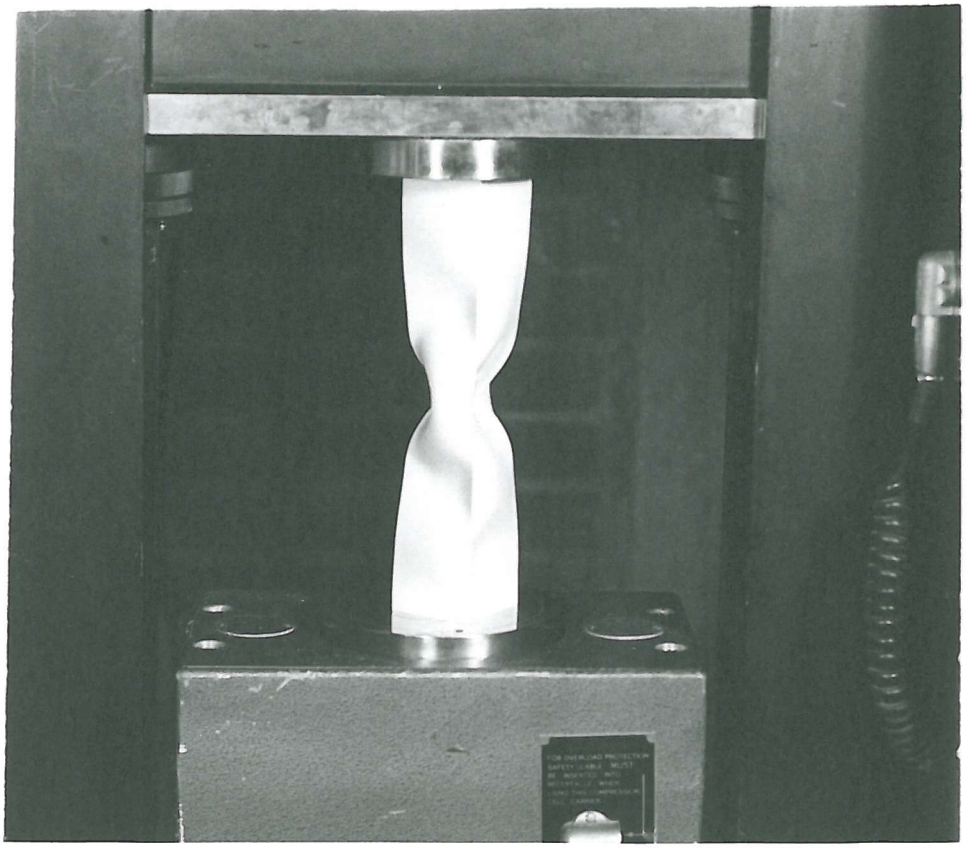

that the snapthrough type of buckling occurs, the specimen jumping from one state of equilibrium to another. In the case of a square box column, there is an additional feature. The displacement profile across the section of the column has two axes of symmetry prior to snap buckling. (Fig. 6.8 (a)). But the equilibrium configuration after collapse has no symmetry about either axis. This indicates that there occurs a bifurcation of equilibrium between the point C at which snap buckling occurs and the point D in the post-collapse equilibrium path DE with the bifurcation mode being symmetric with respect to the diagonals (Fig. 6. 8(b)). But this is a complication which is due to the symmetry of the cross-section and not an inherent feature of the crinkly collapse of the junctions which , as will be shown later, can be simply explained using a mechanical model.

6.4.2 Behaviour of the longer specimens

The collapse behaviour of specimens with $\gamma = 9$ deviates in some important respects from the general pattern described in the previous section. The differences arise as a result of the intervention of the overall buckling in the vicinity of collapse.

Of the specimens tested (ref. Table 6.1), there are two pairs identified as B4 and B9 which have the highest value of γ equal to 9. Of these, the specimens B4 which have a smaller value of β (equal 20), fail by an interaction of the overall buckling mode with the local buckling mode. With the appearance of the overall buckling mode, the stress-strain characteristic takes a turn to become flat and the collapse is precipitated earlier than what may otherwise be expected (Fig. 6.9 (a)). The coupled buckling mode at the instant of failure of the specimen B4(1) is shown in Fig. 6.9 (b). Since the ends of the specimen are made to be fully in contact with the flat crossheads, the overall buckling mode

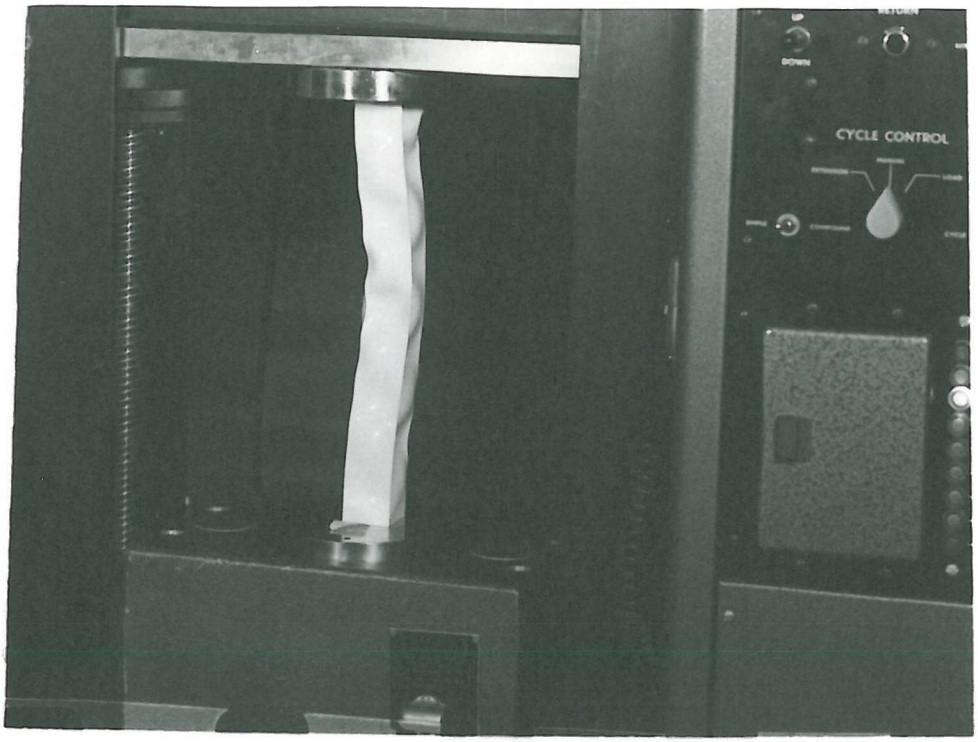

Fig. 6. 9(b) Interaction of Local and Overall Buckling for the Specimen B4

Fig. 6.10(b) Crinkly-cum-overall Buckling of the Specimen B9

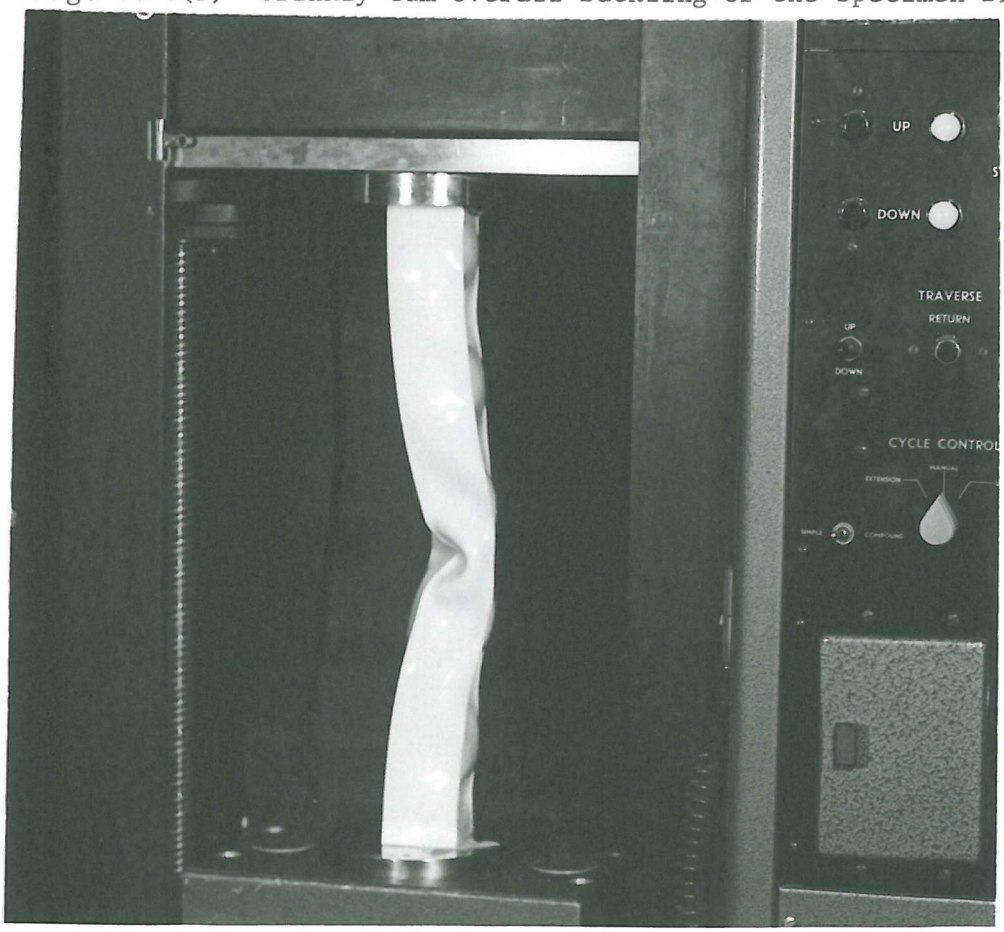

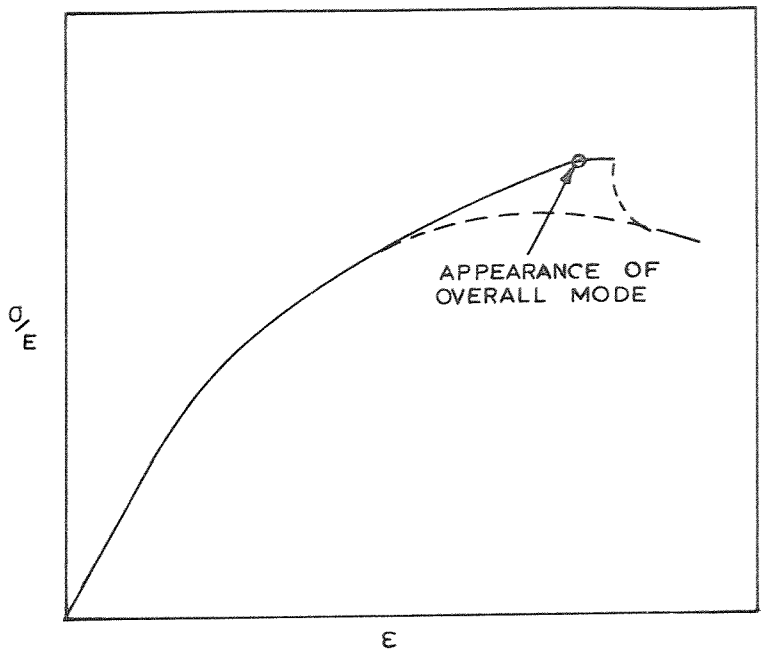

Fig.6.9(a) Stress-Strain relation (not to scale) of Specimen B4 ($\gamma = 9, \beta = 20$)

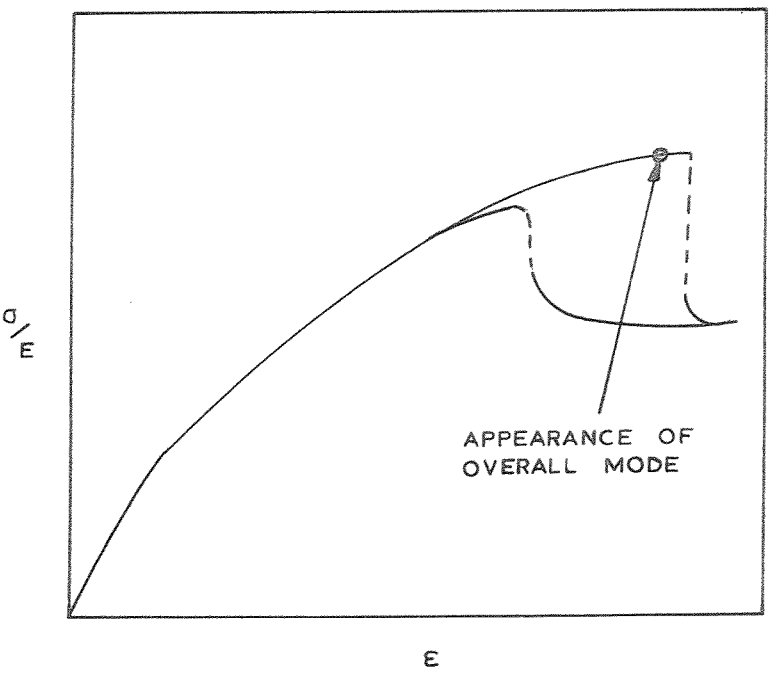

Fig.6.10(a) Stress-Strain relation (not to scale) of Specimen B9 ($\gamma = 9, \beta = 30$)

resembles that of a column clamped at either end.

The behaviour of the specimens B9 (with $\beta = 30$) is different from that of B4 in the following respects. The overall buckling mode does not make its appearance till the stiffness of the specimens is almost completely lost, and the stress-strain characteristic becomes very nearly flat (Fig. 6.10(a)). The postcollapse mode is a combination of the usual 'crinkly' mode and the overall buckling mode and is shown in Fig. 6.10(b).

6.4.3 Reproducibility of test results

Fig. 6.12 shows the nondimensional load displacement characteristics of a set of four specimens with the same value of 'β' and γ ($\gamma = 4$, $\beta = 30$). The set is made up of two groups of a pair of specimens each, with the same nominal dimensions and the same value of 'E' for the material. The actual load displacement relations obtained for the first group (specimens A1(1) and A1(2)) are shown in Fig. 6.11(a) and those for the second group (specimens A2(1) and A2(2)) in Fig. 6.11(b). As seen from the figures, there is a remarkably good agreement between the results of each group as well as the nondimensional plots of the stress-strain relations of all the four specimens. The collapse stresses (given by σ/E) of the specimens are almost identical, but slight differences are noticed in the corresponding 'ε', the average strain. Generally the stress-strain relationship has a much better reproducibility until the collapse than afterwards. In the vicinity of collapse, the structure loses its stiffness almost completely, and large increments in strain correspond to very small increases in stress; and the imperfections in loading and geometry now play a part in precipitating or delaying the collapse. Thus, while the collapse stress is insensitive to imperfections, the same can not be said of collapse strain.

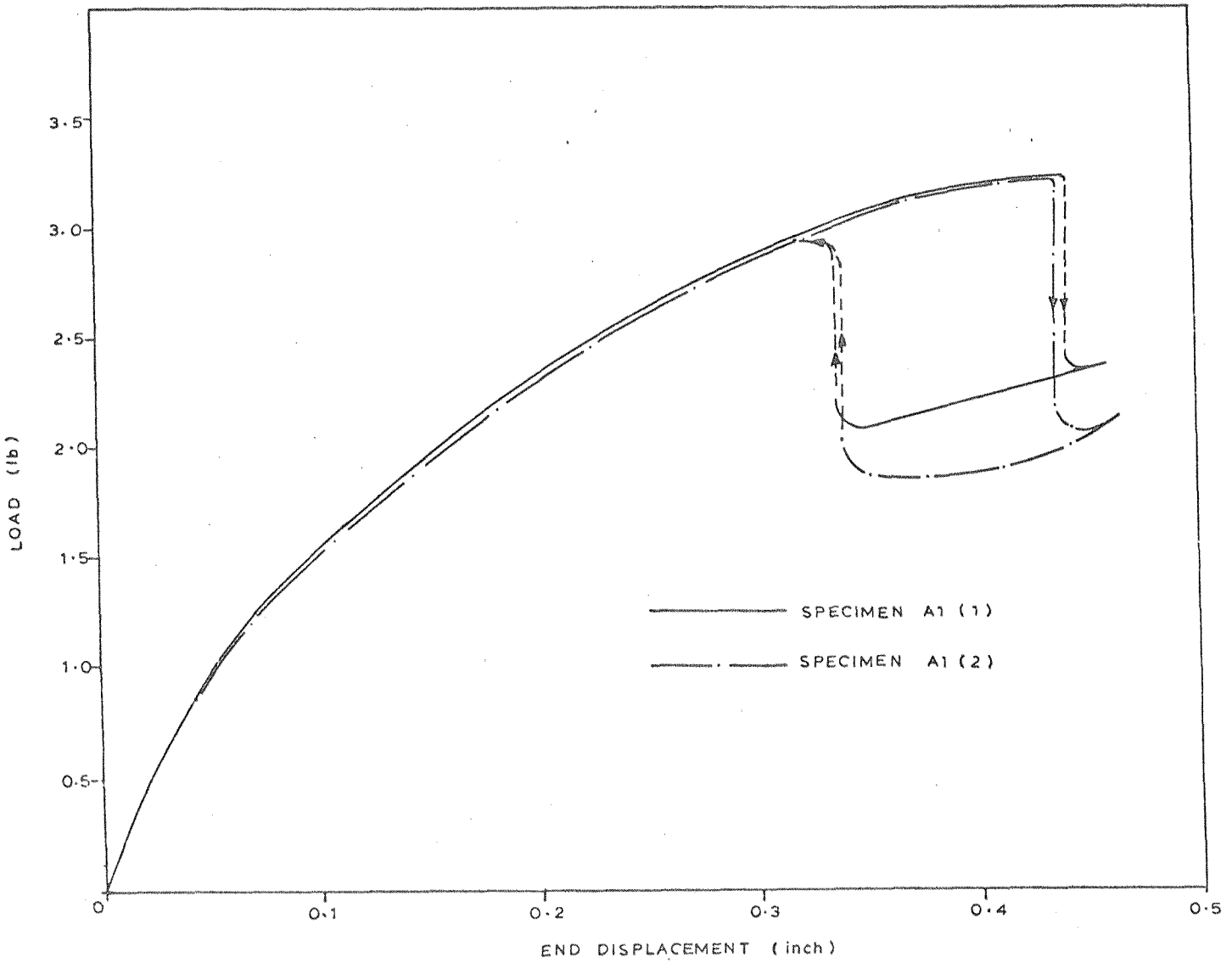

Fig.6.11(a)
Load - End displacemnet relations of Specimens A1 (1) and A1 (2).

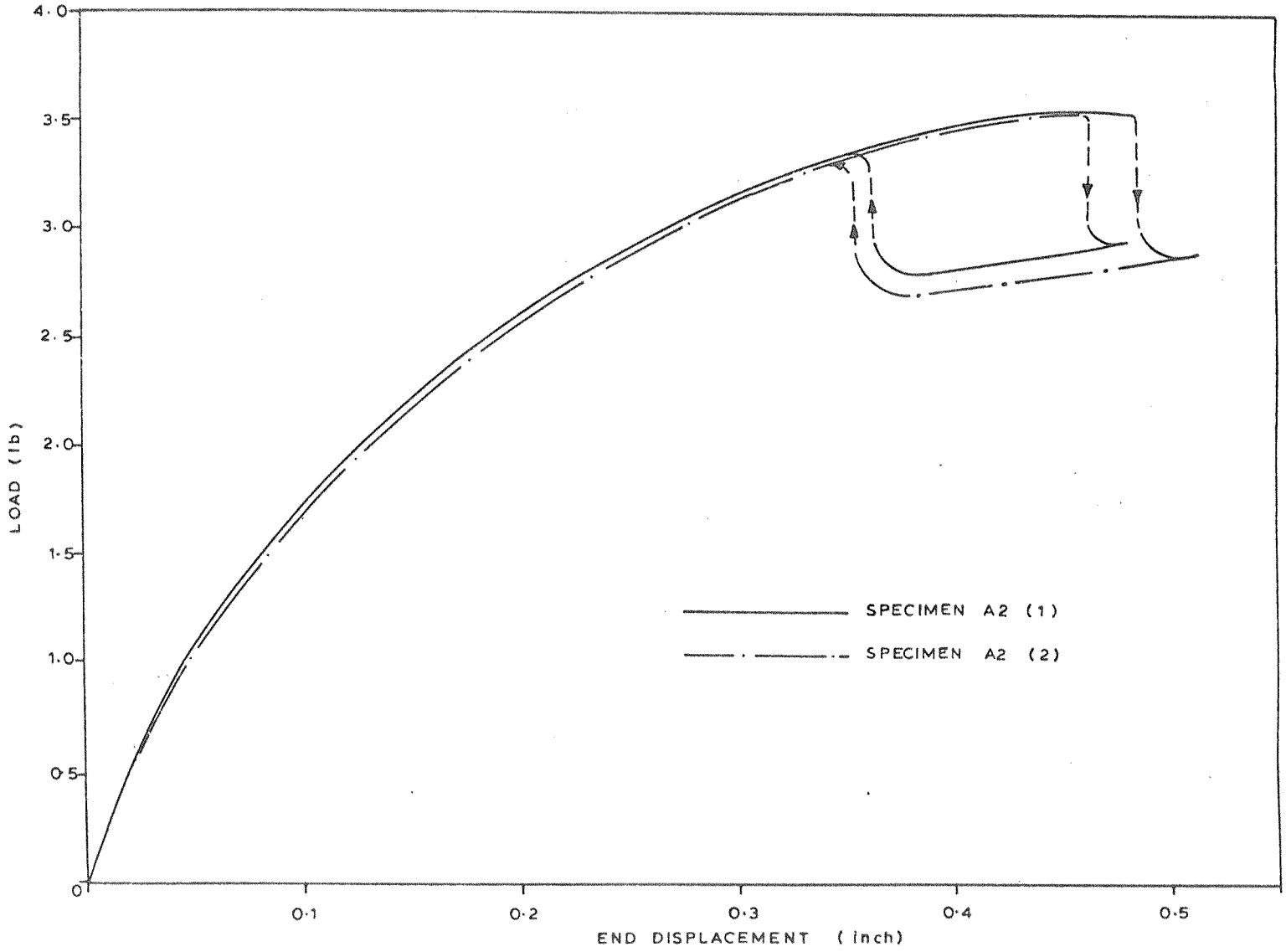

Fig.6.11(b) Load - End displacement relations of the Specimens A2 (1) and A2 (2).

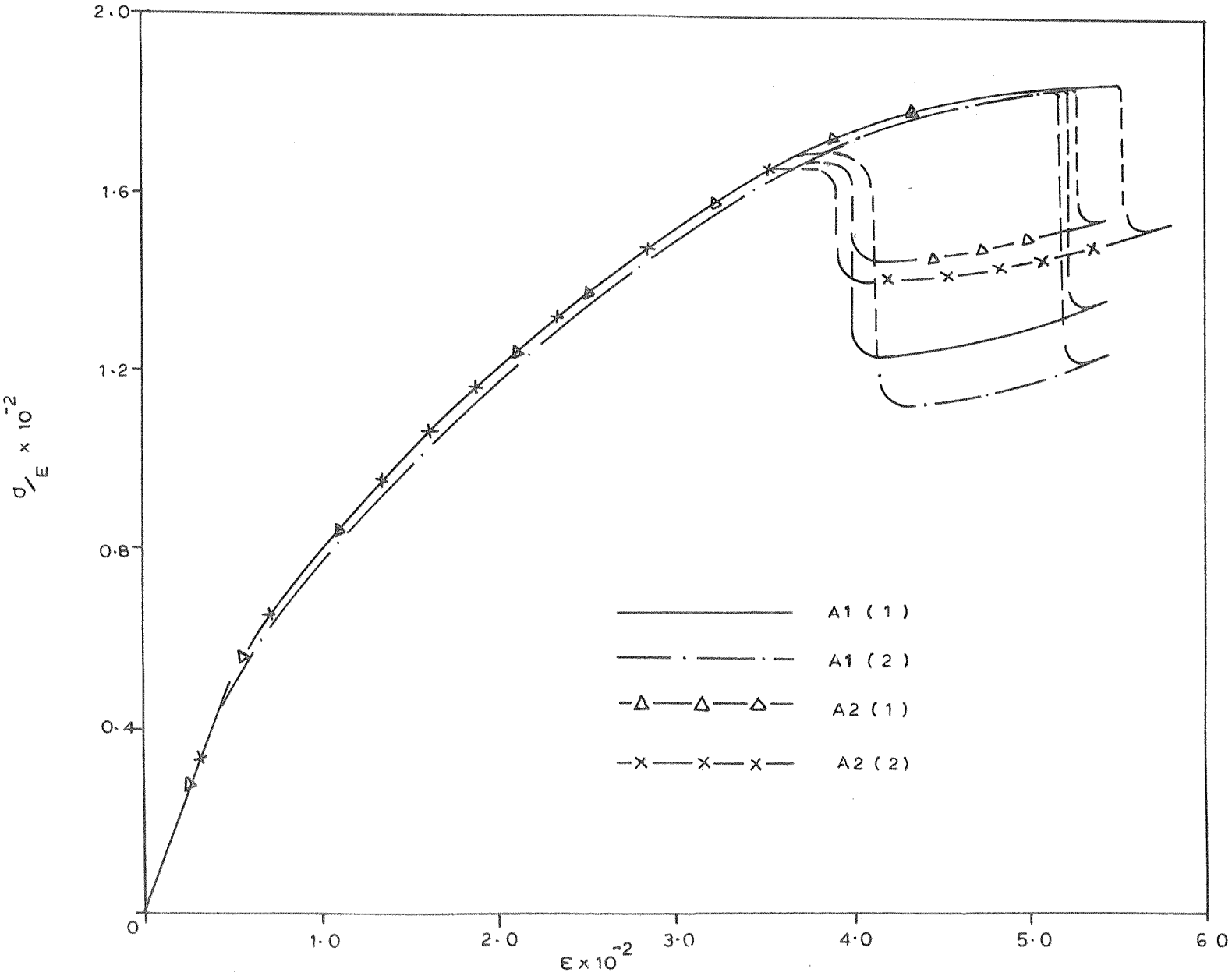

Fig. 6.12
Stress - Strain relations for the Specimens A1(1), A1(2), A2(1) & A2(2).

The collapse of structure is caused by the geometric instability of the buckled surface and was seen in chapter 5 to occur as the ratio of the maximum deflection to the width reaches a certain value (1/7 to 1/5). Thus the displacements in the vicinity collapse are larger than any imperfections that would be normally present in the plate structure, by an order of magnitude; thus the latter are of little importance in the determination of collapse load.

As seen from the Fig. 6.11(a-b) and 6.12, the postcollapse behaviour is somewhat less reproducible than the precollapse behaviour; but in view of the high degree of nonlinearity associated with the crinkly collapse mode and the predominance of the compressive stresses in the structure, the degree of reproducibility seen during the tests must be considered high. In all the four cases the collapse mode was characterised by two diagonally opposite junctions caving in simultaneously. It was seen, however, in subsequent tests, this was not always the case. There were cases where two adjacent junctions gave way, at times simultaneously and on other occasions sequentially. This shows that there are several equilibrium paths possible for the structure to any of which the specimen can jump once the stability of the post-local-buckling path is lost, dictated by imperfections in loading and geometry.

6.4.4 Effect of parameters 'γ' and 'β'

A study of the nondimensional stress-strain relations for the 14 cases (Fig. 6.13(a-e)) reveals the following features:-

(i) The comparison of the results for the same value of 'β' shows that specimen with smaller values of 'γ' (the shorter specimens for a given cross-section) take more load before collapsing. This is due to the clamping of the ends of the specimen, the effect of which is felt to a

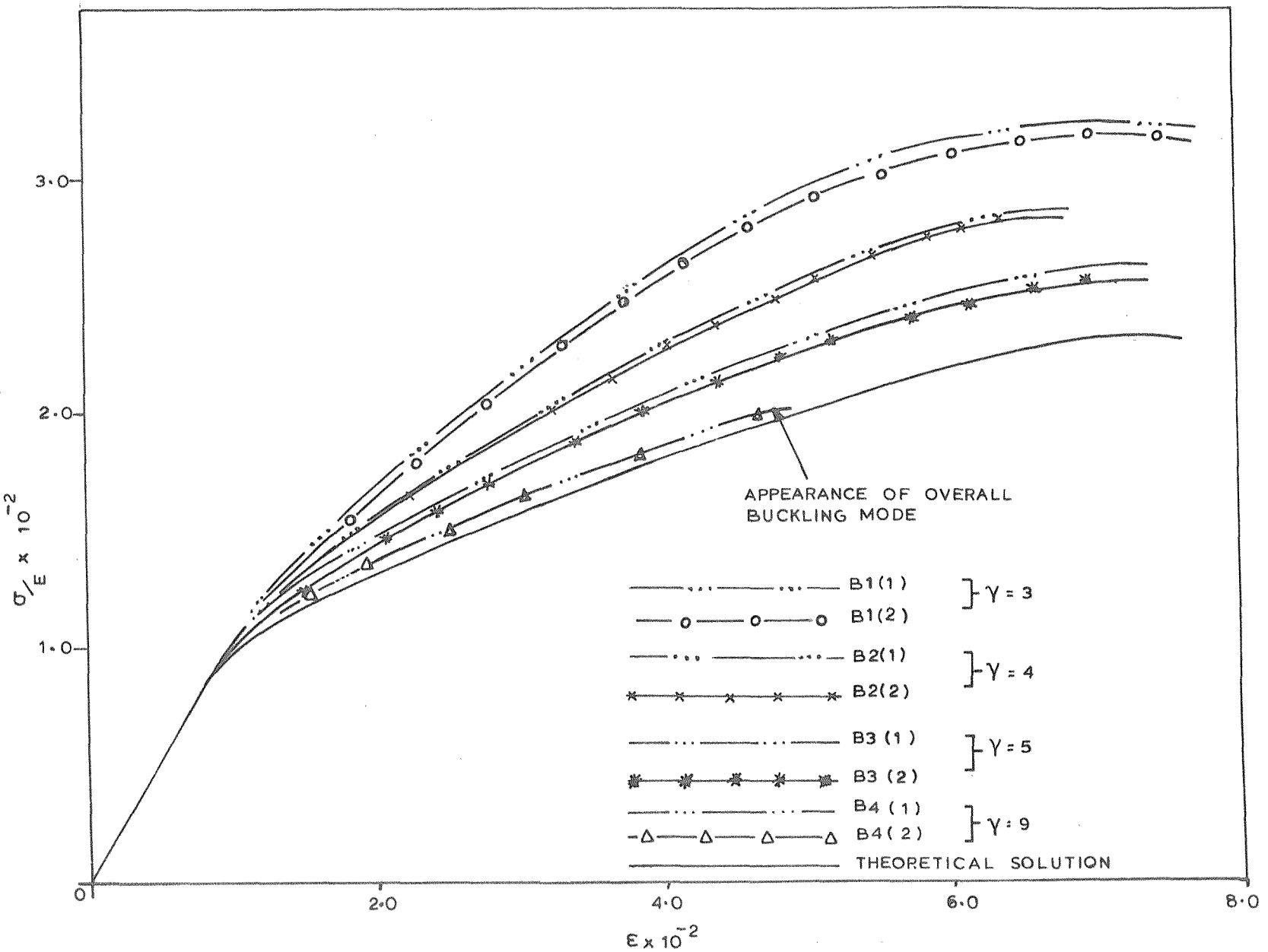

Fig.6.13(a)
Experimental and Theoretical Stress-Strain relations for the case 'β'=20.

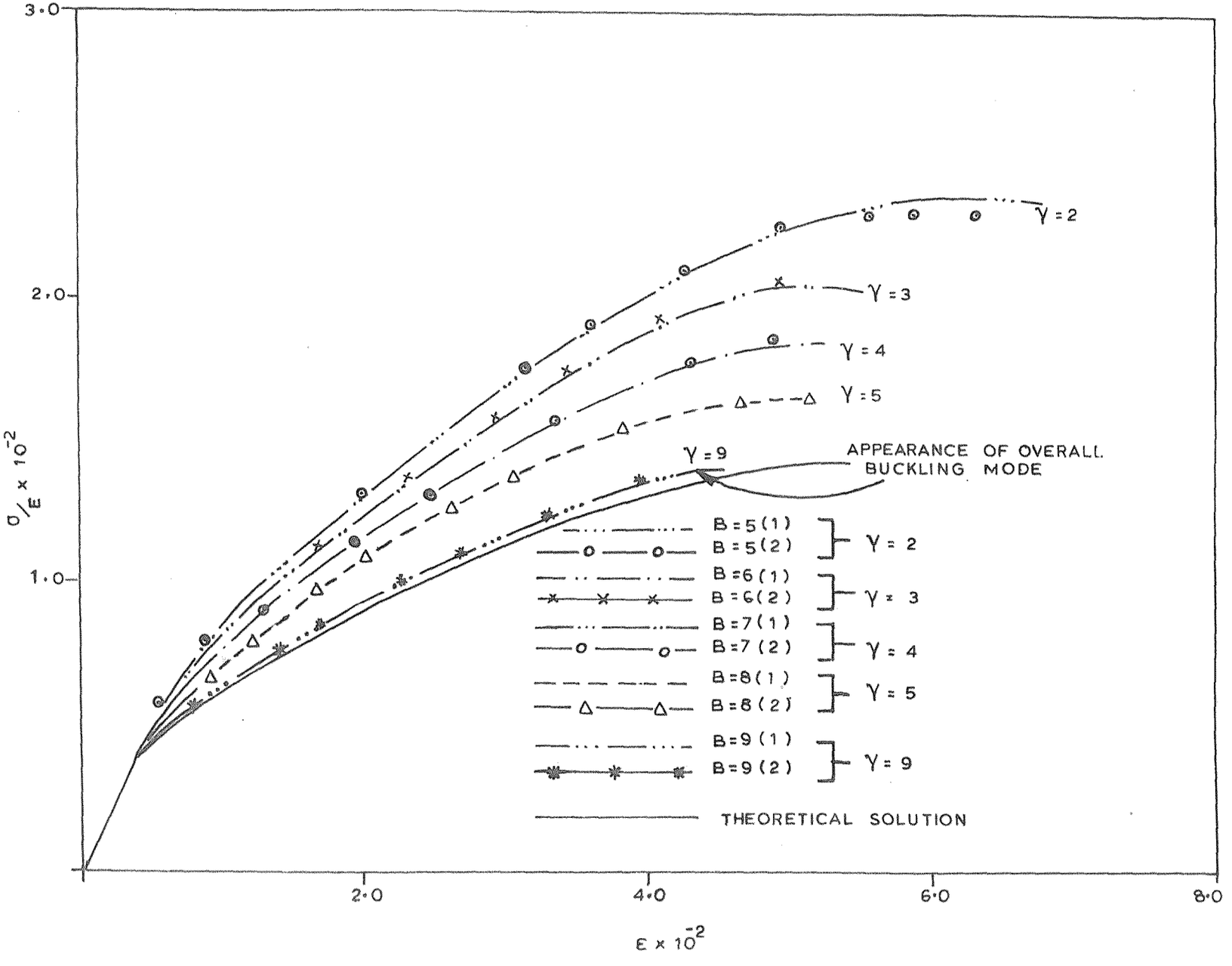

Fig.6.13(b)

Experimental and Theoretical Stress-Strain relations for the case 'β'=30.

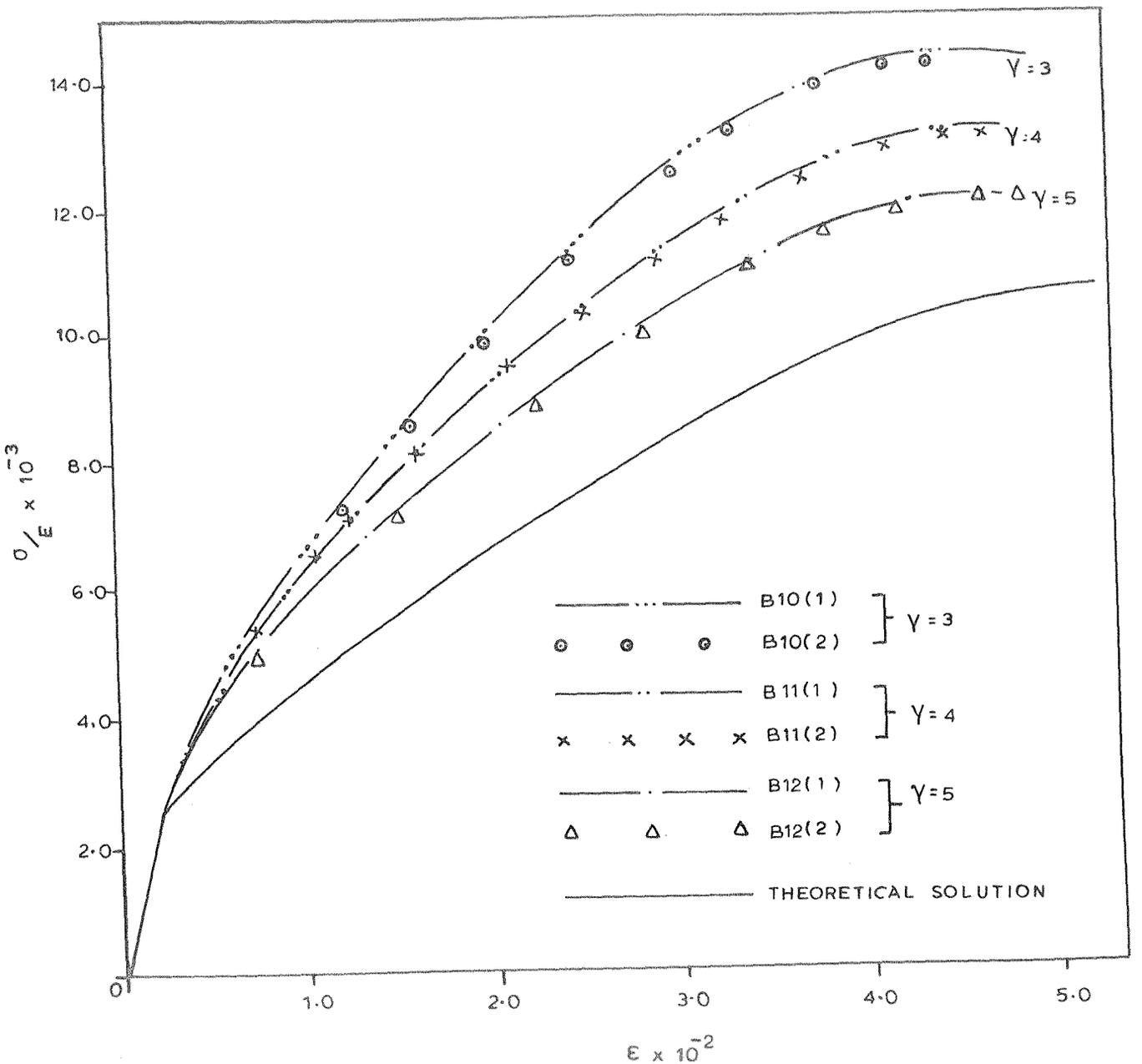

Fig.6.13(c)
Experimental and Theoretical Stress-Strain relations for the case 'β'=40.

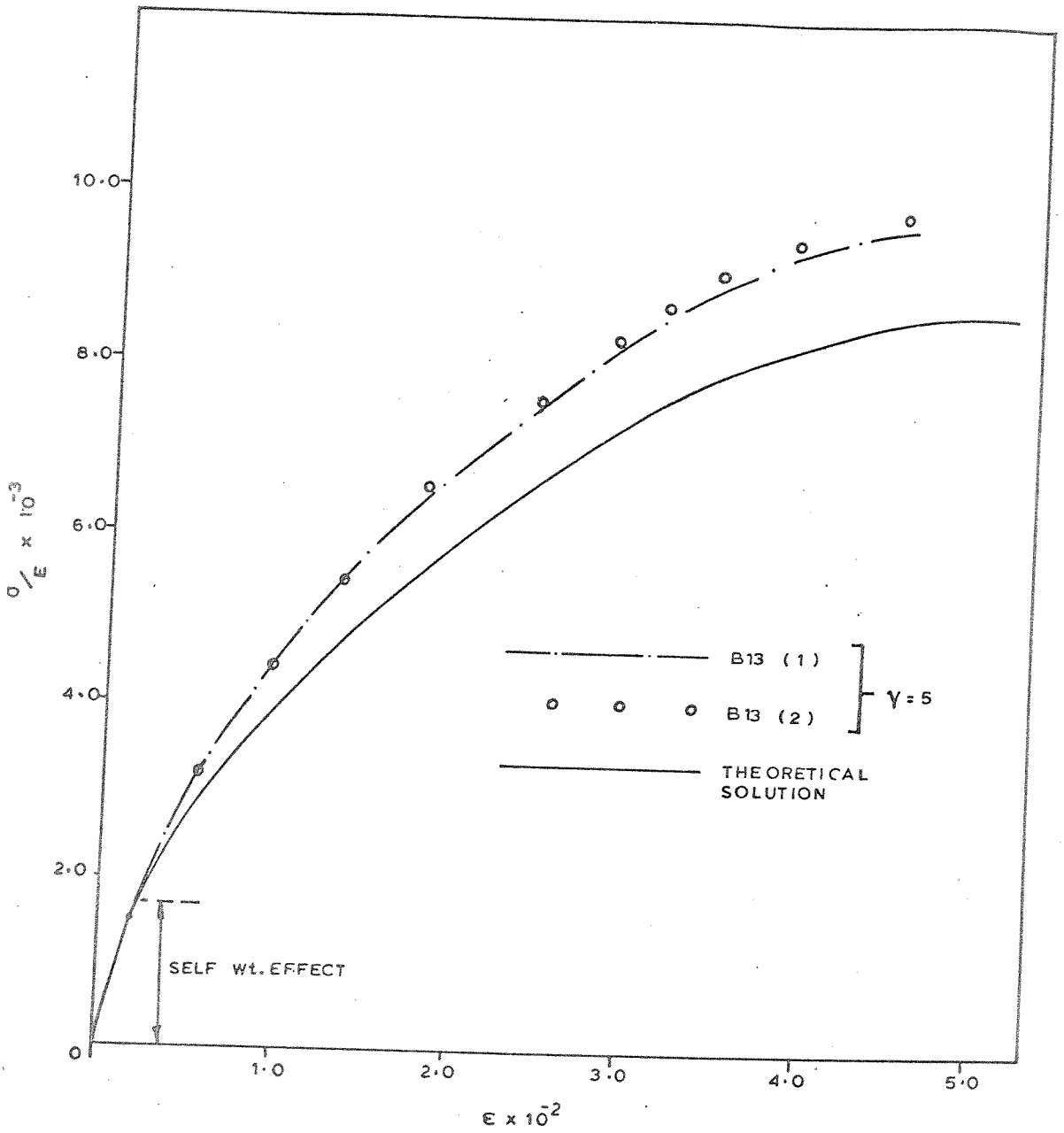

Fig.6.13(d) Experimental and Theoretical Stress-Strain relations for the case 'β' = 50.

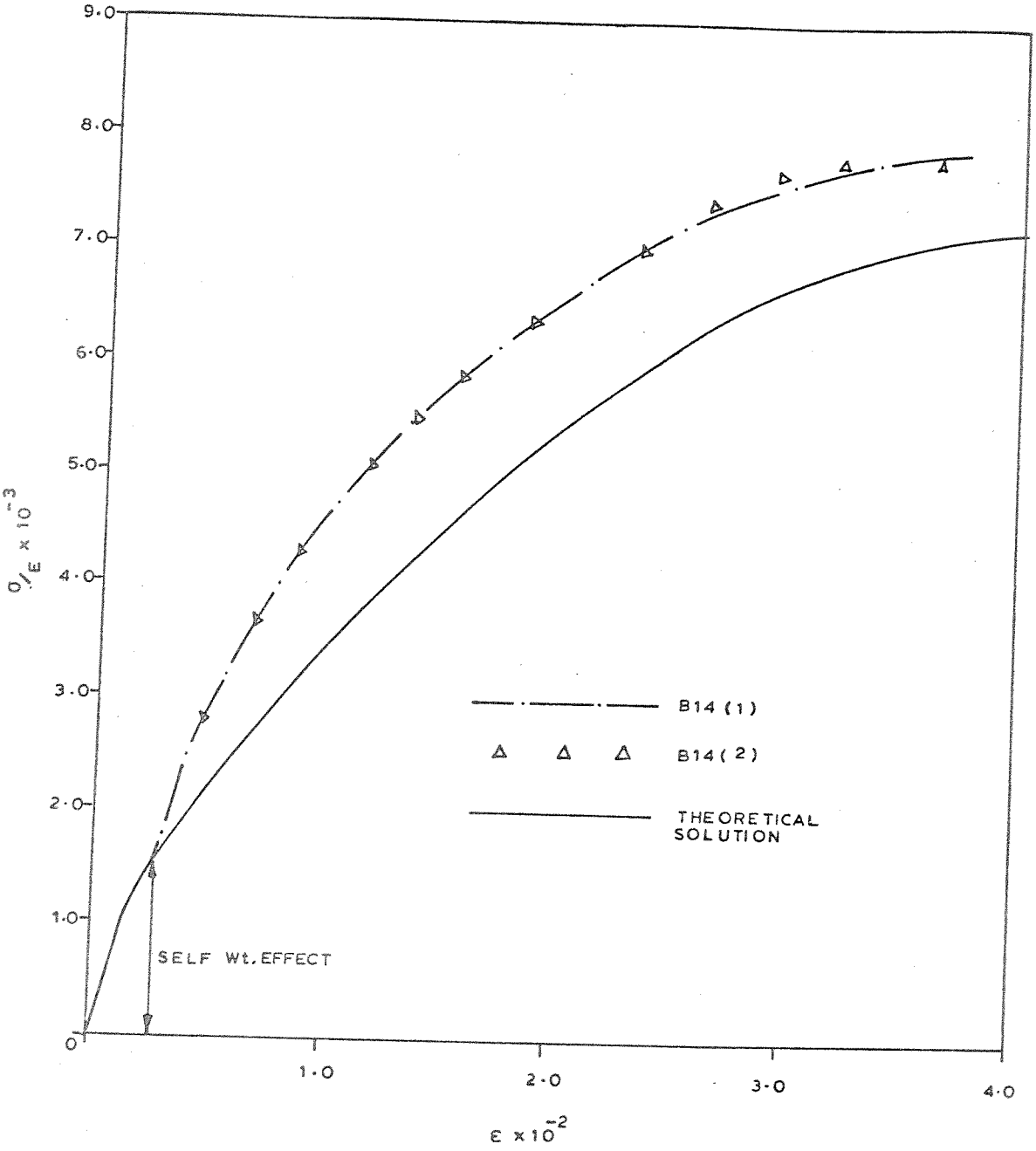

Fig. 6.13(e) Experimental and Theoretical Stress-Strain relations for the case 'β' = 60, 'γ' = 5.

greater extent all along the length in shorter specimens than in longer specimens where it is localised near the ends. From Fig. 6.14, it may be seen that the depth of the buckles in the vicinity of the ends is definitely smaller than those in the interior. A small extra stiffening effect seems to be all that is required to cause significant differences in the collapse load in view of large range of average strain involved. With increasing length, the discrepancies tend to diminish as demonstrated by the fact that the difference in the collapse stress between the cases with $\gamma = 5$ and $\gamma = 9$ ($\beta = 20,30$) are roughly the same as that between $\gamma = 4$ and $\gamma = 5$. If, on the other hand, the specimens were simply supported, the local buckling mode would consist of a set of identical buckles and the collapse load would be independent of the actual length of the specimen.

(ii) The comparison of the results for the same value of γ shows that there occurs a reduction of the nondimensional average stress (σ/E) corresponding to collapse, as 'β' increases; on the other hand the ratio of the ultimate to the initial buckling stress is found to increase with 'β'. These observations are consistent with the results of the theoretical study reported in chapter 5.

(iii) As mentioned earlier, the collapse behaviour of the longer specimens with $\gamma = 9$ is influenced by the intervention of the overall buckling mode.

The Euler buckling stress of a column clamped at both ends, is given by

$$\frac{\sigma_E}{E} = 4 \cdot \frac{\pi^2}{\left(\frac{a}{k}\right)^2} ,$$

where 'k' stands for the radius of gyration of the cross-section. For column with a hollow square cross-section and $\gamma = 9$, $\sigma_E/E = 0.0812$. The

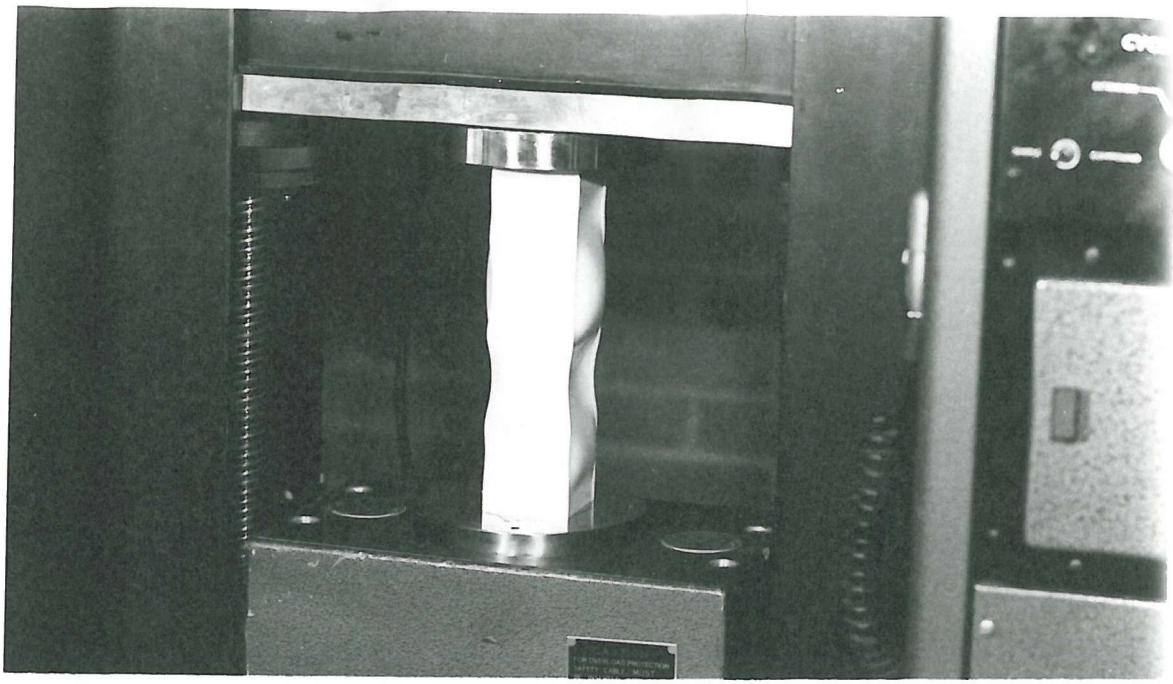

(a)

Fig. 6.14 The Effect of Clamped End Conditions on the Buckle Displacement

(b)

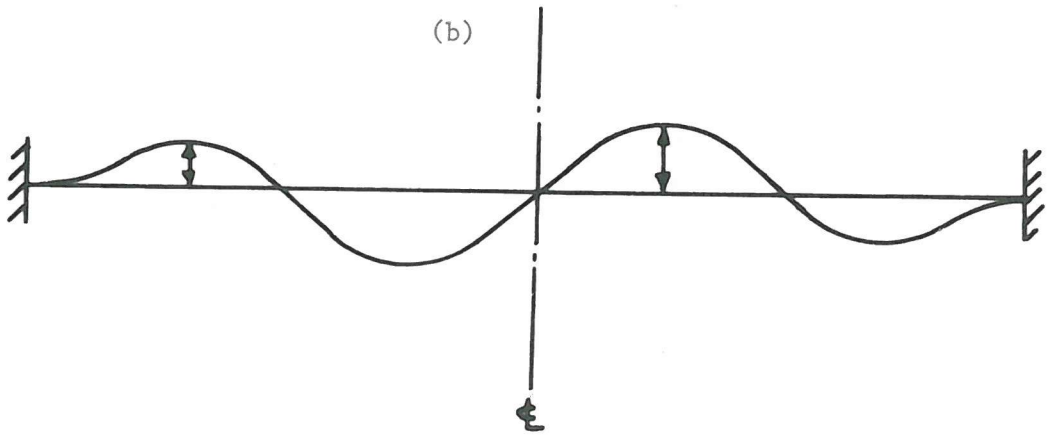

ratios of overall to local buckling stresses σ_E/σ_{cr} take the values 8.98 and 20.21 for columns with β = 20 and 30 respectively. Thus the risk of interaction of overall buckling is higher for the case with β = 20 and this is supported by the tests. In this case, as already noted in 6.4.2, the failure is precipitated by the interaction of overall buckling mode with the local mode, unlike in the case with β = 30, where the overall buckling mode does not make its appearance till the stiffness of the specimen is almost fully exhausted.

6.4.5 Comparison of the experimental and theoretical results

In Fig. 6.13(a-e) the theoretical stress-strain relations for the five cases of β = 20,30 ... 60, are shown against the characteristics obtained in the experiments upto the point of collapse. It is seen from Fig. 6.13(a-b), the theoretical solutions are in close agreement with the experimental characteristics for the case γ = 9. Excellent agreement between theoretical and experimental collapse loads exists for the specimens B9 with β = 30; however this is not the case with the specimens B4 (β = 20), which as already explained, fail by the interaction of overall buckling with the local mode.

As a rule, it is seen that the longer the specimen, the closer the agreement with the theoretical solution. In longer specimens, the end conditions have relatively smaller influence on the behaviour of the specimens than in shorter ones. The theory is based on conditions of simple support at the ends whereas the specimens have clamped end conditions in the experiments. It stands to reason, therefore, that the theoretical predictions of collapse load are always smaller than the experimental values. Thus the experimental and theoretical results are

consistent with each other for all the cases and are in good agreement for the case with $\gamma = 9$ (Specimens B9).

The consistency between the theoretical predictions and experimental observations, confirms the validity of the theoretical approach. It shows that in very thin plate structures, which remain elastic till very near the collapse, the destabilising influence of the inplane displacements 'v' must be taken into account and that it can be done in a simple manner suggested in chapter 5. This validates the notion - which itself is based on experimental observation - that the plate junction fails as a column.

However as stated in chapter 5, the theory cannot explain the machanics of collapse and the post-collapse-behaviour and in order to get an insight into the same, a theoretical mechanical model of a column resting on an elastic medium is proposed in the next section.

6.5 A theoretical mechanical model to explain the crinkly collapse of plate structures

The theoretical mechanical model proposed in this section is based on the notion that the plate junction acts as a column supported laterally by the restraint offered by the locally buckled plates. Thus the problem resembles one of a column resting on an elastic foundation.

In order to model realistically the behaviour of plate junctions, the properties of the mechanical model must be chosen carefully. The prime requisites are that the column must buckle locally and have a positive postbuckling stiffness. Now, it is known that a column resting on a linearly elastic foundation is unstable at the onset of initial buckling[97,107], unlike the locally buckled plate junction. From this it follows that the elastic foundation must have a nonlinear

stiffening response to displacements in order that the postbuckling equilibrium of the column may be stable.

Thus the model proposed is one of a column resting on a nonlinearly elastic foundation. In order to simplify the analysis, the column is represented by a series of rigid links connected at joints (marked 1,2, ... 9 in Fig.6.15(a)each of which rests on a nonlinear compression spring and carries linear moment springs, each connected to a link. This special arrangement is necessary in order to make possible application of the finite element procedure for the model. (vide Appendix XII). There are, however, additional features of the junction-plate interaction which must be incorporated into the model in order to make it more realistic. These are:-

(i) The plate junction has a definite preference to bend inwards, i.e. the resistance offered by the locally buckled plates to inward movements is considerably smaller than to outward movements. This is especially so in the precollapse behaviour. This feature can be taken into account by prescribing an asymmetric response to the compression springs with respect to the direction of loading (Fig. 6.15(b)).

(ii) In the vicinity of collapse, the locally buckled plates start losing their stiffness and offer increasingly small resistance to the inward movement of the plate junction. This feature can be built into the model by prescribing the stiffness of the spring to drop after its initial stiffening behaviour. (Fig. 6.15(b)).

(iii) After snap buckling of the plate structure, the deflection under the crinkle is quite large and the plate structure regains its stability. This can be interpreted as being due to the fact that the stiffness of the elastic foundation begins to improve beyond a certain value of applied displacement.

Thus the reactive force offered by the compression spring, at first increases, drops and then increases again with increasing displacement. This response can be obtained by choosing the load-displacement relationship in the form:

$$F = \sum_{i}^{n} C_i \, q^i$$

where $q = \delta/L$, δ being the displacement of the spring and L, the length of the link,

and choosing the coefficients C_i suitably.

The details of the theoretical analysis are given in Appendix XII, but here a typical solution is presented. Fig. 6.15(a) shows the mechanical model analysed and the coefficients C_i as well as the stiffness of the moment spring. Fig. 6.15(b) shows the load-displacement relationship for each spring.

The number of unknowns involved in the solution are the displacements of each spring (m) and the applied load, making up a total of m+1 while the number of equations available is only 'm'. Thus either the load, or the total end displacement or one of the displacements must be prescribed in order to obtain the rest. The most convenient parameter in the present case was found to be the displacement of the central spring, for this enables the determination of the equilibrium path where both load and end displacement are retrograde simultaneously.

The relationship between end load and end compression of the column is shown in Fig. 6.15(c) and the deflection profiles at a few key points are shown in Fig. 6.15(d-h). Under controlled compression, 'C' is a 'limit' point and in an experiment where the end compression is applied by a very rigid platten on the model, there would occur a dynamic snap

buckling at 'C' to reach the equilibrium configuration at 'E'. As shown in Fig. 6.15(h), the displacement profile in the post-collapse equilibrium path DEF is a localised crinkly one such as would accompany the elastic collapse of a plate structure. At this stage, much of the energy in the remaining part of the column is drained into the sharp crinkle at the middle of the column.

The equilibrium path loses and regains the stability at points P and Q respectively, under controlled compression. On decompression of the column after collapse the column would follow the path EQD and snap back at Q to the initial post local buckling equilibrium path.

The similarity of the snap buckling of the plate junction and that of the mechanical model discussed in the example is apparent. Thus the model serves to explain in qualitative terms the mechanics of crinkly collapse of plate structures.

6.6 Concluding remarks

An experimental investigation of elastic collapse of square box columns made of Silcoset has been described. The experimental results are compared with the theoretical solutions discussed in chapter 5. A mechanical model of a column resting on discrete nonlinear springs is proposed to explain the mechanics of collapse and the crinkly collapse mode. The main conclusions of the investigation may be summarised as follows:

(i) The experiments demonstrate the suitability of Silcoset as a modelling material for the elastic behaviour of box type structures.

(ii) The crinkly collapse of the plate junctions, often the mode of failure of the plate structures can occur entirely elastically. This

type of failure is shown to be a snap through type of buckling which the locally buckled column undergoes at the limit point of controlled compression.

(iii) The phenomenon of elastic collapse of box structures and in particular the collapse load, was found to be very reproducible, using a relatively simple experimental technique described in the chapter. This shows the collapse load is unaffected by initial imperfections.

(iv) The theoretical results are found to be consistent with the experimental ones and for the cases of long columns (Specimen B9) the agreement between the two sets of results upto the collapse of the structure is remarkably good. This confirms the validity of the simplifying approximations used in the theoretical approach.

(v) The mechanical model of a column resting on discrete nonlinear springs exhibits all the essential features of the behaviour of plate junctions.

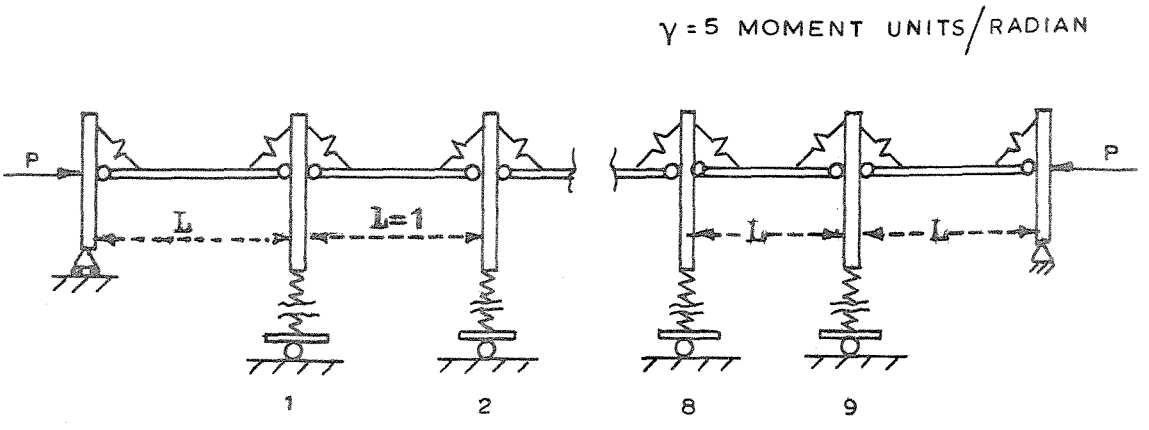

C_1 = 20 Force Units.

C_2 = - 30 "

C_3 = 600 "

C_4 = - 2250 "

$C_5 = C_6 = C_7 = C_8 = 0.$

C_9 = 60000 Force Units.

Fig. 6.15(a) Theoretical Mechanical Model of a Column Resting on an Elastic Foundation.

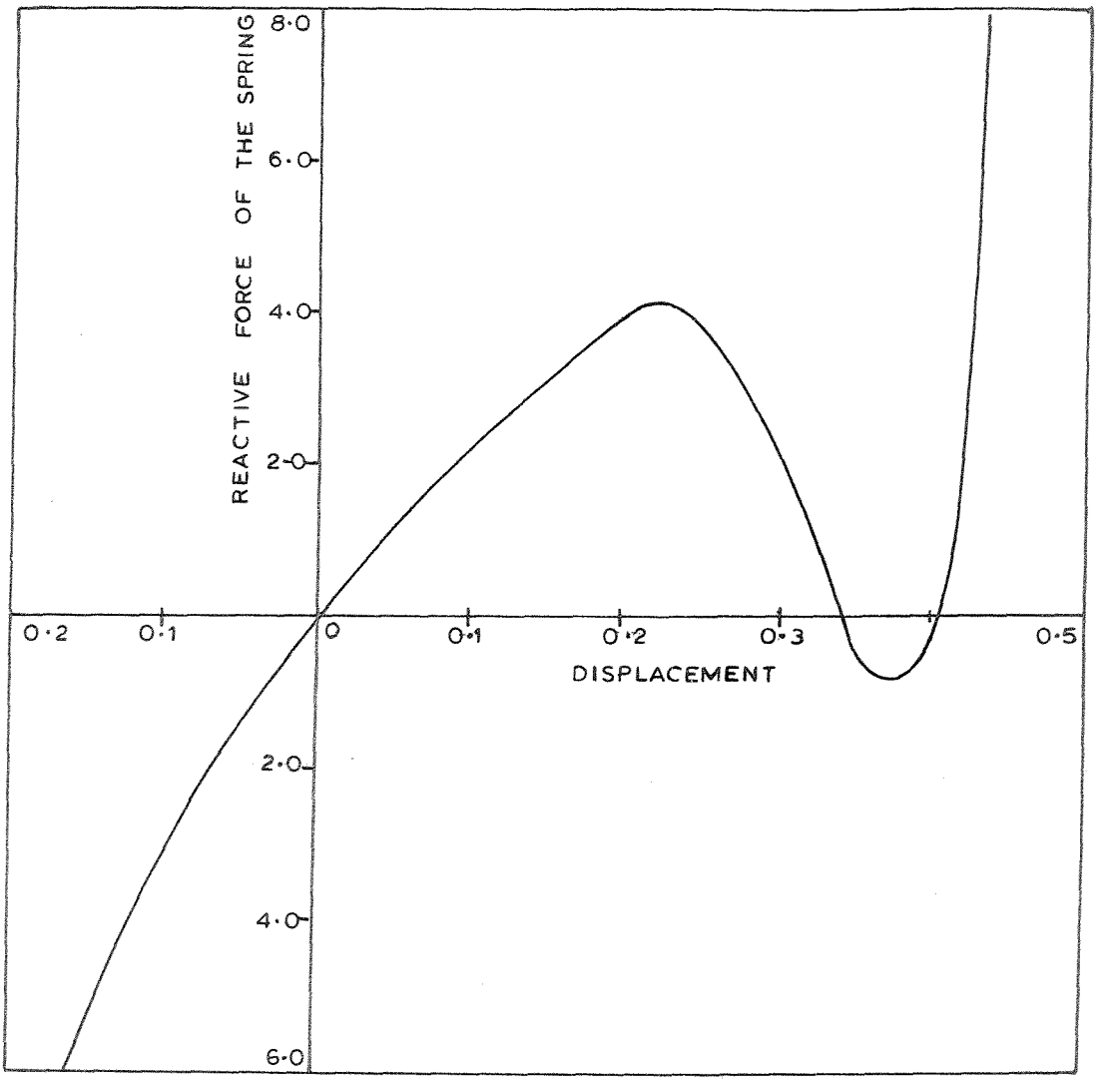

Fig 6.15(b) Load displacement relation for the Compression Springs in the example.

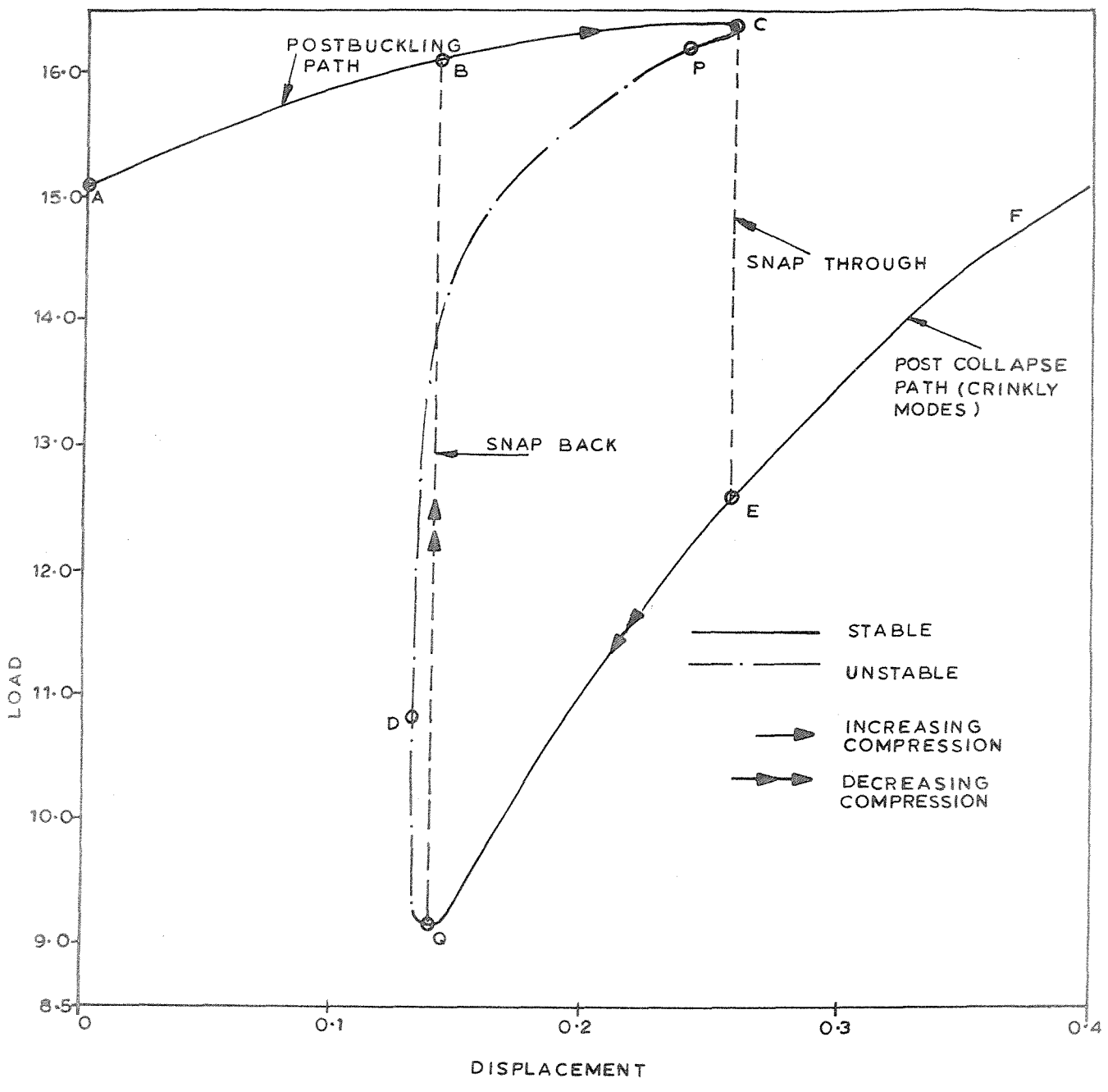

Fig.6.15(c) Load - end displacement relationship of the mechanical model.

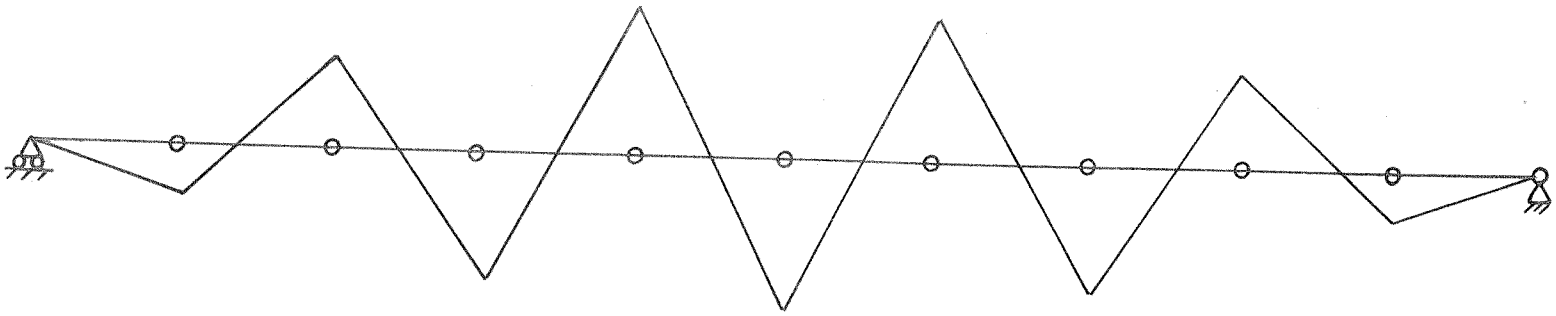

Fig. 6.15(d) Initial Buckling Mode.

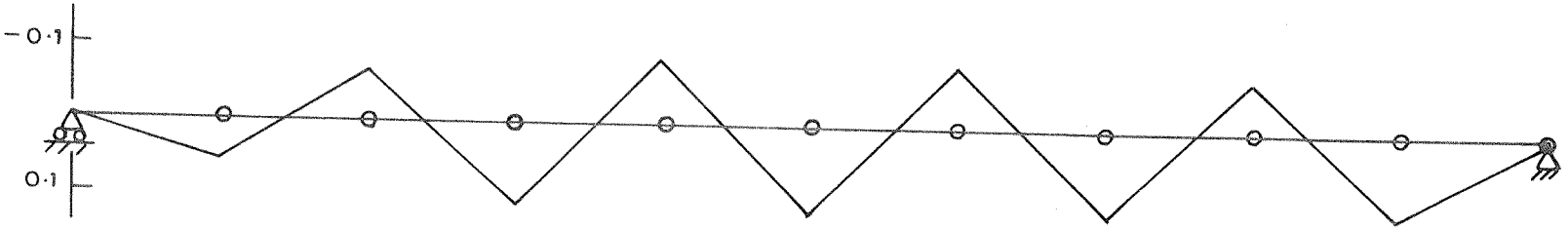

Fig. 6.15(e) Deflection Profile at B in Fig.6.15(c)

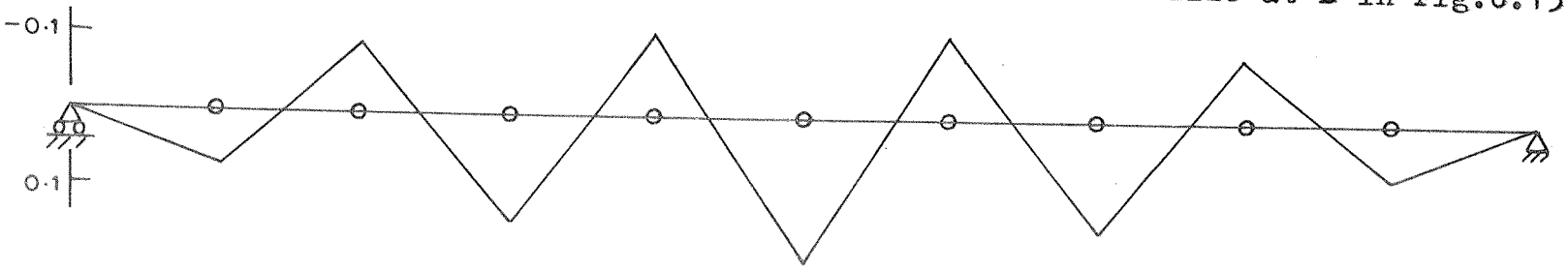

Fig. 6.15(f) Deflection Profile at C in Fig.6.15(c)

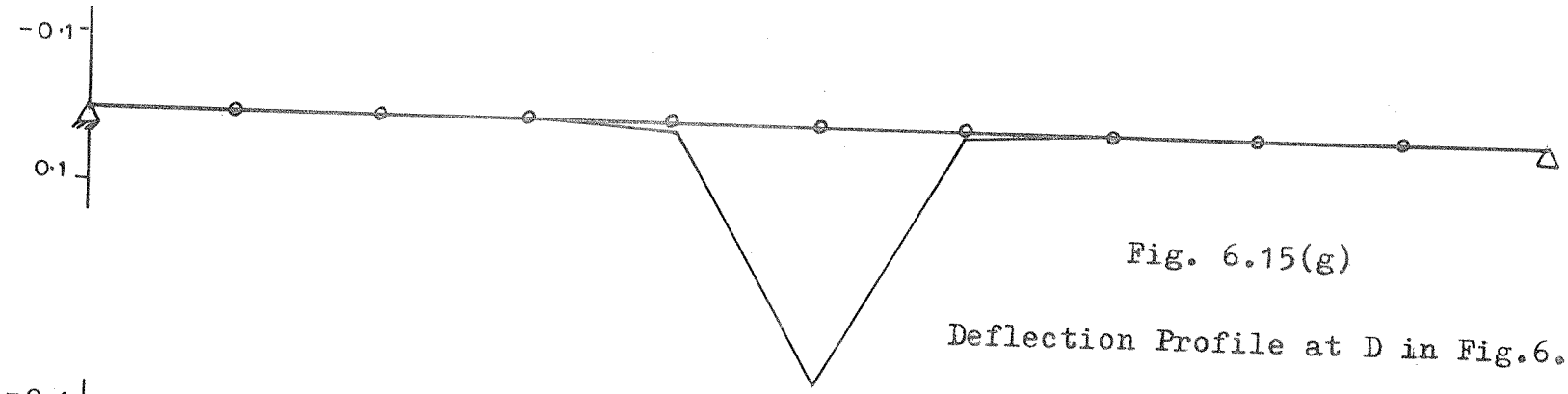

Fig. 6.15(g)

Deflection Profile at D in Fig.6.15(c)

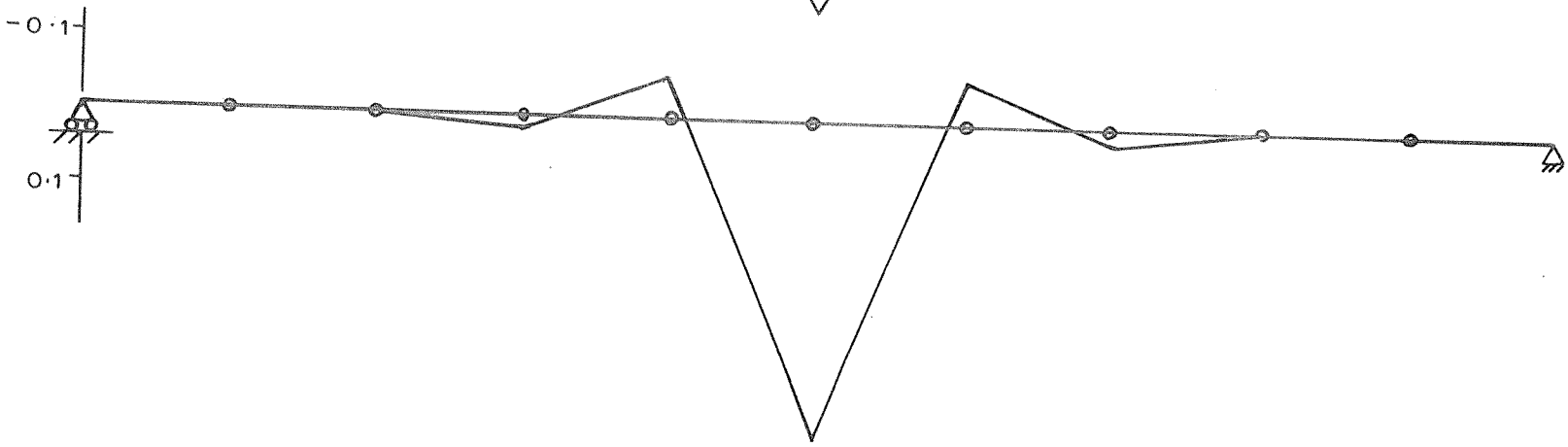

Fig. 6.15(h) Deflection Profile at E in Fig.6.15(c)

CHAPTER 7

CONCLUSIONS AND SCOPE FOR FURTHER WORK

7.1 Introduction

The failure of plate structures by crinkly collapse observed in tests and that such a failure can occur elastically provided the motivation for initiating the investigation reported in the preceding chapters. The objectives with which the author set out were to understand the mechanics of the phenomenon of crinkly collapse and estimate the elastic collapse load for a given plate structure. This necessitated a study of buckling and postbuckling behaviour of plate structures, particularly the latter in its advanced stages - a study which in itself proved rewarding in many respects. But because of the highly complicated strain-displacement relations which are required in the description of post collapse behaviour and the attendant increase both in the volume and complexity of numerical work, the post collapse behaviour could not be modelled; however, with the background material available in this respect, the different aspects of this problem have become clearer so that the problem has become less difficult to tackle in future. However, an insight into the mechanics of crinkly collapse of the plate junctions has been gained by a study of a mechanical model of a column resting on a nonlinear elastic foundation.

In this chapter some of the more important conclusions of the investigation are summarised. These fall into two categories - those which are of interest from an analytical stand point and others which give insight into the phenomena. The scope for extensions of the present work are discussed towards the end of the chapter.

7.2 Conclusions pertaining to analysis

It is believed that a major contribution of the present studies is the development of finite strip technique for the analysis of buckling and postbuckling behaviour of combinations of plates. In the case of the buckling problem, the analysis presented in chapter 2 represents an advance over the buckling analysis in the literature available so far on the finite strip method, in that the prebuckling stress distribution, however complex, is taken into account as an integral part of the procedure and buckling modes which are not necessarily sinusoidal along the length of the plates can be modelled by a suitable combination of harmonics. Using this technique a number of worked examples have been presented such as the problem of columns with 'indeterminate'* configurations and patch loaded plate structures. The savings in computational effort are found to be considerable; in the cases studied the finite strip method required only about 1% of the time required by the finite element method.

The finite strip method is also found to be efficient for dealing with post-local-buckling problems of plate structures; this is especially true of the Version I (of the finite strip method) which neglects the coupling of inplane and out of plane displacements (and forces) of the constituent plates along the junctions. The method is found to take only 3-5% of the computing time taken by a finite element approach for the study of postbuckling analysis of plates. Using this approach post local buckling analysis of a number of typical plate assemblies has been performed; the effects of variation of the widths and thicknesses of the

* The term 'indeterminate' refers to configurations of columns whose constituent plates develop in addition to the longitudinal stresses, inplane transverse stresses as well, even though subjected only to axial loads at the ends.

member plates have been studied.

An alternative version of the finite strip method which takes into account the 'coupled' nature of the boundary conditions, is found to be helpful in the study of advanced post-local-behaviour leading to the collapse of the plate structure. In order to model the collapse behaviour properly, it is found necessary to take into account the destabilising influence of inplane displacements in the transverse direction and to do this simply an approximation based on the conception that the junctions behave as columns, has been suggested. It is believed that this approximation may prove useful in the elastoplastic analysis of plate structures built up of thin plates.

7.3 Conclusions from the experimental study

The phenomenon of crinkly collapse, often the observed mode of failure of plate structures, can occur entirely elastically; the failure is due to snap buckling to a remote equilibrium state under controlled compression. The collapse load of square box columns is found to be quite reproducible, thus indicating that it is insensitive to initial imperfections. Good agreement between the theoretical and experimental results is observed. This confirms the validity of the assumptions made in the theory. In general, it may be concluded that the behaviour of junctions is similar to that of a column resting on the nonlinear elastic support provided by the locally buckled plates. This is demonstrated by an analysis of a mechanical model of a column resting on discrete non-linear springs which exhibit all the features of the plate problem: the phenomenon of local buckling, the exhaustion of the capacity to carry loads in the postbuckling range and the snap buckling to a remote equilibrium state characterised by the 'crinkly' deflection mode.

7.4 Scope for further work

The present investigation has opened up new directions of research, pursuit of which, it is believed will prove rewarding. These will be mentioned briefly in the following.

First of all there exists considerable scope for undertaking parametric studies on buckling and post-local-buckling analysis with the analytical techniques and computer programmes available. These include:

1. The problem of initial buckling of different types of prismatic plate structures under a combination of axial and lateral loading, using the finite strip technique discussed in chapter 2.
2. The post-local-buckling analysis of chosen configurations of the plate assemblies using Version I of the finite strip technique developed in chapter 3.

Buckling and postbuckling behaviour of plate structures under a combination of axial and lateral loading using version II of th finite strip technique developed in chapter 3. (Note that version I is not suitable for this problem for the calculation of inplane stresses under lateral loading, in general, is not possible with the 'uncoupled' boundary conditions of Version I).

3. Elastic collapse analysis of plate structures made of rubber-like materials, using the method discussed in chapter 5.

In addition there are other problems of interest which can be solved by making the necessary modifications to the techniques outlined in this report. These are

(i) Initial buckling of plate structures under varying compressive loading.

(ii) Post-local-buckling behaviour of plate assemblies under increasing end compression applied along the centroid and prescribed constant end rotations about the principal axes; with a set of solutions for various values of rotations produced, it is possible to study the problem of the plate assembly acted upon by a load at given eccentricities with respect to the principal axes.

(iii) The influence of initial imperfections varying sinusoidally in the longitudinal direction and having any arbitrarily given variation in the transverse direction.

(iv) Interaction of the overall buckling mode with the local mode In the post-local-buckling equilibrium path of plate structures, this problem can be tackled with a slight modification of Version I of the finite strip method in the following manner:-

In addition to the degrees of freedom corresponding to the local buckling mode, those corresponding to overall buckling mode (u_o, v_o and w_o) must be included in the formulation in the form:

$$w_o = w_o(y) \sin \frac{\pi x}{a}$$

$$v_o = v_o(y) \sin \frac{\pi x}{a}$$

$$u_o = u_o(y) \cos \frac{\pi x}{a}$$

The strain displacement relations must include nonlinear terms in 'v' as well as in 'w'. The overall buckling mode will begin to operate at any point on the post-local-buckling equilibrium path at which the second variation of total potential energy ceases to be positive definite.

7.5 The final word

The chapter is concluded with the expression of hope that the findings reported in the thesis go some way towards filling a gap in the literature available on the nonlinear behaviour of plate structures.

APPENDIX I

POST LOCAL BUCKLING ANALYSIS OF PLATE ASSEMBLIES BY SOLUTION OF VON KARMAN EQUATIONS

I.1 Introduction

In sec. 1.2.1.2 a reference was made to the earlier work of the author[92] on the postbuckling analysis of plate assemblies by the solution of von Karman equations. This analysis is briefly summarised in this Appendix.

I.2 Governing equations

The structural behaviour of elastic plates subjected to edge loads and undergoing large deflections may be studied with the aid of von Karman equations:

$$\nabla^4 \phi = E \left\{ \left(\frac{\partial^2 w}{\partial x \partial y} \right)^2 - \frac{\partial^2 w}{\partial x^2} \cdot \frac{\partial^2 w}{\partial y^2} \right\}$$

$$\nabla^4 w = \frac{h}{D} \left\{ \frac{\partial^2 \phi}{\partial y^2} \cdot \frac{\partial^2 w}{\partial x^2} - 2 \frac{\partial^2 \phi}{\partial x \partial y} \cdot \frac{\partial^2 w}{\partial x \partial y} + \frac{\partial^2 \phi}{\partial x^2} \cdot \frac{\partial^2 w}{\partial y^2} \right\}$$

. . . I.1(a-b)

Fig. I.A shows the plate with the coordinate axes and the positive directions of stress resultants. In the above equation 'ϕ' is the stress function defined by

$$N_y = h \frac{\partial^2 \phi}{\partial x^2}, \quad N_x = h \frac{\partial^2 \phi}{\partial x^2} \quad \text{and} \quad N_{xy} = - h \frac{\partial^2 \phi}{\partial x \partial y}$$

I.3 Fourier Series Approach

Considering the case of a longitudinally compressed plate assembly, we take for w and ϕ for a typical constituent plate

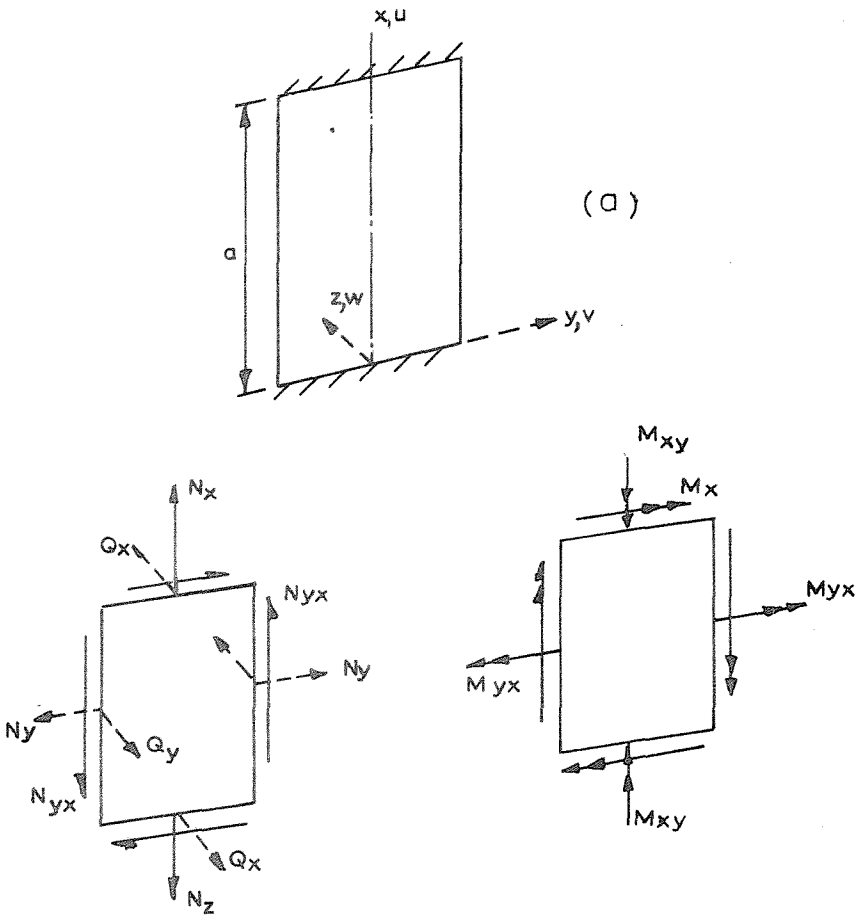

Fig. I.A (a) Plate with the axes of coordinates.

Fig. I.A.(b) Positive Directions of Stress resultants.

N_x, N_y, N_{xy} Normal and Shear forces

Q_x, Q_y Transverse Shears

M_x, M_y, M_{xy} Bending and Twisting Moments.

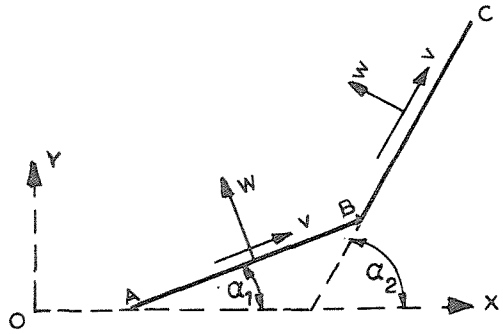

Fig. I.B Orientation of Plates AB & BC

$$w = \sum w_m(y) \sin \frac{m\pi x}{a}$$

$$\phi = \sum \phi_m(y) \sin \frac{m\pi x}{a} - \frac{1}{2} \sigma_x y^2 \qquad \ldots \text{ I.2(a-b)}$$

The boundary conditions at the ends of the plate assembly associated with such a representation of 'w' and 'ϕ' will be discussed in the next section.

Introducing I.2(a-b) into I.1(a-b), we obtain

$$\sum_m \left(\phi_m^{iv} - 2 \frac{m^2\pi^2}{a} \phi_m'' + \frac{m^4\pi^4}{a} \phi_m\right)$$

$$= E \frac{\pi^2}{a^2} \sum_i \sum_j \left\{ w_i' w_j' ij \cos \frac{i\pi x}{a} \cos \frac{j\pi x}{a} + w_i w_j'' i^2 \sin \frac{i\pi x}{a} \sin \frac{j\pi x}{a} \right\}$$

$$\sum_m \left(w_m^{iv} - 2 \frac{m^2\pi^2}{a^2} w_m'' + \frac{m^4\pi^4}{a^4} w_m - \frac{h}{D} \frac{m^2\pi^2}{a^2} \cdot \sigma_x\right)$$

$$m$$

$$= - \frac{h}{D} \frac{\pi^2}{a^2} \sum_i \sum_j \left\{ (\phi_i'' . w_j . j^2 + \phi_i w_j'' i^2) \sin \frac{i\pi x}{a} \sin \frac{j\pi x}{a} \right.$$

$$\left. + 2\phi_i' w_j' ij \cos \frac{i\pi x}{a} \cos \frac{j\pi x}{a} \right\}$$

$$\ldots \text{ I.3(a-b)}$$

We now expand terms $\sin \frac{i\pi x}{a} \sin \frac{j\pi x}{a}$ and $\cos \frac{i\pi x}{a} \cos \frac{j\pi x}{a}$ in Fourier series in the interval $0 < x < a$ in the following manner:

$$\cos \frac{i\pi x}{a} \cos \frac{j\pi x}{a} = \sum_m C_{ijm} \sin m\pi\xi$$

$$\sin \frac{i\pi x}{a} \sin \frac{j\pi x}{a} = \sum_m S_{ijm} \sin m\pi\xi$$

$$\ldots \text{ I.4(a-b)}$$

Truncating the series in I.2 and I.4 at a suitably chosen number of terms

'N', we obtain for each 'm' the following pair of equations:

$$L_m(\phi_m) = \frac{E\pi^2}{a^2} \sum_i \sum_j \left[w_i' \, w_j' \, ij \, C_{ijm} + w_i \, w_j'' \, i^2 \, s_{ijm} \right]$$

$$\bar{L}_m(w_m) = -\frac{h}{D} \cdot \frac{\pi^2}{a^2} \sum_i \sum_j \left[(\phi_i'' \, w_j \, j^2 + \phi_i \, w_j'' \, i^2) S_{ijm} + 2 \, \phi_i' \, w_j' \, ij \, C_{ijm} \right] \quad \ldots \text{ I.5(a-b)}$$

where L_m and $\bar{L}_m$ represent the linear differential operators

$$L_m = \frac{\partial^4}{\partial y^4} - 2 \frac{m^2\pi^2}{a^2} \frac{\partial^2}{\partial y^2} + \frac{m^4\pi^4}{a^4}$$

$$\bar{L}_m = \frac{\partial^4}{\partial y^4} - 2 \frac{m^2\pi^2}{a^2} \frac{\partial^2}{\partial y^2} + \frac{m^2\pi^2}{a^2} \left(\frac{m^2\pi^2}{a^2} - \frac{h}{D} \sigma_x \right)$$

The equations I.4(a-b) represent a pair of ordinary nonlinear differential equations written for each 'm' for each plate.

I.4 Boundary Conditions

At the ends x = 0 and x = a

For simply supported ends we may prescribe

$$w = 0$$
$$\frac{\partial^2 w}{\partial x^2} = 0$$
$$v = 0$$
$$\frac{\partial^2 \phi}{\partial y^2} = -\sigma_x \quad \ldots \text{ I.6(a-d)}$$

It may be readily seen that the conditions I.6(a), (b) and (d) are satisfied by the choice 'w' and 'ϕ' made in I.2(a-b). Regarding I.6(c), it may be easily verified that

$$\frac{\partial v}{\partial y} = \frac{\nu}{E} \sigma_x$$

This represents the transverse strain of the plate owing to the Poisson's effect of uniform applied longitudinal stress. Thus the expressions I.2(a-b) imply that the plate is allowed freedom at the ends to expand to the extent given by $\nu\sigma_x/E$. It is believed that this does not constitute a serious enough violation of the boundary conditions to have any significant effect on the final results of the analysis, especially for long plates.

Along the longitudinal edges:

Along a common edge (B in Fig. I.B) where two plates (AB and BC) meet, compatibility and equilibrium conditions must be satisfied.

Compatibility conditions:

$$w_{BA} \cos \alpha_1 + v_{BA} \sin \alpha_1 = w_{BC} \cos \alpha_2 + v_{BC} \sin \alpha_2$$

$$w_{BA} \sin \alpha_1 - v_{BA} \cos \alpha_1 = w_{BC} \sin \alpha_2 - v_{BC} \cos \alpha_2$$

$$u_{BA} = u_{BC}$$

$$\left(\frac{\partial w}{\partial y}\right)_B \text{ for AB} = \left(\frac{\partial w}{\partial y}\right)_B \text{ for BC} \qquad \ldots \text{ I.7(a-d)}$$

Equilibrium conditions:

$$(\bar{Q}_y)_{BA} \cos \alpha_1 + (N_y)_{BA} \sin \alpha_1 = (\bar{Q}_y)_{BC} \cos \alpha_2 + (N_y)_{BC} \sin \alpha_2$$

$$(\bar{Q}_y)_{BA} \sin \alpha_1 - (N_y)_{BA} \sin \alpha_2 = (\bar{Q}_y)_{BC} \sin \alpha_2 - (N_y)_{BC} \cos \alpha_2$$

$$(N_{xy})_{BA} = (N_{xy})_{BC}$$

$$(M_y)_{BA} = (M_y)_{BC} \qquad \ldots \text{ I.7(e-h)}$$

In the foregoing the suffix BA refers to the force or displacement quantity at B for the plate AB; and the suffix BC refers to the same for plate BC. $\bar{Q}_y$ refers to the Kirchoff's equivalent shear force.

I.5 Buckling and Initial postbuckling analysis using the perturbation technique

The sequentially linear perturbation equations at w = 0 (i.e. $w_m = 0$ for each 'm') may be written in the form:

$$L_m(\Phi_{m_1}) = 0$$

$$\bar{L}_m(w_{m_1}) = 0 \qquad \ldots \text{ I.8(a-b)}$$

$$L_m(\phi_{m_2}) = \frac{2E\pi^2}{a^2} \sum \sum \left[w'_{i_1} \, w'_{j_1} \, ij \, C_{ijm} + w_{i_1} \, w''_{j_1} \, i^2 \, S_{ijm} \right]$$

$$\bar{L}_m(w_{m_2}) = 2 \frac{h}{D} \cdot \frac{m^2\pi^2}{a^2} \sigma_{x_1} \, w_{m_1}$$

$$- 2 \frac{h}{D} \cdot \frac{\pi^2}{a^2} \sum \sum \left[(i^2 \, \phi_{i_1} \, w''_{j_1} + j^2 \, \phi''_{i_1} \, w_{j_1}) S_{ijm} \right.$$

$$\left. + 2\phi'_{i_1} \, w'_{j_1} \, ij \, C_{ijm} \right] \qquad \ldots \text{ I.9(a-b)}$$

$$L_m(\phi_{m_3}) = \frac{3E\pi^2}{a^2} \sum \sum \left[(w'_{i_1} \, w'_{j_2} + w'_{i_2} \, w'_{j_1}) ij \, C_{ijm} \right.$$

$$\left. + (w_{i_2} \, w''_{j_1} + w_{i_1} \, w''_{j_2}) i^2 \, S_{ijm} \right]$$

$$L_m(w_{m_3}) = 3\frac{h}{D} \cdot \frac{m^2\pi^2}{a^2}(\sigma_{x_1} w_{m_2} + \sigma_{x_2} w_{m_1})$$

$$- \frac{3h}{D} \cdot \frac{\pi^2}{a^2} \sum\sum \left[\left\{ i^2(\phi_{i_1} w''_{j_2} + \phi_{i_2} w''_{j_1}) + j^2(\phi''_{i_1} w_{j_2} + \phi''_{i_2} w_{j_1}) \right\} S_{ijm} \right.$$

$$\left. + 2ij(\phi'_{i_1} w'_{j_2} + \phi'_{i_2} w'_{j_1}) C_{ijm} \right]$$

. . . I.10(a-b)

Higher order equations may be set up in a similar way, but will not be shown here.

Solution of these equations together with the appropriate boundary conditions gives the buckling load and characteristics of the secondary path in the vicinity of the bifurcation. The solution of these sets of equations is discussed in section I.7.

I.6 Treatment of nonlinear boundary conditions I.7(a-b)

Of the boundary conditions I.7(a-h), the conditions I.7(d-h) are linear in 'w' and 'ϕ'. The equation I.7(c) can be replaced by the condition of compatibility of longitudinal strain which is a linear relationship in 'ϕ'. The conditions I.7(a-b) are nonlinear as 'v' is related to 'w' and 'ϕ' in the following manner:

$$\frac{\partial^2 v}{\partial x^2} = -\frac{1}{E}\left\{\frac{\partial^3 \phi}{\partial y^3} + (2+\nu)\frac{\partial^3 \phi}{\partial x^2 \partial y}\right\} - \frac{\partial^2 w}{\partial x^2} \cdot \frac{\partial w}{\partial y}$$

Taking 'v' in the form

$$v = v_m(y) \sin\frac{m\pi x}{a} \quad , \quad \text{we obtain}$$

$$v_m\left(\frac{m^2\pi^2}{a}\right) = \frac{1}{E}\{\phi'''_m - (2+\nu)\frac{m^2\pi^2}{a^2}\phi'_m\} - \frac{\pi^2}{a^2}\sum\sum i^2 w_i w'_j S_{ijm}$$

This nonlinear relationship must be reduced to a set of sequentially linear relationships by the perturbation technique and used in the formulation of boundary conditions.

I.7 Solution of perturbation equations

The first order equations are a set of homogeneous equations and give rise to an eigenvalue problem for the buckling stress $\sigma_{x_{cr}}$. Note that the equations corresponding to any 'm' are uncoupled from the rest so that the buckling mode is exclusively in terms of a single harmonic say 'n'. The differential equations are rendered algebraic by the use of a finite difference grid in the transverse direction. In order to obtain the values of ϕ_{m_1} and w_{m_1}, it is necessary to choose a path parameter ε, which may be one of the key displacement coefficients corresponding to the governing harmonic 'n'.

It is important to note that in the present formulation, the higher order equations for each harmonic 'm' are also uncoupled from the rest, so that they can be solved separately. This represents a considerable saving in computing effort.

Second order perturbation equations for the nth harmonic involve an additional unknown viz. σ_{x_1}. But one extra equation can be brought into play viz. $\varepsilon_2 = 0$.

The solution of the higher order system of equations is similar.

I.8 Postbuckling path in the immediate vicinity of bifurcation

The expressions for w and ϕ in the immediate vicinity of the bifurcation may be constructed using Taylor's series:

$$w = \sum \left(w_{m_1} \varepsilon + \frac{1}{2!} w_{m_2} \varepsilon^2 + \frac{1}{3!} w_{m_3} \varepsilon^3 \ \ldots\right) \sin m\pi\xi$$

$$\phi = \sum \left(\phi_{m_1} \varepsilon + \frac{1}{2!} \phi_{m_2} \varepsilon^2 + \frac{1}{3!} \phi_{m_3} \varepsilon^3 \ \ldots\right) \sin m\pi\xi$$

and $$\sigma_x = \sigma_{x_{cr}} + \sigma_{x_1} \varepsilon + \frac{1}{2!} \sigma_{x_2} \varepsilon^2 \ \ldots$$

I.9 Direct solution of nonlinear equations

In view of the possible inaccuracies in a solution based on the perturbation technique and the need for assessing the same, a solution based on a direct attack on the nonlinear problem represented by the equations I.5 and I.7 is desirable.

This has been done by the use of perturbation technique for prediction of increments in displacements for a given increment in the path parameter and Newton-Raphson correction. The procedure is fully explained in Ref. 92. However it must be noted that there occurs an interaction of all the harmonics in the solution process and as a result the computing effort is considerably increased.

I.10 Worked example

An example of a square box column solved using the analytical approach described herein, is now presented.

A square box column shown in Fig. I.C has been solved employing 5 nontrivial harmonics for both 'w' and 'ϕ' and 6 finite difference grid points on each half of the constituent plates (1) and (2). The variation of central deflection of the plate (1) with the applied stress is shown in Fig. I.C for three types of solution:

(i) The perturbation technique employing upto the 3rd order

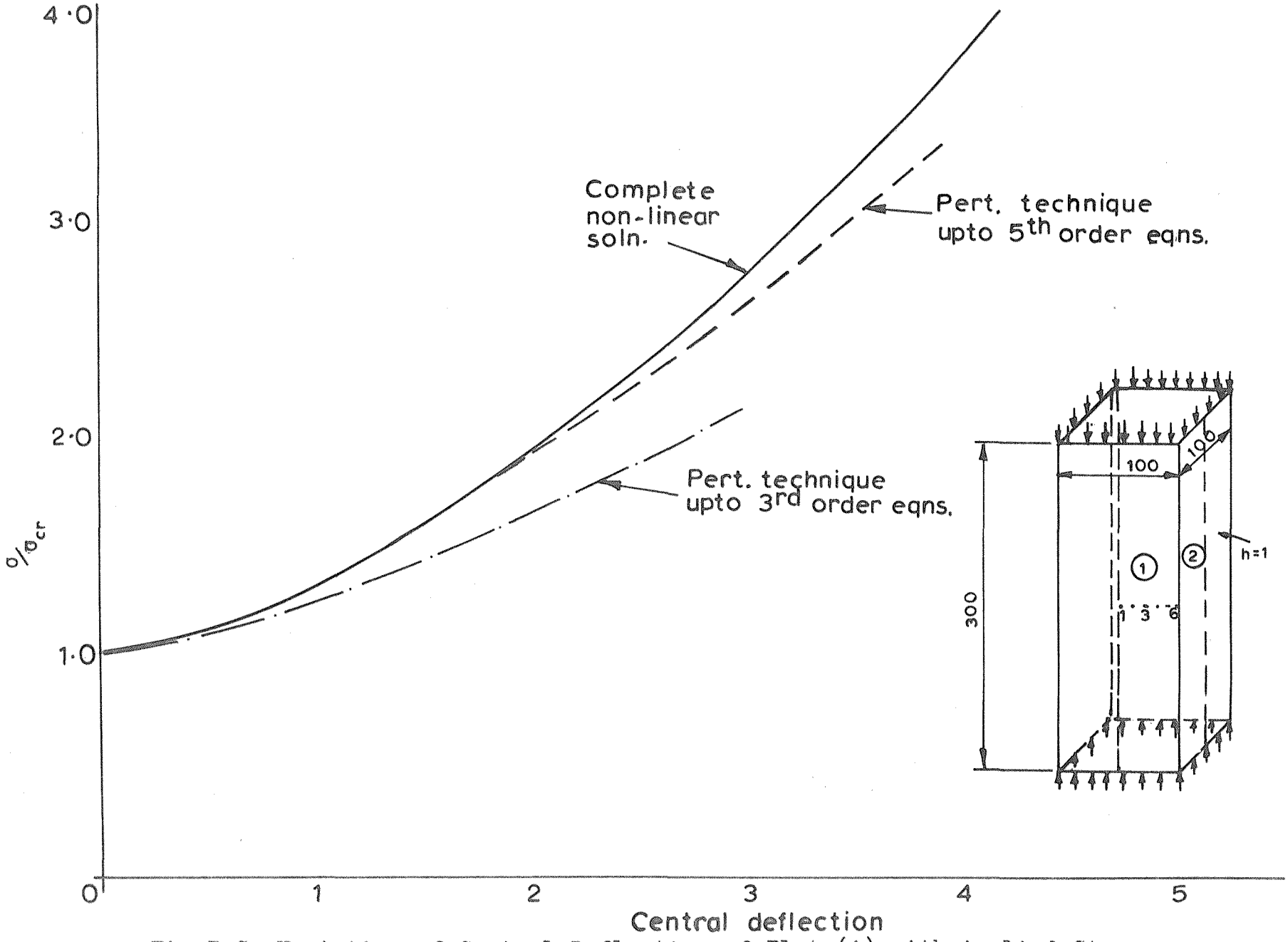

Fig.I.C. Variation of Central Deflection of Plate(1) with Applied Stress.

equations. The curvature at the centre of the column (1) was used as the perturbation parameter. This choice is based on the consideration that its rate of increase decreases with increasing deflection

(ii) The perturbation technique employing upto the 5th order equations, using the same perturbation parameter as in (i).

and (iii) The complete solution of the nonlinear equations governing the problem.

It is seen that the agreement between the solutions (ii) and (iii) are very satisfactory upto about $2\frac{1}{2}$ times the critical load.

APPENDIX II

TOTAL POTENTIAL ENERGY EXPRESSION FOR A STRIP FOR THE INITIAL BUCKLING ANALYSIS

Context: Sec. 2.2.3

Content: In this Appendix, an expression for the total potential energy W of a strip for the initial buckling analysis outlined in chapter 2, is presented.

Section 1. The expression takes the form:

$$W = \frac{Ehab}{2(1-\nu^2)} \{ -\nu e.v_{im}\,\chi_{im}$$

$$+ u_{im}\,u_{jn}\,\alpha_{ijmn} + v_{im}\,v_{jn}(\beta_{ijmn} - e\,\bar{\rho}_{ijmn})$$

$$+ u_{im}\,v_{jn}\,\gamma_{ijmn} + w^*_{rm}\,w^*_{sn}\,(\varepsilon_{rsmn} - e\,\rho_{rsmn})$$

$$+ u_{im}\,w^*_{rn}\,w^*_{sp}\,\psi_{irsmnp} + u_{im}\,v_{jn}\,v_{kp}\,\bar{\psi}_{ijkmnp}$$

$$+ v_{im}\,w^*_{rn}\,w^*_{sp}\,x_{irsmnp} + v_{im}\,v_{jn}\,v_{kp}\,\bar{x}_{ijkmnp} \}$$

$m,n,p = 1 \ldots M$

$i,j = 1,2$

$r,s = 1, \ldots 4$

Section 2. The summation convention has been used in the above expression. 'M' stands for the total number of harmonics considered in the solution. The displacement coefficients u_{im} and v_{im} have already been defined in chapter 2 and the coefficients w^*_{rm} are related to w_{im} and θ_{im} (already defined) in the following manner

$$w^*_{1m} = w_{1m}$$

$$w^*_{2m} = \theta_{1m}$$

$$w^*_{2m} = w_{2m}$$

$$w^*_{4m} = \theta_{2m}$$

The other terms are defined below:

$$\delta_{mn} = 1.0 \qquad (m = n)$$

$$= 0 \qquad (m \neq n)$$

$$\gamma_m = m\pi\beta/\alpha$$

$$\chi_{im} = \frac{2}{m\pi\beta}\left[1 - (-1)^m\right]A_i$$

$$\alpha_{ijmn} = \delta_{mn} \cdot \frac{1}{2}\left\{\left(\frac{m\pi}{\alpha}\right)\left(\frac{n\pi}{\alpha}\right) A^1_{ij} + \frac{(1-\nu)}{2\beta^2} A^2_{ij}\right\}$$

$$\beta_{ijmn} = \delta_{mn} \cdot \frac{1}{2}\left\{\frac{1}{\beta^2} A^2_{ij} + \frac{(1-\nu)}{2}\left(\frac{m\pi}{\alpha}\right)\left(\frac{n\pi}{\alpha}\right) A^1_{ij}\right\}$$

$$\gamma_{ijmn} = \delta_{mn} \cdot \frac{1}{2} \cdot \left(\frac{m\pi}{\alpha}\right) \cdot \frac{1}{\beta} \{-2\nu A^3_{ij} + (1-\nu)A^3_{ji}\}$$

$$\varepsilon_{ijmn} = \delta_{mn} \cdot \frac{1}{24} \cdot \frac{1}{\beta^4} \{B^2_{ij} - \gamma_m \gamma_n (B^4_{ij} + B^4_{ji}) + \gamma^2_m \gamma^2_n B^1_{ij}$$

$$+ (1-\nu) \gamma_m \cdot \gamma_n (B^4_{ij} + b^4_{ji} + 2B^3_{ij})\}$$

$$\rho_{ijmn} = \delta_{mn} \cdot \frac{1}{2}\left\{\left(\frac{m\pi}{\alpha}\right)\left(\frac{n\pi}{\alpha}\right) \cdot B^1_{ij} + \frac{\nu}{\beta^2} \cdot B^3_{ij}\right\}$$

$$\bar{\rho}_{ijmn} \quad \delta_{mn} \cdot \frac{1}{2}\left\{\left(\frac{m\pi}{\alpha}\right)\left(\frac{n\pi}{\alpha}\right) A^1_{ij} + \frac{\nu}{\beta^2} A^2_{ij}\right\}$$

$$\psi_{ijkmnp} = \left(\frac{m\pi}{\alpha}\right)\left(\frac{n\pi}{\alpha}\right)\left(\frac{p\pi}{\alpha}\right) I^1_{mnp}\, C^1_{ijk} + \nu\left(\frac{m\pi}{\alpha}\right)\frac{1}{\beta^2}\cdot I^3_{mnp}\, C^4_{ijk}$$

$$+ \frac{(1-\nu)}{2\beta^2}\left\{\left(\frac{p\pi}{\alpha}\right)\cdot I^5_{mnp}\, C^5_{ijk} + \left(\frac{n\pi}{\alpha}\right) I^5_{mpn}\, C^5_{ikj}\right\}$$

$$\bar{\psi}_{ijkmnp} = \left(\frac{m\pi}{\alpha}\right)\left(\frac{n\pi}{\alpha}\right)\left(\frac{p\pi}{\alpha}\right) I^1_{mnp}\, \bar{C}^1_{ijk} + \nu\left(\frac{m\pi}{\alpha}\right)\cdot\frac{1}{\beta^2} I^3_{mnp}\, \bar{C}^4_{ijk}$$

$$+ \frac{(1-\nu)}{2\beta^2}\left\{\left(\frac{p\pi}{\alpha}\right) I^5_{mnp}\, \bar{C}^5_{ijk} + \left(\frac{n\pi}{\alpha}\right) I^5_{mpn}\, \bar{C}^5_{ikj}\right\}$$

$$x_{ijkmnp} = \frac{1}{\beta^3}\cdot I^2_{mnp}\, C^2_{ijk} + \frac{\nu}{\beta}\cdot\left(\frac{n\pi}{\alpha}\right)\left(\frac{p\pi}{\alpha}\right) I^4_{mnp}\, C^3_{ijk}$$

$$+ \frac{(1-\nu)}{2\beta}\cdot\left(\frac{m\pi}{\alpha}\right)\left\{\left(\frac{p\pi}{\alpha}\right)\cdot I^6_{mnp}\, C^6_{ijk} + \left(\frac{n\pi}{\alpha}\right) I^6_{mpn}\, C^6_{ikj}\right\}$$

$$\bar{x}_{ijkmnp} = \frac{1}{\beta^3}\cdot I^2_{mnp}\, C^2_{ijk} + \frac{\nu}{3\beta}\{F_{mnpijk} + F_{npmjki} + F_{pmnkij}\}$$

$$\text{where } F_{mnpijk} = \left\{\left(\frac{n\pi}{\alpha}\right)\left(\frac{p\pi}{\alpha}\right)\cdot I^4_{mnp}\, \bar{C}^3_{ijk} + (1-\nu)\left(\frac{m\pi}{\alpha}\right)\left(\frac{p\pi}{\alpha}\right) I^6_{mnp}\, \bar{C}^6_{ijk}\right\}$$

Section 3. In the foregoing,

$$A_i = \int_0^1 f_i'\, d\eta$$

$$\{A^1_{ij} \quad A^2_{ij} \quad A^3_{ij}\} = \int_0^1 \{f_i f_j \quad f_i' f_j' \quad f_i f_j'\}\, d\eta$$

$$\{B^1_{ij} \quad B^2_{ij} \quad B^3_{ij} \quad B^4_{ij}\} = \int_0^1 \{\phi_i\phi_j \quad \phi_i''\phi_j'' \quad \phi_i'\phi_j' \quad \phi_i''\phi_j\}\, d\eta$$

$$\{C^1_{ijk} \quad C^2_{ijk} \quad C^3_{ijk} \quad C^4_{ijk} \quad C^5_{ijk} \quad C^6_{ijk}\} = \int_0^1 \{f_i\phi_j\phi_k \quad f'_i\phi'_j\phi'_k \quad f'_i\phi_j\phi_k \quad f_i\phi'_j\phi'_k \quad f'_i\phi'_j\phi_k \quad f_i\phi'_j\phi_k\}d\eta$$

$$\{\bar{C}^1_{ijk} \quad \bar{C}^2_{ijk} \quad \bar{C}^3_{ijk} \quad \bar{C}^4_{ijk} \quad \bar{C}^5_{ijk} \quad \bar{C}^6_{ijk}\} = \int_0^1 \{f_if_jf_k \quad f'_if'_jf'_k \quad f'_if_jf_k \quad f_if'_jf'_k \quad f'_if'_jf_k \quad f_if'_jf_k\}d\eta$$

$$I^2_{mnp} = -I^3_{mnp} = \int_0^1 \sin m\pi\xi \cdot \sin n\pi\xi \cdot \sin p\pi\xi \, d\eta$$

$$I^4_{mnp} = -I^1_{mnp} = \int_0^1 \sin m\pi\xi \cdot \cos n\pi\xi \cdot \cos p\pi\xi \, d\eta$$

$$I^6_{mnp} = I^5_{mnp} = \int_0^1 \cos m\pi\xi \cdot \sin n\pi\xi \cdot \cos p\pi\xi \, d\eta$$

wherein

$$\{f_1 \quad f_2\} = \{1-\eta \quad \eta\}$$

$$\{\phi_1 \quad \phi_2 \quad \phi_3 \quad \phi_4\} = \{1-3\eta^2+2\eta^3 \quad \eta-2\eta^2+\eta^3 \quad 3\eta^2-2\eta^3 \quad -\eta^2+\eta^3\}$$

and dashes denote differentiation with respect to η , e.g.

$$\phi'_i = \frac{\partial\phi_i}{\partial\eta} \quad , \quad \phi''_i = \frac{\partial^2\phi_i}{\partial\eta^2}$$

APPENDIX III

DETAILS OF THE COMPUTER PROGRAMME FOR THE INITIAL BUCKLING ANALYSIS

Context: Sec. 2.2.6

Content: Details of the computer programme for the initial buckling analysis of plate assemblies taking into account the pre-buckling stress distribution are described.

Description: The programme will be described in three sections (i) Input data (ii) Scheme of Computation and (iii) Output

(i) Input data

Number of strips

Number of local degrees of freedom per harmonic

Number of global degrees of freedom in the prebuckling analysis at a time

Semi bandwidth of stiffness matrix for the prebuckling analysis at a time

Number of boundary conditions for the prebuckling analysis at a time

Number of harmonics in the prebuckling analysis

Number of harmonics entering the description of the buckling mode

Number of global degrees of freedom in the stiffness matrix for the buckling analysis

Index which indicates whether the structure carries an axial compression, transverse loading or a combination of both

Length of the plate structure

Width and thickness, orientation of each strip

The global degrees of freedom corresponding to the local degrees of freedom associated with each strip in both the stages of analysis

The actual integers (which enter into the arguments of the trigonometric terms in the displacement functions) corresponding to each of the harmonics in both the stages of analysis

The numbers of the global degrees of freedom which vanish by virtue of boundary conditions in each stage of the analysis

In the case of transverse loading, external load vector, in terms of Fourier coefficients corresponding to unit load

In the case of combined loading, the ratio of axial load to lateral load

Young's Modulus and Poisson's ratio of the material

(ii) Scheme of computation

Preliminary: Calculation of the integrals A_i, A_{ij}, B_{ij}, C_{ijk}, D_{ijk}, I_{mnp} etc. (Ref. Appendix II)

Prebuckling analysis:

(1) Build stiffness matrices for each of the strips for the prebuckling analysis for the first harmonic

(2) If axial compression is present, build the equivalent load vector given rise to by axial compression for the first harmonic

(3) Transform the element stiffness matrices, and the load vector in (2) to the global system

(4) Assemble the transformed element stiffness matrices to form the global stiffness matrix

(5) Assemble the transformed equivalent load vector in (3) to form the global vector of nodal forces given rise to by axial compression

(6) Add to the global load vector in (5) to the vector of applied lateral loading if any

(7) Solve the system of equations to obtain the displacements corresponding to unit axial load (or lateral load)

(8) Repeat the steps (1) to (7) for each of the harmonics

Buckling Analysis:

(1) Build the stiffness matrix governing the linear problem for all the harmonics entering into the description of the buckling mode, taken together $[A_{ij}]$

(2) Build the stiffness matrix $[B_{ij} + \nu C_{ij} - A_{ijk} q_{k_1}]$ which incorporates the destabilising influence or axial compression and the effects of prebuckling stresses for unit axial compression (or lateral load)

(3) Transform the matrices in (1) and (2) and assemble them to form the corresponding global stiffness matrices $[A]$ and $[B]$

(4) Determine the eigenvalues and vectors of the eigen problem in the form $\{[A] - e [B]\} = \{0\}$

(5) Obtain the stress distribution corresponding to the lowest eigenvalue.

(iii) Output

The buckling load (axial compression or lateral load)

The buckling mode in terms of the global degrees of freedom

The longitudinal stress distribution at various sections of the plate assembly at the onset of buckling.

APPENDIX IV

COMPARISON OF THE COMPUTING EFFORT INVOLVED IN THE FINITE ELEMENT AND STRIP SOLUTIONS

Context: Sec. 2.3.4

Content: A comparison of the computing efforts involved in the finite element and finite strip solutions of the problem of a plate carrying inplane patch loading is made.

As stated in sec. 2.3.3, the problem of the square plate carrying inplane patch loading, with C/B = 0.2, has been solved by Rockey and Bagchi[14] by the finite element technique. The results obtained using the finite strip approach are shown in Fig. 2.17. Comparison of the two sets of results shows that in order to obtain a solution within error of 1%, the finite element solution requires 48 elements (say 8 depthwise and 6 breadthwise) over half the plate, whereas the strip method requires 8 strips and 2 harmonics to describe the buckling mode.

In the case of a plate carrying inplane loading, the prebuckling state is described by inplane displacements u and v alone and w = 0; on the other hand the buckling mode is described entirely by 'w', as it is greater than 'u' and 'v' by an order of magnitude. Thus for each part of the analysis, (prebuckling and buckling) only two degrees of freedom along each edge (nodal line) per harmonic need be taken into consideration. On this basis, a comparison of the computing efforts can be made for each stage of the analysis as shown in the following tables.

Table II.A:Prebuckling Analysis

Finite Element Method

No. of elements	No. of nodes	Degrees of freedom per node	Total No. of unknowns N	Semi-band -width B
8 depthwise 6 breadthwise	(8+1)×(6+1) = 63	2	126	9×2 = 18

Finite Strip Method

No. of Strips	No. of nodal lines	Degrees of freedom per nodal line /harmonic	Total no. of unknowns N/harmonic	Semi-band-width B
8	(8+1) = 9	2	18	4

Total no. of harmonics = 15

Note: Computing effort C may be taken to be proportional to the NB^2.

Thus $$\frac{C_{FSM}}{C_{FEM}} = \frac{18 \times 4^2 \times 15}{126 \times 18^2} \simeq \underline{0.11}$$

i.e. the finite strip solution requires about 11% of the computing effort for the finite element solution for the prebuckling analysis. It must be noted that the computing effort required for the prebuckling analysis is only a small fraction of that required by the second part of the analysis which involves solution of the eigenvalue problem and therefore the following comparative study on this aspect is of far greater relevance.

TableII.B: Buckling Analysis

Finite Element Solution

No. of elements	No. of Nodes	Degrees of freedom per node	Total no. of unknowns N	Semi-band-width
8 depthwise 6 breadthwise	(8+1)×(6+1) = 63	3	189	27

Finite Strip Solutions

No. of Strips	No. of nodal lines	Degrees of freedom/ nodal line (two harmonics)	Total no. of unknowns	Semi-band -width
8	9	2×2 = 4	36	8

Note: Following Ref. 103, the computing effort in the determination of finding the eigenvalues and vectors is proportional to the cube of the total number of unknowns, so that

$$\frac{C_{FSM}}{C_{FEM}} = \left(\frac{36}{189}\right)^3 \simeq 0.007$$

Thus the computing effort involved in the strip method is less than 1% of that in the finite element method.

APPENDIX V

MATHEMATICAL BASIS OF THE CHOICE OF THE TERMS IN 'u' and 'v' IN VERSION I OF THE FINITE STRIP METHOD

Context: Sec. 3.2.1.2

Content: Sec. 3.2.1.2 describes the manner of choosing the trigonometric terms in the functions to describe 'u' and 'v' for a given function for 'w' in version I of the finite strip method. The mathematical reasoning underlying this procedure is set forth.

Let $$w = w_m(y) \sin \frac{m\pi x}{a} \qquad \ldots \text{(i)}$$

$$(m = i_1, i_2, \ldots i_n)$$

where $i_1, i_2 \ldots i_n$ are integers.

von Karman compatibility equation relating the stress function 'ϕ' and 'w' reads:

$$\nabla^4 \phi = E \left[\left(\frac{\partial^2 w}{\partial x \partial y} \right)^2 - \frac{\partial^2 w}{\partial x^2} \cdot \frac{\partial^2 w}{\partial y^2} \right] \qquad \ldots \text{(ii)}$$

Substituting (i) in the expression on the right hand side of (ii) and rearranging, it can be expressed in the form

$$F_{i+j}(y) \cos \left[(i+j)\frac{\pi x}{a} \right] + F_{i-j}(y) \cos \left[(i-j)\frac{\pi x}{a} \right]$$

$$(i = 1, \ldots i_n$$

$$j = 1, \ldots i_n)$$

The terms containing 'y' in the brackets, throughout this discussion, represent appropriate functions of 'y'.

A solution for 'ϕ' may therefore be taken in the form

$$\phi = \phi_{i+j}(y)\ \cos\left[(i+j)\frac{\pi x}{a}\right] + \phi_{i-j}(y)\ \cos\left[(i-j)\frac{\pi x}{a}\right]$$

$$+ A_2 y^2 + A_3 y^3 \qquad \ldots \text{(iii)}$$

satisfying the conditions

$$\tau_{xy}\Big|_{\substack{x=o\\x=a}} = 0 \quad , \quad \frac{\partial^2\phi}{\partial x^2}\Big|_{\substack{x=o\\x=a}} = 0$$

The middle surface strain components ε_x, ε_y and γ_{xy} are related to 'ϕ' in the following manner

$$\varepsilon_x = \frac{1}{E}\left\{\frac{\partial^2\phi}{\partial y^2} - \nu\frac{\partial^2\phi}{\partial x^2}\right\}$$

$$\varepsilon_y = \frac{1}{E}\left\{\frac{\partial^2\phi}{\partial x^2} - \nu\frac{\partial^2\phi}{\partial y^2}\right\}$$

$$\gamma_{xy} = -\frac{1}{G}\frac{\partial^2\phi}{\partial x\partial y} \qquad \ldots \text{(iv)(a-c)}$$

Substituting (iii) in (iv), each of the strain components can be expressed in the form:

$$\varepsilon_x = A_2' + A_3' y + \varepsilon_{x_{i+j}}(y)\ \cos\left[(i+j)\frac{\pi x}{a}\right] + \varepsilon_{x_{i-j}}(y)\ \cos\left[(i-j)\frac{\pi x}{a}\right]$$

$$\varepsilon_y = -\nu(A_2'+A_3'y) + \varepsilon_{y_{i+j}}(y)\cos\left[(i+j)\frac{\pi x}{a}\right] + \varepsilon_{y_{i-j}}(y)\cos\left[(i-j)\frac{\pi x}{a}\right]$$

and

$$\gamma_{xy} = \gamma_{i+j}(y)\ \sin\left[(i+j)\frac{\pi x}{a}\right] + \gamma_{i-j}(y)\ \sin\left[(i-j)\frac{\pi x}{a}\right] .$$

$$\ldots \text{(v)(a-c)}$$

where A_2', and A_3' are appropriate constants.

Since

$$\varepsilon_x = \frac{\partial u}{\partial x} + \frac{1}{2}\left(\frac{\partial w}{\partial x}\right)^2 ,$$

$$\frac{\partial u}{\partial x} = A_2' + A_3' y + \bar{u}_{i+j} \cos\left[(i+j)\frac{\pi x}{a}\right] + \bar{u}_{i-j}(y) \cos\left[(i-j)\frac{\pi x}{a}\right]$$

Integrating,

$$u = A_1' x + A_3' yx + A_4 + u_{i+j}(y)\sin\left[(i+j)\frac{\pi x}{a}\right] + u_{i-j}(y) \sin\left[(i-j)\frac{\pi x}{a}\right] \quad \ldots \text{(vi)}$$

where A_4 is an arbitrary constant.

Again,

$$\varepsilon_y = \frac{\partial v}{\partial y} + \frac{1}{2}\left(\frac{\partial w}{\partial y}\right)^2$$

so that $\frac{\partial v}{\partial y} = -\nu(A_2' + A_3' y) + \bar{v}_{i+j}(y) \cos\left[(i+j)\frac{\pi x}{a}\right] + \bar{v}_{i-j}(y) \cos\left[(i-j)\frac{\pi x}{a}\right]$

Integrating

$$v = -\nu(A_2' y + A_3' \frac{y^2}{2}) + A_5 + f(x) + v_{i+j}(y) \cos\left[(i+j)\frac{\pi x}{a}\right] + v_{i-j}(y) \cos\left[(i-j)\frac{\pi x}{a}\right] \quad \ldots \text{(vii)}$$

where A_5 is an arbitrary constant.

Substituting (vi) and (vii) into the expression for γ_{xy}, which is

$$\gamma_{xy} = \frac{\partial u}{\partial x} + \frac{\partial v}{\partial y} + \frac{\partial w}{\partial x} \cdot \frac{\partial w}{\partial y}$$

and making use of (v)(c), we obtain

$$A_3'x + f'(x) = 0 \ , \quad \text{so that}$$

$$f(x) = \tfrac{1}{2}A_3'x^2 + C$$

where 'C' is an arbitrary constant.

Considering the case of uniform end compression $A_3' = 0$. In this case the functions 'u' and 'v' take the form:

$$u = A_2'x + A_4 + u_{i+j}(y) \sin\left[(i+j)\frac{\pi x}{a}\right] + u_{i-j}(y) \sin\left[(i-j)\frac{\pi x}{a}\right]$$

$$v = -\ A_2'y + A_5 + v_{i+j}(y) \cos\left[(i+j)\frac{\pi x}{a}\right] + v_{i-j}(y) \cos\left[(i-j)\frac{\pi x}{a}\right] \quad \ldots \text{(viii)(a-b)}$$

The constants A_4 and A_5 are so chosen as to fix the plate in space in any given position. The term A_2' corresponds to 'e' the average strain of the plate.

The trigonometric terms in (viii) are the most relevant terms for the present discussion. It is seen that the functions for 'u' and 'v' include all the trigonometric terms corresponding to (i+j) and (i-j) where i and j are any two of the integers entering into the arguments of the trigonometric terms in the description of 'w'.

APPENDIX VI

AN EXPRESSION OF STRAIN ENERGY OF A STRIP FOR THE POST LOCAL BUCKLING ANALYSIS - VERSION I

Context: Sec. 3.2.1.3

Content: In this Appendix, an expression for the strain energy U of a strip, required in the post-local-buckling analysis of plate assemblies, using Version I (case (i) and (ii)) of the finite strip method as developed in chapter 3, is presented.

Section 1. The expression takes the form:

$$U = \frac{Ehab}{2(1-\nu^2)} \sum_{1}^{8} T_n$$

where

$T_1 = 0$ for case (i)

$= -\nu e\, v_{im}\, \chi_{im}$ $\quad \begin{cases} m = 1, \ldots M_v \\ i = 1,2 \end{cases}$

for case (ii)

$T_2 = u_{im} u_{jn} \alpha_{ijmn}$ $\quad \begin{cases} m,n = 1, \ldots M_u \\ i,j = 1,2 \end{cases}$

$T_3 = v_{im} v_{jn} \beta_{ijmn}$ $\quad \begin{cases} m,n = 1, \ldots M_v \\ i,j = 1,2 \end{cases}$

$T_4 = u_{im} v_{jn} \gamma_{ijmn}$ $\quad \begin{cases} m = 1, \ldots M_u \\ n = 1, \ldots M_v \\ i,j = 1,2 \end{cases}$

$$T_5 = w^*_{im}\, w^*_{jn}\left[\varepsilon_{ijmn} - e\,\rho_{ijmn}\right] \qquad \begin{matrix} m,n = 1, \ldots M_w \\ i,j = 1, \ldots 4 \end{matrix}$$

$$T_6 = u_{im}\, w^*_{jn}\, w^*_{kp}\, \psi_{ijkmnp} \qquad \begin{matrix} m = 1, \ldots M_u \\ n,p = 1, \ldots M_w \\ i = 1,2 \\ j,k = 1, \ldots 4 \end{matrix}$$

$$T_7 = v_{im}\, w^*_{jn}\, w^*_{kp}\, x_{ijkmnp} \qquad \begin{cases} m = 1, \ldots M_v \\ n,p = 1, \ldots M_v \\ i = 1,2 \\ j,k = 1, \ldots 4 \end{cases}$$

$$T_8 = w^*_{im}\, w^*_{jn}\, w^*_{kp}\, w^*_{\ell q}\, \lambda_{ijk\ell mnpq} \qquad \begin{cases} m,n,p,q = 1, \ldots M_w \\ i,j,k,\ell = 1, \ldots 4 \end{cases}$$

Section 2. In the above, M_u, M_v and M_w represent the total number of terms in the displacement functions for 'u', 'v' and 'w' respectively. The other terms are defined in the following:-

$$\chi_{im} = -\frac{2\nu e}{\beta} \cdot A_i \qquad (m^v = 0)$$

$$= 0 \qquad (m \neq 0)$$

$$\alpha_{ijmn} = \delta_{m^u n^u} \cdot \frac{1}{2}\left\{\left(\frac{m^u \pi}{\alpha}\right)\left(\frac{n^u \pi}{\alpha}\right) A^1_{ij} + \frac{(1-\nu)}{2\beta^2} A^2_{ij}\right\}$$

$$\beta_{ijmn} = \delta_{m^v n^v} \cdot \frac{1}{2}\left\{\frac{1}{\beta^2} \cdot A^2_{ij} + \frac{(1-\nu)}{2}\left(\frac{m^v \pi}{\alpha}\right)\left(\frac{n^v \pi}{\alpha}\right) A^1_{ij}\right\}$$

$$(m^v \neq 0)$$

$$= \delta_{m^v n^v} \cdot \frac{1}{\beta^2} A^2_{ij} \qquad (m^v = 0)$$

$$\gamma_{ijmn} = \delta_{m^u n^v} \cdot \frac{1}{2}\left(\frac{m^u \pi}{\alpha}\right) \cdot \frac{1}{\beta}\left\{2\nu A^3_{ij} - (1-\nu) A^3_{ji}\right\}$$

$$\varepsilon_{ijmn} = \delta_{m^w n^w} \cdot \frac{1}{24\beta^4} \cdot \{B^2_{ij} - \gamma_{m^w}\gamma_{n^w}(B^4_{ij} + B^4_{ji})$$

$$+ \gamma^2_{m^w}\gamma^2_{n^w} B^1_{ij} + (1-\nu)\gamma_{m^w}\gamma_{n^w}(B^4_{ij} + B^4_{ji} + 2B^3_{ij})\}$$

$$\rho_{ijmn} = \tfrac{1}{2}\delta_{m^w n^w}(1-\nu^2) \cdot \left(\frac{m^w\pi}{\alpha}\right)\left(\frac{n^w\pi}{\alpha}\right) B^1_{ij} \qquad \text{in case (i)}$$

$$= \tfrac{1}{2}\delta_{m^w n^w}\left[\left(\frac{m^w\pi}{\alpha}\right)\left(\frac{n^w\pi}{\alpha}\right) B^1_{ij} + \frac{\nu}{\beta^2} B^3_{ij}\right] \qquad \text{in case (ii)}$$

$$\psi_{ijkmnp} = \left(\frac{m^u\pi}{\alpha}\right)\left(\frac{n^w\pi}{\alpha}\right)\left(\frac{p^w\pi}{\alpha}\right) I^1_{m^u n^w p^w} C^1_{ijk}$$

$$+ \nu\left(\frac{m^u\pi}{\alpha}\right) \frac{1}{\beta^2} I^3_{m^u n^w p^w} C^4_{ijk}$$

$$+ \frac{(1-\nu)}{2\beta^2}\left\{\left(\frac{p^w\pi}{\alpha}\right) I^5_{m^u n^w p^w} C^5_{ijk} + \left(\frac{n^w\pi}{\alpha}\right) I^5_{m^u p^w n^w} C^5_{ikj}\right\}$$

$$x_{ijkmnp} = \frac{1}{\beta^3} I^2_{m^v n^w p^w} C^2_{ijk} + \frac{\nu}{\beta}\left(\frac{n^w\pi}{\alpha}\right)\left(\frac{p^w\pi}{\alpha}\right) I^4_{m^v n^w p^w} C^3_{ijk}$$

$$+ \frac{(1-\nu)}{2\beta}\left(\frac{m^v\pi}{\alpha}\right)\left\{\left(\frac{p^w\pi}{\alpha}\right) I^6_{m^v n^w p^w} C^6_{ijk} + \left(\frac{n^w\pi}{\alpha}\right) I^6_{m^v p^w n^w} C^6_{ikj}\right\}$$

$$\lambda_{ijk\ell mnpq} = \frac{1}{4}\left\{m^w n^w p^w q^w \frac{\pi^4}{\alpha^4} \cdot J^1_{m^w n^w p^w q^w} D^1_{ijk\ell}\right.$$

$$+ \frac{1}{\beta^4} J^2_{m^w n^w p^w q^w} D^2_{ijk\ell}$$

$$+ \frac{1}{6}\left[F_{mnpqijk\ell} + F_{mpnqikj\ell} + F_{mqnpi\ell jk}\right.$$

$$\left.\left. + F_{npmqjki\ell} + F_{nqmpj\ell ik} + F_{pqmnk\ell ij}\right]\right\}$$

where $F_{mnpqijk\ell} = \dfrac{2}{\beta^2}\left(\dfrac{m^w\pi}{\alpha}\right)\left(\dfrac{n^w\pi}{\alpha}\right) J^3_{mnpq} D^3_{ijk\ell}$

Section 3. In the above:

1. m^u, m^v, m^w represent integers occurring in the argument of the trigonometric function in the mth term in the series for u, v and w respectively.

2. $$\{D^1_{ijk\ell} \quad D^2_{ijk\ell} \quad D^3_{ijk\ell}\} = \int_0^1 \{\phi_i\phi_j\phi_k\phi_\ell \quad \phi_i'\phi_j'\phi_k'\phi_\ell' \quad \phi_i\phi_j\phi_k'\phi_\ell'\}d\eta$$

3. $$\{I^1_{mnp} \quad I^3_{mnp} \quad I^5_{mnp}\} = \int_0^1 \{C_mC_nC_p \quad C_mS_nS_p \quad C_mS_nC_p\}\, d\xi$$

$$= \{I^4_{mnp} \quad I^2_{mnp} \quad I^6_{mnp}\}$$

$$\{J^1_{mnpq} \quad J^2_{mnpq} \quad J^3_{mnpq}\} = \int_0^1 \{C_mC_nC_pC_q \quad S_mS_nS_pS_q \quad C_mC_nS_pS_q\}\, d\xi$$

(where $C_m = \cos m\pi\xi$, $S_m = \sin m\pi\xi$)

All the other terms (not defined in this Appendix) have the same meaning as in Appendix II.

APPENDIX VII

DETAILS OF THE COMPUTER PROGRAMMS PLAPAV 1 AND PLAPAV2

Context: Sec. 3.2.1.8

Contents: In this Appendix is described the computer programmes entitled "PLAPAV1" and "PLAPAV2" for the post-local-buckling analysis of plate assemblies using Version I and II respectively of the finite strip method, as developed in chapter 3.

I Description of PLAPAV1:

The programme is described in three sections: (i) Input data (ii) General scheme of the computation (iii) Computer output.

1. Input data:

Number of terms in the displacement functions of u, v and w;

Number of strips;

Number of local degrees of freedom;

Number of global degrees of freedom;

Semi-bandwidth of the stiffness matrix;

Number of boundary conditions;

Length of the plate assembly, width and thickness of each strip;

The integers (m_u, m_v, m_w) entering into the argument of trigonometric terms in the displacement functions of u, v and w;

The number corresponding to each of the degrees of freedom which vanishes by virtue of boundary conditions;

The number of the global degree of freedom which is to be used as a path parameter in the perturbation solution (Number corresponding to Q_r);

The number of independent quartic terms (Ref. Table 4.1) in the solution;

The number of steps in which the solution is to be traced;

The value of $e_{cr}(\sigma_{cr}/E)$; the value of $Q_r(\varepsilon)$ to be used in the solution using perturbation technique; the magnitude of increment of 'e' in each step for tracing the postbuckling equilibrium path.

2. Scheme of computation

(i) Preliminary: Calculate the integrals A_i, A_{ij}, B_{ij}, C_{ijk}, D_{ijk} I_{mnp}, J_{mnpq}

(ii) Perturbation

Solution: (1) Build stiffness matrices for the strips with the displacements $u = v = w = 0$ and $e = e_{cr}$.

(2) Assemble the stiffness matrices to form the global stiffness matrix; apply boundary conditions

(3) Making use of $Q_{r_1} = 1$, obtain the buckling mode.

(4) Build the right hand side of the second order equations

(5) Using the contraction mechanism obtain the value of e_1; with $Q_{r_2} = 0$, solve the 2nd order equations (Note, however, $e_1 = 0$ for version I)

(6) Build the right hand side of the third order equations

(7) Using the "Contraction Mechanism", obtain e_2

(8) With $Q_{r_3} = 0$, solve the 3rd order equations

(9) With $Q_r = \varepsilon$, obtain the value of 'e' and those of the local degrees of freedom.

(iii) Tracing the postbuckling equilibrium path

Prediction of the displacements for a given increment in 'e':

(1) Build the incremental stiffness matrix for each strip with the values of u, v, w and e and the vector of incremental forces for unit increment in 'e'

(2) Assemble the stiffness matrices in (1) to obtain the global stiffness matrix and the vector of incremental forces of the strips to form the right hand side of the system of 'incremental' equations. Apply the boundary conditions.

(3) Solve the system of equations to obtain the increments in the values of the degrees of freedom for a chosen increment in 'e'.

Correction of the displacements using Newton Raphson iterations.

(4) Build the incremental stiffness matrix and the vector of edge forces for each strip with the new values of displacements and 'e'

(5) Assemble the stiffness matrices in (4) to obtain the global stiffness matrix and the vector of the edge forces to obtain the vector of global unbalanced forces. Apply the boundary conditions

(6) Obtain the corrections by solving the system of equations given by (5)

(7) Obtain the improved values of displacements and repeat steps (4) to (6) till satisfactory convergence of the solution is obtained

(8) At the end of each step obtain the stresses at various sections of the plate structure

(9) Repeat steps 1-8 for the given number of steps.

3. Output

The buckling mode in terms of the displacements.

The solutions of perturbation displacements as given by the second and third order equations and the value of 'e_2'

The values of 'e', the degrees of freedom, the longitudinal stresses at various sections across the plate assembly and their integrated value at the end of each step.

II Description of PLAPAV2

The details are the same as for PLAPAV1 except for the scheme of computation which includes a preliminary analysis of the prebuckling state of equilibrium.

Scheme of computation:

Preliminary: Calculate the integrals A_i, A_{ij}, B_{ij}, C_{ijk}, $D_{ijk\ell}$, I_{mnp}, J_{mnpq}

Prebuckling solution:

(i) Build the stiffness matrices for the strips with the displacements $u = w = w = 0$ and $e = 0$, and the vector of edge forces with $e_1 = 1$

(ii) Assemble the stiffness matrices to form the global stiffness matrix and the vector of edge forces to obtain the right hand side of the system of equations. Apply the boundary conditions

(iii) Solve the system of equations to obtain the prebuckling displacements u_p, v_p and w_p for $e_1 = 1$ and thus for $e = e_{cr}$.

(v) Build the stiffness matrix for each of the strips with the values of prebuckling buckling displacements at $e = e_{cr}$

and the vector of incremental forces for unit increment in e.

The rest of the procedure is the same as for PLAPAV1.

APPENDIX VIII

AN EXPRESSION OF STRAIN ENERGY OF A STRIP FOR THE POST-LOCAL-BUCKLING ANALYSIS - VERSION II

Context: Sec. 3.2.2.3

Content: In this Appendix, an expression for the strain energy U of a strip, required in the post-local-buckling analysis of plate assemblies, using Version II of the finite strip method as developed in chapter 3, is presented.

The expression takes the same form as for Version I given in Appendix VI but for the following changes in definition of the terms.

Changes in Section 1.

$$T_1 = -\nu e \; v_{im} \; \chi_{im} \qquad \begin{cases} m = 1, \ \ldots \ M_v \\ i = 1,2 \end{cases}$$

Changes in Section 2.

$$\chi_{im} = -\frac{2\nu e}{m\pi\beta} \{1 - (-1)^{m^v}\}.A_i$$

$$\gamma_{ijmn} = \frac{1}{\beta}\left\{2\nu\left(\frac{m^u\pi}{\alpha}\right) \; \mu_{m^u n^v} \; A^3_{ij} + (1-\nu)\left(\frac{n^v\pi}{\alpha}\right) \; \mu_{n^v m^u} \; A^3_{ji}\right\}$$

$$\text{where } \mu_{mn} = \int_0^1 \cos m\pi\xi \,.\, \sin n\pi\xi \; d\xi$$

Changes in Section 3.

$$\{ I^1_{mnp} \quad I^2_{mnp} \quad I^3_{mnp} \quad I^4_{mnp} \quad I^5_{mnp} \quad I^6_{mnp} \}$$

$$\int_0^1 \{C_m C_n C_p \quad S_m S_n S_p \quad C_m S_n S_p \quad S_m C_n C_p \quad S_m S_n C_p \quad C_m S_n C_p \}d\xi$$

Section 4.

The following additional term (U_A) must be included in the strain energy expression, if it is necessary to take into account, as proposed in sec. 5.2 (Chapter 5), the destabilising influence of the inplane displacement 'v'.

$$U_A = -\delta_{mn} \cdot \frac{Ehabe}{2} \left\{ \left(\frac{m v_\pi}{\alpha}\right) \left(\frac{n v_\pi}{\alpha}\right) \cdot A^1_{ij} \right\} v_{m_i} v_{n_j}$$

(in the notation of Appendix VI).

APPENDIX IX

OPERATIONS ON AN EXPANSION OF THE TYPE $A_{ijk\ell}\, q_i q_j q_k q_\ell$ USING ONLY INDEPENDENT TERMS

Context: Art 3.3

Contents: A simplified algorithm to perform certain operations e.g. obtaining the first derivative of certain terms in the strain energy expression with respect to q_r, making use of only independent terms, is described. These operations are found to be necessary for computing the edge forces and the elements of stiffness matrices from the strain energy expression.

Consider an expansion of the type

$$U^* = A_{ijk\ell}\, q_i q_j q_k q_\ell \qquad i,j,k,\ell = 1, \ldots N$$

which occurs in the strain energy expression given in Appendix V.

The terms in the expansion can be divided into the following five groups

(i) $q_i q_j q_k q_\ell$ with i,j,k,ℓ all different from each other

(ii) $q_i^2 q_j q_k$ with i,j,k all different from each other

(iii) $q_i^2 q_j^2$ $(i \neq j)$

(iv) $q_i^3 q_j$ $(i \neq j$

(v) q_i^4

In order to obtain the value of the functions

$$\frac{\partial U^*}{\partial q_i} \qquad (i = 1, \ldots N)$$

and

$$\frac{\partial^2 U^*}{\partial q_i \partial q_j} \qquad (i,j = 1, \ldots N)$$

(which occur the expressions of edge forces and the elements of stiffness matrix respectively)

We may take up terms in each of the groups (i) to (v) separately.

It may be noted that the terms in group (i) repeat themselves 24 times each, those in group (ii) 12 times, those in group (iii) 6 times, those in group (iv) 4 times and finally those in (v) only once. A computational scheme that may be adopted to obtain the derivatives is given in the following:-

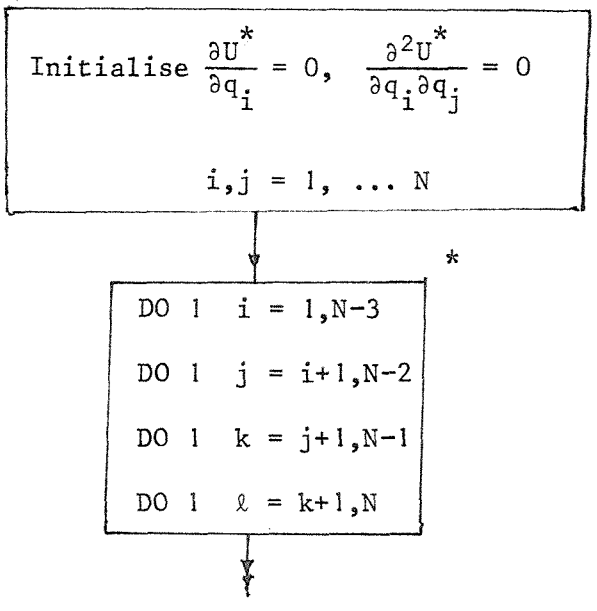

Contd of next page

* Refer to footnote on next page

Contd from previous page

Terms in Group (i)

$$\frac{\partial U^*}{\partial q_i} \rightarrow \frac{\partial U^*}{\partial q_i} + 24A_{ijk\ell}q_j q_k q_\ell$$

$$\frac{\partial U^*}{\partial q_j} \rightarrow \frac{\partial U^*}{\partial q_j} + 24A_{ijk\ell}q_i q_k q_\ell$$

$$\frac{\partial U^*}{\partial q_k} \rightarrow \frac{\partial U^*}{\partial q_k} + 24A_{ijk\ell}q_i q_j q_\ell$$

$$\frac{\partial U^*}{\partial q_\ell} \rightarrow \frac{\partial U^*}{\partial q_\ell} + 24A_{ijk\ell}q_i q_j q_k$$

$$\frac{\partial^2 U^*}{\partial q_i \partial q_j} \rightarrow \frac{\partial^2 U^*}{\partial q_i \partial q_j} + 24A_{ijk\ell}q_k q_\ell$$

$$\frac{\partial^2 U^*}{\partial q_i \partial q_k} \rightarrow \frac{\partial^2 U^*}{\partial q_i \partial q_k} + 24A_{ijk\ell}q_j q_\ell$$

$$\frac{\partial^2 U^*}{\partial q_i \partial q_\ell} \rightarrow \frac{\partial^2 U^*}{\partial q_i \partial q_\ell} + 24A_{ijk\ell}q_j q_k$$

$$\frac{\partial^2 U^*}{\partial q_j \partial q_k} \rightarrow \frac{\partial^2 U^*}{\partial q_j \partial q_k} + 24A_{ijk\ell}q_i q_\ell$$

$$\frac{\partial^2 U^*}{\partial q_j \partial q_\ell} \rightarrow \frac{\partial^2 U^*}{\partial q_j \partial q_\ell} + 24A_{ijk\ell}q_i q_k$$

$$\frac{\partial^2 U^*}{\partial q_k \partial q_\ell} \rightarrow \frac{\partial^2 U^*}{\partial q_k \partial q_\ell} + 24A_{ijk\ell}q_i q_j$$

```
1       CONTINUE                                    *

        DO 2  i =1,N
        DO 2  j =1,N-1
        DO 2  k =j+1,N
```

Contd on next page

---

* Note that the terms 'DO' and 'CONTINUE' have the same meaning as in Fortran language. ' → ' indicates replacement.

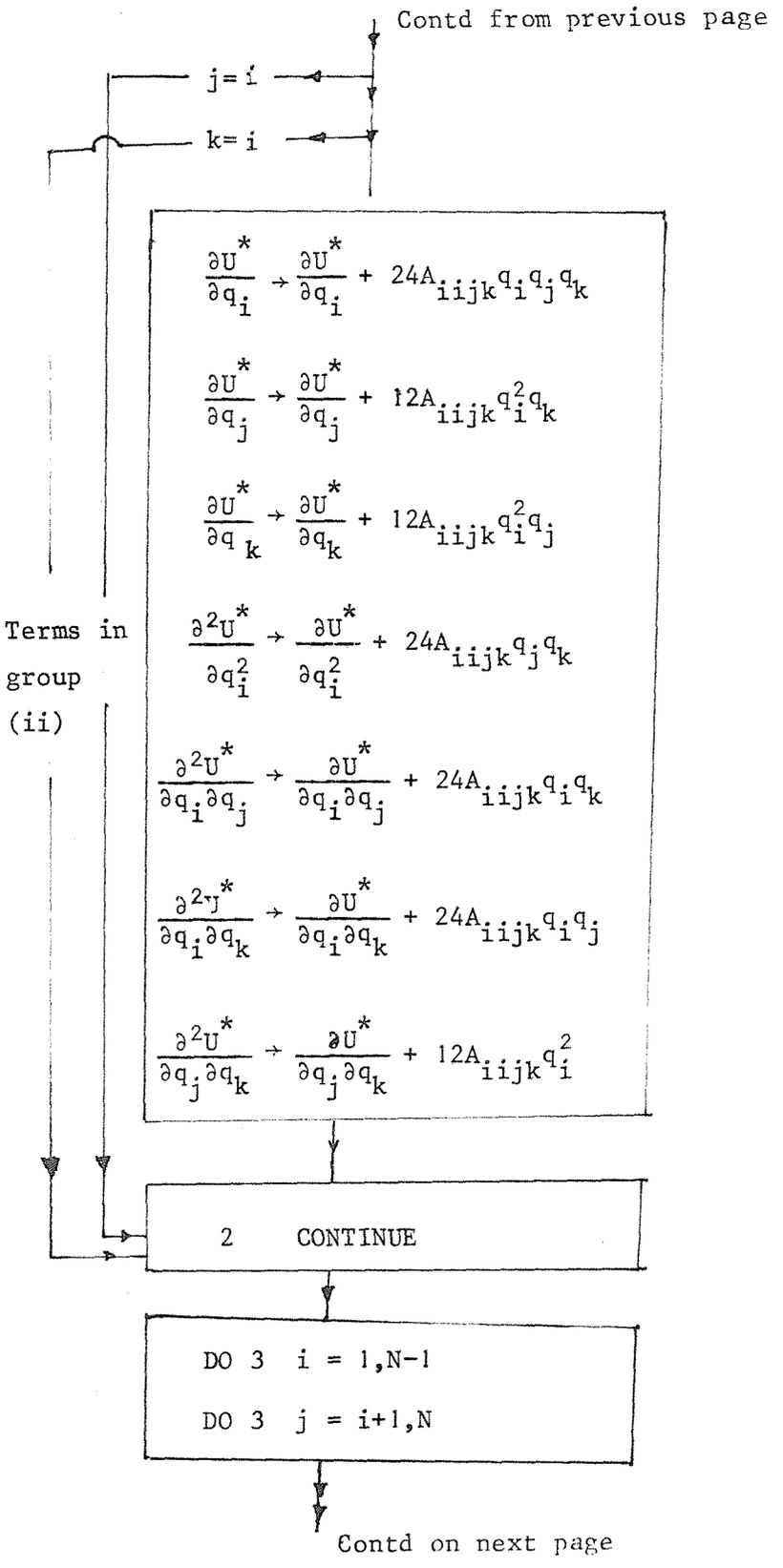
Contd from previous page
j=i
k=i
Terms in group (ii)
$\frac{\partial U^*}{\partial q_i} \rightarrow \frac{\partial U^*}{\partial q_i} + 24A_{iijk}q_i q_j q_k$
$\frac{\partial U^*}{\partial q_j} \rightarrow \frac{\partial U^*}{\partial q_j} + 12A_{iijk}q_i^2 q_k$
$\frac{\partial U^*}{\partial q_k} \rightarrow \frac{\partial U^*}{\partial q_k} + 12A_{iijk}q_i^2 q_j$
$\frac{\partial^2 U^*}{\partial q_i^2} \rightarrow \frac{\partial U^*}{\partial q_i^2} + 24A_{iijk}q_j q_k$
$\frac{\partial^2 U^*}{\partial q_i \partial q_j} \rightarrow \frac{\partial U^*}{\partial q_i \partial q_j} + 24A_{iijk}q_i q_k$
$\frac{\partial^2 U^*}{\partial q_i \partial q_k} \rightarrow \frac{\partial U^*}{\partial q_i \partial q_k} + 24A_{iijk}q_i q_j$
$\frac{\partial^2 U^*}{\partial q_j \partial q_k} \rightarrow \frac{\partial U^*}{\partial q_j \partial q_k} + 12A_{iijk}q_i^2$
2 CONTINUE
DO 3 i = 1,N-1
DO 3 j = i+1,N
Contd on next page

Contd from previous page

Terms in group (iii)

$$\frac{\partial U^*}{\partial q_i} \rightarrow \frac{\partial U^*}{\partial q_i} + 12A_{iijj}\, q_i q_j^2$$

$$\frac{\partial U^*}{\partial q_j} \rightarrow \frac{\partial U^*}{\partial q_j} + 12A_{iijj}\, q_i^2 q_j$$

$$\frac{\partial^2 U^*}{\partial q_i^2} \rightarrow \frac{\partial U^*}{\partial q_i^2} + 12A_{iijj}\, q_j^2$$

$$\frac{\partial^2 U^*}{\partial q_i \partial q_j} \rightarrow \frac{\partial U^*}{\partial q_i \partial q_j} + 24A_{iijj}\, q_i q_j$$

$$\frac{\partial^2 U^*}{\partial q_j^2} \rightarrow \frac{\partial U^*}{\partial q_j^2} + 12A_{iijj}\, q_i^2$$

```
3   CONTINUE
```

```
DO 4  i = 1,N
DO 4  j = 1,N
```

j=i

Terms in group (iv)

$$\frac{\partial U^*}{\partial q_i} \rightarrow \frac{\partial U^*}{\partial q_i} + 12A_{iiij}\, q_i q_j$$

$$\frac{\partial U^*}{\partial q_j} \rightarrow \frac{\partial U^*}{\partial q_j} + 4A_{iiij}\, q_i^3$$

$$\frac{\partial^2 U^*}{\partial q_i^2} \rightarrow \frac{\partial^2 U^*}{\partial q_i^2} + 24A_{iiij}\, q_i q_j$$

$$\frac{\partial^2 U^*}{\partial q_i \partial q_j} \rightarrow \frac{\partial^2 U^*}{\partial q_i \partial q_j} + 12A_{iiij}\, q_i^2$$

```
4   CONTINUE
```

Contd on next page

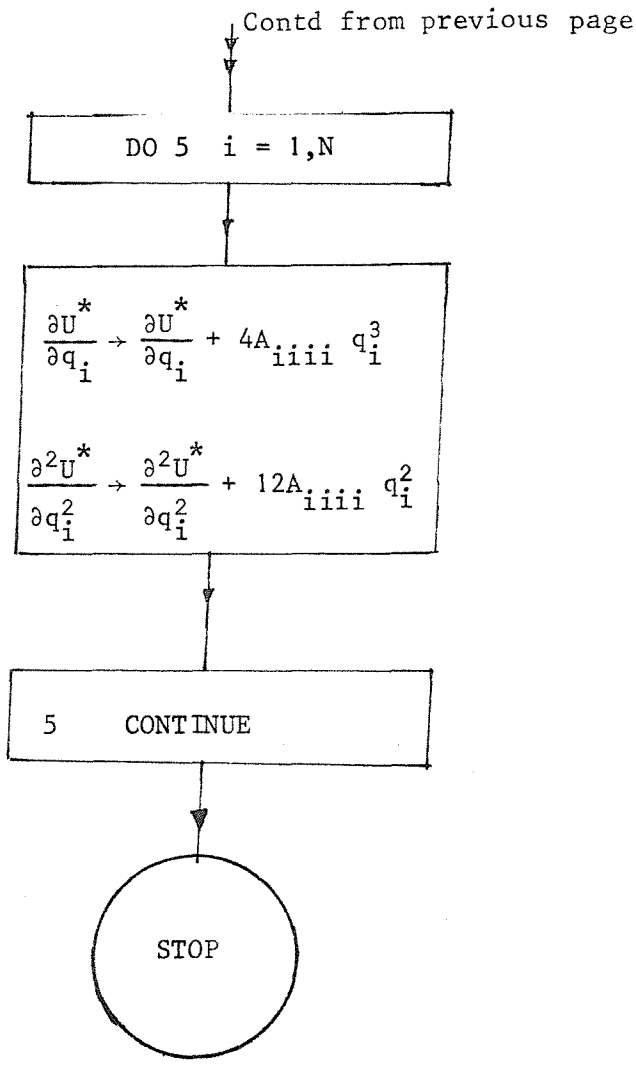
Contd from previous page
DO 5 i = 1,N
$\frac{\partial U^*}{\partial q_i} \rightarrow \frac{\partial U^*}{\partial q_i} + 4A_{iiii}\, q_i^3$
$\frac{\partial^2 U^*}{\partial q_i^2} \rightarrow \frac{\partial^2 U^*}{\partial q_i^2} + 12A_{iiii}\, q_i^2$
5 CONTINUE
STOP

APPENDIX X

A TYPICAL SET OF READINGS OF THICKNESS ON A SHEET OF SILICONE RUBBER

Context: Sec. 6.2.1.2.2

Content: In order to illustrate the quality of the sheets of silcoset used in making the test specimens, a typical set of readings of the thickness on a coupon of material (Fig. X.A) is given, in Table X.A.

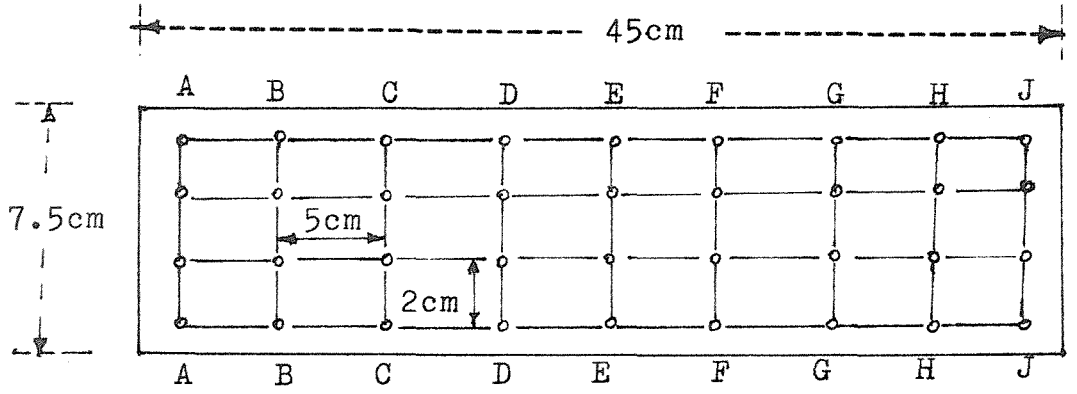

Fig. X.A

Table X.A

READINGS ALONG LINE	Thickness in mm
AA	1.52, 1.50, 1.53, 1.54
BB	1.52, 1.51, 1.52, 1.52
CC	1.51, 1.50, 1.50, 1.51
DD	1.52, 1.51, 1.51, 1.51
EE	1.51, 1.51, 1.50, 1.50
FF	1.51, 1.53, 1.49, 1.50
GG	1.52, 1.53, 1.51, 1.51
HH	1.53, 1.52, 1.52, 1.54
JJ	1.55, 1.52, 1.53, 1.48

Mean thickness = 1.515 mm

Standard deviation = 0.015 mm

APPENDIX XI

DETAILS OF THE SPECIMENS TESTED

Context: Art. 6.3

Contents: Dimensions, the value of 'E' of the material, the self weight and the collapse loads of the square box specimen tested. These are summarised in Table XI.A. This is followed by a discussion on the properties of the material.

Table XI.A

Identification	γ	β	Dimensions length×width×thickness of wall	'E' of the material in psi	Selfwt. in gms (inc. the caps)	Observed collapse load* in lb.
A1(1)	4	30	21.40×5.35×0.178	293	147	3.08
A1(2)	4	30	21.40×5.35×0.178	293	146	3.07
A2(1)	4	30	22.30×5.60×0.186	296	168	3.40
A2(2)	4	30	22.30×5.60×0.186	296	166	3.40
B1(1)	2	30	10.8×5.4×0.180	300	97	3.80
B1(2)	2	30	10.8×5.4×0.180	312	98	3.90
B2(1)	3	20	12.0×4.0×0.205	207	54	3.20
B2(2)	3	20	12.0×4.0×0.200	187	55	2.95
B3(1)	3	30	15.60×5.20×0.175	287	112	3.10
B3(2)	3	30	16.65×5.55×0.185	328	139	3.90
B4(1)	3	40	21.60×7.00×0.180	300	174	3.15
B4(2)	3	40	21.60×7.20×0.180	293	174	3.10
B5(1)	4	20	16.0×4.0×0.200	235	73	3.35
B5(2)	4	20	16.0×4.0×0.200	235	73	3.33
B6(1)	4	30	21.40×5.35×0.178	293	147	3.08
B6(2)	4	30	21.40×5.35×0.178	293	146	3.07

Identification	γ	β	Dimensions length×width×thickness of wall	'E' of the material in psi	Selfwt. in gms (inc. the caps)	Observed collapse load* in lb.
B7(1)	4	40	28.50×7.10×0.178	318	220	3.08
B7(2)	4	40	27.80×6.95×0.174	309	199	2.85
B8(1)	5	20	20×4.0×0.200	175	83	2.20
B8(2)	5	20	20×4.0×0.200	207	84	2.56
B9(1)	5	20	26.50×5.30×0.177	313	165	2.80
B9(2)	5	30	26.50×5.30×0.177	293	166	2.65
B10(1)	5	40	37.00×7.40×0.185	302	404	2.85
B10(2)	5	40	37.00×7.40×0.185	321	391	3.00
B11(1)	5	50	40.00×8.00×0.169	386	401	2.08
B11(2)	5	50	39.30×7.85×0.157	306	381	1.88
B12(1)	5	60	45.0×9.0×0.150	258	513	1.16
B12(2)	5	60	44.4×8.90×0.148	249	521	1.10
B13(1)	9	20	33.10×3.68×0.184	355	132	2.96
B13(2)	9	20	33.50×3.72×0.186	355	141	3.00
B14(1)	9	30	49.70×5.50×0.184	355	269	2.80
B14(2)	9	30	49.70×5.50×0.184	355	277	2.76

Properties of the material

From Table XI.A, it is seen that there is a wide variation of the value of 'E' of the material. This is due to

(i) the change in the quality of the material with increasing age of the rubber fluid.

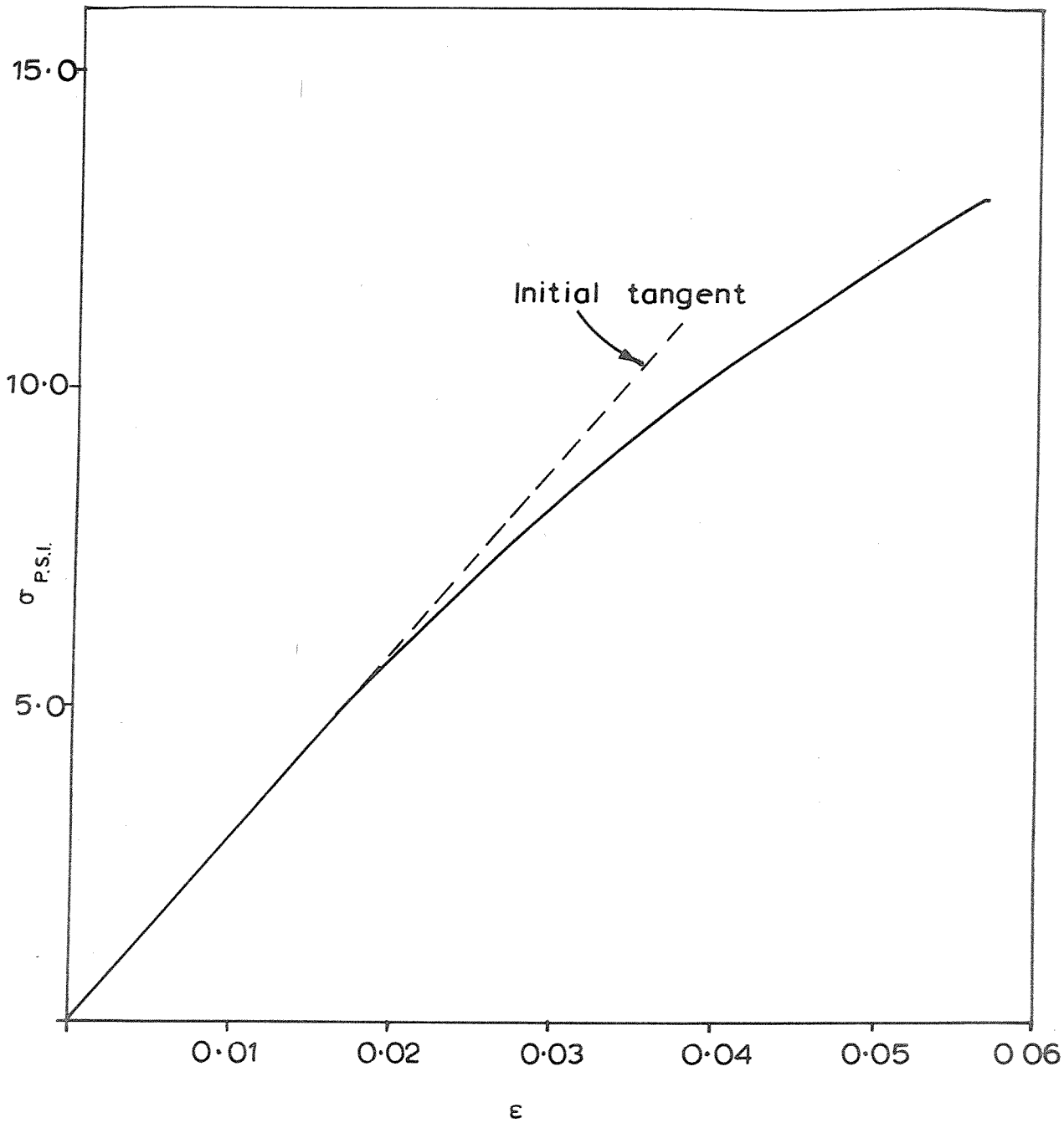

Fig.XI.A. A Typical Stress-Strain Characteristic of a Silcoset Tension Specimen

(ii) the variation of density of the rubber fluid from the top to bottom layers in the vessel in which it is stored.

It was not found practicable to maintain the same value of 'E' throughout the investigation. Instead, the material is transferred to a smaller jar each time a specimen is made, thoroughly stirred with the aid of a mechanical stirrer and a tension specimen cast along with the specimen in order to be able to determine the value of 'E'.

A typical stress-strain characteristic is shown in Fig. XI.A. It is seen that the material has a linear response upto a certain stress (5 psi in this case) whereafter the nonlinearity tends to get pronounced. In view of the very low stresses involved in the compression tests, the initial tangent modulus has been taken to represent 'E'. The value of 'E' in compression is assumed to be the same as that in tension. The value of Poisson's ratio has been taken to be 0.3 for making comparisons with the theory.

APPENDIX XII

ANALYSIS OF THE THEORETICAL MODEL OF THE COLUMN RESTING ON DISCRETE NONLINEAR SPRINGS (DISCUSSED IN CHAPTER 6)

XII.1 Introduction

This appendix describes the analysis of the mechanical model of a column made up of rigid links connected at joints, each of which rest on a nonlinear compression spring and carry a linear moment spring. (Fig. XII.A-B). A finite element procedure is employed for the analysis.

XII.2 Theory

Consider an element AB of the model (Fig. XII.A) with its left end A resting on the compression spring. The total potential energy stored in the element consists of

(i) The strain energy stored in the compression spring at A (U_1)

(ii) The strain energy stored in the moment springs at A and B (U_2)

(iii) The loss of potential of the applied horizontal load, as the horizontal distance between A and B diminishes as the element rotates under the application of load (V).

XII.2.1 The strain energy stored in the compression spring:

Let the resistance offered by the spring F be given by

$$F = \sum_{i=1}^{n} C_i \, q^i$$

where $q = \delta/L$, δ being the applied displacement on the spring and C_i are coefficients having the dimension of force.

The strain energy stored in the spring at a displacement δ ,

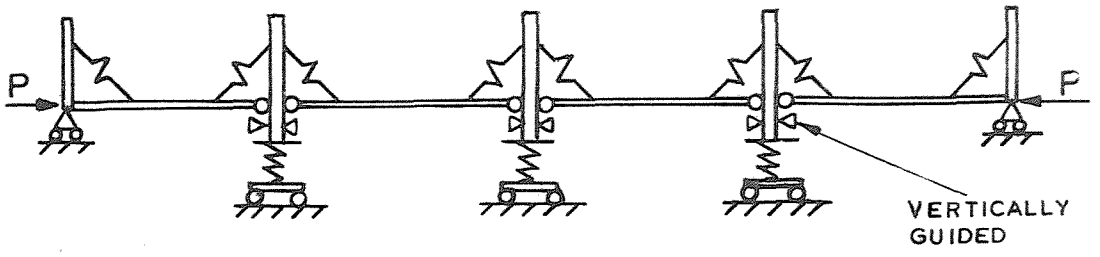

(i) The General Arrangement

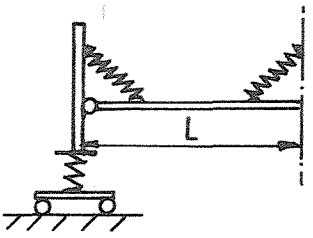

(ii) The Finite Element

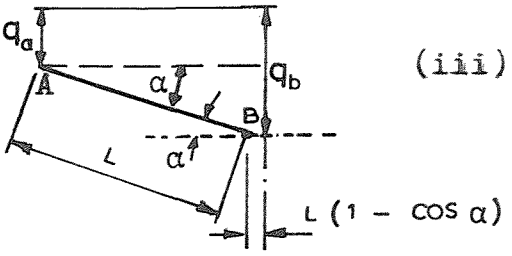

(iii) The Deformation of the Element

Fig. XII.A . The Mechanical Model

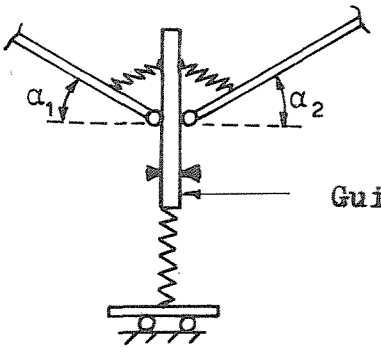

Fig. XII.B . The Details at a Joint

$$U_1 = \int_0^{\delta} (\sum C_i \, q^i) d\delta = \sum A_i \, q^{i+1}$$

where $A_i = \frac{L.C_i}{(i+1)}$

XII.2.2 The strain energy stored in the moment springs

Fig. XII.B shows the details at a joint of the model. It may be seen that at the joint there are two moment springs, one on either side of the joint, each connected to a link and working independently of each other. This special arrangement assumed here is to make possible computation of the strain energy stored in each element separately in terms exclusively of the degrees of freedom associated with it so that the usual finite element procedure can be applied.

The rotation of the element is given by

$$\alpha = \sin^{-1}(q_b - q_a)$$

and the strain energy stored in the moment spring at A

$$U_2 = \frac{1}{2} \gamma_a \, \alpha^2$$

where γ_a is the stiffness of the moment spring. Therefore

$$U_2 = \frac{1}{2} \gamma_a \{\sin^{-1}(q_b - q_a)\}^2$$

The term $\sin^{-1}(q_b - q_a)$ can be accurately represented by the expression

$$\sin^{-1}(q_b - q_a) = \theta + \frac{\theta^3}{6}, \quad \text{where} \quad \theta = q_b - q_a$$

as long as $\theta << 1$.

Thus the strain energy stored in both the springs works out to be

$$U_2 = \frac{\theta^2}{2} (1 + \frac{1}{6} \theta^2)^2 \, (\gamma_a + \gamma_b)$$

If the moment springs have all the same stiffness given by

$$\gamma_a = \gamma_b = \gamma \ , \quad \text{then}$$

$$U_2 = \gamma\theta^2\left(1 + \frac{\theta^2}{6}\right)^2$$

XII.2.3 The loss of potential of the applied load

The change in the horizontal distance between the ends of the rigid slement AB

$$\Delta = L(1 - \cos\alpha)$$

$$= L(1 - \sqrt{1 - \sin^2\alpha})$$

But $\sin\alpha = (q_b - q_a) = \theta$

so that $\Delta = L(1 - \sqrt{1-\theta^2})$.

Thus the loss of potential of the applied load

$$V = -PL(1 - \sqrt{1-\theta^2})$$

Thus the total potential energy of the element

$$U_E = \sum A_i \, q_a^{i+1} + \gamma\theta^2\left(1 + \frac{\theta^2}{6}\right)^2 + PL\sqrt{1-\theta^2} \qquad \ldots \text{(i)}$$

neglecting the constant term -PL.

XII.2.4 Governing equations of the problem:

We now invoke the principle of stationary potential energy to generate the nonlinear equations governing the problem. As a first step, we differentiate U_E, the potential energy of the element, by the nodal degrees of freedom q_a and q_b respectively. Thus

$$E_a = \frac{\partial U_E}{\partial q_a} = \sum A_i (i+1) q_a^i - 2\gamma\theta\left(1 + \frac{\theta^2}{6}\right)\left(1 + \frac{\theta^2}{2}\right) + PL\theta(1-\theta^2)^{\frac{1}{2}}$$

$$E_b = \frac{\partial U_E}{\partial q_b} = 2\gamma\theta\left(1 + \frac{\theta^2}{6}\right)\left(1 + \frac{\theta^2}{2}\right) - PL\theta(1-\theta^2)^{\frac{1}{2}}$$

. . . (ii)(a-b)

These expressions stand for the nodal forces corresponding to q_a and q_b respectively in the element. The nonlinear equations governing the problem can be obtained by summing up the reactive forces at each node corresponding to each of the two elements that meet at the node. These will not be explicitly developed here.

XII.2.5 The buckling analysis of the column

In order to examine the possibility of bifurcation from the trivial equilibrium path of the model, characterised by zero deflections, we employ the perturbation technique to develop a set of sequentially linear equations and examine the first equation thereof with all the displacements vanishing. As a first step in this procedure, we differentiate the expressions (ii) with respect to a path parameter 'ε'(which need not be specified at this stage) and then examine the expressions obtained thereby, at $q_a = q_b = 0$. Thus

$$\left.\frac{\partial E_a}{\partial \varepsilon}\right|_{q=o} = q_{a_1}\left[2A_1 + 2\gamma - PL\right] + q_{b_1}\left[-2\gamma + PL\right]$$

$$\left.\frac{\partial E_b}{\partial \varepsilon}\right|_{q=o} = q_{a_1}\left[-2\gamma + PL\right] + q_{b_1}\left[2\gamma - PL\right]$$

These represent the first order perturbation expressions of the nodal forces of the element AB. Expressed in a matrix notation

$$\frac{\partial}{\partial \varepsilon} \begin{Bmatrix} E_a \\ E_b \end{Bmatrix}_{q=o} = [A_e] \{q_1\} - P [B_e]$$

where $A_e = \begin{bmatrix} 2(A+\gamma) & -2\gamma \\ -2\gamma & 2\gamma \end{bmatrix}$

$$B_e = \begin{bmatrix} L & -L \\ -L & L \end{bmatrix}$$

$$\{q_1\} = \begin{Bmatrix} q_{a_1} \\ q_{b_1} \end{Bmatrix} = \frac{\partial}{\partial \varepsilon} \begin{Bmatrix} q_a \\ q_b \end{Bmatrix}$$

The first order perturbation equations for the entire column written with respect to the trivial equilibrium state, can be obtained by a systematic assembly of the element matrices A_e and B_e to obtain the global matrices A_G and B_G and can be expressed in the form

$$\{[A_G] - P[B_G]\} \{Q_1\} = \{0\}$$

where $\{Q_1\}$ stands for the vector of global displacements.
These are a set of linear homogeneous equations and lead to an eigenvalue problem. The lowest eigenvalue and the corresponding eigenvector of the above set of equations give the buckling load and mode.

XII.2.6 Solution of nonlinear equations to trace the postbuckling equilibrium path

It is possible to continue with the procedure outlined in the last section by setting up higher order perturbation equations, the solution of which would yield information regarding the characteristics of the

postbuckling equilibrium path in the vicinity of the buckling load. Such a procedure has been discussed in the context of the plate problem in chapter 3, and will not be repeated here. But the procedure for tracing the nonlinear equilibrium path by a direct solution of the governing equations will be discussed in this section - as this differs from the previously discussed procedure in a few significant details.

Let a certain point A on the equilibrium path be characterised by the deflections (q_{a_o}, q_{b_o} ... etc) and the load P_o. Let 'ε' be the chosen path parameter and let its value at A be ε_o. In order to obtain the next point on the solution path, we increment ε by Δε. The new value of the path parameter is $\varepsilon_o + \Delta\varepsilon$. It is required to obtain the displacements and load corresponding to this new value of the path parameter. It is important to note that it is better not to identify this path parameter with 'P' or the end displacement (δ), as there would be portions of the solution path where both P and δ will be simultaneously retrograde.

The procedure consists of the following steps:

(i) To predict the displacements and load corresponding to the new value of the path parameter, by using a perturbation technique, and

(ii) To correct the predicted values of displacements and load by a Newton-Raphson iterative procedure. The procedure is very similar, in principle, to the one proposed by Walker[108] and used by Svensson and Croll[71].

Prediction of displacements and load

The expressions E_a and E_b in (ii)(a-b) are differentiated by the path parameter to develop a set of sequentially linear equations therefrom. In most nonlinear problems it is quite sufficient to consider only the first equation thereof. But in view of the high degree of

nonlinearity of the problem, the first two perturbation equations are considered here, to make the predicted values more accurate, so that convergence can be obtained in a fewer number of iterations in the correction process.

The first order perturbation expressions of the nodal forces are

$$\frac{\partial E_a}{\partial \varepsilon} = q_{a_1}\left\{ \sum_1^n i(i+1)A_i\, q_{a_o}^{i-1} + 2\gamma\left(1 + 2\theta_o^2 + \frac{5}{12}\theta_o^4\right) - P_o L(1-\theta_o^2)^{-3/2} \right\}$$

$$+ q_{b_1}\{-2\gamma(1 + 2\theta_o^2 + \frac{5}{12}\theta_o^4) + P_o L(1-\theta_o^2)^{-3/2}\}$$

$$+ P_1 . L\theta_o(1-\theta_o^2)^{-\frac{1}{2}}$$

$$\frac{\partial E_b}{\partial \varepsilon} = q_{a_1}\{-2\gamma(1 + 2\theta_o^2 + \frac{5}{12}\theta_o^4) + P_o L(1-\theta_o^2)^{-3/2}\}$$

$$+ q_{b_1}\{2\gamma(1 + 2\theta_o^2 + \frac{5}{12}\theta_o^4) - P_o L(1-\theta_o^2)^{-3/2}\}$$

$$- P_1 L\theta_o(1-\theta_o^2)^{-\frac{1}{2}}$$

In the matrix notation these take the form:

$$\frac{\partial}{\partial \varepsilon}\begin{Bmatrix} E_a \\ E_b \end{Bmatrix} = [S_E]\{q_1\} + P_1\{c\} \qquad \ldots \text{(iii)}$$

$$\{q_1\} = \begin{Bmatrix} q_{a_1} \\ q_{b_1} \end{Bmatrix}$$

$$[S_E] = \begin{bmatrix} S_{11} & S_{12} \\ S_{21} & S_{22} \end{bmatrix}$$

in which $S_{11} = \sum_{1}^{n} i(i+1)A_i\, q_{a_o}^{i-1} + 2\gamma(1 + 2\theta_o^2 + \frac{5}{12}\theta_o^4) - P_o L(1-\theta_o^2)^{-3/2}$

$$S_{12} = -2\gamma(1 + 2\theta_o^2 + \frac{5}{12}\theta_o^4) + P_o L(1-\theta_o^2)^{-3/2}$$

$$S_{21} = S_{12}$$

$$S_{22} = 2\gamma(1 + 2\theta_o^2 + \frac{5}{12}\theta_o^4) - P_o L(1-\theta_o^2)^{-3/2}$$

and $\{c\} = \begin{Bmatrix} c_1 \\ c_2 \end{Bmatrix}$

in which

$$c_1 = L\theta_o(1-\theta_o^2)^{-\frac{1}{2}}$$

$$c_2 = -c_1$$

Systematic assembly of the first order perturbation nodal forces to express the corresponding equilibrium conditions for the entire column leads to a set of equations in the form

$$[S_G]\ \{Q_1\} + P_1\{C\} = \{0\} \qquad \ldots \text{(iv)}$$

where, $\{Q_1\}$ stands for the first order perturbation quantities corresponding to the global degrees of freedom

$[S_G]$ is the global stiffness matrix obtained by assembling the element stiffness matrices $[S_E]$

and $\{C\}$ is the column vector, built up by the column vectors $\{c\}$ in (iii).

The set (iv) gives 'N' equations (N being the number of global degrees of freedom) in N+1 unknowns, comprising of 'N' degrees of freedom and P_1. An additional equation is required which is supplied by $\varepsilon_1 = 1$. In the present problem, it appears best to choose the deflection of the spring at the middle of the column as the path parameter, as this increases monotonically all along the equilibrium path.

The solution of these equations leads to q_1's and P_1.

In the same notation, the second order perturbation expressions for the nodal forces take the form:

$$\frac{\partial^2}{\partial\varepsilon^2}\begin{Bmatrix} E_a \\ E_b \end{Bmatrix} = [S_E]\{q_2\} + P_2\{c\} + \{d\}$$

where $\{q_2\} = \begin{Bmatrix} q_{a_2} \\ q_{b_2} \end{Bmatrix}$ in which $q_{a_2} = \frac{\partial^2 q_a}{\partial\varepsilon^2}$ and so on.

$$P_2 = \frac{\partial^2 P}{\partial\varepsilon^2}$$

and $\{d\} = \begin{Bmatrix} d_1 \\ d_2 \end{Bmatrix}$

in which

$$d_1 = \sum (i-1)i(i+1)A_i\, q_{a_o}^{i-2}\, q_{a_1}^2 - \frac{2}{3}\gamma\theta_1^2\theta_o(12+5\theta_o^2) + 3P_oL\theta_o\theta_1^2(1-\theta_o^2)^{-5/2} + P_1L\theta_1(1-\theta_o)^{-3/2}$$

$$d_2 = \frac{2}{3}\gamma\theta_1^2\theta_o(12+5\theta_o^2) - 3P_oL\theta_o\theta_1^2(1-\theta_o^2)^{-5/2} - P_1L\theta_1(1-\theta_o^2)^{-3/2}$$

and the second order perturbation equations for the entire structure take the form:

$$[S_G]\{Q_2\} + P_2 \{C\} = - \{D\} \qquad \ldots (v)$$

where {D} is the column vector obtained assembling the column vectors {d}. Again these equations number 'N' and involve N+1 unknowns (comprising of 'N' global degrees of freedom and P_2) and the extra equation is supplied in this case by the condition $\varepsilon_2 = 0$.

The solution of these equations leads to the determination of q_2's and P_2; the displacements and load corresponding to the incremented value of the path parameter, can be obtained as

$$q_a^* = q_{a_o} + \Delta\varepsilon . q_{a_1} + \frac{1}{2!}(\Delta\varepsilon)^2 \, q_{a_2}$$

$$q_b^* = q_{b_o} + \Delta\varepsilon . q_{b_1} + \frac{1}{2!}(\Delta\varepsilon)^2 \, q_{b_2}$$

$$P^* = P_o + \Delta\varepsilon . P_1 + \frac{1}{2!}(\Delta\varepsilon)^2 \, P_2$$

These values provide an approximate solution of the equilibrium state corresponding to $\varepsilon = \varepsilon_o + \Delta\varepsilon$ and are in need of correction.

Newton-Raphson Correction

Let q^c and P^c represent corrections to the displacements q^* and P^*, so that

$$q_a = q_a^* + q_a^c$$

$$q_b = q_b^* + q_b^c$$

and $$P = P^* + P^c$$

Substituting these expressions in the nonlinear expressions for the nodal forces E_a and E_b in (ii)(a-b) and linearising with respect to corrections, the nodal forces can be expressed in the form:

$$\begin{Bmatrix} E_a \\ E_b \end{Bmatrix} = [S_E]\{q^c\} + P_c \{c\} + \{e\} \qquad \ldots (vi)$$

where $\{e\} = \begin{Bmatrix} e_1 \\ e_2 \end{Bmatrix}$ and $\{q^c\} = \begin{Bmatrix} q_a^c \\ q_b^c \end{Bmatrix}$

in which e_1 and e_2 are the values of nodal forces as given by the approximate displacements q_a^*, q_b^* and load P^*. Assembling these matrices, the global system of equations can be expressed in the form

$$[S_G] \{Q^c\} + P_c \{C\} = \{E\} \qquad \ldots \text{(vii)}$$

These again are N equations involving N+1 unknowns and the required additional equation is supplied by $\varepsilon^c = 0$, as no change in the path parameter is to be allowed during the correction process.

The solution of (vii) gives the corrections, but the corrected displacements are still approximate due to the linearisation in obtaining the expression (vi). Therefore, the correction process is repeated till the corrections obtained become negligible.

XII.2.7 Check for stability

It is sometimes necessary to determine whether a certain equilibrium state is stable or otherwise. The stability can be affected by the precise nature of application of compression, whether the load or end compression is prescribed. In the former case, the application of the virtual work theorem leads to the principle of stationary potential energy and in the latter to that of stationary strain energy. Thus in order to check the stability under controlled compression, it is necessary to examine the second variation of strain energy. If it is positive definite, the equilibrium is stable; otherwise it is unstable.

Recalling the strain energy stored in the element

$$U_E = \sum A_i \, q_a^{i+1} + \gamma\theta^2 \left(1 + \frac{\theta^2}{6}\right)^2$$

The second variation of strain energy is given by

$$\delta^2 U_E = \frac{1}{2!}\left\{ \frac{\partial^2 U}{\partial q_a^2}\left(\delta q_a\right)^2 + 2\,\frac{\partial^2 U}{\partial q_a \partial q_b}\,\delta q_a . \delta q_b + \frac{\partial^2 U}{\partial q_b^2}\left(\delta q_b\right)^2 \right\}$$

$$= \{q_a \quad q_b\}\,[S]\begin{Bmatrix} q_a \\ q_b \end{Bmatrix}$$

where $[S] = \begin{bmatrix} S_{11} & S_{12} \\ S_{21} & S_{22} \end{bmatrix}$

in which

$$S_{11} = \sum_{i=1}^{n} A_i\, i(i+1) q_a^{i-1} + 2\gamma\left(1 + 2\theta^2 + \frac{5}{12}\theta^4\right)$$

$$S_{12} = -2\gamma\left(1 + 2\theta^2 + \frac{5}{12}\theta^4\right)$$

$$S_{21} = S_{12}$$

$$S_{22} = 2\gamma\left(1 + 2\theta^2 + \frac{5}{12}\theta^4\right)$$

The second variation matrix of the strain energy of the entire structure can be obtained by assembling the matrices $[S]$ to form the corresponding global matrix. This is but the stiffness matrix $[S_G]$ wherefrom the terms involving P have been deleted. The second variation of strain energy is positive definite if this matrix is positive definite i.e. if the determinant and all the principal minors are positive.

XII.2.8 Computer programme

A computer programme for the analysis of the theoretical mechanical model based on the finite element procedure outlined above has been developed. The programme can deal with columns consisting of any given number of links and the coefficients defining response of the supporting springs.

REFERENCES

1. S.P. Timoshenko and J.M. Gere, "Theory of Elastic Stability", McGraw-Hill Book Co. Inc., 1961.

2. P.S. Bulson, "Stability of Flat Plates" Chatto and Windus, 1970.

3. F. Bleich, "Buckling Strength of Metal Structures" McGraw Hill Book Co. Inc. 1952

4. G. Gerard and H. Becker, "Hand Book of Structural Stability PART I - Buckling of Flat Plates", N.A.C.A. T.N.3781, 1957.

5. W.H. Wittrick, "A Unified Approach to the Initial Buckling of Stiffened Panels in Compression", The Aeronatuical Quarterly, Vol.XIX, pp.265-283, 1968.

6. F.W. Williams and W.H. Wittrick, "Computational Procedures for a Matrix Analysis of the Stability and Vibration of Thin Flatwalled Structures in Compression", International Journal of Mechanical Sciences, Vol.11, pp.979-998, 1969.

7. W.H. Wittrick, 'General Sinusoidal Stiffness Matrices for Buckling and Vibrational Analyses of Thin Flatwalled Structures", International Journal of Mechanical Sciences, Vol.10, pp.949-966, 1968.

8. W.H. Wittrick and F.W. Williams, "Algorithm for Computing Critical Buckling Loads of Elastic Structures" Journal of Structural Mechanics, Vol.1, No.4, pp.497-518, 1973.

9. W.H. Wittrick and F.W. Williams, "Buckling and Vibration of Anisotropic or Isotropic Plate Assemblies under Combined Loadings", International Journal of Mechanical Sciences, Vol.16, pp.209-239, 1974.

10. V.V. Novozhilov, "Foundations of Nonlinear Theory of Elasticity" Graylock Press, Rochester, N.Y., 1953.

11. G.J. Turvey, "A Contribution to the Elastic Stability of Thinwalled Structures Fabricated from Isotropic and Orthotropic Materials" Ph.D. Thesis, University of Birmingham, 1971.

12. Y.K. Cheung, "Finite Strip Method in Structural Analysis" Pergamon Press, 1976.

13. J.G.A. Croll and A.C. Walker, "Elements of Structural Stability", The Macmillan Press Ltd., 1972, p.70, 100, 144, 176.

14. K.C. Rockey and D.K. Bagchi, "Buckling of Plate Girder Webs under Partial Edge Loadings", International Journal of Mechanical Sciences, Vol.12, pp.64-76, 1970.

15. Th. von Karman, "Festigkeitsprobleme in Maschinenbau" Vol.IV, pt.4 of Encyk. der Math Wiss 1910 art 27 p.349.

16. Y.C. Fung, "Foundations of Solid Mechanics" Englewood Cliffs, N.J., Prentice-Hall, 1965.

17. N.T. Koiter, "On the Nonlinear Theory of Thin Elastic Shells", Proc. K. ned. Akad. Wet., Series B, I. Introductory Sections, II. Basic Shell Equations, III. Simplified Shell Equations, 69, 1966.

18. S. Levy, "Bending of Rectangular Plates with Large Deflections", NACA TR 737, 1942.

19. J.M. Coan, "Large Deflection Theory for Plates with Small Initial Curvature Loaded in Edge Compression" Trans. ASME 73, pp.143-151, 1951.

20. W.S. Hemp, "The Theory of Flat Panels Buckled in Compression", R & M 2178 ARC 1945.

21. M. Stein, "Loads and Deformations of Buckled Rectangular Plates" NACA Technical Report R40, 1959.

22. M. Stein, "Behaviour of Buckled Rectangular Plates" Journal of the Engineering Mechanics Division, ASCE, EM2, pp.59-76, 1960.

23. K. Marguerre, "Apparent Width of the Plate in Compression" NACA RM832, 1937.

24. N. Yamaki, "Postbuckling Behaviour of Rectangular Plates with Small Initial Curvature Loaded in Edge Compression", Journal of Applied Mechanics, pp.407-414, Sept. 1959 and pp.335-342, June 1960.

25. A.C. Walker, "The Postbuckling Behaviour of Simply Supported Square Plates" Aeronautical Quarterly, Vol.XX, pp.203-222, 1969.

26. J. Rhodes and J.M. Harvey, "The Postbuckling Behaviour of Thin Plates in Compression with the Unloaded Edges Elastically Restrained against Rotation", Journal of Mechanical Engineering Science, Vol.13, No.2, pp.82-91, 1971.

27. J. Rhodes and J.M. Harvey, "Plates in Uniaxial Compression with Various Support Conditions at the Unloaded Boundaries", International Journal of Mechanical Science, Vol.13, pp.787-802, 1971.

28. J. Rhodes and J.M. Harvey, "Effects of Eccentricity of Load or Compression on the Buckling and Postbuckling Behaviour of Flat Plates", International Journal of Mechanical Science, Vol.13, pp.867-879, 1971.

29. J. Rhodes and J.M. Harvey, "Examination of Plate Postbuckling Behaviour", Journal of Engineering Mechanics Division, ASCE, EM3, pp.461-478, 1977.

30. Washizu, K. "Variational Methods in Theory of Elasticity and Plasticity", Pergamon Press, 1968.

31. H.L. Cox, "The Buckling of Flat Rectangular Plate under Axial Compression and its Behaviour after Buckling" R & M, No.2041 (8641), A.R.C. Tech. Report.

32. Ref. 1, pp.411-417.

33. A.C. Walker, "Thinwalled Structural Forms under Eccentric Compressive Load Action", Ph.D. Thesis, University of Glasgow, 1964.

34. O.C. Zienkiewicz, "Finite Element Method in Engineering Science", McGraw-Hill Publishing Co. Inc., 1970.

35. J.S. Przemeniecki, "Theory of Matrix Structural Analysis", McGraw-Hill Book Co. Inc., 1968.

36. M.J. Turner, E.H. Dill, H.C. Martin and R.J. Melosh, "Large Deflection Analysis of Complex Structures Subjected to Heating and External Loads", Journal of Aero-Space Science, Vol.27, pp.97-106, Feb. 1960.

37. H.C. Martin, "Derivation of Stiffness Matrices for the Analysis of Large Deflection and Stability Problems" Proceedings of the First Conference on Matrix Methods in Structural Mechanics, AFFDL-TR-66-80, pp.697-715, 1966.

38. R.H. Gallagher, R.A. Gellatly, J. Padlog and R.H. Mallet, "Discrete Element Procedure in Thin Shell Stability Analysis" AIAA Journal, Vol.5, No.1, pp.138-144, 1967.

39. L.A. Schmidt, F.K. Bogner and R.L. Fox, "Finite Deflection Structural Analysis using Plate and Shell Discrete Elements" AIAA Journal, Vol.6, No.5, pp.781-791, 1968.

40. J.T. Oden, "Numerical Formulation of Nonlinear Elasticity Problems," Journal of the Structural Division, ASCE, Vol.93, No.ST3, pp.235-255, 1967.

41. D.W. Murray and E.L. Wilson, "Finite Element Large Deflection Analysis of Plates", Journal of the Engineering Mechanics Division, ASCE, Vol.95, EM1, pp.143-165, 1969.

42. D.W. Murray and E.L. Wilson "Finite Element Postbuckling Analysis of Thin Elastic Plates" AIAA Journal, Vol.7, No.10, pp.1915-1920, 1969.

43. C. Brebbia and J. Connor, "Geometrically Nonlinear Finite Element Analysis", Journal of the Engineering Mechanics Division, ASCE, Vol. 95, No.EM2, 1969, pp.463-483.

44. T.M. Roberts and D.G. Ashwell, "The Use of Finite Element Mid-Increment Stiffness Matrices in the Postbuckling Analysis of Imperfect Structures", International Journal of Solids and Structures, Vol.7, pp.805-823, 1971.

45. Akin Ecer, "Finite Element Analysis of the Postbuckling Behaviour of Structures", Vol.11, No.11, AIAA Journal, pp.1532-1538, 1973.

46. P.G. Bergan, "Nonlinear Analysis of Plates Considering Geometric and Material Effects" Division of Structural Mechanics, The Norwegian Institute of Technology, The University of Trondheim, Report No. 72-1, 1972.

47. Y. Ueda, M. Matsuishi, Y. Yamauchi and M. Topaka, "Nonlinear Analysis of Plates using the Finite Strip Method" Journal of the Kansai Society of Naval Architects No.154, pp.83-92, Sept. 1974.

48. A.S.L. Chan and A. Firmin, "Analysis of Cooling Towers by the Matrix Finite Element Method" Part II, Large displacements, The Aeronautical Journal of the Royal Aeronautical Society, pp.971-982, December 1970.

49. J.A. Stricklin and W.E. Haisler, H.R. MacDougall and F.J. Stebbins, "Nonlinear Analysis of Shells of Revolution by the Matrix Displacement Method", AIAA Journal, Vol.6, No.12, pp.2306-2312, 1968.

50. W.H. Haisler and J.A. Stricklin, "Nonlinear Finite Element Analysis Including Higher Order Strain Energy Terms" AIAA Journal Vol.8, No.6, pp.1158-1159, 1970.

51. J.A. Stricklin, J.E. Martinez, J.R. Tillerson, J.H. Hong and W.E. Haisler, "Nonlinear Dynamic Analysis of Shells of Revolution by Matrix Displacement Method" AIAA Journal, Vol.9, No.4, pp.629-636, 1971.

52. Chi-Teh Wang, "Nonlinear Large Deflection Boundary Value Problems of Rectangular Plates" NACA Technical Note No.1425, 1948.

53. A.K. Basu and J.C. Chapman, "Large Deflection Behaviour of Rectangular Orthotropic Plates", Proceedings of the Institution of Civil Engineers, Vol.35, pp.79-109, 1966.

54. B. Aalami and J.C. Chapman, "Large Deflection Behaviour of Rectangular Orthotropic Plates under Transverse and Inplane Loads" Proceedings of the Institution of Civil Engineers, Vol.42, pp.347-379, 1969.

55. D. Greenspan, "On Approximating Extremals of Functionals - I - The Method and Examples for Boundary Value Problems" - Bull. Int. Comp. Centre, Vol.4, University of Rome, pp.99-120, 1965.

56. D. Greenspan, "On Approximating Extremals of Functionals - II, Theory and Generalisations Related to Boundary Value Problems for Nonlinear Differential Equations", International Journal of Engineering Science, Vol.5, pp.571-588, 1967.

57. D. Bushnell and B.O. Almroth, "Finite-Difference Energy Method for Nonlinear Shell Analysis", Proc. LMSC/AFFDL Shell Conference, Palo Alto, California, Aug. 1970.

58. J.P. Benthem, "The Reduction in Stiffness of Combinations of Rectangular Plates in Compression After Exceeding the Buckling Load" NLL-TR S.539, June, 1969.

59. T.R. Graves-Smith, "The Postbuckled Behaviour of Thinwalled Columns," Eighth Congress of the IABSE, New York, 1968, pp. 311-320.

60. T.R. Graves-Smith, "The Postbuckled Behaviour of Thinwalled Box Beam in Pure Bending", International Journal of Mechanical Science, Vol.14, pp.711-722, 1972.

61. J. Rhodes and J.M. Harvey, "The Local Buckling and Post Local Buckling Behaviour of Thinwalled Beams", Aeronautical Quarterly Vol.XIX, pp.363-388, 1970.

62. J. Rhodes and J.M. Harvey, "Plain Channel Section Struts in Compression and Bending Beyond the Local Buckling Load", International Journal of Mechanical Science, Vol.8 , pp.511-519, 1976.

63. M. Stein, "The Phenomenon of Change in Buckle Pattern in Elastic Structures", NASA TR, R-39, 1959.

64. W.J. Supple, "Coupled Branching Configurations in the Elastic Buckling of Symmetrical Structural Systems" International Journal of Mechanical Sciences, Vol.9, pp.97-112, 1967.

65. W.J. Supple, "On the Change in Buckle Pattern in Elastic Structures", International Journal of Mechanical Sciences, Vol.10, pp.737-745, 1968.

66. W.J. Supple, "Changes in Wave-form of Plates in the Postbuckling Range", International Journal of Solids and Structures, Vol.6, pp.1243-1258, 1970.

67. T.R. Graves-Smith, "The Ultimate Strength of Locally Buckled Columns of Arbitrary Length", Ph.D. Thesis, Cambridge University, 1966.

68. A. van Der Neut, "The Interaction of Local Buckling and Column Failure of Thinwalled Compression Members", Proc. XII International Congress of Applied Mechanics, Stanford, 1968.

69. W.T. Koiter and G.D.C. Kuiken, "The Interaction between Local Buckling and Overall Buckling on the Behaviour of Built-up Columns", Report no. 447, Laboratory of Engineering Mechanics, Delft, May 1971.

70. A. van Der Neut, "The Sensitivity of Thinwalled Compression Members to Column Axis Imperfection", International Journal of Solids & Structures, Vol.9, pp.9-9 to 1011, 1973.

71. S.E. Svensson and J.G.A. Croll, "Interaction between Local and Overall Buckling", International Journal of Mechanical Sciences, Vol.17, pp.307-321, 1975.

72. A.C. Walker, "Interactive Buckling of Structural Components" Science Progress, Vol.62, pp.579-597, 1975.

73. J.D. Tulk and A.C. Walker, "Model Studies on the Elastic Buckling of a Stiffened Plate" Journal of Strain Analysis Vol.11, No.3, July 1976, pp.137-143.

74. W.C. Fok, J. Rhodes and A.C. Walker "Local Buckling of Outstands in Stiffened Plates", Aeronautical Quarterly, pp.277-291, November 1976.

75. R. Hill, "Mathematical Theory of Plasticity" Oxford University Press, 1950.

76. P.M. Naghdi, "Stress-Strain Relations in Plasticity and Thermo-plasticity", Plasticity - Proceedings of the Second Symposium on Naval Structural Mechanics, (Editors: E.H. Lee and P.S. Symonds) Pergamon Press, 1960.

77. G. Pope, "A Discrete Element Method for the Analysis of Plane Elastic-Plastic Stress Problems", Royal Aeronautical Establishment, TR65028, 1965.

78. T.R. Graves-Smith, "A Variational Method for Large Deflection-Elasto-Plastic Theory in its Application to Arbitrary Flat Plates", Structure, Solid Mechanics and Engineering Design, The Proceedings of the Southampton 1969 Civil Engineering Materials Conference, (Editor: M. Te'eni) pp.1249-1255.

79. M.A. Crisfield, "Fullrange Analysis of Steel Plates and Stiffened Plating under Uniaxial Compression" Proceedings of the Institution of Civil Engineers, Part 2, pp.1249-1255, 1975.

80. P.A. Frieze, P.J. Dowling and R.E. Hobbs, "Ultimate Load Behaviour of Plates in Compression", Steel Plated Structures, pp.24-50, An International Symposium,(Editors: P.J. Dowling, J.E. Harding and P.A. Frieze), Crosby Lockwood Staples, London 1977.

81. T.H. Soreide, P.G. Bergan and T. Moan, "Ultimate Collapse Behaviour of Stiffened Plates using Alternative Finite Element Formulations", Steel Plated Structures, pp.618-637. An International Symposium Ed. P.J. Dowling et al, Crosby Lockwood Staples, London, 1977.

82. M. Crisfield and R. Puthli, "A Finite Element Method Applied to Collapse Analysis of Stiffened Boxgirder Diaphragms" Steel Plated Structures, pp.311-317, An International Symposium, Ed. P.J. Dowling et al, Crosby Lockwood Staples, London, 1977.

83. A.N . Sherbourne and R.M. Korol, "Ultimate Strength of Plates in Uniaxial Compression" Preprint No. 1386, ASCE National Structural Meeting, Baltimore, April 1971.

84. A.N. Sherbourne, C.Y. Lian and C. Marsh, "Stiffened Plates in Uniaxial Compression" Publication of the IABSE, Vol.31, pp.146-177, 1971.

85. N.W. Murray, "Behaviour of Thin Stiffened Steel Plates" Publication of the IABSE, Vol.33-I, pp.191-201, 1973.

86. A.C. Walker, and N.W. Murray, "A Plastic Collapse Mechanism for Compressed Plates", Publication of the IABSE, Vol.35-I, pp.217-236, 1975.

87. M.R. Horne, "Plastic Theory of Structures" Nelson, 1971.

88. A.N. Sherbourne, "The Ultimate Strength of Circular, Mild Steel Plates in Uniform Compression" Publications of the IABSE, Vol.22, pp.289-310, 1962.

89. T.R. Graves-Smith, "The Effect of Initial Imperfections on the Strength of Thin Walled Box Columns", International Journal of Mechanical Sciences, Pergamon Press, Vol.13, pp.911-925, 1971.

90. J.R. Jombock and J.W. Clark, "Postbuckling Behaviour of Flat Plates", Transactions of the ASCE, Vol.127, Part I, pp.227-240, 1962.

91. B. Rawlings and P. Shapland, "The Behaviour of Thin-walled Box Sections under Gross Deformation", The Structural Engineer No.4, Vol.53, pp.181-186, 1975.

92. S. Sridharan, "Elastic Postbuckling Behaviour of Plate Assemblies and Crinkly Buckling of Plate Junctions", Progress Report, Dept. of Civil Engineering, University of Southampton, Nov. 1975.

93. K. Yoshida, "Buckling Analysis of Plate Structures by Strip Elements" Proceedings of Japanese Society of Naval Architects, 130, 1971.

94. M.Z. Khan and A.C. Walker, "Buckling of Plates subjected to Localised Edge Loading", The Structural Engineer, Vol.50, No.6, pp.225-232, 1972.

95. M.Z. Khan, K.C. Johns and B. Hayman, "Buckling of Plates with Partially Loaded Edges" Journal of the Structural Division, ASCE, ST3, pp.547-558, 1977.

96. P.R. Bensom and E. Hinton, "A Thick Finite Strip Formulation for Static, Free Vibration and Stability Problems", International Journal of Numerical Methods in Engineering, Vol.10, pp.665-678, 1976.

97. J.M.T. Thompson and A.C. Walker, "A General Theory of Elastic Stability" A Wiley-Interscience Publication, 1973.

98. J.M.T. Thompson and A.C. Walker, "The Nonlinear Perturbation Analysis of Discrete Structural Systems" International Journal of Solids and Structures, Vol.4, pp.757-768, 1968.

99. Y.K. Cheung, "Folded Plate Structures by the Finite Strip Method", Journal of the Structural Division, ST12, pp.2963-79, 1969.

100. J.H. Wilkinson and C. Reinsch, "Handbook of Automatic Computation" Vol. II, Linear Algebra, pp.303-314, 212-226 & 227-240, Springer-Verlag, 1971.

101. F.W. Williams, "Initial Buckling Curves for a Simply Supported Plate with a Vee-shaped Corrugation" Civil Engineering and Public Works Review, pp.239-242, March 1972.

102. S.P. Timoshenko and D.H. Young, "Theory of Structures", McGraw Hill Book Co. Inc., 1945.

103. NAG Library Manual, Mark 5, (University of Southampton Computing Services Library) 1977.

104. J.A. Stricklin and W.E. Haisler, "Formulations and Solution Procedures for Nonlinear Structural Analysis" Computers and Structures, Vol.7, pp.125-136, 1977.

105. W. H. Wittrick and F.W. Williams, "Initial Buckling of Channels in Compression", Journal of the Engineering Mechanics Division, EM3, pp.711-726, 1971.

106. N. Patterson, "Modelling with Silcoset", Honours Project Dept. of Civil Engineering, University of Southampton, 1975.

107. J.G. Lekkerkerker, "On the Stability of an Elastically Supported Beam Subjected to its Smallest Buckling Load", Proc. K. ned. Akad. Wet., Series B. 65, 1962.

108. A.C. Walker, "A Method of Solution for Nonlinear Simultaneous Algebraic Equations" International Journal of Numerical Methods in Engineering", Vol.1, pp.177-180, 1969.

109. K.S. Prabhu, S. Gopalacharyulu and D.J. Johns, "Buckling of Cylindrical Shells under Non-Uniform Lateral Pressures" Report TT7514, Loughborough,University of Technology, November 1975.